



SYNTHESIS OF GLYCOLIPIDS AND GLYCODENDRITIC POLYMERS THAT BIND HIV RGP120

José Antonio Morales Serna

ADVERTIMENT. L'accés als continguts d'aquesta tesi doctoral i la seva utilització ha de respectar els drets de la persona autora. Pot ser utilitzada per a consulta o estudi personal, així com en activitats o materials d'investigació i docència en els termes establerts a l'art. 32 del Text Refós de la Llei de Propietat Intel·lectual (RDL 1/1996). Per altres utilitzacions es requereix l'autorització prèvia i expressa de la persona autora. En qualsevol cas, en la utilització dels seus continguts caldrà indicar de forma clara el nom i cognoms de la persona autora i el títol de la tesi doctoral. No s'autoritza la seva reproducció o altres formes d'explotació efectuades amb finalitats de lucre ni la seva comunicació pública des d'un lloc aliè al servei TDX. Tampoc s'autoritza la presentació del seu contingut en una finestra o marc aliè a TDX (framing). Aquesta reserva de drets afecta tant als continguts de la tesi com als seus resums i índexs.

ADVERTENCIA. El acceso a los contenidos de esta tesis doctoral y su utilización debe respetar los derechos de la persona autora. Puede ser utilizada para consulta o estudio personal, así como en actividades o materiales de investigación y docencia en los términos establecidos en el art. 32 del Texto Refundido de la Ley de Propiedad Intelectual (RDL 1/1996). Para otros usos se requiere la autorización previa y expresa de la persona autora. En cualquier caso, en la utilización de sus contenidos se deberá indicar de forma clara el nombre y apellidos de la persona autora y el título de la tesis doctoral. No se autoriza su reproducción u otras formas de explotación efectuadas con fines lucrativos ni su comunicación pública desde un sitio ajeno al servicio TDR. Tampoco se autoriza la presentación de su contenido en una ventana o marco ajeno a TDR (framing). Esta reserva de derechos afecta tanto al contenido de la tesis como a sus resúmenes e índices.

WARNING. Access to the contents of this doctoral thesis and its use must respect the rights of the author. It can be used for reference or private study, as well as research and learning activities or materials in the terms established by the 32nd article of the Spanish Consolidated Copyright Act (RDL 1/1996). Express and previous authorization of the author is required for any other uses. In any case, when using its content, full name of the author and title of the thesis must be clearly indicated. Reproduction or other forms of for profit use or public communication from outside TDX service is not allowed. Presentation of its content in a window or frame external to TDX (framing) is not authorized either. These rights affect both the content of the thesis and its abstracts and indexes.

José Antonio Morales Serna

**SYNTHESIS OF GLYCOLIPIDS AND GLYCODENDRITIC
POLYMERS THAT BIND HIV rgp120**

THESIS DOCTORAL

Supervisor: Dr. Sergio Castellón Miranda

Department of Analytic Chemistry and Organic Chemistry



UNIVERSITAT ROVIRA I VIRGILI

Tarragona
2009

UNIVERSITAT ROVIRA I VIRGILI



Departament de Química Analítica

i Química Orgànica

Campus Sescelades

Carrer Marcel·lí Domingo,s/n

43007 Tarragona

Sergio Castellón Miranda, Catedràtic de Química Orgànica del Departament de Química Analítica i Química Orgànica de la Universitat Rovira i Virgili,

CERTIFICA:

Que el present treball, titulat "**Synthesis of glycolipids and glycodendritic polymers that binds HIV-1 rgp 120**", que presenta Jose Antonio Morales Serna per a l'obtenció del títol de Doctor, ha estat realitzat sota la meva direcció al Departament de Química Analítica i Química Orgànica i que aconsegueix els requeriments per poder optar al grau de doctor.

Tarragona, 30 d'Abril de 2009

This research was supported by a grant from the DGI CTQ2005-03124 (Ministerio de Educación y Ciencia, Spain), and a fellowship from DURSI (Generalitat de Catalunya) and Fons Social Europeu.

Acknowledgements

I would like to express my deep gratitude to Prof. Sergio Castellón Miranda, Dr. Maribel I. Matheu and Dr. Yolanda Díaz for providing continuous support and tutorial to this work.

I also owe my sincere appreciation to Prof. Dr. Angels Serra i Albert who gave important comments about hyperbranched polymers.

Special thanks go Prof. Varinder K. Aggarwal, Dr. Guillermo Negrón Silva and Dr. Jorge Cárdenas Pérez for numerous discussions, suggestions and advices which were important contribution to this research.

To David Foix, Isidro Cobo, and Josep Llaveria I would like to thank for their help with NMR measurements.

To Daniela S. Miles and Harry Surman I owe my thanks for their help with SPR.

Special appreciation goes to David Benito, Omar Boutureira, Miguel A. Rodriguez, Patricia Marcé, Núria Almacellas, Andrea Köver, Irene Martín, Javier Castilla, Gerard Lligadas, Lucas Montero, Robert Andreu, Lidia González, Mercé Arasa, Marta Sacristan and Mariza Spontón for pleasant working atmosphere.

Finally, I dedicate this work to my family.

Summary

Several viral envelope glycoprotein oligomers assembled into a viral fusion machine, form a molecular scaffold that brings the viral and target cell membranes into close apposition and allow the subsequent fusion events. The fusion pore formation and its sequential expansion are orchestrated by viral and cellular lipids and proteins. The HIV entry process is understood in some detail at the molecular level. It is coordinated by the HIV envelope glycoprotein complex, a trimer of three gp120 surface glycoproteins, each noncovalently attached to three gp41 transmembrane glycoprotein subunits.

It is known that changes in GSLs expression in target membranes can modulate viral fusion and entry. These studies on structure–function relationship of target membrane GSLs, the gp120-gp41 and the viral receptors suggest that plasma membrane GSLs support HIV-1 entry by stabilizing the intermediate steps in the fusion cascade. These observations, led it to hypothesize that upregulation of GSLs metabolites (such as ceramide) and/or modulation of GSLs, which preferentially partition in the plasma membrane microdomains, could have a significant influence on HIV-1 entry.

Based on these findings, in this work has been developed a strategy to synthesize glycodendritic polymers that bind HIV gp120 and inhibit HIV-1 entry. To reach this goal, first it was carried out the total synthesis of *D-erythro*-sphingosine with high enantioselectivity and diastereoselectivity. Then, an efficient protocol of glycosylation of ceramides employing stannyl derivatives as strategy was developed. Finally, water-soluble hyperbranched glycodendritic polymers for the study of carbohydrate interactions were synthesized. These glycoconjugate consists of Boltorn H30 hyperbranched polymers, based on the monomer 2,2-bis(hydroxymethyl)propionic acid, functionalized with naturally occurring β -Galceramide. The click chemistry permits functional group tolerance during the derivatization of Boltorn H30. Their ability to bind HIV-1 gp 120 was demonstrated using surface plasmon resonance (SPR).

Acronyms

AA	Asymmetric aminohydroxylation
Ac	Acetyl
Ac ₂ O	Acetic anhydride
AcOH	Acetic acid
AFM	Atomic force microscopy
AgOTf	Silver triflate
AIBN	2,2'-azobisisobutyronitrile
Arg	Arginine
AW	Acid washed
BCD	β -cyclodextrin
BINAP	2,2'-bis-(diphenylphosphino)-1-1'-binaphthyl
Bn	Benzyl
Boc	<i>tert</i> -Butyloxycarbonyl
<i>t</i> -Bu	<i>tert</i> -Butyl
<i>t</i> -BuLi	<i>tert</i> -Butyllithium
Bz	Benzoyl
Cbz	Benzyloxycarbonyl
CDI	Carbonyldimidazol
Cer	Ceramide
CM	Cross-metathesis reaction
<i>m</i> -CPBA	<i>meta</i> -Chloroperoxybenzoic acid
CSO	Camphorsulfonyl
D	doublet
DBN	1,5-Diazabicyclo[4.3.0]non-5-ene
DBU	1,8-Diazabicyclo[5.4.0]undec-7-ene
DCC	<i>N,N'</i> -Dicyclohexylcarbodiimide
DDQ	2,3-Dichloro-5,6-dicyano-1,4-benzoquinone

de	Diastereomeric excess
DEAD	Diethyl azodicarboxylate
DIBAL-H	Diisobutylaluminium hydride
DIPEA	<i>N,N</i> -Diisopropylethylamine
DIPT	Diisopropyl tartrate
DMAP	4- <i>N,N</i> -Dimethylaminopyridine
DME	1,2,-Dimethoxyethane
DMF	Dimethylformamide
DMS	Dimethylsulfide
DMSO	Dimethylsulfoxide
DMP	2,2-Dimethoxypropane
DMTST	Dimethyl(methylthio)sulfonium triflate
DNA	Deoxyribonucleic acid
DS	Dextran sulphate
DTBMP	2,6-di- <i>tert</i> -butyl-4-methylpyridine
DTBS	4,6-O-di- <i>tert</i> -butylsilylene
EDC	1-Ethyl-3-(3-dimethylaminopropyl) carbodiimide
ee	Enantiomeric excess
EGC	Endoglycoceramidase
equiv	Equivalent
ER	Endoplasmic reticulum
Et ₂ O	Diethyl ether
EtP ₂	Phosphazene base
EtOAc	Ethyl Acetate
FCC	Flash column chromatography
FmocCl	Fluorenylmethyloxycarbonyl chloride
g	Grams
GPI	Glycosylphosphatidylinositol
GSLs	Glycosphingolipids
h	Hour
HIV-1	Human immunodeficiency virus

HMPT	Hexamethylphosphoric triamide
HOBt	Hydroxybenzotriazole
HR-TEM	High-resolution transmission electron microscopy
HSPGs	Heparan sulphate proteoglycans
Hz	Hertz
IBX	<i>o</i> -Iodoxybenzoic acid
Ile	Isoleucine
<i>i</i> -PrOH	<i>iso</i> -Propanol
K_A	Equilibrium association constants
k_a	Association rate constant
K_D	Equilibrium dissociation constants
k_d	Dissociation rate constant
KHMDS	Potassium hexamethyldisilazane
LCA	<i>Candida antarctica</i> lipase
LiAlH ₄	Lithium aluminium hydride
LiHMDS	Lithium hexamethyldisilazane
LTMP	Lithium 2,2,6,6-tetramethylpiperidine
Lys	Lysine
MALDI-TOF	Matrix-Assisted Laser Desorption/Ionization
MeOH	Methanol
MeONa	Sodium methoxide
MDMs	Monocyte-derived macrophages
MeLi	Methyl lithium
mg	Milligrams
MHz	Megahertz
mL	Millilitres
MS	Molecular sieve
MsCl	Mesyl chloride
NaHMDS	Sodium hexamethyldisilazane
NaOAc	Sodium acetate
NaO <i>t</i> Bu	Sodium tert-butoxide

NBD	Norbornadiene
NIS	<i>N</i> -Iodosuccinimide
NMM	<i>N</i> -Methyl morpholine
NMP	<i>N</i> -Methyl-2-pyrrolidone
NMR	Nuclear magnetic resonance
Nu	Nucleophile
<i>O</i> -PFB-COCl	<i>O</i> -Pentafluorobenzoyl chloride
PCC	Pyridinium chlorochromate
PDC	Pyridinium dichromate
Ph	Phenyl
PhLi	Phenyl lithium
Piv	Pivaloyl
PMB	<i>p</i> -Methoxybenzyl
PMBCl	<i>p</i> -Methoxybenzyl chloride
PPTS	Pyridinium <i>p</i> -toluenesulfonate
PS	Phosphatidylserine
Py	Pyridine
q	quadruplet
RCM	Ring-Closing Metathesis
Red-Al	Sodium bis(2-methoxyethoxy)aluminium hydride
rt	Room temperature
SBD	Sphingolipid-binding domain
S _N 1	Unimolecular nucleophilic substitution
S _N 2	Bimolecular nucleophilic substitution
SPR	Surface Plasmon Resonance
t	triplet
TA	Tethered aminohydroxylation
TBAF	Tetrabutylammonium fluoride
TBAI	Tetrabutylammonium iodide
TBDMS	<i>tert</i> -Butyldimethylsilyl
TBDMSCl	<i>tert</i> -Butyldimethylsilyl chloride

TBDMSOTf	<i>tert</i> -Butyldimethylsilyl triflate
TBDPSCI	<i>tert</i> -Butyldiphenylsilyl chloride
TCA	Trichloroacetimidate
TEA	Triethylamine
TEMPO	2,2,6,6-Tetramethylpiperidine 1-oxyl
TESOTf	Triethylsilyl triflate
Tf	Triflate (Trifluoromethanesulfonate)
TFA	Trifluoroacetic acid
TFAA	Trifluoroacetic anhydride
TfN ₃	Triflate azide
Tf ₂ O	Triflic anhydride
Tf ₂ OH	Triflic acid
THF	Tetrahydrofuran
TIPSOCI	Triisopropylsilyl chloride
TIPSOTf	Triisopropylsilyl triflate
TLC	Thin layer chromatography
TM	Transmembrane
TMEDA	<i>N,N,N',N'</i> -Tetramethylethylenediamine
TMNO	Trimethylamine-N-oxide
TMS	Tetramethylsilane
TMSCN	Trimethylsilyl cyanide
TMSI	Trimethylsilyl iodide
TMSN ₃	Trimethylsilyl azide
TMSOTf	Trimethylsilyl triflate
TMP	Tetramethylpiperidine
Tol	Toluene
Troc	Trichloroethoxycarbonyl
Ts	Tosyl
TsCl	<i>p</i> -Toluenesulfonyl chloride
TsOH	<i>p</i> -Toluenesulfonyl acid

List of Publications

1. **Recent advances in the glycosylation of sphingosines and ceramides.** Morales-Serna, J. A.; Boutureira, O.; Díaz, Y.; Matheu, M. I.; Castellón, S. *Carbohydr. Res.* **2007**, *342*, 1595–1612.
2. **Highly efficient and stereoselective synthesis of β -glycolipids.** Morales-Serna, J. A.; Boutureira, O.; Díaz, Y.; Matheu, M. I.; Castellón, S. *Org. Biomol. Chem.* **2008**, *6*, 443–446.
3. **Direct and efficient glycosylation protocol for synthesizing α -glycolipids: Application to the synthesis of KRN7000.** Boutureira, O.; Morales-Serna, J. A.; Díaz, Y.; Matheu, M. I.; Castellón, S. *Eur. J. Org. Chem.* **2008**, 1851–1854.
4. **Stannyl ceramides as efficient acceptors for synthesising β -galactosyl ceramides.** Morales-Serna, J. A.; Díaz, Y.; Matheu, M. I.; Castellón, S. *Org. Biomol. Chem.* **2008**, *6*, 3831–3836.
5. **Asymmetric sulfur ylide based enantioselective synthesis of D-erythro-sphingosine.** Morales-Serna, J. A.; Llaveria, J.; Díaz, Y.; Matheu, M. I.; Castellón, S. *Org. Biomol. Chem.* **2008**, *6*, 4502–4504.
6. **Synthesis of D/L-erythro-sphingosine using a tethered aminohydroxylation reaction as the key step.** Morales-Serna, J. A.; Díaz, Y.; Matheu, M. I.; Castellón, S. *Synthesis* **2009**, 710–712.
7. **Efficient synthesis of β -glycosphingolipids by reaction of stannylceramides with glycosyl iodides promoted by TBAI/AW 300 molecular sieves.** Morales-Serna, J. A.; Díaz, Y.; Matheu, M. I.; Castellón, S. *Eur. J. Org. Chem.* **2009**, *Submitted*.
8. **Recent advances in the synthesis of sphingosine and phytosphingosine, molecules of biological significance.** Morales-Serna, J. A.; Llaveria, J.; Matheu, M. I.; Díaz, Y.; Castellón, S. *Curr. Org. Chem.* **2009**, *Submitted*.
9. **Synthesis of novel glycodendritic polymers of β -galceramide that bind HIV-1 rgp 120.** Morales-Serna, J. A.; Boutureira, O.; Serra, A.; Matheu, M. I.; Díaz, Y.; Castellón, S. *In preparation*.

Table of Contents

1. Introduction	1
1.1. Chemistry and Biology of glycosphingolipids	3
1.2. Cluster Effect	12
1.3. Human Immunodeficiency Virus	14
2. Objectives	23
3. Results	27
3.1. Synthesis of <i>D-erythro</i> -sphingosine	29
3.1.1. Chemistry and biology of sphingosine	30
3.1.2. Recent contributions in the synthesis of sphingosine reported in the literature (1998-2008)	32
3.1.2.1. Carbohydrate approach	32
3.1.2.2. From Serine and Garner's aldehyde	37
3.1.2.3. From tartaric acid	41
3.1.2.4. Synthesis from phytosphingosine	43
3.1.2.5. Using chiral reagents and auxiliaries	46
3.1.2.6. Enantioselective catalytic procedures	50
3.1.3. Results	53
3.1.3.1. Synthesis of <i>D/L-erythro</i> -sphingosine using a tethered aminohydroxylation (TA) as key step	53
3.1.3.2. Synthesis of <i>D-erythro</i> -sphingosine employing an asymmetric sulfur ylide reaction as key step	56
3.1.4. Experimental Part	61
3.2. Glycosilation of ceramides	69
3.2.1. Strategy of glycosylation	71

3.2.2. Recent contributions in the synthesis of α -glycosyl sphingosines and ceramides reported in the literature (2000-2007)	72
3.2.2.1. Glycosylation of azido-sphingosines	72
3.2.2.2. Glycosylation of ceramides	77
3.2.3 Recent contributions in the synthesis of β -glycosyl sphingosines and ceramides reported in the literature (2000-2007)	83
3.2.3.1. Glycosylation of azidosphingosine	83
3.2.3.2. Glycosylation of ceramides	87
3.2.3.3. Enzymatic procedures	90
3.2.4 Results	91
3.2.4.1. Stannyl ceramides as efficient acceptors for synthesising β -galactosyl ceramides	91
3.2.4.1. Synthesis of iGb3	103
3.2.4.2. Synthesis of KRN7000	104
3.2.5. Experimental Part	108
3.3. Synthesis of novel glycodendritic polymers of β -Galcer that bind HIV-1 rgp 120	121
3.3.1. The HIV process	123
3.3.2. Hyperbranched polymers	124
3.3.3. Results	128
3.3.3.1. Synthesis of modified β -glycosphingolipid	128
3.3.3.2. A click approach to unprotected glycodendritic structure	130
3.3.3.3. Functionalization of Boltorn H30 hyperbranched dendritic polymer	131
3.3.3.4. Sulfation of glycodendritic polymer of β -GalCer	137
3.3.3.5. Biological Evaluation	141
3.3.4. Experimental Part	148

4. Conclusions	155
Annex	161

1. INTRODUCCION

1.1. Chemistry and Biology of Glycosphingolipids

In the fluid mosaic model of biological membranes, lipids form a homogeneous two-dimensional solvent phase for membrane proteins. Yet membrane lipids comprise several hundreds of distinct molecules that exist in different physical states controlled by several physicochemical parameters such as the temperature, presence of cholesterol and chemical nature of the hydrocarbon chains. Biological membranes (Figure 1) are thus better described as a ‘mosaic of lipid domains’ rather than a homogeneous fluid mosaic. Membrane cholesterol, for instance, is unevenly distributed into cholesterol-rich and cholesterol-poor domains, consistent with the notion that specialized lipid domains with specific biochemical composition and physicochemical properties do exist in membranes.¹

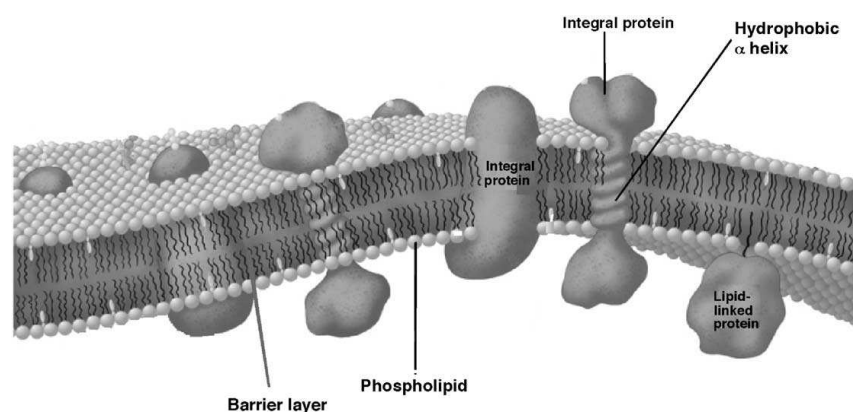


Figure 1. Schematic representation of the bilayer fluid mosaic model of the cell membrane.

Among these domains, those containing sphingolipids and cholesterol, referred to as lipid rafts or caveolae (when associated with the integral membrane protein caveolin), have been extensively studied.² For cell biologists, lipid rafts are chiefly involved in cellular trafficking and signalling functions.³ For pathologists, these membrane areas are preferential sites for host–pathogen/toxin interactions⁴ and for the generation of pathological/infectious forms of proteins associated with Alzheimer’s and

¹ Taïeb, N.; Yahi, N.; Fantini, *Adv. Drug Deliv. Rev.* **2004**, *56*, 779–794.

² Simona, K.; Ikolen, E. *Nature* **1997**, *387*, 569–572.

³ (a) Sprong, H.; van der Sluijs, P.; van Meer, G. *Nat. Rev.* **2001**, *2*, 504–513. (b) Kasahara, K.; Sanai, Y. *Glycoconj. J.* **2000**, *17*, 153–162.

⁴ Duncan, M. J.; Shin, J.-S.; Abraham, S. N. *Cell. Microbiol.* **2002**, *4*, 783–791.

prion diseases.⁵ As a matter of fact, both the physiological and pathological aspects of lipid raft functions have been the subject of excellent recent reviews.⁶

Glycosphingolipids⁷ (GSLs) are characteristic membrane components of eukaryotic cells where they are found in the carbohydrate-rich glycocalyx, which consists of glycoproteins and glycosaminoglycans in addition to GSLs.⁸ Minor sites of location are the subcellular organelles where glycosphingolipid metabolism occurs, or the vesicles, or other transport structures, involved in glycosphingolipid intracellular traffic. Gangliosides are major components of neuronal membranes, where they constitute 10-12% of the total lipid content (20-25% in the outer membrane layer). Details regarding glycosphingolipids, particularly gangliosides, structure and cellular location can be found in classical reviews.⁹ Each GSL carries a hydrophobic ceramide (Cer) moiety and a hydrophilic extracellular oligosaccharide chain which protrudes from the membrane surface (Figure 2).

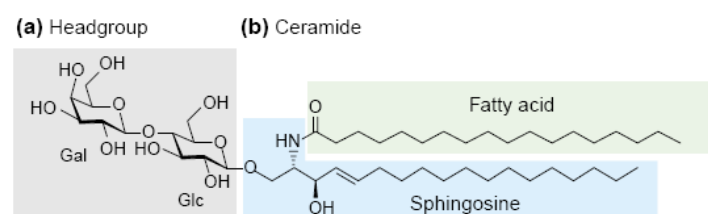


Figure 2. Structure of a glycosphingolipid

Ceramide is constituted by a long amino alcohol chain (sphingoid base) linked to a fatty acid, most commonly with a long chain of carbons atoms (18-20), sometimes hydroxylated. The most frequently occurring long chain bases contain a C4-C5 double bond in the *trans-D-erythro* configuration, and are C₁₈ and C₂₀ sphingosines. Less frequent are sphinganines, that lack the double bond, and phytosphingosine that carries a hydroxyl group on C4. The saccharide moiety is represented by a single saccharide

⁵ Mahfoud, R.; Garmy, N.; Maresca, M.; Yahi, N.; Puigserver, A.; Fantini, J. *J. Biol. Chem.* **2002**, *277*, 11292–11296.

⁶ (a) Smart, E. J.; Graf, G. A.; McNiven, M. A.; Sessa, W. C.; Engelman, J. A.; Scherer, P. E.; Okamoto, T.; Lisanti, M. P. *Mol. Cell. Biol.* **1999**, *19*, 7289–7304. (b) Hakomori, S.-I. *Glycoconj. J.* **2000**, *17*, 143–151. (c) Norkin, L. C. *Adv. Drug Deliv. Rev.* **2001**, *49*, 301–315.

⁷ (a) Vankar, Y. D.; Schmidt, R. R. *Chem. Soc. Rev.* **2000**, *29*, 201–216. (b) Miller-Pedraza, H. *Chem. Rev.* **2000**, *100*, 4663–4682.

⁸ Sweely, C. c. *Biochemistry of Lipids, Lipoproteins and Membranes*, (Eds.: Vance, D. E. and Vance, J. E.) Benjamin/Elsevier, Amsterdam, **1991**.

⁹ (a) Huwiler, A.; Kolter, T.; Pfeilschifter, J.; Sandhhooff, K. *Biochim. Biophys. Acta*, **2000**, *1485*, 63–69. (b) Shayman, J. A. *Kidney Inter.* **2000**, *58*, 11–26.

unit, as in the case of cerebrosides (β -Galcer **1**, Figure 3); sulphated mono- or disaccharides, as in the case of sulphatides (Sulfatide β -Galcer **2**, Figure 3); and as linear or branched oligosaccharide chain (iGB₃ **3** or GM₃ **4**, Figure 3). The saccharide units present in glycosphingolipids are glucose, galactose, *N*-acetylglucosamine, *N*-acetylgalactosamine, fucose, sialic acid and glucuronic acid. The mono- or multi-sialosylated glycosphingolipids are named gangliosides that, together with sulphatides, constitute the group of acidic glycosphingolipids. The remainder glycosphingolipids are neutral glycosphingolipids. Thus, GSLs are generally classified as follows:

- (i) Cerebrosides, which contain one sugar residue (β -Galcer **1**)
- (ii) Sulfatides whose structure contain one sugar residue with a sulphate group (Sulfatide β -Galcer **2**)
- (iii) Neutral Glycosphingolipids (iGB₃ **3**)
- (iv) Gangliosides (GM₃ **4**)

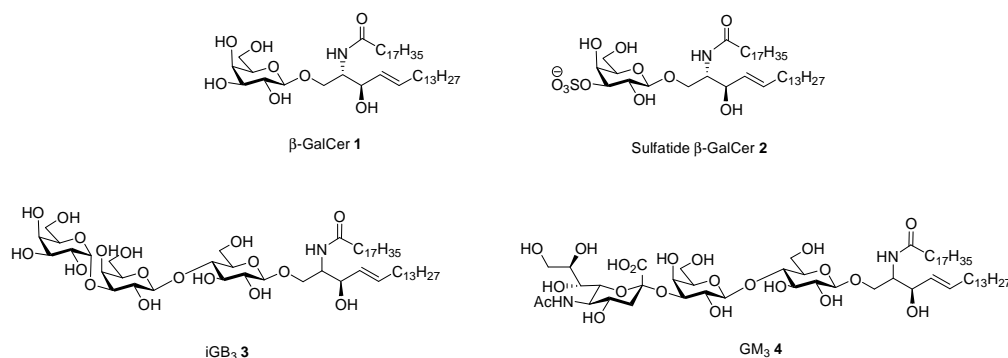
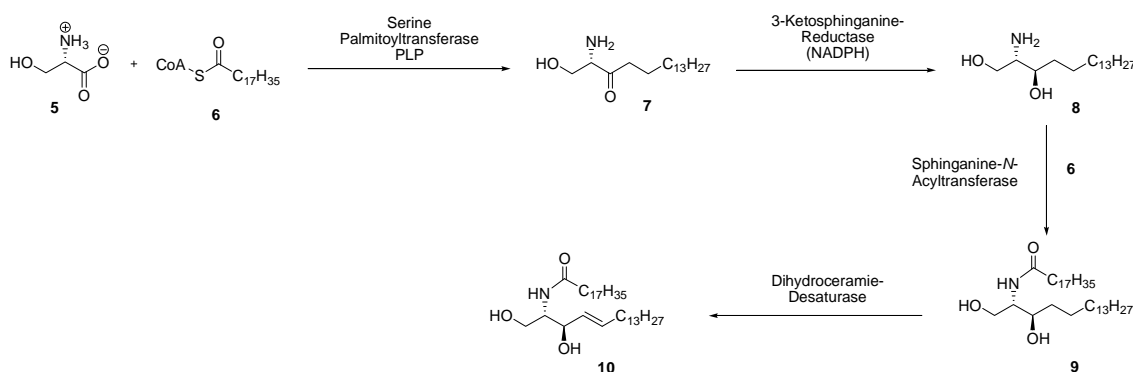


Figure 3. Naturally occurring glycosphingolipids

The formation of ceramide is catalysed by membrane bound enzymes on the cytosolic leaflet of the endoplasmic reticulum (ER).¹⁰ Starting from the amino acid L-serine **5** and two molecules of the palmitoyl-coenzyme A **6**, dihydroceramide **9** is formed in three steps (Scheme 1). This *N*-acyl-2-aminoalkyl-1,3-diol (*N*-acylsphinganine) is dehydrogenated to ceramide **10** with a 4,5-*trans*-double bond by a dihydroceramide desaturase. At the membranes of the Golgi apparatus, hydrophilic head groups are attached to ceramide leading to sphingomyelin, galactosylceramide, glucosylceramide, and higher glycosphingolipids, which are synthesised by the stepwise

¹⁰ Merrill Jr., A. H. *J. Biol. Chem.* **2002**, 277, 25843–25846.

addition of monosaccharides to glucosylceramide. Their biosynthesis is coupled to exocytotic vesicle flow to the plasma membrane (Figure 4).



Scheme 1. Biosynthesis of ceramide 10

The constitutive degradation of sphingolipids occurs in both the endosomes and the lysosomes.¹¹ Parts of the plasma membrane are endocytosed and transported via the endosomal to the lysosomal compartment. Hydrolytic enzymes cleave the carbohydrate residues of glycolipids sequentially. Many glycosphingolipids, and also ceramide, require the additional presence of activator proteins and negatively charged lysosomal lipids for degradation.¹² In humans, inherited defects of glycosphingolipid and sphingolipid catabolism give rise to lysosomal storage diseases, the sphingolipidoses.¹³

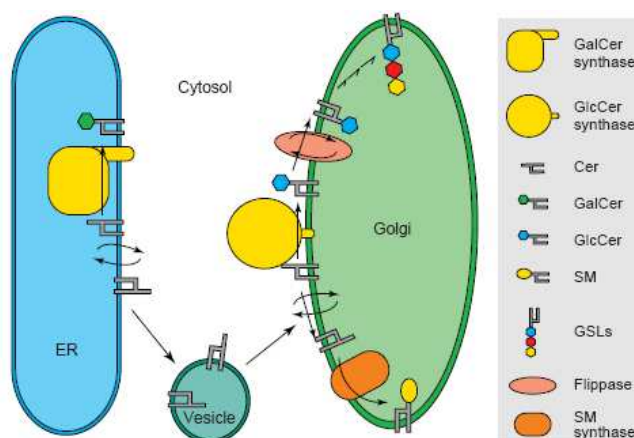


Figure 4. Localization and topology of ceramide-metabolizing enzymes

¹¹ (a) Kolter, T.; Sandhoff, K. *Angew. Chem.* **1999**, *111*, 1633–1670. (b) Kolter, T.; Sandhoff, K. *Angew. Chem. Int. Ed.* **1999**, *38*, 2532–1568. (c) Kolter, T.; Sandhoff, K. *Trends Cell Biol.* **1996**, *6*, 98–103.

¹² Kolter, T.; Sandhoff, K. *Phil. Trans. R. Soc. London B* **2003**, *358*, 847–861.

¹³ Kolter, T.; Sandhoff, K. *Brain Pathology* **1998**, *8*, 79–100.

Several external proteins that are specifically associated with lipid rafts are bound to the membrane by a glycosylphosphatidylinositol (GPI) anchor consisting of two saturated chains (1-alkyl-2-acyl-glycerol) that can tightly pack with raft lipids.¹⁴ Although sphingolipids are usually not found in the cytoplasmic leaflet of the plasma membrane, specific glycerophospholipids such as phosphatidylserine (PS) with saturated or monounsaturated chains may form liquid-ordered domains through interaction with long sphingolipid acyl chains of the outer monolayer.¹⁵ On the other side of the membrane, acylated proteins anchored in the internal leaflet with two or more saturated acyl chains (generally myristyl and palmityl) are constitutively associated with lipid rafts. It is likely that these proteins may significantly contribute to the formation of a Lo phase in the inner leaflet of lipid rafts.¹⁶

The situation is even more complex for transmembrane proteins, which have three main distinct possibilities of interaction with the specific lipid components of the rafts: (i) the extracellular domain, which interacts with the polar head of glycosphingolipids (ii) the cytoplasmic juxtamembrane domain, which faces anionic glycerophospholipids such as PS, and (iii) the transmembrane (TM) domain (Figure 5). Since lipid rafts are enriched in cholesterol, it can be predicted that the TM domain contains amino acid side chains particularly suited for interacting with this sterol. Although the relative affinity of the 20 amino side chains for cholesterol is not known, it can be anticipated from the chemical structure that Phe and Ile residues would ideally fit with the aliphatic cycles and the isooctyl tail of the lipid (Figure 5). In support of this hypothesis, it has been shown that replacement of the TM domain of CD40, a raft-associated protein, by the one of CD45, a non-raft protein, resulted in the exclusion of CD40 from lipid rafts.¹⁷ The TM domains of CD40 and CD45 are both composed of 22 amino acids, but CD40 has 6 Ile and 3 Phe residues, whereas CD45 has only 4 Ile and 2 Phe residues. Basically, a TM domain is an α -helix buried in the hydrophobic region of the membrane. The assembly of cholesterol molecules around a TM domain enriched in Ile and Phe residues may contribute to stabilize the interaction of the α -helix with the Lo phase of lipid rafts. Mutating these residues in the TM domain of CD40 and other raft-associated proteins will help to validate this hypothesis.

¹⁴ Benting, J. *FEBS Lett.* **2003**, *462*, 47–50.

¹⁵ Pike, L. J.; Han, X.; Chung, K.-N.; Gross, R. W. *Biochemistry* **2002**, *41*, 2075–2088.

¹⁶ Edidin, M. *Annu. Rev. Biophys. Biomol. Struct.* **2003**, *32*, 257–283.

¹⁷ Bock, J.; Gulbins, E. *FEBS Lett.* **2003**, *534*, 169–174.

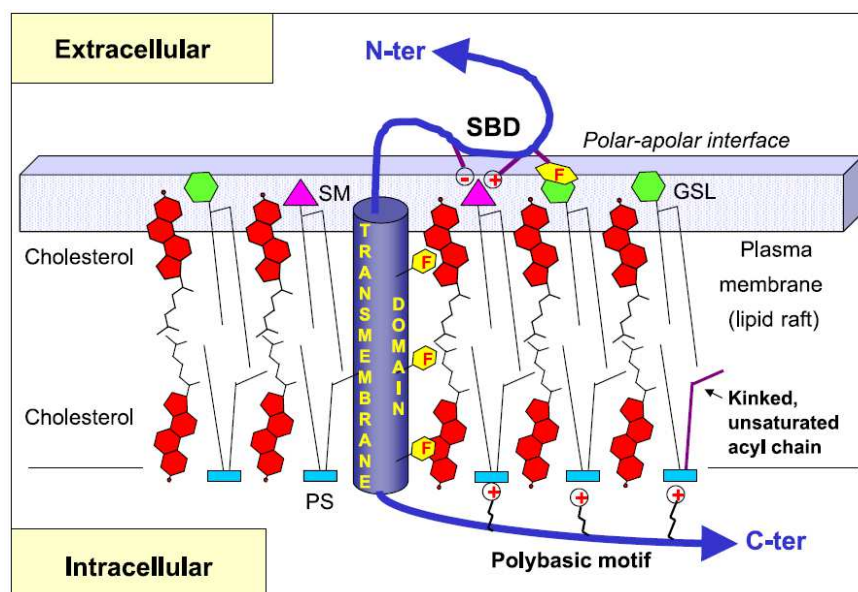


Figure 5. Interaction of membrane proteins with lipid rafts

A polybasic motif enriched in Arg or, to a lesser extent, Lys residues is often found in the juxtamembrane cytoplasmic domain of raft-associated proteins (e.g. human CD4, EGF and PDGF receptors). The positive charge of these basic amino acids may interact with the net negative charge of PS through electrostatic interactions. Finally, the extracellular domain of raft-associated proteins faces sphingomyelin, which carries one positive and one negative charge, and GSLs which may be either neutral or negatively charged in the case of gangliosides. Ideally, a sphingolipid-binding domain (SBD) should be composed of a charged residue (preferentially basic) for interacting with the polar head of sphingomyelin and gangliosides. Moreover, the SBD should also contain a solvent-exposed aromatic side chain conveniently oriented to stack against the sugar rings of GSLs. In any case, the three modes of interaction of transmembrane proteins with lipid rafts (i.e. SBD, TM domain and polybasic motif) may allow the assembly of a lipid shell around the protein.¹⁸ According to this model, lipid shells have a preferential affinity for lipid rafts, so that they are assumed to target the protein they encase to these microdomains.

Since bacterial adhesins and toxins may interact first (if not exclusively) with the extracellular side of lipid rafts, they can be considered as foreign competitors for host membrane proteins associated with lipid rafts. On this basis, it could be anticipated that bacterial adhesins and toxins could present in their three-dimensional structure a SBD

¹⁸ Anderson, R. G. W.; Jacobson, K. *Science* **2002**, 296, 1821–1825.

domain similar to the one found in the raft proteins of the host. The first identification of a microbial SBD came from the study of HIV-1 surface envelope glycoprotein gp120 and its GSL intestinal receptor GalCer.⁵ The region of gp120 responsible for GalCer recognition is a disulfide-linked domain referred to as the V3 loop.¹⁹ Searches for structure similarities revealed the presence of a V3-like SBD in various sphingolipid-binding proteins including cellular proteins such as the prion protein isoform PrPc or the Alzheimer β -amyloid peptide⁵ and bacterial toxins.²⁰

The GSLs are used as cellular binding sites for a wide variety of pathogens, including viruses, bacteria, fungi and parasites.²¹ The oligosaccharide residues of GSLs protrude into the extracellular space, providing a considerable number of carbohydrate-binding sites for microbial adhesions. However, specificity of a carbohydrate sequence is not the unique parameter controlling pathogen binding, and density levels of GSLs on the host cell surface may also be critical. Indeed, a threshold level of GSLs is often required to ensure microbial adhesion, suggesting that those GSLs are active only when concentrated in a lipid raft to form an operational attachment platform. Thus, although individual GSLs–protein interactions may be weak, the resulting avidity of the pathogen for the raft may be very high. To complicate further the story, the same pathogen (e.g. HIV-1) may use either high or low affinity GSLs binding sites to infect various cellular targets. Moreover, the binding of a pathogen on the cell surface may also require, in addition to the GSLs, a second component, generally a protein which can be either GPI-anchored or an integral transmembrane protein. In this case, the lipid and the protein cooperate and the binding reaction proceeds in three steps. First, the pathogen selects a raft with appropriate GSLs binding sites. Once stabilized on this attachment platform, the raft float on the cell surface, allowing the pathogen to ‘browse’ over the cell surface, looking for a high affinity receptor. Third, a ternary ‘GSL-pathogen-receptor’ complex is formed within the raft area. It should also be noted that the role of GSLs in this process has been remarkably anticipated to viruses²² and bacterial neurotoxins,²³ several years before the elaboration of the raft concept. Basically, this mechanism can be viewed as a pathological exploitation of the coalescence model (Figure 6).

¹⁹ Cook, D. G.; Fantini, J.; Spitalnik, S. L.; Gonzales-Scarano, F. *Virology*, **1994**, *201*, 206–214.

²⁰ Fantini, J. *Cell. Mol. Life Sci.* **2003**, *60*, 1027–1032.

²¹ Van der Goot, F. G. *Semin. Immunol.* **2001**, *13*, 89–97.

²² Haywood, A. J. *J. Virol.* **1994**, *68*, 1–5.

²³ Montecucco, C. *Trends Biochem. Sci.* **1986**, *11*, 314–317.

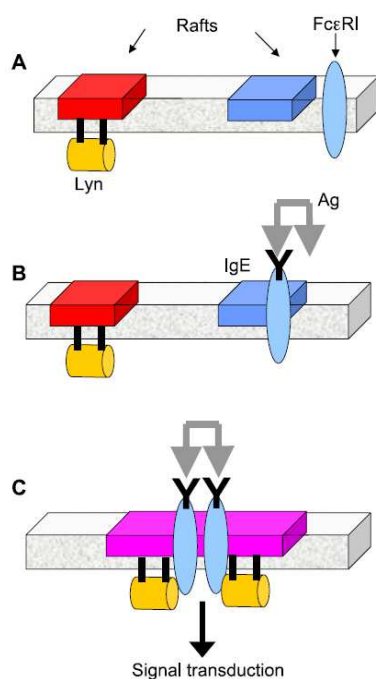


Figure 6. Signal transduction pathway

In the coalescence model, the IgE receptor FcεRI is a multichain immune recognition receptor which is not constitutively associated with raft microdomains. Upon crosslinking with their physiological ligand (i.e. the IgE-antigen complex), FcεRI receptors are rapidly recruited in raft areas.²⁴ The co-compartmentation of FcεRI receptors with the raft-associated tyrosine kinase Lyn provides an adequate spatial proximity allowing the phosphorylation of FcεRI on tyrosine-based activation motifs (ITAMs). This membrane-coordinated signal triggers the intracellular cascade that leads to release of mediators of

the allergic response. Finally, it is important to mention that some signal transduction units may pre-assembled in lipid rafts of quiescent cells, allowing rapid and efficient signal initiation upon activation.²⁵ As shown in Figure 6 (A) in quiescent mast cells, the IgE receptor (FcεRI) is localized outside membrane rafts, so that it cannot interact with Lyn, a kinase of the src family anchored to the inner leaflet of the plasma membrane with acyl chains. (B) Upon binding of the antigen (Ag)-IgE complex to FcεRI, Lyn and FcεRI are recruited in rafts. (C) The coalescence of rafts induced by the multivalent antigen allows the interaction between FcεRI and Lyn, resulting in phosphorylation of FcεRI and activation of the signal transduction pathway.

In the other hand, it has long been recognized that the aglycone, hydrophobic part of GSLs has a major impact on the conformation of their glycone moiety and thus on GSLs receptor function.²⁶ Moreover, it has been demonstrated that cholesterol, which functions as ‘molecular spacer’ in lipid rafts,² may have a critical effect on the conformation and thus on the binding properties of raft GSLs. This is the case for Gb3,

²⁴ Prieschl, E. L.; Baumruker, T. *Immunol. Today*, **2000**, *21*, 555–560.

²⁵ Drevot, P.; Langlet, C.; Guo, X. J.; Bernard, A. M.; Colard, O.; Chauvin, J. P.; Lasserre, R.; He, H. T. *EMBO J.* **2000**, *15*, 1899–1908.

²⁶ Kiarash, A.; Boyd, B.; Lingwood, C. A. *J. Biol. Chem.* **1994**, *269*, 11138–11146.

which requires cholesterol to interact optimally with the SBD of HIV-1 gp120²⁷ and for cholera toxin, which binds to GM1 only when presented as condensed complexes in artificial cholesterol/phospholipid membranes.²⁸ Therefore, although cholesterol has been described as a specific binding site for a number of bacterial pore-forming toxins (the so-called cholesterol-dependent cytolysins),²⁹ it may also act as a fine regulator of most GSLs–pathogen interactions.

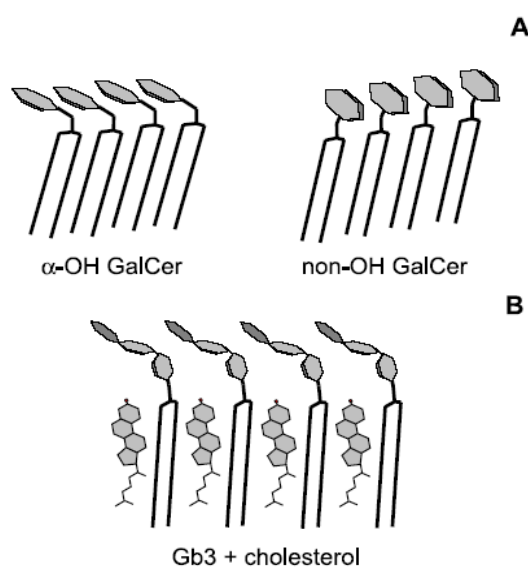


Figure 7. Influence of the hydrophobic moiety of GSLs on the orientation of the glycone polar head

Yet in some instances, cholesterol has an inhibitory rather than a stimulatory effect on GSLs–pathogen interactions. This is the case for GalCer, a major GSLs of the apical brush border of enterocytes.³⁰ Due to the relatively small size of its polar head (only one sugar ring), GalCer can form a tightly packed platform in absence of cholesterol (Figure 7A). In contrast, Gb3 with three sugar rings may

require cholesterol to form a condensed complex on the cell surface,²⁷ as proposed in Figure 7B. This is consistent with the body of data suggesting that different types of lipid rafts, with and without cholesterol, exist in the apical brush border.³¹ In particular, a high concentration of cholesterol may suppress the formation of membrane domains by impairing the tight packing of GalCer, a major GSLs of brush border membranes.

²⁷ Mahfoud, R.; Mylvaganam, M.; Lingwood, C. A.; Fantini, J. *J. Lipid Res.* **2002**, *43*, 1670–1679.

²⁸ Radhakrishnan, A.; Anderson, T. G.; McConnell, H. M. *Proc. Natl. Acad. Sci. U.S.A.* **2000**, *97*, 12422–12427.

²⁹ Alouf, J. E.; *Int. J. Med. Microbiol.* **2000**, *290*, 351–356.

³⁰ Hammache, d.; Piéroni, G.; Maresca, M.; Ivaldi, S.; Yahi, N.; Fantini, J. *Methods Enzymol.* **2000**, *312*, 495–506.

³¹ (a) Corbeil, D.; Röper, K.; Fargeas, C. A.; Joester, A.; Huntner, W. B. *Traffic*, **2001**, *2*, 82–91. (b) Milhiet, P. E.; Giocondi, M.-C.; Le Grimellec, C. *J. Biol. Chem.* **2002**, *277*, 875–878. (c) Braccia, A.; Villani, M.; Immerdal, L.; Niels-Christiansen L.-L.; Nystrom, B. T.; Hansen, G. H.; Danielsen, E. M. *J. Biol. Chem.* **2003**, *278*, 15679–15684.

This may explain the opposite effects of cholesterol on GalCer and Gb3 receptor functions.²⁷

The potential absence of cholesterol in GalCer enriched intestinal rafts does not mean that the aglycone part of this GSLs does not influence the orientation of the galactose ring. The presence of an α -OH group in the acyl chain of the ceramide backbone of GalCer allows the formation of a H-bond which orientates the galactose ring of GalCer so that the molecule adopts a typical L-shape structure³² (Figure 7A). In contrast, the galactose ring of GalCer containing a non hydroxylated acyl chain protrudes at 180° with respect to the plane of the membrane (Figure 7A). As a result, vicinal sugar units share a stacking interaction and are thus not available for pathogens. For these reasons, many microbial adhesins and toxins specifically recognize alpha-hydroxylated vs. nonhydroxylated galactose-containing GSLs.³³ In this respect, it is interesting to note that the α -OH group of the fatty acid chain and cholesterol have a comparable conformational effect on GSLs, allowing in both cases an orientation of the sugar head compatible with the establishment of CH- π stacking interactions with aromatic amino acid side chains of the SBD.

1.2. Cluster effect

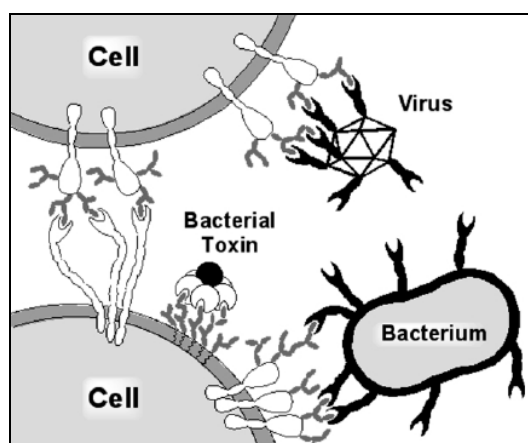


Figure 8. A graphical representation of cell surface protein-carbohydrate interactions

Although protein-carbohydrate interactions (Figure 8) are essential to many biological processes, individual interactions usually exhibit weak binding³⁴ affinities (K_d values in the mM to μ M range) as well as apparently relatively low selectivities between similar carbohydrate ligands. These characteristics and properties are at odds with the observed biological activities which demand interactions

³² Nyholm, P. G.; Pasher, I.; Sundell, S. *Chem. Phys. Lipids* **1990**, *52*, 1–10.

³³ (a) Tang, W.; Seino, K.; Ito, M.; Konishi, T.; Senda, H.; Makuuchi, M.; Kojima, N.; Mizuochi, T. *FEBS Lett.* **2001**, *504*, 31–35. (b) Fantini, J.; Maresca, M.; Hammache, D.; Yahi, N.; Delézay, O. *Glycoconj. J.* **2000**, *17*, 173–179. (c) Fantini, J.; Cook, D. G.; Nathanson, N.; Spitalnik, S. L.; Gonzalez-Scarano, F. *Proc. Natl. Acad. Sci. U.S.A.* **1993**, *90*, 2700–2704. (d) Karlsson, K. K. *Ann. Rev. Biochem.* **1989**, *58*, 309–350.

³⁴ Lee, R. T.; Lee, Y. C. *Acc. Chem. Res.* **1995**, 321–327.

that are both extremely selective and of high affinity. Nature's answer to this problem is to use multivalency.³⁵ Thus, multiple copies of the carbohydrate ligands are arranged on glycoprotein scaffolds or in patches of glycolipids on the surface of one cell, and multiple copies of lectins (or lectins each with multiple binding sites) are displayed at the surface of another cell. When these two surfaces come together, the individual interactions reinforce one another to give overall a high avidity, not unlike molecular scale Velcro.

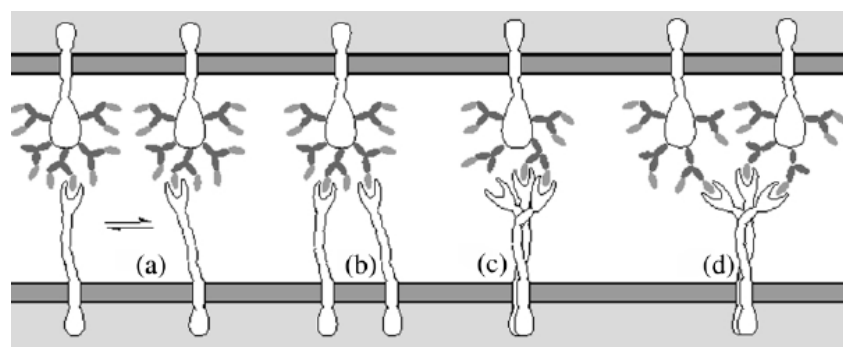


Figure 9. The glycoside cluster effect

The glycoside cluster effect was defined initially³⁶ as the ‘binding affinity enhancement exhibited by a multivalent carbohydrate ligand over and beyond that expected from the concentration increase resulting from its multivalency’. This enhancement in binding affinity can be the consequence of two different mechanisms³⁷ at the molecular level: 1) a statistical effect in which the multivalent compound gives rise (Figure 9a) to a highly localized concentration of the ligand at the receptor binding site; and 2) a chelate effect in which the multivalent ligand cross-links binding sites either in adjacent receptors (Figure 9b) or in a single multivalent receptor (Figure 2c and 2d). It has been observed that,³⁷ in those cases where cross-linking lectin binding sites with a multivalent ligand (chelation) are not possible, a small increase (five-fold to 10-fold) in binding affinity still occurs as a consequence of the statistical effect. By contrast, however, exponential increases in binding affinities are possible in situations that favor the chelation mechanism. Furthermore, just as the multivalent display of

³⁵ Mammen, M.; Choi, S.-K.; Whitesides, G. M. *Angew. Chem. Int. Ed.* **1998**, *37*, 2754–2794.

³⁶ Lee, R. T.; Lee, Y. C. *Neoglycoconjugates: Preparation and Applications*, **1994**, Academic Press, San Diego, 23–50.

³⁷ Pohl, N. L.; Kiessling, L. L. *Synthesis* **1999**, 1515–1519.

ligands can occur on different scales (multivalent glycans attached to multivalent proteins clustered in a multivalent fashion at a cell surface) the glycoside cluster effect can operate at different levels of complexity. This phenomenon has been described³⁶⁻³⁸ in terms of the so-called minicluster (Figure 9b) and maxicluster (Figure 9c) effects, which can express themselves separately or in unison.

Although the observation that multivalency is important in protein-carbohydrate interactions formed the original rationalization for developing a whole range of synthetically engineered glycoconjugate systems the pioneering work in the field by Lee³⁹ has also contributed to understanding of multivalency. An important aspect of multivalency that has been observed, in addition to high affinity, is the enhancement of the selectivity of a particular interaction. Small differences in the intrinsic binding affinity (monovalent binding affinity) can be ‘amplified’ greatly on displaying the ligands in a multivalent fashion.⁴⁰

1.3. Human Immunodeficiency Virus

The human immunodeficiency virus (HIV) has proven to be a difficult pathogen to overcome; there are currently no effective vaccines that provide specific and long-lasting immunity to the virus. Moreover, there are only a few currently FDA-approved drugs that target HIV proteins such as reverse transcriptase, protease, and the surface envelope protein. Although these drug combination therapies provide effective suppression of HIV virions in individuals, the cost, toxicity, and drug resistance remain common concerns. Until recently, with the FDA approval of Fuzeon® (enfuvirtide), there were no drugs on the market that specifically target and prevent the entry of HIV into human cells. Inhibitors of reverse transcriptase and protease are designed to work only after viral contents have entered into cells, whereas enfuvirtide works by binding to the HIV transmembrane envelope subunit gp41 and preventing the fusion of the viral membrane with the host membrane.⁴¹ Other fusion inhibitors involving the blocking of

³⁸ Yi, D.; Lee, R. T.; Longo, P.; Berger, E. T.; Lee, Y. C.; Petri, W. A.; Jr. Schnaar, R. L. *Glycobiology*, **1998**, *8*, 1037–1043.

³⁹ Lee, Y. C. *Carbohydr. Res.* **1978**, *67*, 509–514.

⁴⁰ (a) Pieters, R. J. *Med. Res. Rev.* **2007**, *27*, 796–816. (b) Schengrund, C.-L. *Biochem. Phar.* **2003**, *65*, 699–707. (c) Bezouška, K. *Rev. Mol. Biotech.* **2002**, *90*, 269–290. (d) Turnbull, W. B.; Stoddart, J. F. *Rev. Mol. Biotech.* **2002**, *90*, 231–255. (e) Ortiz-Mellet, C.; Defaye, J.; García-Fernández, J. M. *Chem. Eur. J.* **2002**, *8*, 1982–1990. (f) Lee, R. T.; Lee, V. C. *Glycoconj. J.* **2000**, *17*, 543–551.

⁴¹ Kilby, J. M.; Hopkins, S.; Venetta, T. M.; DiMassimo, B.; Cloud, G. A.; Lee, J. Y.; Alldredge, L.; Hunter, E.; Lambert, D.; Bolognesi, D.; Matthews, T.; Johnson, M. R.; Nowak, M. A.; Shaw, G. M.; Saag, M. S. *Nat. Med.* **1998**, *4*, 1302–1307.

host chemokine receptors are currently being investigated in preclinical models and clinical trials.⁴² Despite the development of such potential therapeutics, the spread of HIV worldwide continues unabated with no promising cure in sight. Further pursuit of its understanding of HIV will lead to new possibilities for preventing HIV infection that can be effective and affordable.

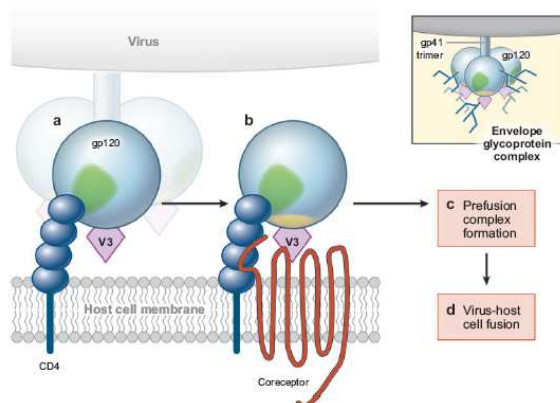


Figure 10. Binding of HIV to cell

molecule-3 (ICAM-3)-grabbing nonintegrin (DC-SIGN), macrophage mannose receptor, lymphocyte function-associated antigen-1 (LFA-1), intercellular adhesion molecule-1 (ICAM-1), and glycosaminoglycans.⁴⁴ Subsequent to the initial binding to CD4, a conformational change in gp120 allows it to bind to chemokine receptors, generally, either CCR5 or CXCR4, although a number of other chemokine receptors may serve as HIV coreceptors (Figure 10). This binding then triggers a conformational change that exposes a previously buried portion of the transmembrane glycoprotein, gp41, resulting in its insertion into the host cell membrane. The host and viral membranes then fuse, permitting the contents of the virus to enter the cell cytoplasm.

Lipid rafts, which are cholesterol- and sphingolipid-enriched membrane domains, appear to be involved in HIV fusion and infection.⁴⁵ The formation of lipid

⁴² Shaheen, F.; Collman, R. G. *Curr. Opin. Infect. Dis.* **2004**, *17*, 7–16.

⁴³ Eckert, D. M.; Kim, P. S. *Annu. Rev. Biochem.* **2001**, *70*, 777–810.

⁴⁴ (a) Bobardt, M. D.; Saphire, A. C.; Hung, H. C.; Yu, X.; Van der Schueren, B.; Zhang, Z.; David, G.; Galloway, P. A. *Immunity* **2003**, *18*, 27–39. (b) Nguyen, D. G.; Hildreth, J. E. *Eur. J. Immunol.* **2003**, *33*, 483–493. (c) Triantafyllou, K.; Takada, Y.; Triantafyllou, M. *Crit. Rev. Immunol.* **2001**, *21*, 311–322. (d) Su, S. V.; Gurney, K. B.; Lee, B. *Curr. HIV Res.* **2003**, *1*, 87–99.

⁴⁵ (a) Viard, M.; Parolini, I.; Sargiacomo, M.; Fecchi, K.; Ramoni, C.; Ablan, S.; Ruscetti, F. W.; Wang, J. M.; Blumenthal, R. *J. Virol.* **2002**, *76*, 11584–11595. (b) Hug, P.; Lin, H. M.; Krote, T.; Xiao, X.; Dimitrov, D. S.; Wang, J. M.; Puri, A.; Blumenthal, R. *J. Virol.* **2000**, *74*, 6377–6385. (c) Graham, D. R.; Chertova, E.; Hilburn, J. M.; Arthur, L. O.; Hildreth, J. E. *J. Virol.* **2003**, *77*, 8237–8248. (d) Liao,

rafts arises from the tight packing of cholesterol with saturated sphingolipid chains that allows for increased order in the membrane and resistance to non-ionic detergents at 4°C.⁴⁶ Studies using β -cyclodextrin (BCD) to remove cholesterol from target cell membranes have demonstrated significant inhibition of HIV infection. Similarly, chemical inhibition of glycosphingolipid production also resulted in the inhibition of HIV infection.⁴⁷ Thus, perturbation of lipid raft-specific lipids in the target cell membrane can influence the cell's ability to be infected. A supposed minor alteration in the cholesterol molecule by oxidation of carbon-3 (to form 4-cholesten-3-one) also results in significant inhibition of HIV infection.⁴⁸ Although it was initially thought that cholesterol is simply required for membrane mixing, studies have demonstrated that the HIV inhibitory effects of treating cells with BCD can be overcome by over-expressing chemokine receptors.

The CD4 molecule is predominantly localized in lipid rafts under normal physiological conditions; however, the requirement for the interaction of CD4 and lipid rafts in HIV infection is currently being debated: some researchers have demonstrated the interaction to be essential for infection,⁴⁹ whereas others have found it to be non-essential.⁵⁰ An additional point of interest regarding cholesterol is that statin drugs, originally identified as cholesterol-lowering agents, inhibit HIV infection both by blocking the interaction of ICAM-1 with LFA-1 and by inhibiting Rho GTPase activity.⁵¹ Because lipid-altering drugs can influence a number of cell signaling pathways and cell responsiveness, the question: "Is the effect a pure membrane inhibitory effect or is it inhibiting cell signaling pathways that may be required for productive infection?" remains to be determined.

Cholesterol in the HIV membrane is also essential for infectivity. As viruses bud from infected cells they do so at cholesterol-rich lipid rafts, resulting in the enrichment

Z.; Cimasky, L. M.; Hampton, R.; Nguyen, D. H.; Hildreth, J. E. *AIDS Res. Hum. Retroviruses* **2001**, *17*, 1009–1019.

⁴⁶ Brown, D. A.; London, E. *Annu. Rev. Cell. Dev. Biol.* **1998**, *14*, 111–136

⁴⁷ (a) Manes, S.; del Real, G.; Lacalle, R. A. *EMBO Rep.* **2000**, *1*, 190–196. (b) Nguyen, D. H.; Taub, D. *J. Immunol.* **2002**, *168*, 4121–4126. (c) Popik, W.; Alce, T. M.; Au, W. C. *J. Virol.* **2002**, *76*, 4709–4722.

⁴⁸ Nguyen, D. H.; Taub, D. D. *Exp. Cell. Res.* **2003**, *291*, 36–45.

⁴⁹ del Real, G.; Jimenez-Baranda, S.; Lacalle, R. A.; Mira, E.; Lucas, P.; Gomez-Mouton, C.; Carrera, A. C.; Martinez, A. C.; Manes, S. *J. Exp. Med.* **2002**, *196*, 293–301.

⁵⁰ (a) Kozak, S. L.; Heard, J. M.; Kabat, D. *J. Virol.* **2002**, *76*, 1802–1815. (b) Percherancier, Y.; Lagane, B.; Planchenault, T.; Staropoli, I.; Altemeyer, R.; Virelizier, J. L.; Arenzana-Seisdedos, F.; Hossli, D.; Bachelier, F. *J. Biol. Chem.* **2003**, *278*, 3153–3161.

⁵¹ (a) Giguere, J. F.; Tremblay, M. J. *J. Virol.* **2004**, *78*, 12062–12065. (b) del Real, G.; Jimenez-Barada, S.; Mira, E.; Lacalle, R. A.; Lucas, P.; Gómez-Moutón, C.; Alegret, M.; Peña, J. M.; Rodríguez-Zapata, M.; Alvarez-Mon, M.; Martínez-A. C.; Mañes, S. *J. Exp. Med.* **2004**, *200*, 541–547.

of cholesterol in viral membranes as compared to the levels of cholesterol found on host cells.⁵² Hildreth and colleagues have proposed the use of BCD in topical formulations, which would remove cholesterol from free virions, in order to prevent HIV infection.⁵³ Preclinical studies using such topical compounds are currently underway. Moreover, the HIV Gag protein, which is the major viral structural protein, is modified by the addition of a saturated myristoyl tail promoting its incorporation into lipid rafts. This finding has led others to demonstrate that the addition of unsaturated fatty acids to HIV producing cells can inhibit the production of virions, most likely by covalent modification of Gag, resulting in non-raft protein localization.⁵⁴

Although the common approach to manipulating lipid rafts is to target cholesterol into the cell membrane, another approach is to alter raft-associated sphingolipids. In a recent publication, Blumenthal and colleagues have demonstrated that increasing cellular ceramide can inhibit HIV infection.⁵⁵ The addition of a phosphocholine group produces sphingomyelin, a known raft-associated lipid. In their study, the retinoic acid derivative 4-HPR (fenretinide) was utilized to increase cellular ceramide levels in HeLa cells, peripheral blood activated T cells, and monocyte-derived macrophages (MDMs). Such treatment resulted in a significant decrease in the HIV infectivity of the three cell models and with all of the viral strains tested. Some viral strains demonstrated nearly complete inhibition of infection at concentrations of <5 mM 4-HPR, but there was significant variability in the IC50 values and maximal inhibition among the different strains. This HIV inhibition was a ceramide-specific effect, as evidenced through the use of sphingomyelinase, which cleaves sphingomyelin to create ceramide, and by the addition of exogenous ceramide. Unlike BCD, which removes cholesterol from cell membranes, 4-HPR did not affect chemokine receptor function. The increase in cellular ceramide levels inhibited cell-cell fusion, leading to the hypothesis that increasing ceramide affects membrane lipid-raft organization and structure. Based on these data, the authors propose that 4-HPR could potentially be used as an anti-HIV drug in combination with current therapies, based on its low toxicity. The potential for targeting ceramide raises some interesting aspects regarding HIV therapy. Further studies will need to be done in order to fully characterize how

⁵² (a) Nguyen, D. H.; Hildreth, J. E. *J. Virol.* **2000**, *74*, 3264–3272. (b) Ono, A.; Freed, E. O. *Proc. Natl. Acad. Sci. U.S.A.* **2001**, *98*, 13925–13930.

⁵³ Khanna, K. V.; Whaley, K. J.; Zeitlin, L. *J. Clin. Invest.* **2002**, *109*, 205–211.

⁵⁴ Lindwasser, O. W.; Resh, M. D. *Proc. Natl. Acad. Sci. U.S.A.* **2002**, *99*, 13037–13042.

⁵⁵ Finnegan, C. M.; Rawat, S. S.; Puri, A.; Wang, J. M.; Ruscetti, F. W.; Blumenthal, R. *Proc. Natl. Acad. Sci. U.S.A.* **2004**, *1001*, 15452–15457.

increased ceramide levels may influence the cell membrane. How does 4-HPR and ceramide impact the formation, integrity, and structure of lipid rafts, including signalling protein association and CD4 association?

It should be noted that Blumenthal and coworkers also reported that this ceramide-mediated inhibition of HIV infectivity was not observed using VSV-gene-containing pseudotyped or surrogate virions. Given that VSV-pseudotyped viruses do not depend on lipid rafts for entry into cells, these data strongly support a lipid raft-specific but not a whole-membrane effect. Another recent study has demonstrated that ceramide also efficiently displaces cholesterol from lipid rafts,⁵⁶ thus potentially explaining the raft-specific effect without interfering with CXCR4 cholesterol interactions. Can ceramide somehow prevent the ability to cluster CD4 and chemokine receptors into microdomains that may be required for infection? As there is no known physiologic reason that CD4 would need to interact with chemokine receptors, inhibiting such clustering could potentially be quite specific for HIV infection (Figure 11). On T cells, the HIV receptor CD4 is constitutively associated with lipid rafts at the cell surface, whereas chemokine receptors such as CXCR4 are normally excluded. Upon HIV binding and cell signaling, CXCR4 is recruited to rafts where they can interact with gp120, resulting in viral fusion to the cell membrane (bottom left).

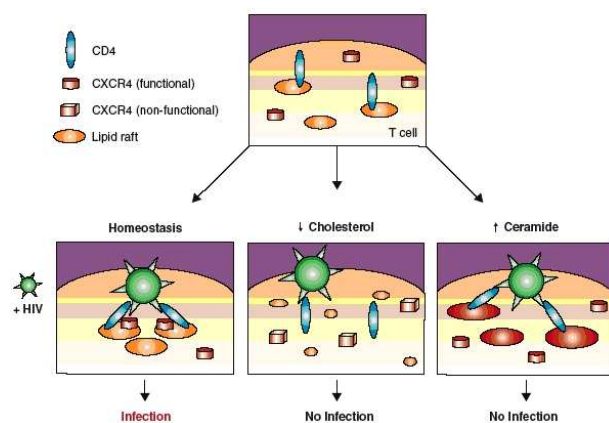


Figure 11. Model for inhibit HIV infection

Treatment with BCD or statins to remove membrane cholesterol disrupts lipid rafts and cell signaling, resulting in an inhibition of HIV infection and a loss of chemokine receptor function (bottom center). Increasing membrane ceramide levels also alter the properties of lipid rafts (bottom right), possibly by displacing cholesterol from lipid rafts, which results in the inhibition of HIV

infection. In contrast to treatment with BCD, increased ceramide in the cell membrane does not result in the loss of chemokine receptor function (Figure 11).

⁵⁶ London, M.; London, E. *J. Biol. Chem.* **2004**, *279*, 9997–10004.

For now, as we expect HIV infected patients to be treated with anti-retrovirals for the rest of their lives, thus, the use of lipid concentration-altering drugs could elicit serious long-term effects, especially in cells such as neurons that are rich in gangliosides and sphingolipids. Do these drugs have immune inhibitory effects, such as with T cell activation? As HIV patients already have suppressed immune systems with decreased CD4 T cell counts, any additional suppression may prove dangerous. The path to inhibiting HIV infection remains elusive, in which, we will require the development of new approaches to achieve success. Targeting lipid rafts could possibly provide such a means to inhibiting viral infection. Whether BCD formulations in topical microbiocides or 4-HPR will be clinically effective at slowing or stopping HIV infection remains to be demonstrated. At least we can begin to broaden the scope of HIV therapy by understanding how host cell lipids contribute to HIV infection. In addition, the targeting of non-HIV proteins may provide the path of least resistance to achieving effective HIV therapy.

Studies described above illustrate that glycosphingolipids, ceramide, and their metabolites play a direct and/or auxiliary role during HIV-1 infection. Although the exact mechanisms by which these lipids modulate HIV-infection warrant further investigation, it is certain that the site of action of these lipids at the virus-cell membrane fusion level. Therefore, a number of strategies have been developed to design GSL/glycoconjugate based molecules to inhibit HIV-1 fusion reaction.

In this context, a series of β -GalCer and β -SGalCer-derivatized dendrimers (multivalent neoglycoconjugates) were synthesized to enhance binding affinity with HIV-1 gp120 (Figure 12).^{57,58} The glycodendrimers were evaluated for binding to rgp120 using surface plasmon resonance (SPR). All of the GalCer analogues, when appended to Dab-Am generations 3-5 (with 16, 32, and 64 amino end groups, respectively), gave equilibrium dissociation constants (KD) on the order of 10^{-9} M. The binding affinities for the GalCer glycodendrimers were roughly 2 orders of magnitude

⁵⁷ Kensinger, R. D., Yowler, B. C., Benesi, A. J., and Schengrund, C. L. *Bioconjug. Chem.* **2004**, *15*, 349–358.

⁵⁸ Kensinger, R. D.; Catalone, B. J.; Krebs, F. C.; Wigdahl, B.; Schengrund, C. L. *Antimicrob. Agents Chemother.* **2004**, *48*, 1614–1623.

lower than that observed for the known standard, DS (2.29×10^{-11} M). SPR also indicated that the binding of both the GalCer glycodendrimers and DS was 1:1 with respect to rgp120. In addition to evaluate the binding affinities of the GalCer glycodendrimers, the ability of the glycodendrimers to inhibit HIV infection of U373-MAGI-CCR5 cells by HIV-1 Ba-L was tested, again utilizing DS as a standard. These cells express CD4 and included either cloned CCR5 or CXCR4 coreceptor genes. It was determined that none of the nonsulfated GalCer glycodendrimers were able to inhibit HIV infection in Vitro. However, one of the sulfated derivatives, when attached to the higher order dendrimers (generations 3-5), gave EC50 values of approximately 90, 70, and 20 μ M, respectively. Dextran sulfate was found to be a superior inhibitor with a measured EC50 value of less than 1 μ M.

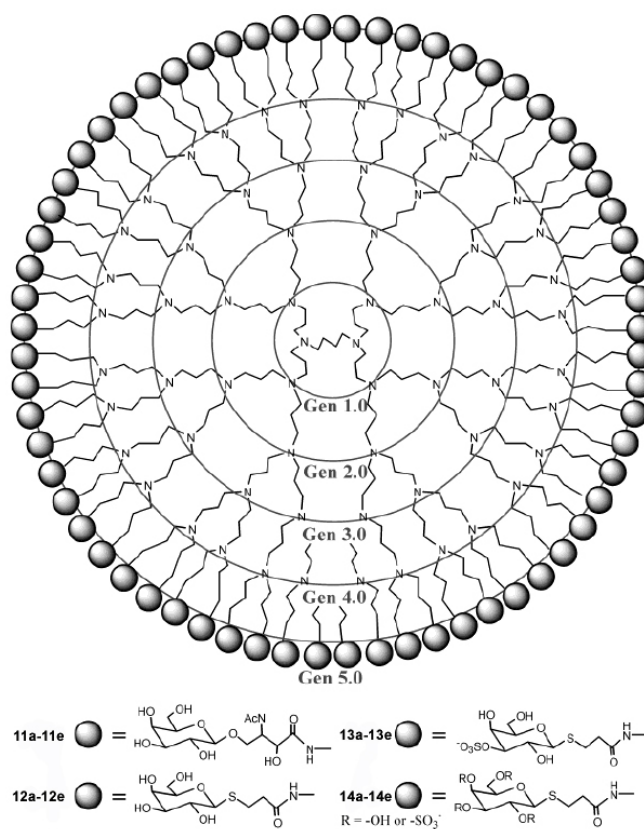


Figure 12. Schematic representation of the glycodendrimers

Multivalent interactions of Au glyconanoparticles containing galactosyl and glucosyl headgroups with recombinant gp120 were recently reported.⁵⁹ The gold nanoparticles were prepared from disulfides containing C-glycosides linked to triethylene glycol via an amide bond (Figure 13). Results from high-resolution transmission electron microscopy (HR-TEM), atomic force microscopy (AFM), UV/Vis absorption spectroscopy, HR-TEM, and elemental analysis data indicated that the nanoparticles averaged 2 nm in diameter and contained approximately 120 carbohydrate head groups per particle. The BNAA was used to evaluate the ability of the Au glyconanoparticles to displace rgp120 from plate-bound GalCer. The results showed divalent disulfides were <10% as active as biotinylated GalCer; however, when these same carbohydrates were presented in a polyvalent display, they were greater than 350 X times more active than the disulfides and at least 20 X more active than biotinylated GalCer.

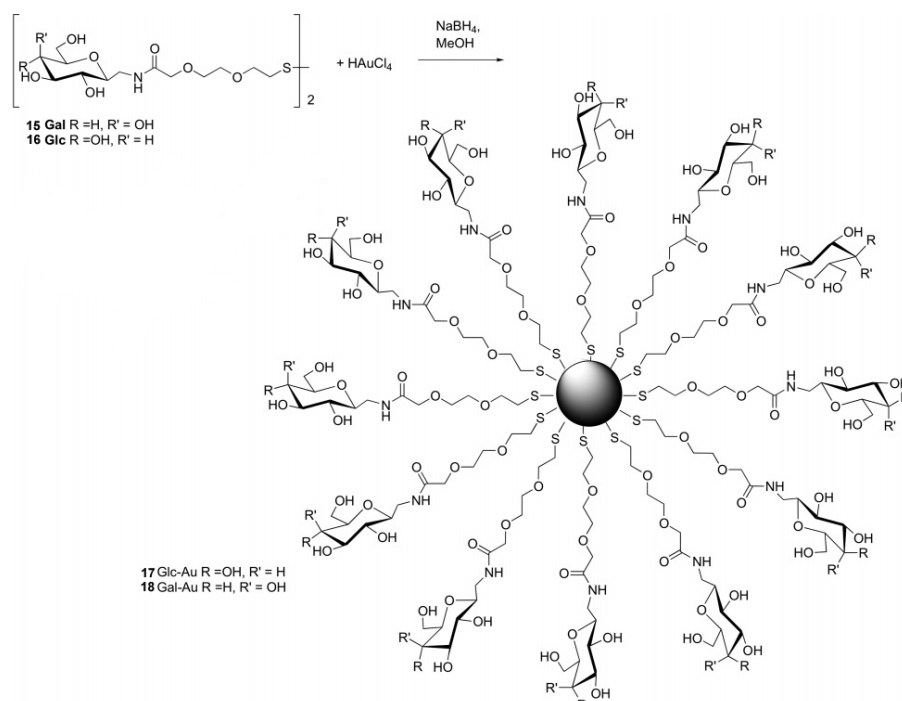


Figure 13. Synthesis of glyconanoparticles

⁵⁹ Yu, J.-J.; Nolting, B.; Tan, Y. H.; Li, X.; Gervay-Hague, J.; Liu, G.-Y. *NanoBiotechnology* **2005**, *1*, 201-210.

2. OBJETIVES

With this background, the objective of this work is the synthesis of novel hyperbranched glycodendritic polymer that bind HIV-1 gp 120. To reach this goal, it glimpses a strategy that involves the next steps:

- i) Synthesis of *D-erythro*-sphingosine with high enantioselectivity and diastereoselectivity (Figure 14).

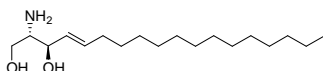


Figure 14

- ii) Glycosylation of ceramides employing stannyl derivatives as strategy (Figure 15).



Figure 15

- iii) Synthesis of glycodendritic polymer based on Boltorn H30 as a dendritic support and β -Galcer as external group. Click chemistry will be the key reaction to explore (Figure 16).

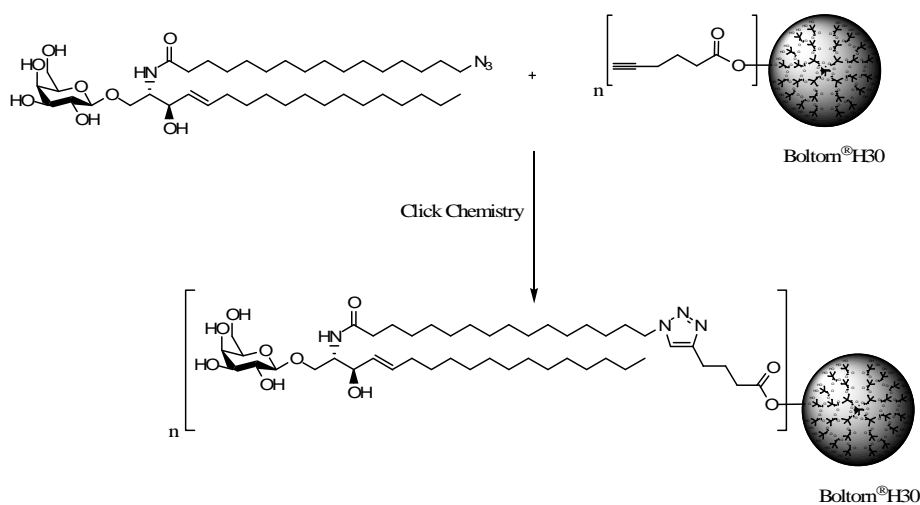


Figure 16

- iv) Finally, evaluate the interaction between this glycoconjugate with HIV-1 gp 120 (Figure 17).

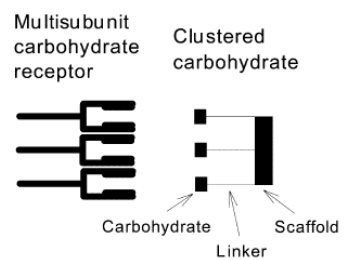
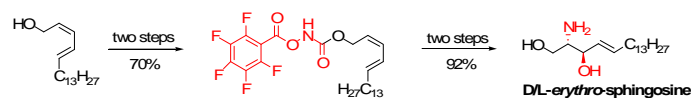


Figure 17

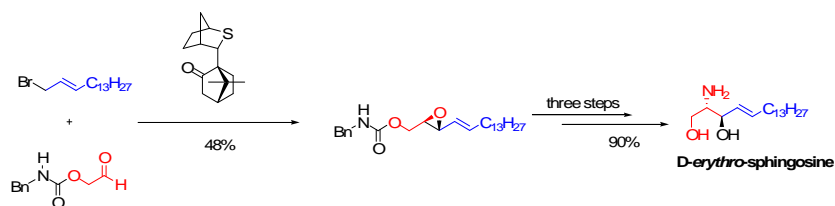
3. RESULTS

3.1. Synthesis of D-erythro-sphingosine

D/L-erythro-sphingosine and D-erythro-sphingosine were efficiently synthesized with 33% overall yield in 8 steps and 60% overall yield in 5 steps, respectively. A key transformation in the synthesis of D/L-erythro-sphingosine is the tethered aminohydroxylation (TA) to introduce the required stereochemistry.



A crucial step in the synthesis of D-erythro-sphingosine comprises an asymmetric sulfur ylide reaction between the bromide of dodecane and the appropriate aldehyde in presencia the EtP₂.



3.1.1. Chemistry and biology of sphingosine

In 1881, when Johann Thudichum first described the compound that would later be fully characterized as sphingosine, he named it after the Greek mythological character, the Sphinx, “in commemoration of the many enigmas which it has presented to the inquirer”.⁶⁰ Sphingolipids (Figure 18) have emerged over the last several decades as a family of key signalling molecules including ceramide **10**, sphingosine **19** and sphingosine-1-phosphate **20**.⁶¹ These compounds together with

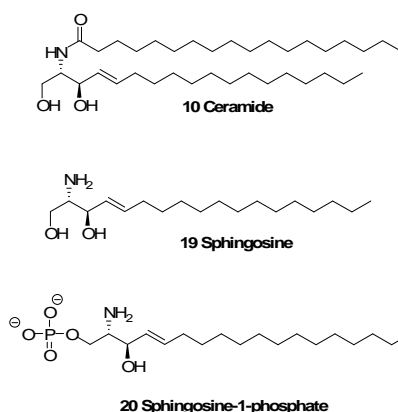


Figure 18. Naturally occurring of sphingolipids

glycerophospholipids and cholesterol are building blocks⁶² that play essential roles as structural cell membrane components⁶³ and participant in higher order physiological processes including inflammation⁶⁴ and vasculogenesis.⁶⁵ Recent studies implicate sphingolipid involvement in many of the most common human diseases including infection by microorganisms,⁶⁶ diabetes,⁶⁷ a range of cancers,⁶⁸ Alzheimer's,⁶⁹ and many others.⁷⁰

The basic structure of a sphingolipids consists of a long-chain sphingoid base backbone linked to a fatty acid via an amide bond with the 2-amino group and to a polar head group at the C-1 position via an ester bond (Figure 18). There are four sphingosine stereoisomers with a wide range of biological activities.⁷¹ The isomer *D*-erythro is the most common metabolite and has been meticulously studied. Since, sphingosine and its

⁶⁰ Thudichum, J. L. W. *A treatise on the Chemical Constitution of the Brain*, **1884**, Bailliere, Tindall and Cox, London.

⁶¹ Tani, M.; Ito, M.; Igarashi, Y. *Cell. Signal.* **2007**, *19*, 229–237.

⁶² Riethmüller, J.; Riehle, A.; Grassmé, H.; Gulbins, E. *Biochim. Biophys. Acta* **2006**, *1758*, 2139–2147.

⁶³ Snook, C. F.; Jones, J. A.; Hannun, Y. A. *Biochim. Biophys. Acta* **2006**, *1761*, 927–946.

⁶⁴ El Alwani, M.; Wu, B. X.; Obeid, L. M.; Hannun, Y. A. *Pharmacol. Ther.* **2006**, *112*, 171–183.

⁶⁵ Argraves, K. M.; Wilkerson, B. A.; Argraves, W. S.; Fleming, P. A.; Obeid, L. M.; Drake, C. J. *J. Biol. Chem.* **2004**, *279*, 50580–50590.

⁶⁶ Heung, L. J.; Luberto, Ch.; Del Poeta, M. *Infect. Immun.* **2006**, *74*, 28–39.

⁶⁷ Summers, S. A.; Nelson, D. H. *Diabetes* **2005**, *54*, 591–602.

⁶⁸ Modrak, D. E.; Gold, D. V.; Goldenberg, D. M. *Mol. Cancer Ther.* **2006**, *5*, 200–208.

⁶⁹ Zhou, S.; Zhou, H.; Walian, P. J.; Jap, B. K. *Biochemistry* **2007**, *46*, 2553–2563.

⁷⁰ Kolter, T.; Sandhoff, K. *Biochim. Biophys. Acta* **2006**, *1758*, 2057–2079.

⁷¹ (a) Merrill, A. H., Jr.; Nimkar, S.; Menaldino, D.; Hannun, Y. A.; Loomis, C.; Bell, R. M.; Tyahi, S. R.; Lambeth, J. D.; Stevens, V. L.; Hunter, R.; Liotta, D. C. *Biochemistry* **1989**, *28*, 3138–3145. (b) Sachs, C. W.; Ballas, L. M.; Mascarella, S. W.; Safa, A. R.; Lewin, A. H.; Loomis, C.; Carroll, F. I.; Bell, R. M.; Fine, R. L. *Biochem. Pharmacol.* **1996**, *52*, 603–612.

derivatives are available a limited amount from natural sources, there is a continuing interest in developing efficient methods for their synthesis. There are many methods for synthesizing sphingosine reported in the literature⁷² and they can be classified into four categories: i) In the first, carbohydrates are used as the source of chirality, ii) the Sharpless asymmetric epoxidation to generate the asymmetric centres, iii) the third relies on the aldol reaction with a chiral auxiliary and finally iv) the use of amino acid serine as the source of chirality. However, most of the methods require multistep reactions that resulted in low total yields. The key to cost-effective and efficient synthesis is the choice of a proper starting material that requires minimal protection-deprotection steps.

3.1.2. Recent contributions in the synthesis of sphingosine reported in the literature (1998-2008)

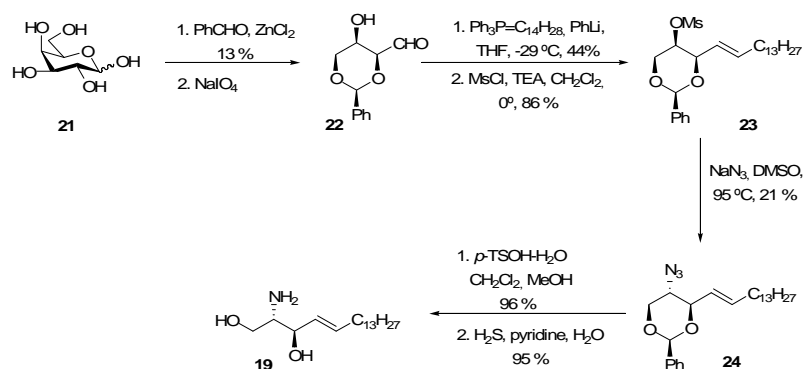
3.1.2.1. Carbohydrate approach

The total synthesis of sphingosine **19** was performed via the azidosphingosine intermediate **24** starting from D-galactose **21** (Scheme 2).⁷³ Thus, D-Galactose **21** was converted to 4,6-benzylidene-D-galactose as a mixture of α and β anomers (85:15), then it was oxidated with NaIO₄ to give **22**, which was employed in the next reaction without column chromatographic purification. The olefination reaction and protection of alcohol group afforded **23** in a 44% yield over two steps, results that agreed with the original report.⁷⁴ Synthesis of azide proceeded via mesylate **23** with inversion of configuration employing NaN₃ in DMSO at 95°C to afford the product **24** with a lower yield (21%). Finally, the bezylidene group was removed by acid-catalyzed and the azide reduced with H₂S to give pure *D-erythro*-sphingosine **19** (Scheme 2). In this work, apparent discrepancies in literature procedures and characterization have been resolved.

⁷² For reviews, see: (a) Merrill, A. H., Jr.; Hannun, Y. A. *Methods Enzymol.* **2000**, *311*, 91–479; (b) Koskinen, P. M.; Koskinen, A. M. P. *Synthesis* **1998**, 1075–1091. (c) Liao, J.; Tao, J.; Lin, G.; Liu, D. *Tetrahedron* **2005**, *61*, 4715–4733.

⁷³ Duclos Jr, R. I. *Chemistry and Physics of Lipids* **2001**, *111*, 111–138.

⁷⁴ Schmidt, R. R.; Zimmermann, P. *Tetrahedron Lett.* **1986**, *27*, 481–484.



Scheme 2

To the synthesis of sulfatides like **2**, which are an antigen presented by CD1a proteins,^{75,76,77} 3-*O*-benzoylazidosphingosine⁷⁸ **29** was stereoselectively prepared through a CuCN-catalyzed allylic alkylation of a hexenitol dimesylate **27**. Thus, D-xylose **25** (Scheme 3) was converted into the 3,5-*O*-isopropylidene derivative **26** and subsequently a Peterson olefination by condensation between **26** and a Grignard reagent gave the β-silyl alcohol. Finally the treatment of the alcohol with potassium hydride and reaction with MsCl afforded the dimesylate **27** (41% overall yield). Allylic displacement of the mesylate group in position 3 was effected with *n*-dodecylmagnesium bromide in the presence of catalytic copper cyanide to give **28**. This compound was treated with tetrabutylammonium azide in toluene, and then acetonide was removed in acid medium. The obtained product was transformed into the desired 3-*O*-benzoylazidosphingosine **29** through standard protection-deprotection reactions.⁷⁹ Alternatively, D-xylose **25** was transformed into the dithioethyl derivative, which without purification was converted to the di-acetonide **30** (Scheme 3). A Wittig reaction and a series deprotection and protection steps allowed to obtain compound **31**.⁸⁰ In the last stage of synthesis, **31** was treated with NaN₃ and a solution of HCl to afford 3-*O*-

⁷⁵ Nazi, K.; Chiu, M.; Mendoza, R.; Degano, M.; Khurana, S.; Moody, D.; Melian, A.; Wilson, I.; Kronenberg, M.; Porcelli, S.; Modlin, R. *J. Immunol.* **2001**, *166*, 2562–2570.

⁷⁶ Melian, A.; Watts, G. F.; Shamshiev, A.; De Libero, G.; Clatworthy, A.; Vincent, M.; Brenner, M. B.; Behar, S.; Niazi, K.; Modlin, R. L.; Almo, S.; Ostrov, D.; Nathanson, S. G.; Porcelli, S. A. *J. Immunol.* **2000**, *165*, 4494–4504.

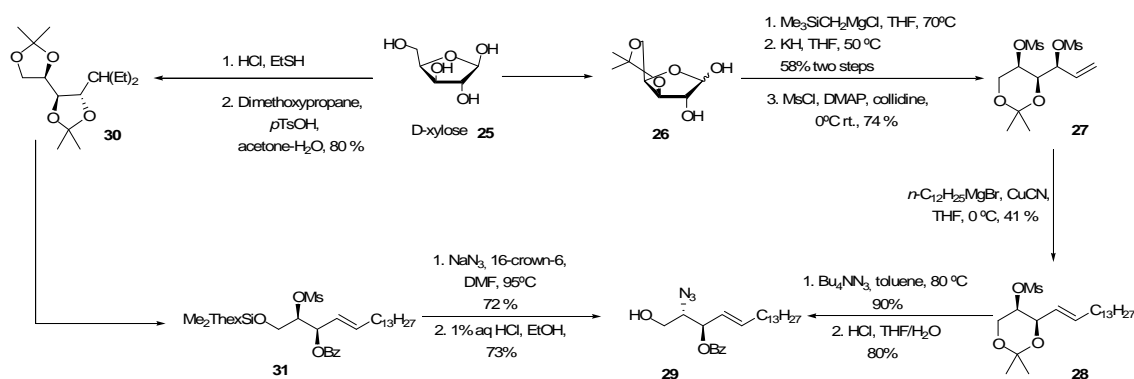
⁷⁷ Shamshiev, A.; Donda, A.; Prigozy, T. I.; Mori, L.; Chigorno, V.; Benedict, C. A.; Kappos, L.; Sonnino, S.; Kronenberg, M.; De Libero, G. *Immunity* **2000**, *13*, 255–264.

⁷⁸ Compostella, F.; Franchini, L.; De Libero, G.; Palmisano, G.; Ronchetti, F.; Panza, L. *Tetrahedron* **2002**, *58*, 8703–8708.

⁷⁹ Zimmermann, P.; Schmidt, R. R. *Liebigs Ann. Chem.* **1988**, 663–667.

⁸⁰ Kumar, P.; Schmidt, R. R. *Synthesis* **1998**, 33–35.

benzoylazidosphingosine **29** in good yield. This synthesis it is reproducible up to at least a 20 g scale (Scheme 3).



Scheme 3

Ceramide **10** was prepared from the 1-thio- β -D-xylopyranoside **32**, through a Cu(I)-mediated 1,2-metallate rearrangement as key step (Scheme 4).⁸¹ The synthesis of the crucial α -lithiated glycol **35** began with the oxidation of **32** to the corresponding sulfone. Subsequent β -elimination using MeLi as base afforded the α -phenylsulfonyl glycol derivative **33** in 72% yield. A Ni(0)-catalyzed⁸² coupling of tributylstannylmagnesium bromide converted the sulfone to the corresponding stannane **34** in 82% yield. Transmetalation with BuLi gave **35**. Alternatively, **32** can be converted into the sulfoxide with hydrogen peroxide catalyzed by ammonium molybdate and subsequent treatment with LDA gives the β -elimination of *t*-BuMe₂SiOLi affording the α -phenylsulfonyl glycol **36** in 69% yield. Reaction of sulfoxide with *t*-BuLi at -78°C gave the α -lithiated glycol **35** (Scheme 4). In the second stage of synthesis, **35** was reacted with *n*-tridecyl lithium in the presence of CuBr·SMe₂ to generate the alkenylsilane **37** in 68% overall yield. The obtention of this product can be explained by the formation of the higher order cuprate and its rearrangement with inversion of configuration at the alkenylmetal centre and the subsequent selective intramolecular O→C silyl transfer of the C3O-silyl group.⁸³ To complete the synthesis, **37** was protected as its bezylidene acetal and then treated with TBAF to give **38**. The C-TBS group was transferred back to oxygen by a Brook rearrangement⁸⁴ employing sodium hydride and 15-crown-5. TBAF was used to obtain the alcohol **39**. A Mitsunobu

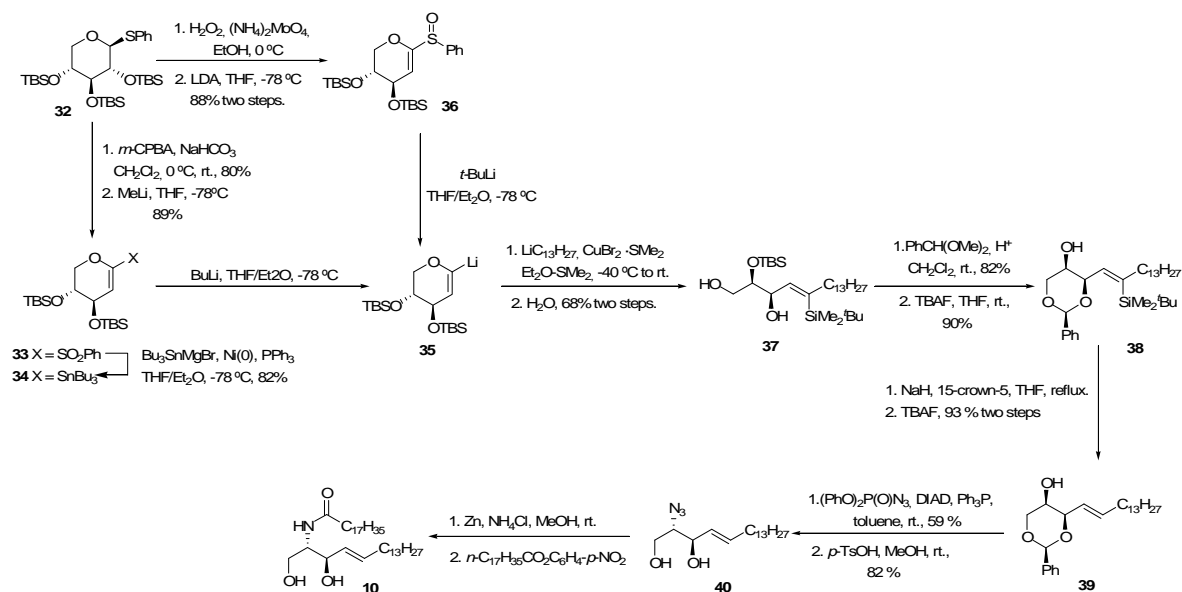
⁸¹ Milne, J. E.; Jarowicki, K.; Kocienski, P. J.; Alonso, J. *Chem. Comm.* **2002**, 426–427.

⁸² Gunn, A.; Jarowicki, K.; Kocienski, P.; Lockhart, S. *Synthesis*, **2001**, 331–338

⁸³ Kocienski, P.; Wadman, S.; Cooper, K. *J. Am. Chem. Soc.* **1989**, *111*, 2363–2365.

⁸⁴ Lutens, M.; Delanghe, P. H. M.; Goh, J. B.; Zhang, C. H. *J. Org. Chem.* **1995**, *60*, 4213–4227.

reaction was used to introduce the azide group and the benzylidene group was removed under acid conditions to afford azido-sphingosine **40**. Finally, the reduction of azide with Zn and acylation of the amine afforded the ceramide **10** (Scheme 4).



Scheme 4

The cross-metathesis (CM) reaction was explored as the key step in the synthesis of *D-eythro* and *D-threo*-sphingosine because the compatibility of Grubb's catalyst (second generation) with sugar azide, and the high *E*-selectivity and functional group tolerance (Scheme 5).⁸⁵ Thus, the required 3-azido-3,5,6-trideoxy-1,2-*O*-isopropylidene- α -*D-ribo*-hexofuran-5-ene **41** was obtained from *D*-glucose,^{86,87} while 3-azido-3,5,6-trideoxy-1,2-*O*-isopropylidene- α -*D-xylo*-hexofuran-5-ene **42** was derived from *D*-allose^{88,89,90} following the same reaction sequence. The use of first generation Grubb's catalyst in the individual reactions of both starting materials with 1-nonene did not provide cross-coupling products, while the second generation catalyst afforded the cross-coupling product in good yield in the same conditions. Consequently, the second

⁸⁵ Chaudhari, V. D.; Kumar, K. S. A.; Dhavale, D. *Org. Lett.* **2005**, *7*, 5805–5807.

⁸⁶ Gruner, S. A. W.; Keri, G.; Schwab, R.; Venetianer, A.; Kessler, H. *Org. Lett.* **2001**, *3*, 3723–3725.

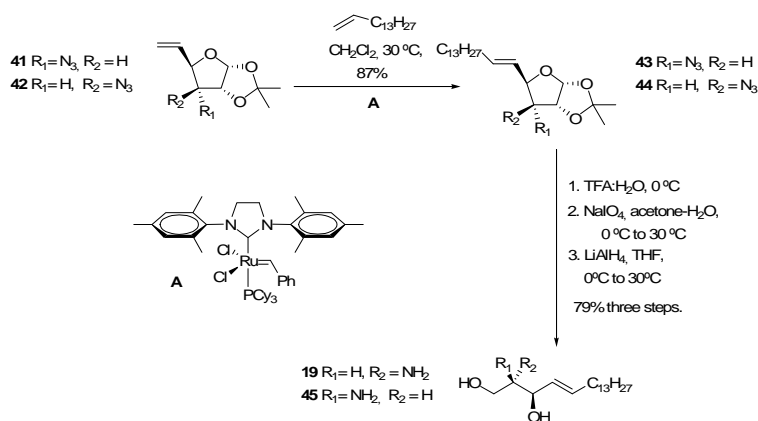
⁸⁷ Gurjar, M. K.; Patil, V. J.; Pawar, S. M. *Indian J. Chem.* **1987**, *26B*, 1115–1120.

⁸⁸ Fernandez, J. M.G.; Mellet, C. O.; Blanco, J. L. J.; Fuentes, J. *J. Org. Chem.* **1994**, *59*, 5565–5572.

⁸⁹ Calvo-Flores, F. G.; Garcia-Mendoza, P.; Hernandez, F.; Isac-Garcia, J.; Santoyo-Gonzalez, F. *J. Org. Chem.* **1997**, *62*, 3944–3961.

⁹⁰ Santoyo-Gonzalez, F.; Garcia-Calvo-Flores, F.; Garcia-Mendoza, P.; Hernandez-Mateo, F.; Isac-Garcia, J.; Perez-Alvarez, M. D. *Chem. Commun.* **1995**, 461–462.

generation Grubb's was employed in the reaction with 1-pentadecene to afford the cross-coupling alkenes **43** and **44** with good yields and excellent stereoselectivities. Finally, **43** and **44** were treated with TFA-water to afford an anomeric mixture of hemiacetals that were treated with sodium periodate the resulted aldehyde was subsequently reduced with LiAlH₄ furnishing *D-erythro*-sphingosine **19** and *D-threo*-sphingosine **45**, respectively, in three steps (Scheme 5).



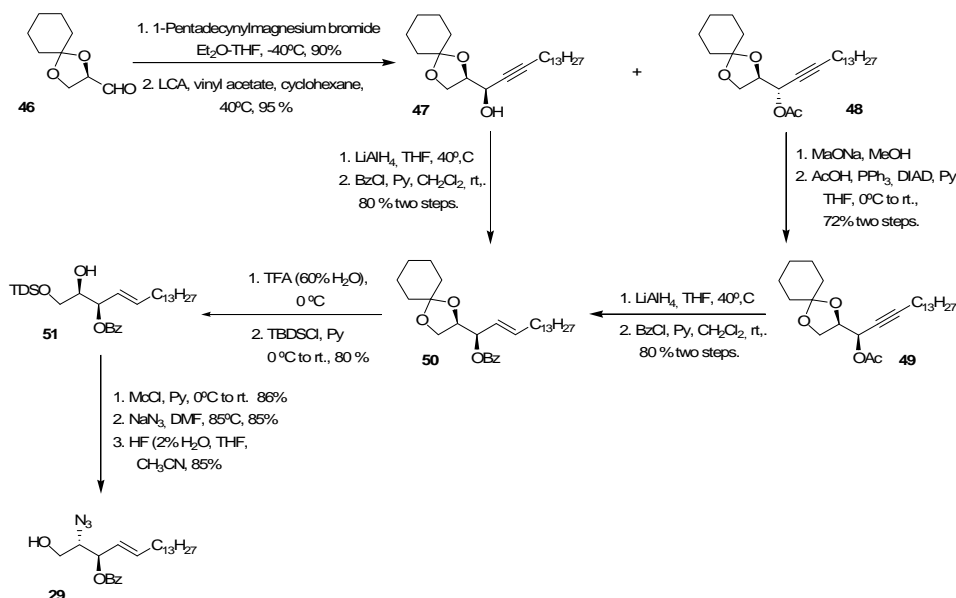
Scheme 5

Glyceraldehyde is also a suitable starting material for the synthesis of sphingosines.⁹¹ Thus, 2,3-*O*-benzylidene-D-glyceraldehyde⁹² **46** (Scheme 6) was generated by periodate cleavage of 1,2:5,6-di-*O*-cyclohexylidene-D-manitol, and the subsequent treatment with 1-pentadecynylmagnesium bromide afforded a diastereoisomeric mixture of propargylic alcohols in a *syn/anti* ratio of 4:6. This mixture of alcohols was resolved with *Candida antarctica* (LCA) lipase and vinyl acetate to furnish the *anti* acetyl derivative **48**, while the *syn* alcohol **47** was recovered unchanged. The undesired *anti* acetyl derivative **48** was hydrolyzed in Zemplén conditions and the configuration was inverted by reaction with acetic acid in Mitsunobu conditions to provide the acetyl derivative **49**. The *trans* allylic alcohol was obtained in quantitative yield from **47** or **49** by reaction with LiAlH₄, and it was used in the next reaction with benzoyl chloride without purification to give the compound **50**. Cleavage of the cyclohexylidene acetal and 1-*O*-silylation furnished the **51**. Hydroxyl group at position

⁹¹ Compostella, F.; Franchini, L.; Giovenzana, G. B.; Panza, L.; Prosperi, D.; Ronchetti, F. *Tetrahedron Asymmetry* **2002**, 13, 867–872.

⁹² Chattopadhyay, A. *J. Org. Chem.* **1996**, 61, 6104–6107.

2 was activated as mesylate for nucleophilic displacement by azide affording the fully protected azidosphingosine, which was treated with HF to give 3-*O*-benzoyl azidosphingosine **29** (Scheme 6).



Scheme 6

3.1.2.2. From Serine and Garner's aldehyde

L-Serine has a hydroxyamino function with the appropriate configuration that makes this compound especially suitable for synthesising sphingosine derivatives. In this context, recently a highly efficient and versatile method for synthesising sphingosine **19** was established by olefin cross metathesis reaction between 1-pentadecene and amino alcohol **55**, which was derived starting from L-serine **52** (Scheme 7).⁹³ The synthesis started with protection of L-serine **52** afforded **53**, followed by the formation of Weinreb amide and the protection of the primary hydroxyl group to give **54** in excellent yield in three steps without column chromatography. The reaction of **54** with vinylmagnesium bromide and reduction of the resulting ketone with tri-*tert*-butoxyaluminumhydride^{94,95} provided the allylic alcohol **55** with excellent yield and as a

⁹³ Yamamoto, T.; Hasegawa, H.; Hakogi, T.; Katsumura, S. *Org. Lett.* **2006**, *8*, 5569–5572.

⁹⁴ Hakogi, T.; Fujii, S.; Morita, M.; Ikeda, K.; Katsumura, S. *Bioorg. Med. Chem. Lett.* **2005**, *15*, 2141–2144.

⁹⁵ Hofmann, R. V.; Maslouh, N. Lee, F.-C. *J. Org. Chem.* **2002**, *67*, 1045–1056.

sole diastereomer. Then **55** was treated with pentadecene in presence of second generation Grubb's catalyst to afford **56** in 75% yield. Reaction of **56** with trifluoroacetic acid furnished unprotected sphingosine **19** (Scheme 7).

The L-serine derivatives were used in an alternative synthesis of sphingosine whose key step relies on the palladium catalyzed cross-coupling between an alkenyl boronic acid and a thiol ester.⁹⁶ Initially, the cross-coupling of a series of *N*-protected serine thiophenyl esters and *trans*-1-pentadecyl boronic acid⁹⁷ were studied. From protective groups studied (i.e. Cbz, Trityl, Fmoc), the *tert*-butyloxycarbonyl (Boc) gave the highest yield of ketone.

Thus, the synthesis started from commercially available *N*-Boc-L-serine **53**, which was converted into the corresponding thiophenyl ester **57** using typical dehydration condition (DCC/HOBT), and silyl protection of alcohol group with TBSCl/NMM/DMAP in DMF (Scheme 7).⁹⁸ The subsequent cross-coupling of thiol ester **57** and the appropriate boronic acid afforded ketone **58** in high yield (94%). Lithium tri-*tert*-butoxyaluminumhydride in ethanol was used for a highly diastereoselective reduction of ketone and, finally, removal of protecting groups in acid medium provided *D-erythro*-sphingosine **19** (Scheme 7).

The syntheses of all four diastereomers of sphingosine from L-serine have been also achieved through highly diastereoselective reduction of the *N*-trityl protected α -amino enone derivative.^{99,100} The synthetic route started with the fully protected serine methyl ester **59** (Scheme 7), which was readily obtained from commercially available L-serine derivative **52**. The protected serine ester was reacted with lithium dimethyl methylphosphonate yielding quantitatively yielding the keto-phosphonate which was treated tetradecyl aldehyde in a Horner-Wadsworth-Emmons olefination reaction to provide the corresponding enone **60** in good yield. Removal of protecting groups with 2N HCl in MeOH-THF and diastereoselective reduction with zinc borohydride afforded *D-erythro*-sphingosine **19** in 90% d.e.; presumably via a cyclic Felkin-Anh transition state, and probably due to the high chelating ability of the zinc ion. When enone **60** was reduced via non-chelation control using NaBH₄ in presence of CeCl₃·7H₂O the *N,O*-diprotected *L-threo*-sphingosine **61** in 92 % d.e. was obtained (Scheme 7). By

⁹⁶ Yang, H.; Li, H.; Wittenberg, R.; Egi, M.; Huang, W.; Liebeskind, L. S. *J. Am. Chem. Soc.* **2007**, *129*, 1132–1140.

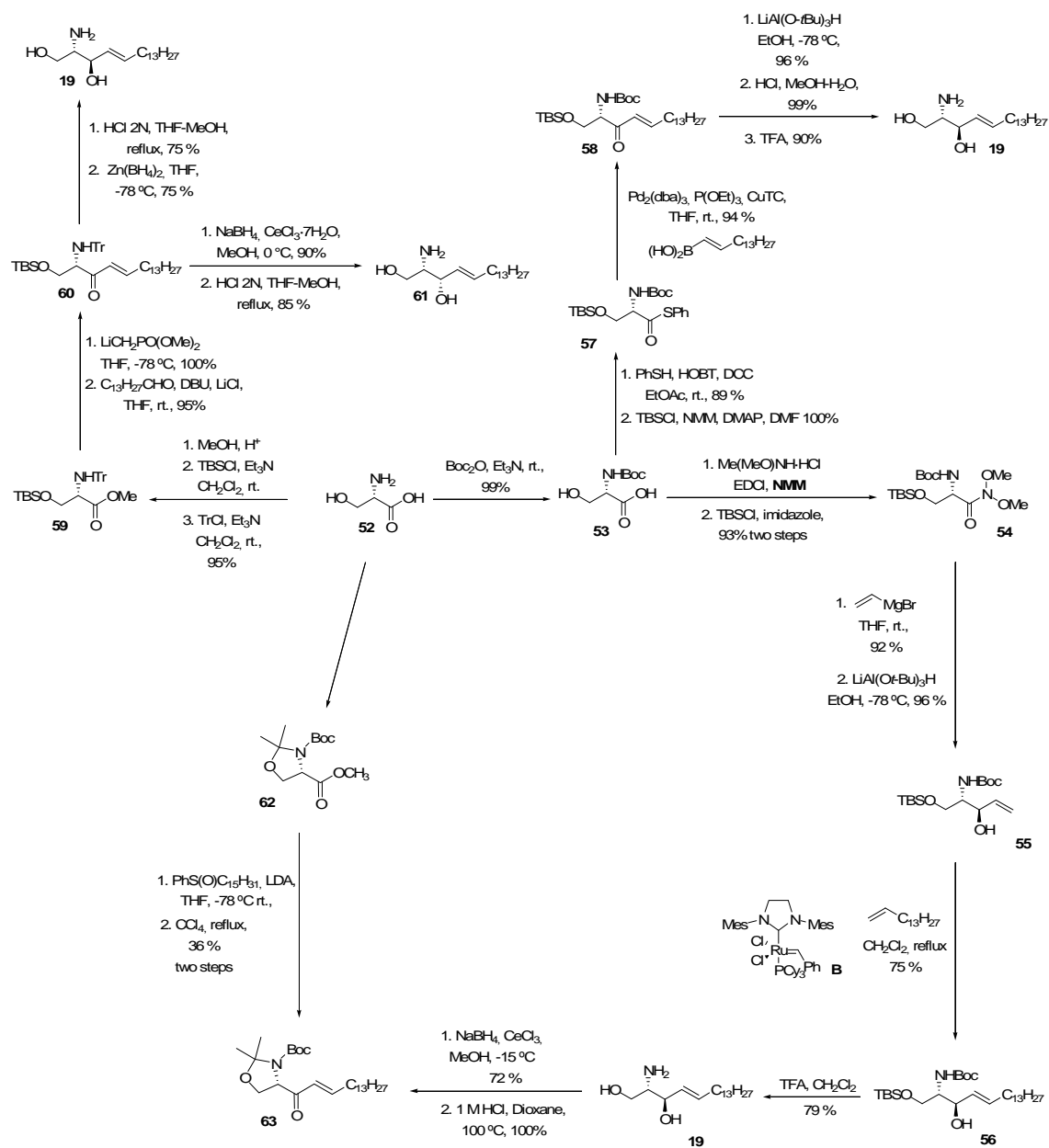
⁹⁷ Brown, H. C.; Bhat, N. G.; Somayaji, V. *Organometallics*, **1983**, *2*, 1311–1316.

⁹⁸ Yang, H.; Liebeskind, L. S. *Org. Lett.* **2007**, *9*, 2993–2995.

⁹⁹ Chung, S. K.; Lee, J. M. *Tetrahedron: Asymmetry* **1999**, *10*, 1441–1444.

¹⁰⁰ Lee, J.-M.; Lim, H.-S.; Chung, S.-K. *Tetrahedron: Asymmetry* **2002**, *13*, 343–347.

employing the same procedures on D-serine esters, L-erythro and D-threo-sphingosines were also synthesized.



Scheme 7

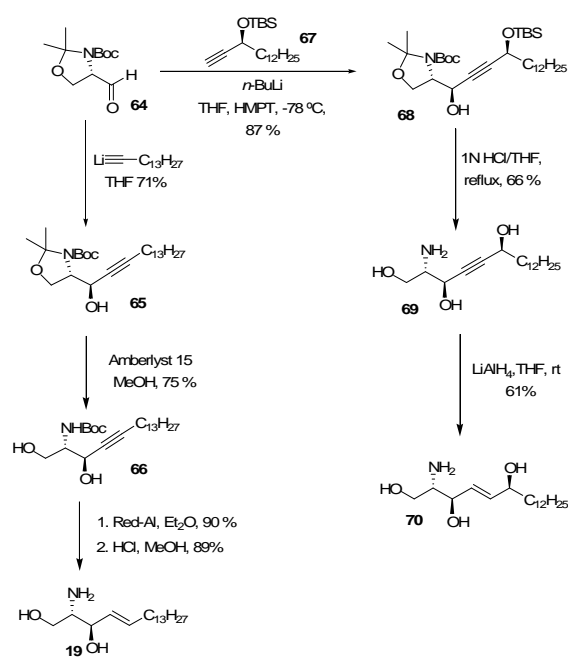
An L-serine derivative was also the starting material for a synthesis of sphingosine relying on the synthesis of an amino-enone by reaction of a serine ester with a sulfur stabilized carbanion followed by elimination (Scheme 7).¹⁰¹ The synthesis began with the reaction of L-serine derived N-Boc-oxazoline methyl ester

¹⁰¹ Chun, J.; Li, G.; Byun, H.-S.; Bittman, R. *Tetrahedron Lett.* **2002**, 43, 375–377.

62¹⁰² with an alkyl phenyl sulfoxide to give a sulfoxide intermediate which was not isolated and that afforded the enone **63** upon heating in CCl₄ overnight. The synthesis of *D-erythro*-sphingosine **19** was completed in two steps, first the diastereoselective reduction with NaBH₄ and CeCl₃ in methanol to provide the alcohol and finally the hydrolysis with HCl (1M) in dioxane furnished *D-erythro*-sphingosine **19** (Scheme 7).

Garner's aldehyde is also an L-serine derivative that is commercially available and that has been widely used as starting material for synthesis of enantiomerically pure compounds. With the objective of preparing of ¹³C- and ¹⁴C-labelled glucosphingolipids,¹⁰³ Garner's

aldehyde¹⁰⁴ **64** was reacted with pentadec-1-ynyllithium to give the acetylenic alcohol **65** in a moderate diastereomeric excess. The removal of acetonide in **65** afforded **66**, which was reacted with Red-Al¹⁰⁵ to stereoselectively reduce the alkyne with concomitant deprotection of amine group. Removal of silyl protecting group afforded *D-erythro*-sphingosine **19** (Scheme 8). This preparative approach was employing in the synthesis of a series of 3-C-methylceramide derivatives¹⁰⁶ and sphingosine 1-phosphate.¹⁰⁷



Scheme 8

6-Hydroxy-4*E*-sphingosine^{108,109,110} **70** was synthesized from Garner's aldehyde following a similar procedure (Scheme 8). Thus, the alkyne **67** was lithiated using *n*-

¹⁰² Garner, P.; Park, J. M. *Org. Synth.* **1991**, *70*, 18–28.

¹⁰³ Duffin, G. D.; Ellames, G. J.; Hartmann, S.; Herbert, J. M.; Smith, D. I. *J. Chem. Soc., Perkin Trans. 1*, **2000**, 2237–2242.

¹⁰⁴ Garner, P.; Park, J. M.; Malecki, E.; *J. Org. Chem.* **1988**, *53*, 4395–4398.

¹⁰⁵ Herold, P. *Helv. Chim. Acta* **1988**, *71*, 354–363.

¹⁰⁶ Sawatzki, P.; Kolter, T. *Eur. J. Org. Chem.* **2004**, 3693–3700.

¹⁰⁷ Blot, V.; Jacquemard, U.; Reissig, H-U.; Kleuser, B. *Synthesis*, **2009**, 759–766.

¹⁰⁸ Yadav, J. S.; Geetha, V.; Krishnam Raju, A.; Gnaneshwar, D.; Chandrasekhar, S. *Tetrahedron Lett.* **2003**, *44*, 2983–2985.

¹⁰⁹ Mori, K.; Masuda, Y. *Tetrahedron Lett.* **2003**, *44*, 9197–9200.

¹¹⁰ Masuda, Y.; Mori, K. *Eur. J. Org. Chem.* **2005**, 4789–4800.

BuLi and reacted with **64** in HMPT at -78°C to give the alcohol **68**. Removal of protecting groups in acid medium provided **69** which was treated with LiAlH_4 to yield 6-hydroxy-4*E*-sphingosine **70**, which have been found in human skin.^{111,112,113}

3.1.2.3. From tartaric acid

The use of tartaric acid and its derivatives as synthons in the synthesis of natural products is amply described in the literature.^{114,115,116,117} In this context, recently D-tartaric acid has been used as chiral starting material¹¹⁸ in the synthesis of D-erythro-sphingosine **6**. (Scheme 9). The synthesis started with the transformation of D-tartaric acid **71** into the alcohol **72**,¹¹⁹ which was oxidized with PCC to afford the aldehyde **73**. The olefination of **73** was achieved by reaction with diisopropyl (ethoxycarbonylmethyl)phosphonate in the presence of lithium bromide and triethylamine, to obtain the ester **74** in good yield. Reduction of the ester with DIBAL and acylation of the resulting alcohol provided the allyl acetate **75**. Chain elongation was carried out by reacting acetate **75** with $\text{C}_{12}\text{H}_{25}\text{MgBr}$ in the presence of catalytic Li_2CuCl_4 . Subsequent acetal deprotection and introduction of azide group by a Mitsunobu reaction furnished the azido sphingosine **76**. Then, the azide was reduced to amine group by means of the Staudinger reaction and the benzyl group was removed by Birch reduction to give D-erythro-Sphingosine **19** (Scheme 9).

In the same context, D-Threose **73** was obtained from tartaric acid and was as starting material to synthesize the ceramide analogue **79**,¹²⁰ which was evaluated as inhibitor of growth mouse embryonic fibroblast cells. Thus, aldehyde **73**, reacted with tetradecylmagnesium bromide to give a diastereomeric mixture of alcohols, which was oxidized to ketone with the Dess-Martin reagent. Methylenation reaction was carried

¹¹¹ Stewart, M. E.; Downing, D. T. *J. Invest. Dermatol.* **1995**, *105*, 613.

¹¹² Bouwstra, J. A.; Gooris, G. S.; Dubbelaar, F. E. R.; Ponc, M. *J. Lipid Res.* **2001**, *42*, 1759

¹¹³ Wakita, H.; Nishimura, K.; Takigawa, M. *J. Invest. Dermatol.* **1992**, *99*, 617.

¹¹⁴ Seebach, D.; Hungerbühler, E. *In Modern Synthetic Methods*, Vol. 2; Scheffold, R., Ed.; Otto Salle-Sauerländer:Frankfurt-Aarau, Germany, **1980**, 91–171.

¹¹⁵ Gawronski, J.; Gawronska, K. *Tartaric and Malic Acids in Synthesis: A Source Book of Building Blocks, Ligands, Auxiliaries, and Resolving Agents*; Wiley: New York, **1999**.

¹¹⁶ Ghosh, A. K.; Koltun, E. S.; Bilcer, G. *Synthesis* **2001**, 1281–1301.

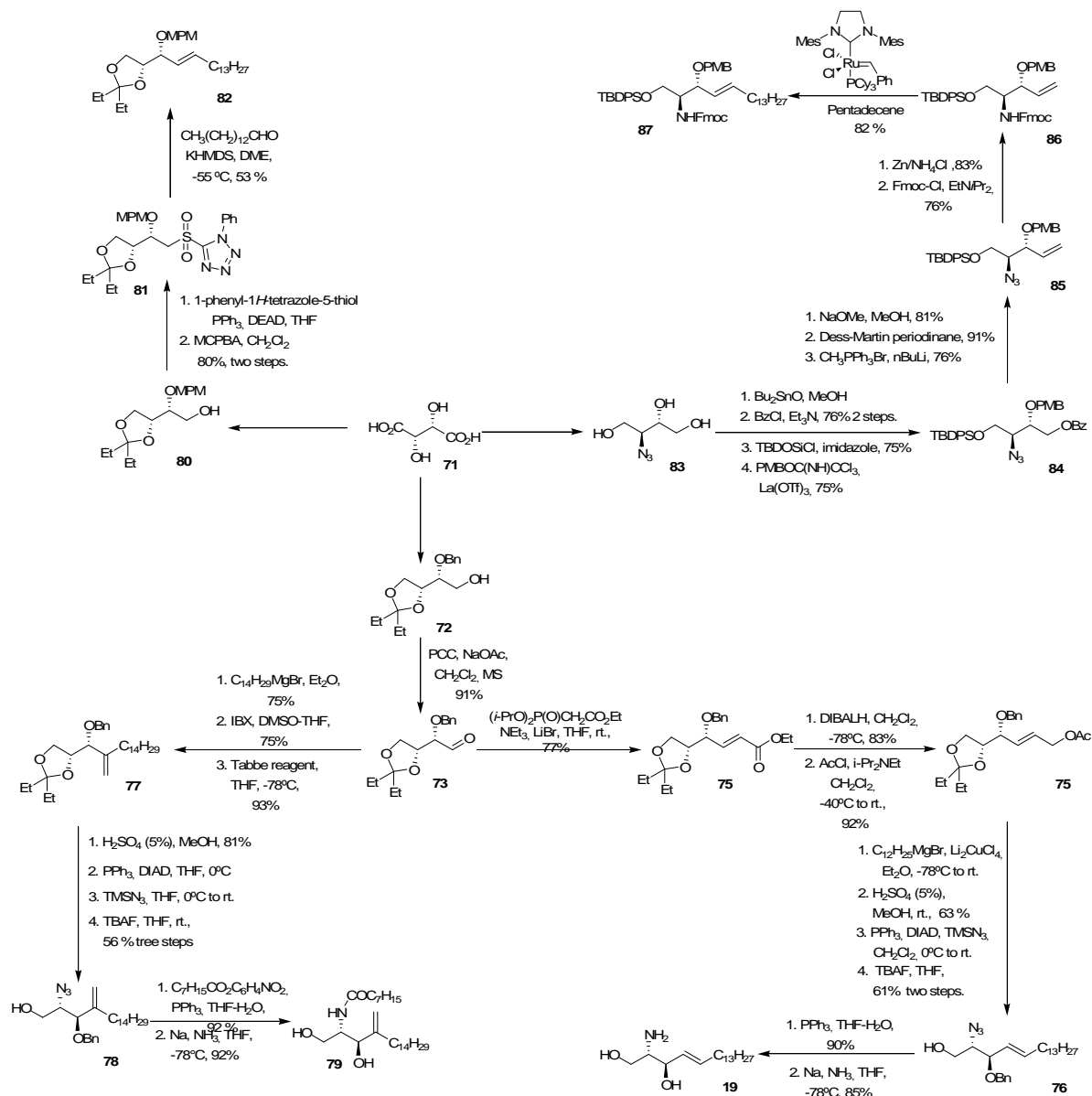
¹¹⁷ Liu, W.; Szewczyk, J. M.; Waykole, L.; Repič, O.; Blacklock, T. J. *Tetrahedron Letters*, **2002**, *43*, 1373–1375.

¹¹⁸ Lu, X.; Bittman, R. *Tetrahedron Lett.* **2005**, *46*, 1873–1875.

¹¹⁹ Lu, X.; Byun, H.-S.; Bittman, R. *J. Org. Chem.* **2004**, *69*, 5433–5438.

¹²⁰ Starting of Lu, X.; Arthur, G.; Bittman, R. *Org. Lett.* **2005**, *7*, 1645–1648.

out with $(C_5H_5)_2TiCH_2ClAl(CH_3)_2$ (Tebbe reagent)¹²¹ to give the alkene **77**. Then, deprotection of diol with 5% H_2SO_4 and introduction of azide group furnished the analogue of azidosphingosine **78**. Reduction of the azido group with PPh_3 , followed by amide formation and elimination of benzyl group furnished compound **79** (Scheme 9).



Scheme 9

The known alcohol **80**¹²² derived from D-tartaric acid **71** was chosen as starting material in the formal synthesis of 3-O-(4-methoxybenzyl)-azidosphingosine.¹²³ This

¹²¹ For a review of Tebbe methylenation see: Hartley, R. C.; McKierman, G. J. *J. Chem. Soc., Perkin Trans. 1* **2002**, 2763–2793.

¹²² Somfai, P.; Olsson, R. *Tetrahedron* **1993**, 49, 6645–6650.

synthetic route is an example of the versatility of the Kocienski¹²⁴ modification of the Julia olefination.¹²⁵ Thus, alcohol **80** was first converted into the 1-phenyl-1*H*-tetrazole-5-yl thioether under Mitsunobu conditions, and then it was oxidized to **81**. A solution of sulfone **81** in DME was treated with KHMDS, followed by the addition of tetradecanal to give the compound **82**, which was transformed into the target 3-*O*-(4-methoxybenzyl)-azidosphingosine (Scheme 9).¹²²

Other important route synthetic from D-tartaric acid **71** employing a highly stereoselective olefin cross metathesis reaction has been recently described.¹²⁶ In this case, the D-tartrate was converted into the known azidotriol **83** in three steps.^{127,128,129} Selective benzoylation of **83** was accomplished via the stannylene ketal intermediate. Silylation of the remaining primary alcohol followed by installation of the *p*-methoxybenzyl ether afforded the differentially protected intermediate **84**. Deacylation followed by oxidation with the Dess-Martin reagent proceeded smoothly to provide the corresponding aldehyde, which was converted into **85** via Wittig methylenation. This building block presented low reactivity in cross metathesis reaction, and in order to increase the yield of the metathesis step, the azide was reduced to the amine and protected as the Fmoc carbamate **86**. Reaction of **86** with pentadecene provided **87** in good yield (Scheme 9).

3.1.2.4. Synthesis from phytosphingosine

The synthesis of D-*erythro*-sphingosine **19** and D-*erythro*-azidosphingosine **40** were achieved from commercially available D-*ribo*-phytosphingosine **88** (Scheme 10).¹³⁰ Their synthesis began with the conversion of the amino function into azide and the protection of primary hydroxyl group of phytosphingosine **88** to give the diol **89**. Conversion of 3,4-vicinal diol **89** to its cyclic sulphite with thionyl chloride followed by oxidation with RuCl₃/NaIO₄ provided cyclic sulphate **90** in high yield (90 %). Then, it was explored the base-mediated direct transformation of cyclic sulphate **90** into allylic

¹²³ Compostella, F.; Franchini, L.; Panza, L.; Prosperi, D.; Ronchetti, F. *Tetrahedron*, **2002**, *58*, 4425–4428.

¹²⁴ Blakemore, P. R.; Cole, W. J.; Kocienski, P. J.; Morley, A. *Synlett* **1998**, 26–28.

¹²⁵ Baudin, J. B.; Hareau, G.; Julia, S. A.; Ruel, O. *Tetrahedron Lett.* **1991**, *32*, 1175–1178.

¹²⁶ Narain, A.; Basu, A. *Org. Lett.* **2004**, *6*, 2861–2863.

¹²⁷ He, L.; Byun, H.-S.; Bittman, R. *Tetrahedron Lett.* **1998**, *39*, 2071–2074.

¹²⁸ Metz, K.; Honda, M.; Komori, T. *Liebigs Ann. Chem.* **1993**, 55–60

¹²⁹ Mori, K.; Kinsho, T. *Liebigs Ann. Chem.* **1991**, 1309–1315.

¹³⁰ Kim, S.; Lee, S.; Lee, T.; Ko, H.; Kim, D. *J. Org. Chem.* **2006**, *71*, 8661–8664.

alcohol **40** by the regioselective abstraction of a β -hydrogen. Thus, **90** was treated with DBU in refluxing toluene to give, after hydrolysis in acid medium an removal of silyl group, compound **40** in low yield (39%). The yield increase notably (87%) when the reaction was carried out in the presence of TBAI.¹³¹ No *cis* olefin was detected by ¹H NMR of the reaction crude. Azide group in **40** was reduced with NaBH₄ to give *D-erythro*-sphingosine **19** (Scheme 10). The sulfate intermediate has been also used in an elegant synthesis of the sphingosine analogue Pachastrissamine.¹³²

Similarly, *D-ribo*-phytosphingosine **88** was transformed into *D-erythro*-sphingosine **19** in high yield,¹³³ by means of a regio- and stereoselective oxirane opening reaction as key step (Scheme 9). Protection of 1,2-aminoalcohol function in one step and selective tosylation of hydroxyl group in position 4 afforded **91**. The synthesis of key intermediate **92** was achieved by treatment of **91** with potassium *tert*-butoxide. Treatment of oxirane **92** with TMSI/DBN¹³⁴ led to the exclusive isolation of *E*-allyl silyl ether **93**. Finally, removal of trimethylsilyl, and phenyloxazoline protecting groups of **93** furnished *D-erythro*-sphingosine **19** (Scheme 10).

Other important contribution to synthesis of *D-erythro*-sphingosine **19** pursuing the same idea of transforming *D-ribo*-phytosphingosine **88** into *D-erythro*-sphingosine **19** was carried out by a regiospecific and stereoselective reduction of a *Z*-enol triflate (Scheme 10).¹³⁵ To achieve this goal, *D-ribo*-phytosphingosine **88** was treated with Boc₂O and di-*tert*-butylsilyl ditriflate to afford the silylene derivative **94**. Oxidation of the 4-hydroxyl group with acetic anhydride in DMSO, followed by treatment with potassium bis(trimethylsilyl)amide and sulfonylation of the *in situ* formed enolate furnished *E*-enol triflate **95**. Reaction of enol triflate function with formic acid¹³⁶ in the presence of Pd(OAc)₂(PPh₃)₂ allowed to obtain compound **96**. Finally, desilylation with TBAF and acidolysis of the *N*-Boc protecting group furnished *D-erythro*-sphingosine **19** (Scheme 10). The same authors obtained *D-erythro*-sphingosine **19** from *D-ribo*-phytosphingosine **88** following the Smith¹³⁷ procedure. Thus, **88** was subjected to diazo transfer and regioselective protection of the 1,3-diol to give **97** (Scheme 10). Triflation

¹³¹ Shing, T. K. M.; Tai, V. W. F. *J. Chem. Soc., Perkin Trans. 1* **1994**, 2017–2025.

¹³² Lee, T.; Lee, S.; Kwak, Y. S.; Kim, D.; Kim, S. *Org. Lett.* **2007**, *9*, 429–432.

¹³³ Van den Berg, R. J. B. H. N.; Korevaar, C. G. N.; Overkleeft, H. S.; Van der Marel, G. A.; Van Boom, J. H. *J. Org. Chem.* **2004**, *69*, 5699–5704.

¹³⁴ Kraus, G. A.; Frazier, J. *J. Org. Chem.* **1980**, *45*, 2579–2581.

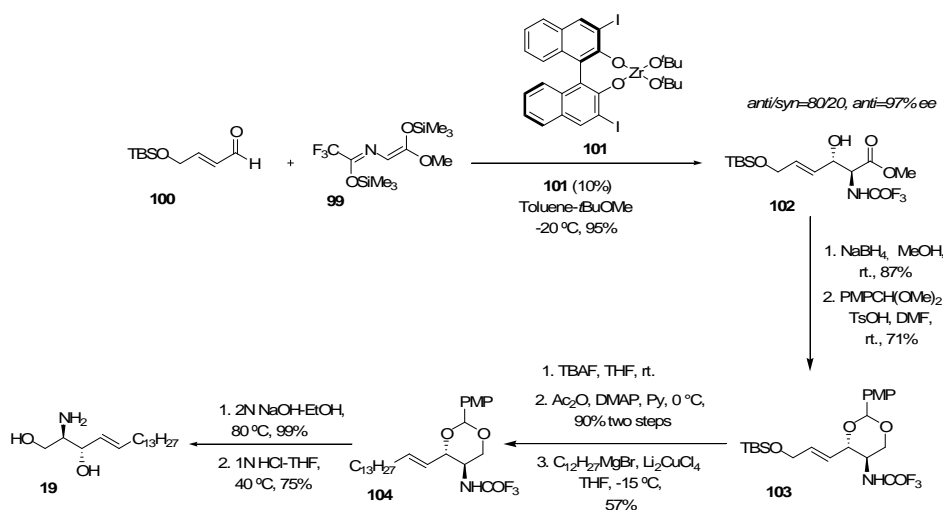
¹³⁵ Van den Berg, R. J. B. H. N.; Korevaar, C. G. N.; van der Marel, G. A.; Overkleeft, H. S.; Van Boom, J. H. *Tetrahedron Lett.* **2002**, *43*, 8409–8412.

¹³⁶ Carchi, S.; Morera, E.; Otrá, G. *Tetrahedron Lett.* **1984**, *25*, 4821–4824.

¹³⁷ Wild, R.; Schmidt, R. R. *Tetrahedron: Asymmetry*, **1994**, *5*, 2195–2208.

3.1.2.5. Using chiral reagents and auxiliaries

Starting from a glycine-derived silicon enolate the main functionalities present in sphingosine could be also prepared by a zirconium-catalyzed asymmetric aldol reaction (Scheme 11).¹³⁸ This procedure was illustrated in the synthesis of *L-erythro*-sphingosine **19** in 7-steps. Thus, the aldol reaction of **99** with aldehyde **100** was performed in the presence of the chiral zirconium complex **101**, prepared from zirconium alkoxide and BINOL,¹³⁹ affording the desired *anti*-aldol adduct **102** with high stereoselectivity and enantioselectivity (*anti/syn*=80/20, *anti*=97% ee). Reduction of **102**, followed by protection of the resulting 1,3-diol as its *p*-methoxybenzylidene acetal furnished **103**. Then, the *t*-butyldiphenylsilyl ether was converted to the corresponding acetate, which was treated with C₁₂H₂₅MgBr in presence of a catalytic amount of Li₂CuCl₄ to afford **104**. Finally, deprotection of 2-amino-1,3-diol gave *L-erythro*-sphingosine **19** (Scheme 11).



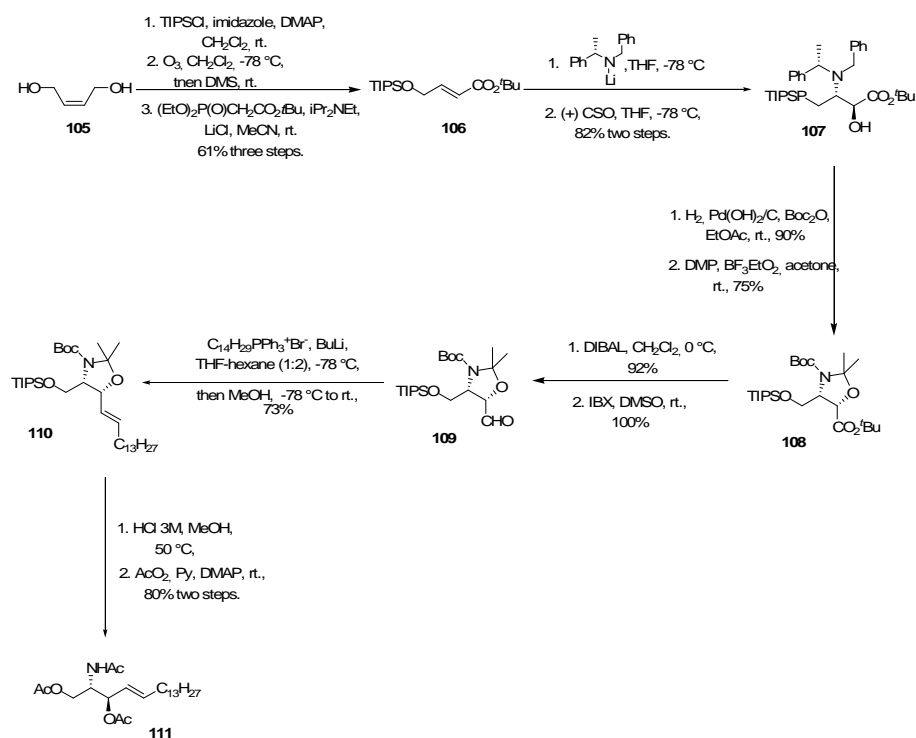
Scheme 11

With the idea of synthesizing asymmetric vicinal amino alcohols, a highly diastereoselective *anti*-aminohydroxylation of α,β -unsaturated esters, *via* conjugate addition of lithium (*S*)-*N*-benzyl-*N*-(α -methylbenzyl)amide and subsequent *in situ* enolate oxidation with (+)-(camphorsulfonyl)oxaziridine (+)-CSO, has been used as the

¹³⁸ Kobayashi, J.; Nakamura, M.; Mori, Y.; Yamashita, Y.; Kobayashi, S. *J. Am. Chem. Soc.* **2004**, *126*, 9192–9193.

¹³⁹ Yamashita, Y.; Ishitani, H.; Shimizu, H.; Kobayashi, S. *J. Am. Chem. Soc.* **2002**, *124*, 3292–3302.

key step in the synthesis of triacetyl *D-erythro*-Sphingosine¹⁴⁰ **111** (Scheme 12). Thus, γ -silyoxy- α,β -unsaturated ester **106** was prepared from *cis*-but-2-ene-1,4-diol **105**. Then, the conjugate addition of lithium (*S*)-*N*-benzyl-*N*-(α -methylbenzyl)amide and subsequent enolate oxidation with (+)-(camphorsulfonyl)oxaziridine (+)-CSO allowed obtain the (2*S*, 3*S*, α *S*)- α -hydroxy- β -amino- γ -silyloxy ester **107** with 98% de. Subsequent hydrogenolysis and *in situ* amino protection, followed by *N,O*-acetal formation afforded the oxazolidine ester **108**. Reduction of oxazolidine esters **108** with DIBAL-H and oxidation of alcohol in presence of IBX furnished the aldehyde **109**. In an attempt to reduce the ester with LiAlH₄, resulted in reduction of the ester and desilylation, giving the corresponding diol. Schlosser modification^{141,142} of the Wittig olefination was used to obtain the (*E*)-alkene **110**. Finally, hydrolysis of the protecting groups and acetylation gave **111** (Scheme 12).

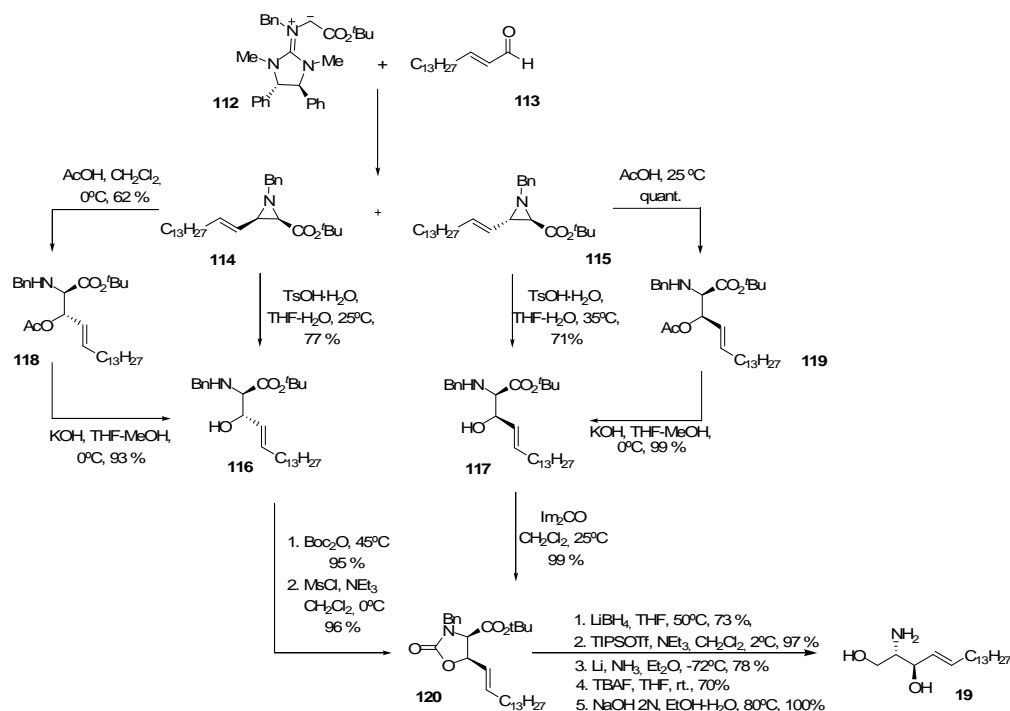


Scheme 12

¹⁴⁰ Abraham, E.; Davies, S. G.; Millican, N. L.; Nicholson, R. L.; Roberts, P. M.; Smith, A. D. *Org. Biomol. Chem.* **2008**, *6*, 1655–1664.

¹⁴¹ Schlosser, M.; Christmann, K. F. *Angew. Chem. Int. Ed. Engl.* **1966**, *5*, 126.

¹⁴² Oh, J. S.; Kim, B. H.; Kim, Y. G. *Tetrahedron Lett.* **2004**, *45*, 3925–3928



Scheme 13

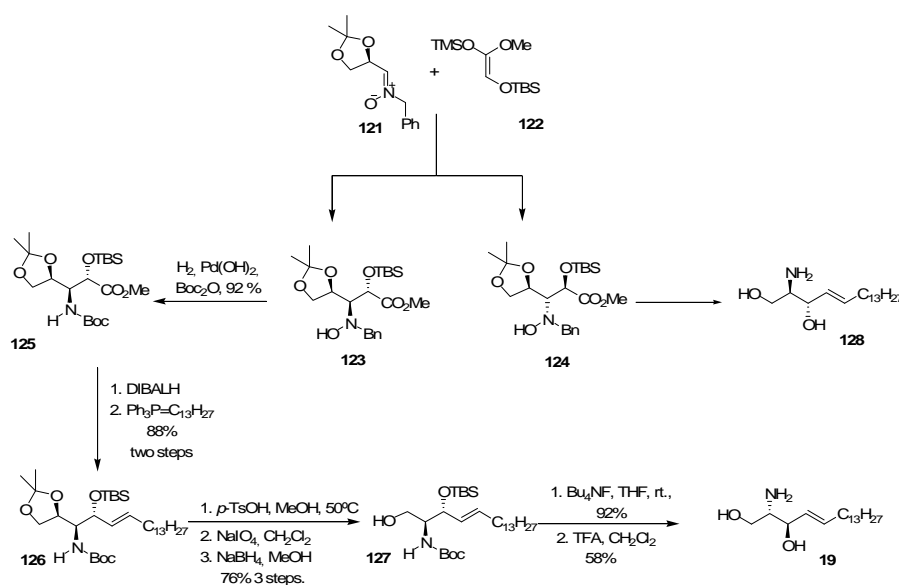
The α -amino- β -hydroxy acid units can be derived from the corresponding aziridine derivatives.¹⁴³ This strategy was applied in the synthesis of *D*-erythro-sphingosine **19**, using the addition reaction of chiral guanidinium ylides to aldehydes (Scheme 13).¹⁴⁴ Thus, reaction of (*R,R*)-guanidinium ylide **112** with aldehyde **113** followed by treatment with silica gel to give the *cis*- and *trans*-3-[(*E*)-pentadec-1-anyl]aziridines **114** and **115** with a poor stereoselectivity (*cis/trans*=53/47). The aziridine ring-opening reactions with TsOH allowed directly to introduce a hydroxyl function into the skeleton affording the esters **116** and **117**. Alternatively, the reaction of aziridines with acetic acid afforded the acetoxy derivatives **118** and **119**, which could be hydrolyzed to the α -amino- β -hydroxy esters **116** and **117** by methanolysis (KOH, THF/MeOH). The configuration of the alcohol at C3 in the *trans* isomer can be inverted by protection of the amino group (Boc), formation of the methanesulfonate and intramolecular cyclization to provide the *cis*-oxazolidine **120**. This oxazoline can be also obtained by reaction of the α -amino- β -hydroxy ester **117** with Im₂CO. The ester function was reduced with lithium borohydride to afford the corresponding alcohol,

¹⁴³ For recent review on the ring-opening reaction of aziridines, see: Hu, X. E. *Tetrahedron* **2004**, *60*, 2701–2743.

¹⁴⁴ Disadee, W.; Ishikawa, T. *J. Org. Chem.* **2005**, *70*, 9399–9406.

and then protecting-desprotecting protocol allowed to obtain *D-erythro*-sphingosine **19** (Scheme 13).

Stereoselective nucleophilic additions of enolates to imines and related compounds were used for the asymmetric synthesis of β -amino carbonyl derivatives. This reaction, as well called Mannich-type reaction, can be stereocontrolled to provide efficient routes to enantiomerically pure polyhydroxy- β -amino acids, which have been apply in the enantiodivergent synthesis of L- and *D-erythro*-sphingosine¹⁴⁵ (Scheme 14). Focusing in this idea, it was studied the reaction between the chiral nitron **121** (derived from glyceraldehyde) and silyl ketene acetal **122** in the presence of Lewis acid. The *2S,3S,4S* isomer **123** being the major product (89%) when $Zn(OTf)_2$ was employed as Lewis acid (*anti/syn*=97/3). If the Lewis acid used is $SnCl_4$ the major product is *2S,3R,4S*, isomer **124** (84%) (*anti/syn*=92/8). Compound **123** was transformed into β -amino- α -hydroxy ester **125** by catalytic hydrogenation in the presence of Boc_2O . The ester **125** was reduced to the corresponding aldehyde, followed of a Schlosser modification of the Wittig condensation with phosphorane to generate the alkene **126**. The dioxolane ring was converted into a hydroxymethyl group to give the orthogonally protected *D-erythro*-sphingosine **127**. Finally, elimination of protecting groups allowed obtained *D-erythro*-sphingosine **19**. The same methodology applied to compound **123** was applied to compound **122** to give *L-erythro*-sphingosine **128** (Scheme 14).

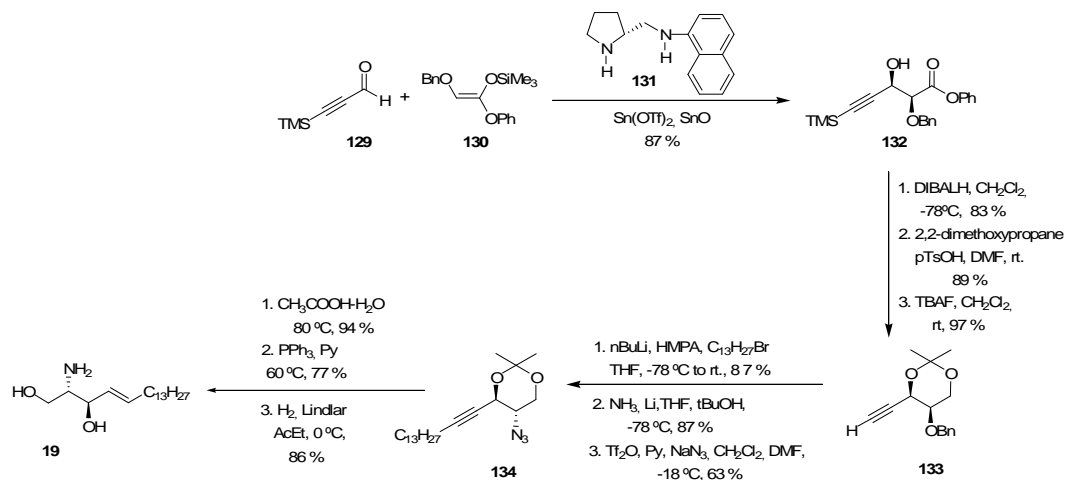


Scheme 14

¹⁴⁵ Merino, P.; Jimenez, P.; Tejero, T. *J. Org. Chem.* **2006**, 71, 4685–4688.

3.1.2.6. Enantioselective catalytic procedures

D-erythro-sphingosine **19** was enantioselectively synthesized¹⁴⁶ by a tin(II)-catalyzed asymmetric aldol reaction (Scheme 15). Thus, when trimethylsilylpropynal **129** was reacted with the silylenol ether **130** in the presence of 20 % of tin(II) triflate and the chiral diamine **131**, compound **132** was obtained in high diastereo- and enantioselectivity (*syn/anti*=97/3, 91% ee for *syn*). The phenyl ester **132** was then reduced with DIBAL to the corresponding diol, which was protected as its acetonide. Finally the desilylation with tetrabutylammonium fluoride gave the desired intermediate **133**. The lipidic chain was introduced by alkylation of the acetylene-lithium derivative. The installation of the amino functionality at position 2 was carried out by removal of benzyl group under Birch conditions, triflation of the resulting alcohol and reaction with NaN₃ to give **134** through an S_N2 process. The synthesis of sphingosine **19** was completed by deprotection of acetonide, reduction of the azide under Staudinger conditions and of the acetylene using Red-Al (Scheme 15).



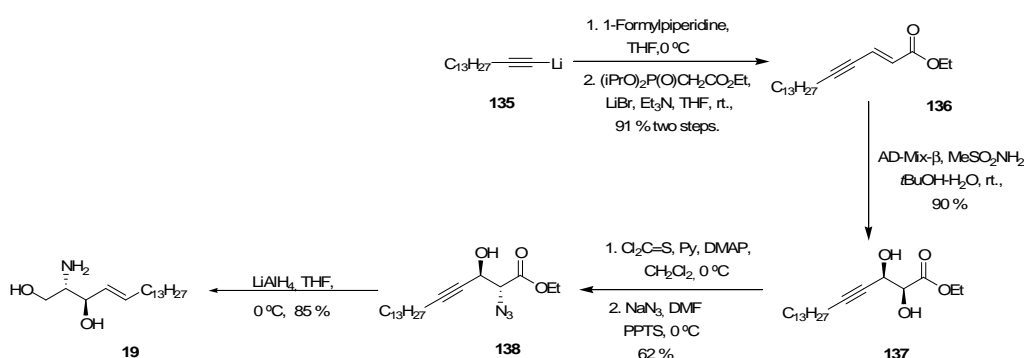
Scheme 15

Sharpless asymmetric dihydroxylation was also used as key step in the synthesis of *D-erythro*-sphingosine **19** (Scheme 16).¹⁴⁷ The synthesis is really short and efficient and starts by formylation of lithium 1-pentadecyne **135** with 1-formylpiperidine to give

¹⁴⁶ Kobayashi, S.; Furuta, T. *Tetrahedron* **1998**, *54*, 10275–10294.

¹⁴⁷ He, L.; Byun, H.S.; Bittman, R. *J. Org. Chem.* **2000**, *65*, 7627–7633.

the hexadec-1-ynal, which was reacted with diisopropyl(ethoxycarbonylmethyl) phosphonate (Horner-Wadsworth-Emmons reaction) to give the unsaturated ester **136**. Then, asymmetric dihydroxylation of enyne ester **136** with AD-mix- β provided the diol **137** in high yield and 98% ee. Reaction of **137** with thiophosgene quantitatively afforded to the corresponding cyclic thionocarbonate, which was subject to a ring-opening reaction with NaN₃. The reaction proceeded with the exclusive attack to the azido group to the α position to yield compound **138**. In the last stage of synthesis, the triple bond, the azido and ester functional groups in **138** were reduced simultaneously by LiAlH₄ in THF to furnish the *D-erythro*-sphingosine **19** (Scheme 16).



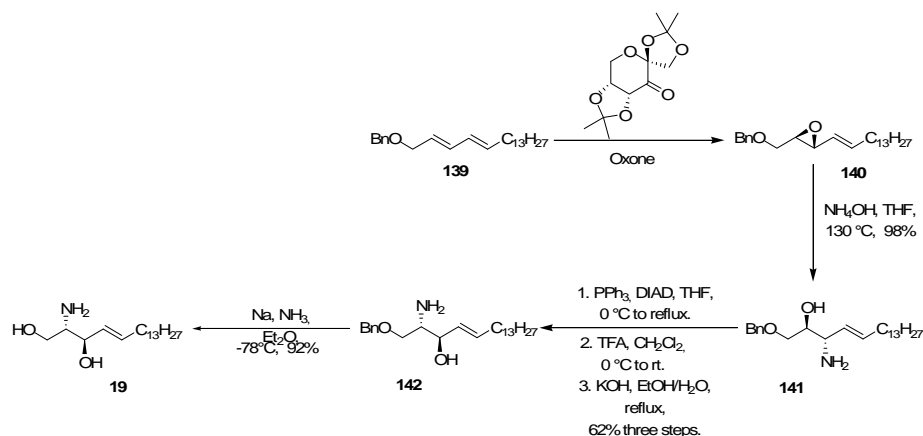
Scheme 16

A divergent synthesis¹⁴⁸ of *D-erythro*-Sphingosine **19** focused on the enantioselective epoxidation of diene **139** (Scheme 17). Thus, the benzylated diene **139** was reacted under the under Shi's asymmetric epoxidation conditions to afford the vinyl epoxide **140** in excellent yield and enantioselectivity (95% ee). Diastereospecific and regioselective opening in the allylic position, of vinyl epoxide **140** was carried out with ammonium hydroxide¹⁴⁹ furnishing the *anti*-amino alcohol **141**. In order to install the amino and the hydroxyl functionalities in the correct positions, compound **141** was reacted under Mitsunobu conditions¹⁵⁰ to give the vinylaziridine which was opened in presence of trifluoroacetic acid to generate the *anti*-amino alcohol **142**. Finally, the synthesis was completed by removal of the benzyl group under Birch conditions (Scheme 17).

¹⁴⁸ Olofson, B.; Somfai, P. *J. Org. Chem.* **2003**, *68*, 2514–2517.

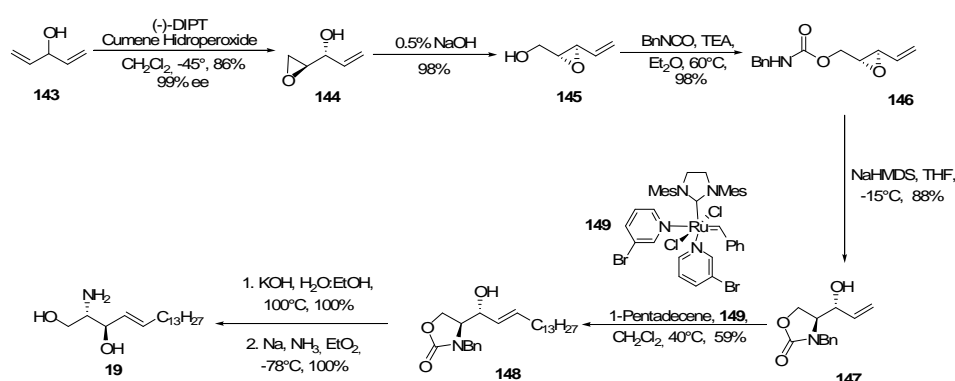
¹⁴⁹ Olofson, B.; Somfai, P. *J. Org. Chem.* **2002**, *67*, 8574–8583.

¹⁵⁰ Olofson, B.; Wijtmans, R.; Somfai, P. *Tetrahedron* **2002**, *58*, 5979–5982.



Scheme 17

Asymmetric Sharpless epoxidation was also used as key step in the synthesis of sphingosine (Scheme 18).¹⁵¹ The synthesis starts with Sharpless epoxidation¹⁵² of **143**, to give the alcohol **144**, followed by base induced Payne rearrangement generated the corresponding epoxide **145**, which was treated with benzyl isocyanate and Et₃N to provide the benzyl carbamate **146**. The subsequent intramolecular ring-opening using NaHMDS afforded the oxazolidinone **147**. The use of Grubbs' phosphine free catalyst **149** in the *E*-selective cross-methathesis allowed to obtain the intermediate **148**. Removal of the benzyl group with sodium in liquid ammonia, and hydrolysis with KOH generated **19** in a quantitative yield (Scheme 18).



Scheme 18

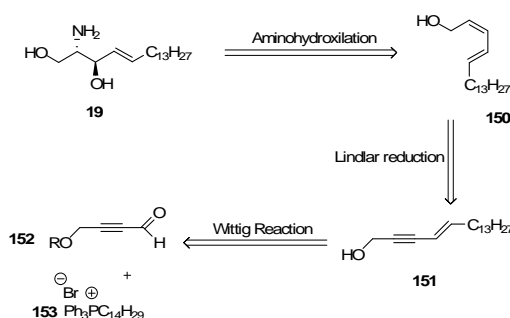
¹⁵¹ Torsell, S.; Somfai, P. *Org. Biomol. Chem.* **2004**, *2*, 1643–1646.

¹⁵² Romero, A.; Wong, C-H. *J. Org. Chem.* **2000**, *65*, 8264–8268.

3.1.3. Results

3.1.3.1 Synthesis of D/L-erythro-sphingosine using a tethered aminohydroxylation (TA) as key step

With the aim to contribute to enrich this diversity of strategies in sphingosine synthesis, in this work we report an efficient method for synthesising of D/L-erythro-sphingosine **19** employing the aminohydroxylation reaction as the key step. Unfortunately, this reaction is not compatible with the use of cinchona alkaloid-derived chiral ligands, which therefore precludes an enantioselective version. Our choice of starting material was dictated by the type of reaction that we planned employed to generate the asymmetric centres. Thus, the amino-hydroxylic functions were introduced in the last step by an aminohydroxylation of diene **150**, which has the proper *E,Z* configuration in the aminohydroxylation reaction. This diene can be prepared by reduction of **151**, which in turn can be obtained from aldehydes **152** by a Wittig reaction (Scheme 19).



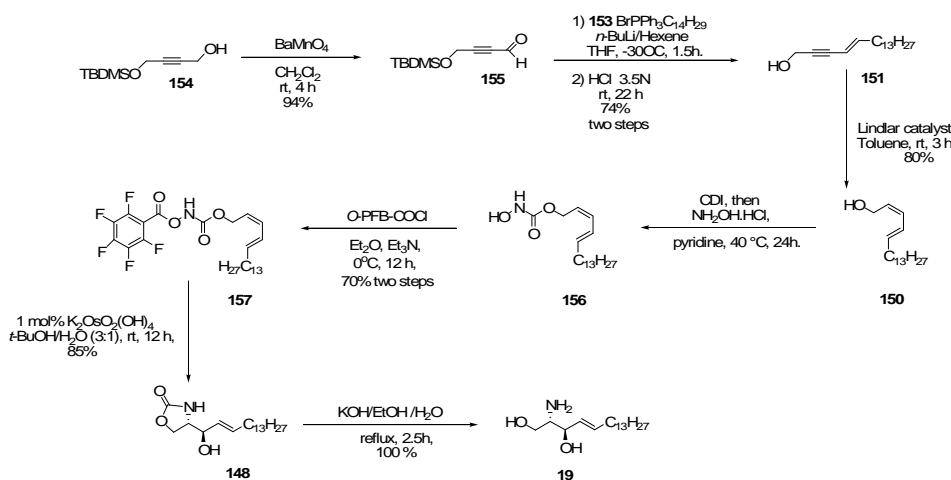
Scheme 19. Retrosynthetic analysis of DL-erythro-sphingosine 19

The synthesis of diene **150** starts from acetylenic alcohol **154** which under oxidation conditions with BaMnO₄ gave aldehyde **155**. Then, the reaction of **155** with the phosphonium salt **153** afforded the *E*-enyne **151**. The desired *E,Z*-diene **150** was obtained in 80% yield by Lindlar reduction of **151**, followed of deprotection of hydroxyl group in acid medium (Scheme 20). The Sharpless asymmetric aminohydroxylation¹⁵³ (AA) and tethered aminohydroxylation¹⁵⁴ (TA) allows the catalytic and diastereoselective synthesis of aminoalcohols. However, in AA persist the drawbacks of regioselectivity during the oxidation of unsymmetrical alkenes. This

¹⁵³ (a) Li, G.; Chang, H.-T.; Sharpless, K. B. *Angew. Chem. Int. Ed. Engl.* **1996**, *35*, 451. For review, see: (b) Bodkin, J. A.; McLeod, M. D. *J. Chem. Soc. Perkin Trans. 1* **2002**, 2733–2746.

¹⁵⁴ (a) Donohoe, T. J.; Helliwell, M.; Johnson, P. D.; Keenan, M. *Chem. Commun.* **2001**, 2078–2079. (b) Donohoe, T. J.; Cowley, A.; Johnson, P. D.; Keenan, M. *J. Am. Chem. Soc.* **2002**, *124*, 12934–12935. (c) Donohoe, T. J.; Johnson, P. D.; Pye, R. J. *Org. Biomol. Chem.* **2003**, *1*, 2025–2028. (d) Donohoe, T. J.; Johnson, P. D.; Keenan, M.; Pye, R. J. *Org. Lett.* **2004**, *6*, 2583–2585. (e) Donohoe, T. J.; Chughtai, M. J.; Klauber, D. J.; Griffin, D.; Campbell, A. D. *J. Am. Chem. Soc.* **2006**, *128*, 2514–2515.

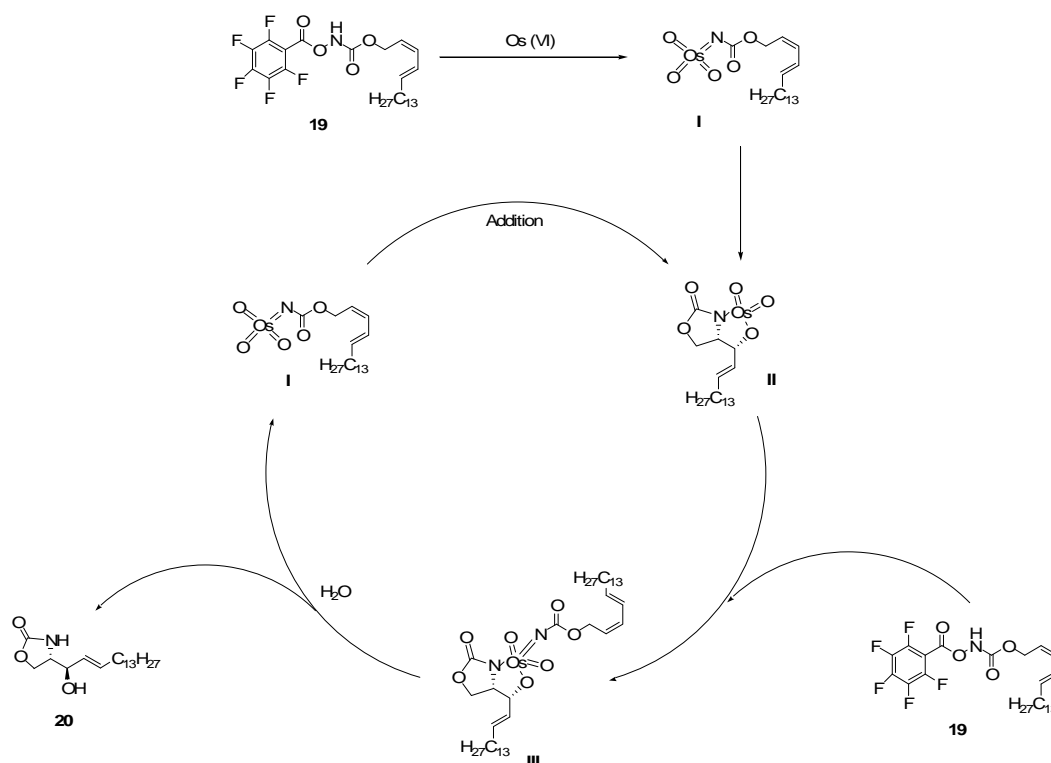
inconvenient can be avoided through the use of TA. At this point of the synthesis, we were interested in extending the TA methodology¹⁵⁵ as a general strategy in order to aminohydroxylate the double bond. Thus, the *E,Z*-diene **150** was reacted with carbonyldimidazol (CDI) in the presence of pyridine, followed by the addition of hydroxylamine hydrochloride, to give the hydroxycarbamate **156**. The latter was treated with *O*-pentafluorobenzoyl chloride (C_6F_5COCl), to yield the hydroxycarbamate **157**, which was then reacted under aminohydroxylation conditions (TA), to give oxazolidinone **148** in 85% yield with complete regio- and stereoselectivity. Alkaline hydrolysis of **148** afforded racemic sphingosine **19** in quantitative yield (Scheme 20).



Scheme 20. Synthesis of sphingosine **19** using a tethered aminohydroxylation reaction as key step

In terms of mechanism, it has suggest that the carbamate **157** (a nitrene equivalent), combines with potassium osmate (OsVI) to form the active osmium species **I**, which then adds to the alkene to form the azaglycolate species **II**. The osmium is first reoxidised through the addition of a second nitrene equivalent **157** to form a second glycolate species **III**. The hydrolysis of the glycolate species **III** releases the hydroxyamination product **148** and regenerates the initial active osmium species **I**, so completing the catalytic cycle (Scheme 21).

¹⁵⁵ Donohoe, T. J.; Bataille, C. J. R; Gattrell, W.; Kloesges, J.; Rossignol, E. *Org. Lett.* **2007**, *9*, 1725–1728.



Scheme 21. Proposed mechanism for the TA reaction

To rationalize the key step in the intramolecular addition, the model **A** (Figure 19) which supports the *syn* selectivity observed during the reaction, is proposed. By X-ray crystallography it has been shown that related transition-metal complexes form linear metal-nitrogen-carbon arrangements (with the metal forming a double bond to an acyl-substituted nitrogen).¹⁵⁶ Thus, such a linear arrangement is present during the TA reaction (Figure 19). The nitrogen and oxygen then overlap with the π -orbitals of the alkene, with deformation of the linear (C=N=Os) arrangement occurring as the reaction proceeds

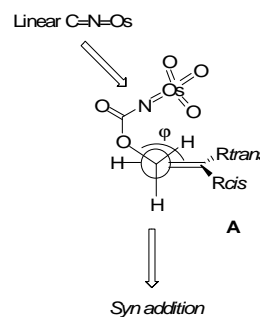


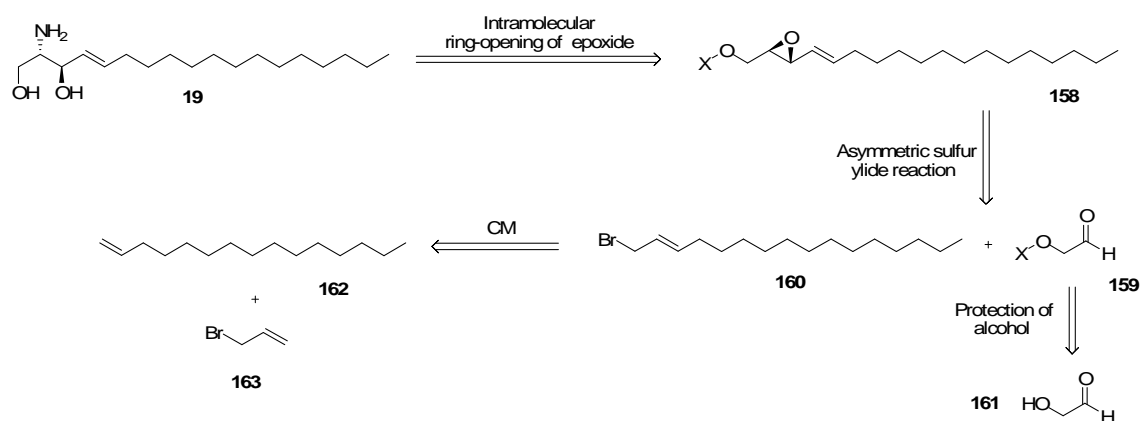
Figure 19. Transition states to rationalize the *syn* selectivity observed during the TA reaction

¹⁵⁶ Thomas, S.; Lim, P. J.; Gable, R. W.; Young, C. G. *Inorg. Chem.* **1998**, *37*, 590–593.

to furnish an azaglycolate osmate ester. A consequence of starting with a linear osmium-nitrogen-carbon bond is that the initial dihedral angle ϕ required to give good orbital overlap between the oxidant and alkene must be large. Therefore, only one reactive conformation need be considered, which lead to the *syn* product (Figure 19).

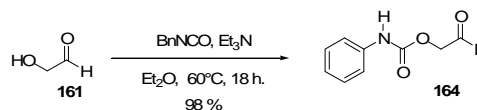
3.1.3.2 Synthesis of *D-erythro*-sphingosine employing an asymmetric sulfur ylide reaction as key step

In the present study, we report a convenient and concise route for the synthesis of *D-erythro*-sphingosine **19**. Based on the retrosynthetic analysis depicted in Scheme 21, compound **19** could be generated from the corresponding epoxide **158** via an intramolecular ring-opening to introduce the amino functionality at C-2. The selectivity of the intermolecular opening is controlled by the double bond and affords the 3-amino derivative. For synthesising epoxide **158** we envisaged an asymmetric reaction between a chiral sulfur ylide obtained from bromide **160** and aldehyde **159**, which can incorporate the nucleophile (X) for epoxide opening in its structure. The aldehyde **159** is readily prepared from the alcohol **161**. Lipophilic chain part **160** should be available from alkenes **162** and allyl bromide **163** by means of cross-metathesis (CM) reaction in order to introduce the required *E*-olefin moiety (Scheme 22).



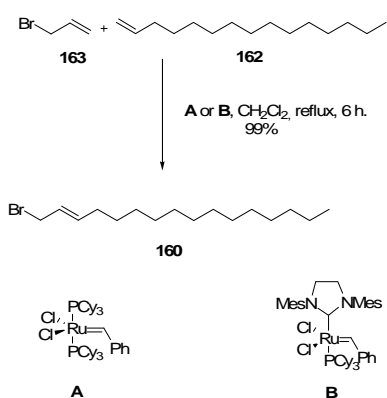
Scheme 22. Retrosynthetic analysis of *D-erythro*-sphingosine **19**

As shown in Scheme 23, the synthesis started with the protection of hydroxyaldehyde **161** as a carbamate, since it is appropriate for opening the epoxide in a subsequent step. Thus, aldehyde **164** for asymmetric sulfur ylide reaction was obtained in excellent yield by reaction of hydroxyaldehyde **161** and benzyl isocyanate (1.5 equiv) in presence of Et₃N, employing Et₂O as solvent.



Scheme 23. Synthesis of carbamate **164**

In the other hand, the high *E*-selectivity and the functional tolerance are attractive features of cross-metathesis olefination in the synthesis of natural products.¹⁵⁷ In recent synthesis of sphingosines and phytosphingosines, CM has been used as carbon chain elongation strategy.¹⁵⁸ Therefore, we reasoned that a cross metathesis reaction of alkene



Scheme 24. Synthesis of allyl bromide **160** by cross-metathesis

162 and allyl bromide **163** and in presence of Grubbs' ¹⁵⁹ catalyst will provide the intermediate **160** with the correct configuration. Thus, substrate **163** was stirred with 4 equiv of olefin **162** and 0.02 equiv of second generation Grubbs' **B** in CH₂Cl₂ for 8 h at reflux. The reaction proceeded smoothly, and desired coupling product **160** was obtained in 97% yield with an *E:Z* selectivity of 52:1. The homocoupling product of **163** was not observed in its ¹H NMR. In this case

the use of Ti(OiPr)₄ or other additive was not necessary to obtain excellent results. A decrease in the selectivity (*E:Z* 11:1) and the yield (78%) was observed when the first generation Grubbs' catalyst **A** was employed under similar conditions (Scheme 24).

¹⁵⁷ For review, see: (a) Franck, R. W.; Tsuji, M. *Acc. Chem. Res.* **2006**, *39*, 692–701. (b) Prunet, J. *Curr. Top. Med. Chem.* **2005**, *5*, 1559–1577. (c) Cannon S. J.; Blechert, S. *Angew. Chem Int. Ed.* **2003**, *42*, 1900–1923.

¹⁵⁸ (a) Yamamoto, T.; Hasegawa, H.; Hakogi T.; Katsumura, S. *Org. Lett.* **2006**, *8*, 5569–5572. (b) Lombardo, M.; Capdevila, M. G.; Pasi F.; Tombini, C. *Org. Lett.* **2006**, *8*, 3303–3305. (c) Chaudhari, V. D.; Kumar K. S. A.; Dhavale, D. D. *Org. Lett.* **2005**, *7*, 5805–5807. (d) Torrsell S.; Somfai, P. *Org. Biomol. Chem.* **2004**, *2*, 1643–1646. (e) Rai A. N.; Basu, A. *Org. Lett.* **2004**, *6*, 2861–2863. (f) Singh, O. V.; Kampf D. J.; Han, H. *Tetraheron Lett.*, **2004**, *45*, 7239–7242.

¹⁵⁹ Trnka T. M.; Grubbs, R. H. *Acc. Chem. Res.* **2001**, *34*, 18–29.

The key step is the synthesis of the epoxide **167** with control of the configuration of the stereogenic centers at C-2 and C-3 by using the stoichiometric sulphur ylide reaction, which is the particular interest because of the valuable synthetic intermediate that have been generated using this reaction.¹⁶⁰ The sequence developed to prepare epoxide **167** is summarized in scheme 25. Sulfide **165** was selected as chiral auxiliary¹⁶¹ in order to prepare the corresponding chiral sulphur ylide. Reaction of sulfide **165** (1 equiv) with allyl bromide **160** (1.2 equiv) in CH₂Cl₂ and in the presence of AgBF₄ (4 equiv) afforded the required sulfonium salt **166** in 80% yield.¹⁶² Subsequent treatment of the salt **166** with EtP₂ base (1.1 equiv) and the aldehyde **164** (1.1 equiv) furnished the desired epoxide **167** in 60% yield. Crucial to the success of the reaction were conditions that favoured the formation of stabilized ylide **168** employing the EtP₂ base at -78 °C in CH₂Cl₂ (Scheme 25).

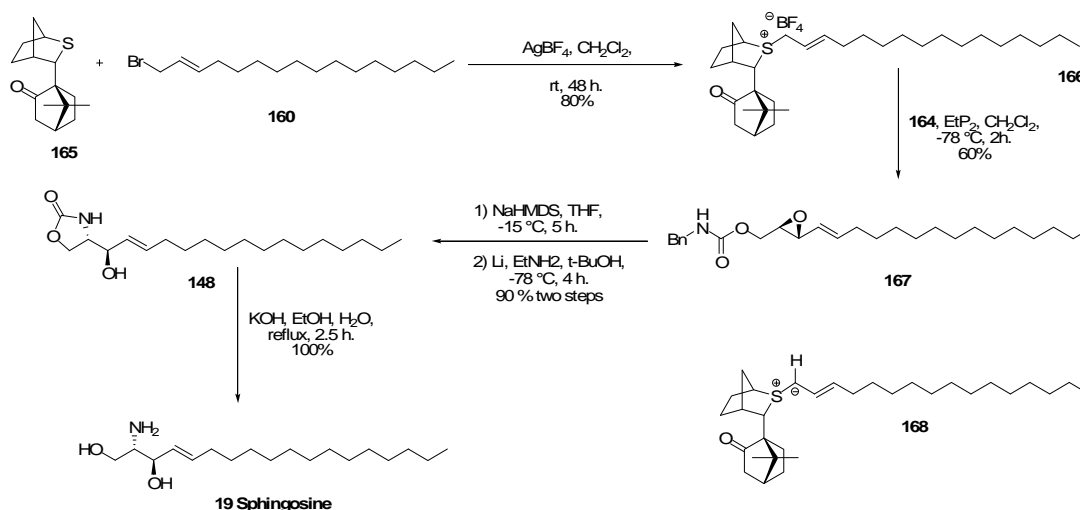
To complete the synthesis (Scheme 25), a highly regioselective intramolecular ring-opening of epoxide **167** was carried out under basic conditions. A complementary chemoselectivity occurred with the internal delivery of a nitrogen nucleophile to the epoxide α -position. Thus, the intermediate **167** was converted to oxazolidinone **148** by first treatment with NaHMDS (1.5 equiv) at -20 °C in THF.¹⁶³ Then, elimination of the benzyl group employing Li (excess) and EtNH₂/t-BuOH at -78 °C gave **148** in 90% yield over two steps. Finally, alkaline hydrolysis of oxazolidinone **148** with KOH at reflux for 2.5 h, allow to obtain *D-erythro*-sphingosine **19** in quantitative yield. Synthetic **19** gave mp 72-74 °C (lit^{158d} mp 72-75 °C), [α]_D = -1.6.0 (lit^{158d} [α]_D = -1.6) 400 MHz ¹H and 125 MHz ¹³C NMR spectroscopic data were consistent with data report for the natural product. The match of optical rotation values indicates that the formation of the epoxide **167** was completely stereoselective.

¹⁶⁰ For a general review about asymmetric sulfur ylide reaction see: (a) McGarrigle, E. M.; Myers, E. L.; Illa, O.; Shaw, M. A.; Riches S. L.; Aggarwal, V. K. *Chem. Rev.* **2007**, *107*, 5841–5883. (b) Fulton, J. R.; Aggarwal V. K.; de Vicente, J. *Eur. J. Org. Chem.* **2005**, 1479–1492. (c) Aggarwal V. K.; Winn, C. L. *Acc. Chem. Res.* **2004**, *37*, 611–620. (d) Aggarwal V. K.; Richardson, J. *Chem. Commun.* **2003**, 2644–2651. (e) Li, A.-H.; Dai L.-X.; Aggarwal, V. K. *Chem. Rev.* **1997**, *97*, 2341–2372.

¹⁶¹ Aggarwal, V. K.; Fang, G.; Kokotos, C. G.; Richardson J.; Unthank, M. G. *Tetrahedron* **2006**, *62*, 11297–11303.

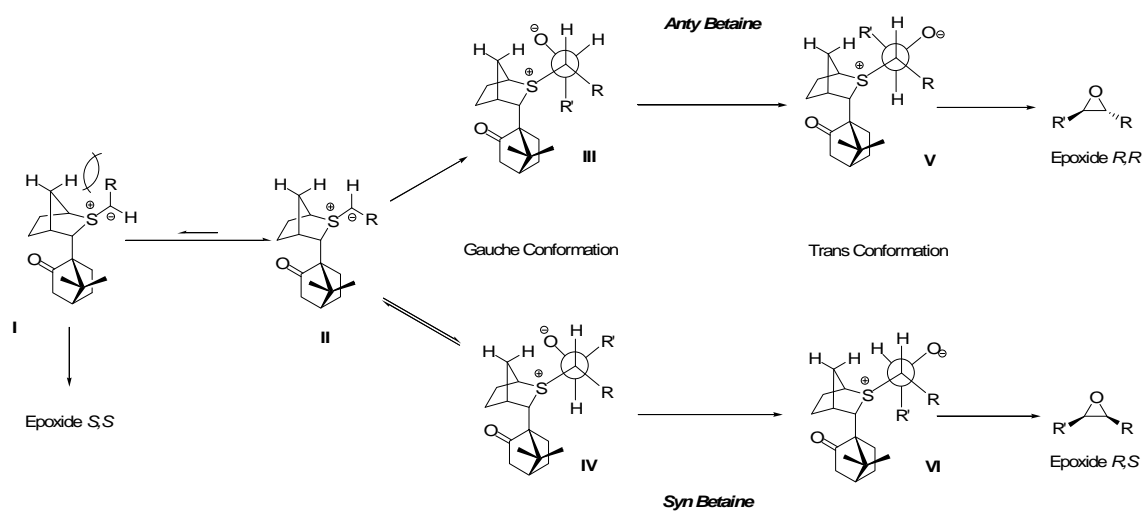
¹⁶² Aggarwal, V. K.; Bae, I.; Lee, H.-Y.; Richardson J.; Williams, D. T. *Angew. Chem. Int. Ed.* **2003**, *42*, 3274–3278

¹⁶³ (a) Bew, S. P.; Bull, S. D.; Davies, S. G.; Savory E. D.; Waltkin, D. J. *Tetrahedron*, **2002**, *58*, 9387–9401. (b) Roush W. R.; Adam, M. A. *J. Org. Chem.*, **1985**, *50*, 3752–3757. (c) Bernet B.; Vasella, A. *Tetrahedron Lett.* **1983**, *24*, 5491–5494. (c) Julina, R.; Herzig, T.; Bernet B.; Vasella, A. *Helv. Chim. Acta*, 1986, **69**, 368–373



Scheme 25. Synthesis of sphingosine 19

The mechanism of epoxidation involves three distinct steps: i) formation of the betaine with charges adjacent to each other, ii) followed by bond rotation to the *trans*-conformation, and finally iii) ring closure (Scheme 26). The high enantioselectivity observed is a consequence of ylide conformer **II** being strongly favoured over conformer **I** owing to 1,4-steric interactions and essentially complete preference for *Si*-face attack, as the *Re* face of the ylide is hindered by the bulky camphor moiety. The diastereoselectivity obtained in depend on the degree of reversibility of the formation of the betaine intermediates arising from the attack of the sulphur ylide on the carbonyl group of the aldehyde. The addition of the ylide to the aldehyde occurs in a “cisoid” manner, which is preferred due to favourable Coulombic interactions, and two rotamers of the *anti*- and *syn*-betaines could be formed (**III** y **IV** Scheme 26). The high *trans* selectivity observed is a consequence of nonreversible formation of the *anti* betaine **III** and the unproductive, reversible formation of *syn* betaine **IV**. Finally, C-C bond rotation to lead to rotamer **V**, followed to the ring-closure step from the *anti*-periplanar rotamers furnished the *trans*-epoxide (Scheme 26).



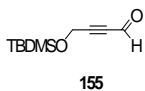
Scheme 26. Proposed mechanism for the asymmetric sulfur ylide reaction

3.1.4 Experimental Part

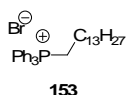
General methods

All reactions were conducted under a dried argon stream. Solvents (CH₂Cl₂ 99.9%, toluene 99.9%) were purchased in capped Pure Solv System-4[®] bottles and used without further purification and stored under argon. Yields refer to the chromatographically and spectroscopically (¹H and ¹³C) homogeneous materials, unless otherwise stated. All other solvents and reagents were used without further purification. All glassware utilized was flame-dried before use. Reactions were monitored by TLC carried out on 0.25 mm E. Merck silica gel plates. Developed TLC plates were visualized under a short-wave UV lamp and by heating plates that were dipped in ethanol/H₂SO₄ (15:1). Flash column chromatography (FCC) was performed using flash silica gel (32–63 μm) and employed a solvent polarity correlated with TLC mobility. Melting points, determined with Reichert apparatus, are uncorrected. Optical rotations were measured at 598 nm on a Jasco DIP-370 digital polarimeter using a 100 mm cell. NMR experiments were conducted on a Varian 400 MHz instrument using CDCl₃ (99.9% D) as the solvent, with chemical shifts (δ) reference to internal standards CDCl₃ (7.26 ppm ¹H, 77.23 ppm ¹³C) or Me₄Si as an internal reference (0.00 ppm) Chemical shifts are relative to the deuterated solvent peak and are in parts per million (ppm).

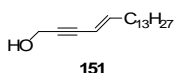
Experimental Procedures



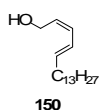
4-[(1,1-Dimethylethyl)dimethylsilyloxy]but-2-yn-1-al 155. To a solution of alcohol **154** (1.50 g, 7.48 mmol) in dry CH₂Cl₂ (100 mL) was added barium manganate (9.00 g, 37.4 mmol), and the mixture was stirred at room temperature for 3.5 h. Filtration of the mixture through a pad of Celite and evaporation of the filtrate *in vacuo* gave aldehyde **155** (1.40 g, 95%) as an oil. The unstable aldehyde was used in the next step without purification: ¹H NMR (400, MHz, CDCl₃): δ 9.6 (1H, s), 4.4 (2H, s), 0.8 (9H, s), 0.1 (6H, s).



Tetradecyltriphenylphosphonium bromide 153. A mixture of triphenylphosphine (8.51 g, 0.032 mmol) and 1-bromotetradecane (10.00 g, 0.036 mL) was heated at 140 °C for 7 h. The reaction mixture was cooled, and tetradecyltriphenylphosphonium bromide **153** was crystallized from acetone/ether (17.00 g, 92%), mp 96-98 °C. ¹H NMR (400 MHz, CDCl₃): δ: 7.29-7.91 (15H, m), 3.77 (2H, m), 1.62 (2H, m), 1.23 (11H, s), 1.19 (11H, s), 0.87 (3H, t, *J*=6.7 Hz). Anal. Calcd for C₃₂H₄₄BrP: C, 71.23; H, 8.21. Found: C, 71.54; H, 8.11.

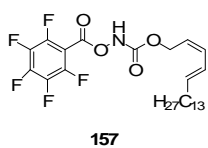


Octadeca-4(E)-en-2-yn-1-ol 151. To a solution of tetradecyltriphenylphosphonium bromide **153** (3.90 g, 7.21 mmol) in anhydrous THF (25 mL) at -78 °C was added 1.55 M *n*-butyllithium in hexane (5.1 mL, 7.95 mmol). The mixture was stirred for 1.5 h at -30 °C. The orange-red reaction mixture was cooled to -78 °C, and aldehyde **155** (1.1g, 5.54 mmol) in anhydrous THF (25 mL) was added. The mixture was stirred for 2 h at -78 °C, and 1.55 M *n*-butyllithium in hexane (5.1 mL, 7.95 mmol) was added. The resulting dark red solution was stirred at -30 °C for 1 h and was diluted with ether (10 mL) and methanol (3 mL). The resulting solution was stirred for 3 h at room temperature. Then, 3.5 N HCl was added until pH 4 was reached, and the mixture was stirred for 22 h. The reaction mixture was diluted with water and extracted with ether (3 x 40 mL). The organic phase was dried and concentrated in *vacuo*. The residue was purified by flash column chromatography on silica gel using hexane-AcOEt-MeOH (80:20) as the eluent to give 154 mg of pure alcohol **151** (75 %). TLC (Hexane-AcOEt 60:40) *R*_f 0.60; m.p. 104–106 °C; ¹H NMR (400 MHz, CDCl₃): δ 6.17 (1H, dd, *J*=15.8, 7.0, Hz), 5.49 (1H, dd, *J*=15.0, 1.7 Hz, Hz), 4.38 (2H, dd, *J*=5.9, 1.6, Hz), 1.54 (2H, q, *J*=6.0 Hz), 1.37(2H, m), 1.26 (18H, m), 0.89 (3H, t, *J*=6.9 Hz); ¹³C NMR (100.6 MHz, CDCl₃): δ 145.8, 108.7, 85.5, 84.6, 51.6, 33, 31.9, 29.6, 29.5, 29.4, 29.3, 29, 28.6, 22.6, 14. Anal. Calcd for C₁₈H₃₂O: C, 81.55; H, 12.19. Found: C, 81.75; H, 12.03.



Octadeca-2(Z),4(E)-dien-1-ol 150. A mixture of propargyl alcohol **151** (0.850 g, 3.21 mmol), dry toluene (25 mL), and Lindlar catalyst (0.100 g) was stirred at room temperature under an atmosphere of hydrogen until TLC indicated the disappearance of

the starting material (-3 h). The reaction mixture was filtered through a Celite pad, and the filtrate was concentrated *in vacuo*. The residue was purified by flash column chromatography on silica gel using hexane-AcOEt (80:20) as the eluent to give 684 mg of pure alcohol **150** (80 %) as a colorless oil. TLC (Hexane-AcOEt 60:40) R_f 0.50; ^1H NMR (400 MHz, CDCl_3): δ 6.38 (1H, m), 6.31 (1H, m), 6.24 (1H, m), 5.58 (1H, m), 4.31 (2H, d, $J=6.8$ Hz), 2.09 (2H, m), 1.26 (22H, m), 0.88 (3H, t, $J=6.7$ Hz); ^{13}C NMR (100.6 MHz, CDCl_3): δ 137.6, 131.3, 127, 124.7, 58.8, 32.8, 31.9. Calcd for $\text{C}_{18}\text{H}_{34}\text{O}$: C, 81.13; H, 12.86. Found: C, 81.19; H, 12.01.

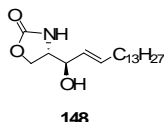


Carbamate 157. *N,N*-Carbonyldiimidazole (182 mg, 1.12 mmol) was added to alcohol **150** (200 mg, 0.75 mmol) in pyridine (20 mL) at 40 °C. When adduct between the alcohol and the *N,N*-carbonyldiimidazole was totally formed, hydroxylamine hydrochloride (130 mg, 1.87 mmol) was

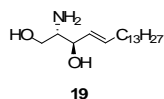
added. The resulting reaction mixture was stirred for 24 h at 40 °C, it was quenched with hydrochloric acid (1M, 10 mL), and finally AcOEt (10 mL) was added. After separation of organic phase, the aqueous phase was extracted with AcOEt (2 x 10 mL). The combined organic layers were then washed sequentially with water (10 mL) and brine (3 x 10 mL) dried (NaSO_4), filtered and the solvent was azeotropically removed with toluene. The crude product was purified by flash column chromatography on silica gel using hexane/AcOEt (85:15) as the eluent to give **156**, which was used directly into next step.

A solution of **156** (243 mg, 0.75 mmol), and Et_3N (83 mg, 0.82 mmol) in 20 mL of dry Et_2O was cooled to 0 °C. The acid chloride *O*-PFB-COCl (172 mg, 0.75 mmol) in 10 mL of dry Et_2O was added drop wise over 1 h at 0 °C, and then the reaction was stirred under argon for 12 h at room temperature. The reaction was quenched with HCl (1M aq. sol., 10 mL) and the aqueous layer was extracted with Et_2O (3 x 10 mL). The combined organic layers were washed sequentially with HCl (10 % aqueous, 1 x 10 mL), NaHCO_3 (7 % aqueous, 1 x 10 mL), and brine (3 x 10 mL). The organic layer was dried over MgSO_4 and concentrated *in vacuo*. The residue was purified by flash column chromatography on silica gel using hexane/AcOEt (85:15) as the eluent to give 270 mg of **157** (70 %) as a clear oil. ^1H NMR (400, MHz, CDCl_3): δ 8.36 (1H, s), 6.3 (1H, dd, $J=13.8, 11.1$ Hz), 6.15 (1H, dd, $J=11.1, 10.6$, Hz), 5.8 (1H, dq, $J=13.8, 6.6$ Hz), 5.4 (1H,

dt, $J=10.6, 7.1$ Hz), 4.73 (2H, d, $J=7.1$ Hz), 2.12 (2H, q, $J=7.0$ Hz), 1.37-1.2 (22H, m), 0.85 (3H, t, $J=6$ Hz); ^{13}C NMR (100.6 MHz, CDCl_3): δ 158.5, 155.7, 148.9, 147.2, 145.6, 143.0, 138.4, 133.1, 124.5, 121.9, 61.1, 32.8, 31.9, 29.6, 29.5, 29.4, 29.3, 29.2, 29.1, 22.6, 14.0. Anal. Calcd. For $\text{C}_{26}\text{H}_{34}\text{F}_5\text{NO}_4$: C, 60.11; H, 6.60; F, 18.28; N, 2.70; O, 12.32. Found: C, 60.13; H, 6.59; N, 2.72.

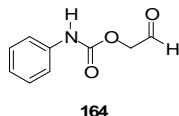


Oxazolidinone 148. To a solution of **157** (250 mg, 0.48 mmol) in a mixture *t*-butanol/water (3:1, 10 mL/mmol) was added dropwise a solution of potassium osmate dihydrate (1.8 mg, 1 mol%) in water (0.25 mL). After, the resulting reaction mixture was stirred for 12 h at room temperature. The reaction was quenched by addition of sodium sulphite (100 mg, mmol), allowed to stir for 30 minutes and then, the solvent azeotropically removed with toluene. The crude product was purified by flash column chromatography on silica gel using hexane/AcOEt (85:15) as the eluent to give 132 mg of **148** (85 %) as a white solid. ^1H NMR (400, MHz, CDCl_3): δ 6.10 (1H, s), 5.83 (1H, ddt, $J = 15.4, 6.8, 0.8$ Hz), 5.37 (1H, ddt, $J=15.4, 6.8, 1.2$ Hz), 4.39 (1H, dd, $J=8.8, 8.5$ Hz), 4.33 (1H, dd, $J=8.8, 5.2$ Hz), 4.12 (1H, m), 3.86 (1H, m), 2.92 (1H, br s), 2.04 (2H, q, $J=7.0$ Hz), 1.37-1.2 (22H, m), 0.81 (3H, t, $J=6.8$ Hz); ^{13}C NMR (100.6 MHz, CDCl_3): δ 160.5, 136.6, 126.6, 73.3, 66.4, 56.4, 32.5, 32.1, 29.81, 29.79, 29.74, 29.6, 29.5, 29.4, 29.1, 22.8, 14.2. Anal. Calcd. For $\text{C}_{19}\text{H}_{35}\text{NO}_3$: C, 70.11; H, 10.84; N, 4.30; O, 14.75. Found: C, 70.19; H, 10.80; N, 4.32.

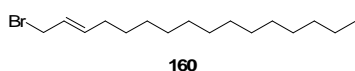


Sphingosine 19. Oxazolidone **148** (100 mg, 0.30 mmol) in 1 M KOH (5 mL, $\text{H}_2\text{O}:\text{EtOH}$ 1:1) was heated to reflux for 2.5 h, cooled to room temperature and then 2 M HCl (2.5 mL) was added. The mixture was extracted with EtOAc (3 x 10 mL) and the combined organic layers were dried over MgSO_4 and concentrated *in vacuo* giving **19** (89 mg, 100 %) as a white solid. TLC (Hexane-AcOEt-MeOH 60:30:10) R_f 0.70; m.p. 104–106 °C; ^1H NMR (400, MHz, CDCl_3): δ 5.76 (dt, 1H, $J=15.4, 6.7$ Hz), 5.47 (dd, 1H, $J=15.4, 7$ Hz), 4.11 (m, 1H), 3.70 (dd, 1H, $J=11, 3$ Hz), 3.65 (dd, 1H, $J=11, 5.8$ Hz), 2.92 (m, 1H), 2.05 (dt, 2H, $J=6.7, 7.3$ Hz), 1.37 (m, 2H), 1.20–1.40 (m, 20H), 0.88 (t, 3H, $J=6.9$ Hz); ^{13}C NMR (100.6 MHz, CDCl_3): δ 134.7, 128.8, 74.7, 63.3, 56.3, 32.5, 31.9, 29.7–29.2,

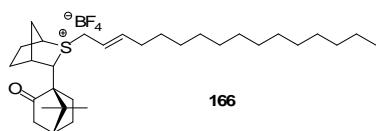
22.7, 14.1. Anal. Calcd. For $C_{18}H_{37}NO_2$: C, 72.19; H, 12.45; N, 4.68; O, 10.68. Found: C, 72.21; H, 12.41; N, 4.70.



Formylmethyl phenylcarbamate 164. To a solution of 2-hydroxyacetaldehyde **161** (184 mg, 3.06 mmol) in 15 mL of dry Et_2O was added freshly distilled Et_3N (10.16 mmol) followed by $BnNCO$ (647 mg, 4.8 mmol). The resultant mixture was heated to $60\text{ }^\circ\text{C}$ in a sealed tube for 17 h, cooled to room temperature and quenched with saturate NH_4Cl (10 mL). The phases were separated and the aqueous layer was extracted with CH_2Cl_2 (2 x 10 mL). The organic layer was dried over $MgSO_4$ and concentrated *in vacuo*. The residue was purified by flash column chromatography on silica gel using hexane-AcOEt (85:15) as the eluent to give 580 mg of pure formylmethyl phenylcarbamate **164** (98 %) as an oil. TLC (Hexane-AcOEt 80:10) R_f 0.70; 1H NMR (400 MHz, $CDCl_3$): δ 9.67 (1H, t, $J=0.7$ Hz), 7.35-7.21 (5H, m), 5.08 (1H, br s) 4.89 (2H, d, $J=0.7$ Hz) 4.4 (2H, d, $J=5.5$); ^{13}C NMR (100.6 MHz, $CDCl_3$): δ 194.2, 153.6, 136.9, 128.5, 124.4, 121.6, 69.5. Anal. Calcd. For $C_{10}H_{11}NO_3$: C, 62.17; H, 5.74; N, 7.25. Found: C, 62.15; H, 5.75; N, 7.26.

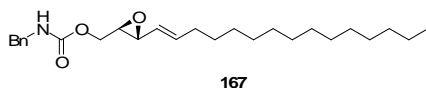


(E)-1-bromohexadec-2-ene 160. To a solution of allyl bromide **163** (240 mg, 0.15 mmol) in 40 mL of dry CH_2Cl_2 was added pentadec-1-ene **162** (1.68 g, 8 mmol). A mixture of catalyst **B** (8 mg, 2%) and 20 mL of CH_2Cl_2 was added, with stirring, at a rate sufficient to reach and maintain refluxing. After the addition was completed, the reaction mixture was kept boiling for 6 h and then cooled to room temperature and concentrated *in vacuo*. The residue was purified by flash column chromatography on silica gel using hexane-AcOEt (98:2) as the eluent to give 590 mg of pure (E)-1-bromohexadec-2-ene **160** (97 %) as colourless oil and with *E:Z* selectivity of 52:1. TLC (Hexane) R_f 0.60; 1H NMR (400 MHz, $CDCl_3$): δ 5.78 (1H, dt, $J=14.8, 7.6$ Hz), 5.68 (1H, dt, $J=14.8, 7.2$ Hz), 3.96 (2H, d, $J=7.6$ Hz), 2.03 (2H, q, $J=7.2$ Hz), 1.34-1.20 (22H, m), 0.86 (3H, t, $J=6.9$ Hz); ^{13}C NMR (100.6 MHz, $CDCl_3$): δ 137, 126.3, 34, 32.3, 32.1, 29.8, 29.6, 29.5, 29.3, 29, 22.9, 14.3. Anal. Calcd. for $C_{16}H_{31}Br$: C, 63.36; H, 10.30. Found: C, 63.34; H, 10.31.



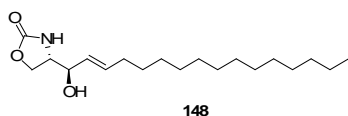
Sulfonium salt 166. To a rapidly stirred solution of chiral sulfide **165** (82 mg, 0.33 mmol) and (*E*)-1-bromohexadec-2-ene **160** (100 mg, 0.33 mmol) in 10 mL CH₂Cl₂ was

added silver tetrafluoroborate (194 mg, 0.99 mmol) in the dark under an argon atmosphere at room temperature. The reaction stirred for 48 h and 10 mL of CH₂Cl₂ was added. Silver bromide precipitate was filtered and the filtrate was concentrated *in vacuo*. The residual brown oil was recrystallized from CH₂Cl₂ and Et₂O to give sulfonium salt **166** as a white precipitate which was used directly into next step.



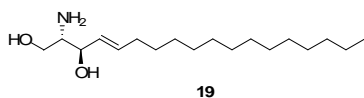
((2*R*,3*R*)-3-((*E*)-pentadec-1-enyl)oxiran-2-yl)methyl benzylcarbamate 167. To a stirred solution of sulfonium salt **166** (465 mg, 0.83 mmol) in 5 mL of CH₂Cl₂ was

added *N,N,N',N'*,-tetramethyl-*N''*-[tris(dimethylamino)phosphoraldidene]phosphoric triamide ethylimine (415 mg, 1.22 mmol) at -78 °C under argon. After 45 min, a mixture of 20 mL of CH₂Cl₂ and formylmethyl phenylcarbamate **164** (240 mg, 1.25 mmol) was added to the solution. After 2 h stirring, the mixture was warmed up to room temperature and then saturated NaCl solution (10 mL) was added. The phases were separated and the aqueous layer was extracted with AcOEt (2 x 10 mL). The organic layer was dried over MgSO₄ and concentrated *in vacuo*. The residue was purified by flash column chromatography on silica gel using hexane-AcOEt (85:15) as the eluent to give 192 mg of pure epoxide **167** (60 %). Compound **165** (180 mg, 87%) was also recovered. TLC (Hexane-AcOEt 70:30) *R*_f 0.60; [α]_D +15.0 (*c* 0.5 in CHCl₃); ¹H NMR (400 MHz, CDCl₃): δ 7.37-7.26 (5H, m), 5.73 (1H, dt, *J*=14.8, 6.5 Hz), 5.10 (1H, dd, *J*=14.8, 9.1 Hz), 5.01 (1H, br s), 4.47 (1H, dd, *J*=12.2, 3.1 Hz), 4.39 (2H, d, *J*=6), 4.05 (1H, dd, *J*=12.2, 6.3 Hz), 3.30 (1H, dd, *J*=9.1, 2.4), 3.15 (1H, ddd, *J*=6.3, 3.1, 2.4 Hz), 2.03 (2H, q, *J*=6.5 Hz), 1.37-1.20 (22H, m), 0.81 (3H, t, *J*=6.8 Hz); ¹³C NMR (100.6 MHz, CDCl₃): δ 156.0, 138.4, 134.6, 128.8, 127.7, 127.6, 120.3, 64.9, 57.6, 56.5, 45.2, 32.5, 32.1, 29.8, 29.6, 29.5, 29.4, 29.3, 22.8, 14.3. Anal. Calcd. for C₂₆H₄₁NO₃: C, 75.14; H, 9.94; N, 3.37. Found: C, 75.12; H, 9.95, N, 3.36.



(S)-4-((R,E)-1-hydroxyhexadec-2-enyl)oxazolidin-2-one 148.

To a stirred solution of epoxide **167** (220 mg, 0.57 mmol) in 15 mL of THF at -15 °C was added dropwise NaHMDS (0.57 mmol, 1 M in THF). The resultant mixture was slowly allowed to reach 0 °C (5 h) and then quenched by addition of saturate NH₄Cl (10 mL). The phases were separated and the aqueous layer was extracted with AcOEt (2 X 10 mL). The organic layer was dried over MgSO₄ and concentrated *in vacuo*. The residue was used directly into next step. Thus, to a stirred mixture of Li (excess) and freshly EtNH₂ (45 mL) under argon at -78 °C was added a solution of first residue in dry 10 mL of Et₂O *via* syringe. solutionthis residue. The reaction mixture was stirred at -78 °C for 4 h and then carefully quenched with saturate NHCl₄. The phases were separated and the aqueous layer was extracted with AcOEt (2 X 10 mL). The organic layer was dried over MgSO₄ and concentrated *in vacuo*. The residue was purified by flash column chromatography on silica gel using hexane-AcOEt-MeOH (85:10:5) as the eluent to give 154 mg of pure oxazolidinone **148** (82 %). TLC (Hexane-AcOEt-MeOH 60:30:10) *R_f* 0.70; m.p. 104–106 °C; ¹H NMR (400, MHz, CDCl₃): δ 6.10 (1H, s), 5.83 (1H, ddt, *J*=15.4, 6.8, 0.8 Hz), 5.37 (1H, ddt, *J*=15.4, 6.8, 1.2 Hz), 4.39 (1H, dd, *J*=8.8, 8.5 Hz), 4.33 (1H, dd, *J*=8.8, 5.2 Hz), 4.12 (1H, m), 3.86 (1H, m), 2.92 (1H, br s), 2.04 (2H, q, *J*=7.0 Hz), 1.37-1.2 (22H, m), 0.81 (3H, t, *J*=6.8 Hz); ¹³C NMR (100.6 MHz, CDCl₃): δ 160.5, 136.6, 126.6, 73.3, 66.4, 56.4, 32.5, 32.1, 29.81, 29.79, 29.74, 29.6, 29.5, 29.4, 29.1, 22.8, 14.2. Anal. Calcd. For C₁₉H₃₅NO₃: C, 70.11; H, 10.84; N, 4.30; O, 14.75. Found: C, 70.19; H, 10.80; N, 4.32.

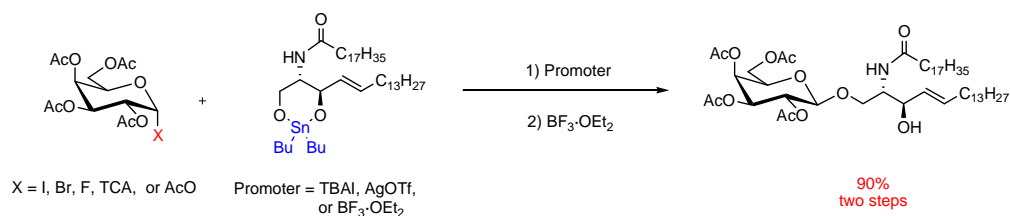


D-erythro-sphingosine 19. The mixture of oxazolidinone **148** (32 mg, 1.31 mmol) and 1 M KOH (20 mL, H₂O:EtOH 1:1) was heated to reflux for 2.5 h, cooled to room temperature and then 2 M HCl (10 mL) was added. The mixture was extracted with EtOAc (3 X 20 mL) and the combined organic layers were dried over MgSO₄ and concentrated *in vacuo* giving 30 mg of pure D-erythro-sphingosine **19** (100 %). TLC (Hexane-AcOEt-MeOH 60:30:10) *R_f* 0.70; m.p. 104–106 °C; ¹H NMR (400, MHz, CDCl₃): δ 5.76 (dt, 1H, *J*=15.4, 6.7 Hz), 5.47 (dd, 1H, *J*=15.4, 7 Hz), 4.11 (m, 1H), 3.70 (dd, 1H, *J*=11, 3 Hz),

3.65 (dd, 1H, $J=11$, 5.8 Hz), 2.92 (m, 1H), 2.05 (dt, 2H, $J=6.7$, 7.3 Hz), 1.37 (m, 2H), 1.20–1.40 (m, 20H), 0.88 (t, 3H, $J=6.9$ Hz); ^{13}C NMR (100.6 MHz, CDCl_3): δ 134.7, 128.8, 74.7, 63.3, 56.3, 32.5, 31.9, 29.7–29.2, 22.7, 14.1. Anal. Calcd. For $\text{C}_{18}\text{H}_{37}\text{NO}_2$: C, 72.19; H, 12.45; N, 4.68; O, 10.68. Found: C, 72.21; H, 12.41; N, 4.70.

3.2. Glycosylation of ceramides

β -Galactosyl ceramides have been obtained in excellent yields and stereoselectivities by reacting disarmed glycosyl donors with stannyl ethers. The broad compatibility of stannyl ethers with various leaving groups has been demonstrated



3.2.1. Strategy of glycosylation

With a stimulating biological background and the complicated availability of GSL's from natural sources,¹⁶⁴ many organic chemists have focused on developing methods for synthesizing GSLs.¹⁶⁵ The retrosynthetic analysis and the disassembly at the strategic glycosidic, amide and ester bonds reveal three important steps in the syntheses of β -GalCer: (i) attachment of the sphingosine moiety, (ii) *N*-acylation with the fatty acid and finally (iii) elimination of the protecting groups (Figure 20).

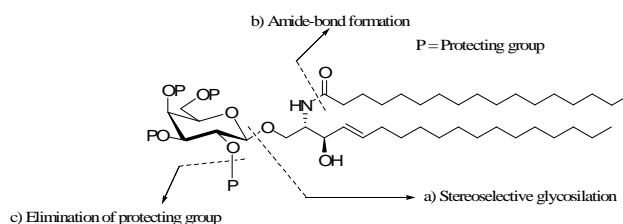


Figure 20. Retrosynthetic analysis of β -galactosylceramide

One of the main synthetic problems in the synthesis of glycosphingolipids is the glycosylation reaction,¹⁶⁶ which gives low yields when ceramides like **172** are directly used in the reaction. That has been attributed to the low nucleophilicity of ceramides,¹⁶⁷ which are extremely ordered as a result of the headgroup hydrogen bonding. This driving force for molecular self-assembly in ceramides allow have hexagonal and orthorhombic phases, structural organization similar in crystalline and hydrated states, with high stability.¹⁶⁸ This problem is usually circumvented by using azido-sphingosine **170**, but that requires further reduction of the azido group and acylation (Scheme 27).¹⁶⁹ The most classical and efficient glycosylation procedures that have been used in the GSLs synthesis include glycosyl trichloroacetamidates and fluorides.^{170,166} In these cases the stereochemistry of the reaction is determined by the participation of the neighbouring groups, solvent, and the kind of promoter.¹⁶⁶

¹⁶⁴ Schengrund, C.-L.; Ringler, N. J. *J. Biol. Chem.* **1989**, *264*, 13233–13237.

¹⁶⁵ (a) Howell, A. R.; So, R. C.; Richardson, S. K. *Tetrahedron* **2004**, *60*, 11327–11347. (b) Brodesser, S.; Sawatzki, P.; Kolter, T. *Eur. J. Org. Chem.* **2003**, 2021–2034. (c) Duclos, Jr. R. I. *Chem. Phys. Lipids*, **2002**, *111*, 111–138.

¹⁶⁶ For a review about the *O*-glycosylation of sphingosines and ceramides see: Morales-Serna, J. A.; Boutoureira, O.; Díaz, Y.; Matheu M. I.; Castellón, S. *Carbohydr. Res.* **2007**, *342*, 1595–1612.

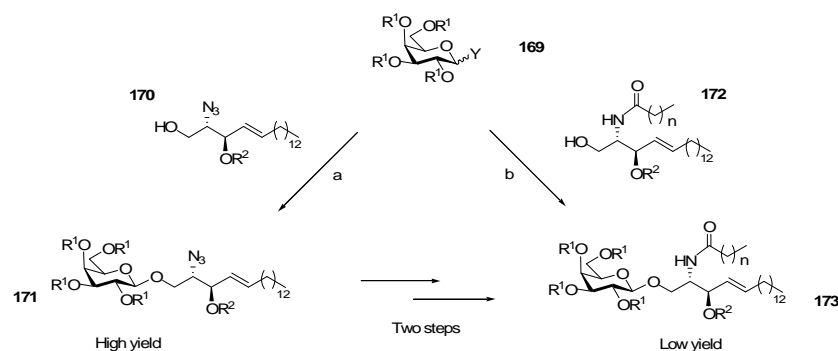
¹⁶⁷ (a) Polt, R.; Szabo, L.; Treiberg, J.; Li Y.; Hruby, V. J. *J. Am. Chem. Soc.* **1992**, *114*, 10249–10258.

(b) Schmidt R. R.; Zimmermann, P. *Angew. Chem. Int. Ed. Engl.* **1986**, *25*, 725–726.

¹⁶⁸ Rerek, M. E.; Chen, H.-C.; Markovic, B.; Van Wyck, D.; Gardiel, P.; Mendelsohn, R.; Moore, D. J. *J. Phys. Chem. B*, **2001**, *105*, 9335–9362.

¹⁶⁹ Schmidt, R. R.; Zimmermann, P. *Tetrahedron Lett.* **1986**, *27*, 481–484.

¹⁷⁰ (a) Pellissier, H. *Tetrahedron* **2005**, *61*, 2947–2993. (b) Toshima, K.; Tatsuta, K. *Chem. Rev.* **1993**, *93*, 1503–1531.



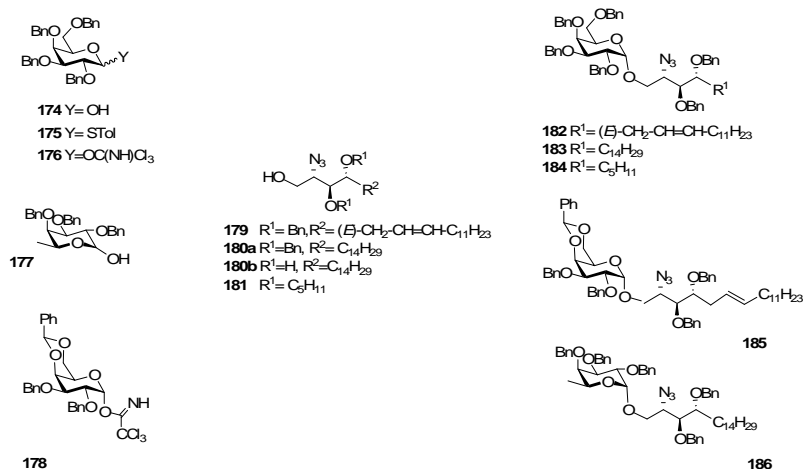
Scheme 27. Strategy of glycosilation

3.2.2. Recent contributions in the synthesis of α -glycosyl sphingosines and ceramides report in the literature (2000-2007)

3.2.2.1. Glycosylation of azido-sphingosines

As mentioned before, interest in α -glycosylceramides derives from the relevant biological properties of these products and particularly of those having phytosphingosine as a part of the ceramide moiety (α -GalCer). Consequently, most works are related with the synthesis of this compound and analogues. While formation of 1,2-*trans* glycosides can be easily achieved by taking advantage of neighbouring group assistance, such as *O*-acetyl or *O*-benzoyl at C-2, the stereospecific construction of 1,2-*cis* galactopyranosyl linkages has been one of the greatest challenges of glycoside synthesis. α -Gal-type linkages can be formed by working under thermodynamic conditions (anomeric effect), in appropriate solvents (ethereal solvent effect), and by using nonparticipating protecting groups at the C2 hydroxyl, typically benzyl groups. Glycosyl thichloroacetimidates are the most popular glycosyl donors for glycosylation of azidosphingosine, although SPh, OAc, and other leaving groups have also been used. In Table 1 are collected several examples of glycosylation of galactose derivatives with azidosphingosines.

Table 1. Synthesis of α -galactosyl-azido-sphingosines 182-186



Entry	Acceptor	Donor	Promoter	Solvent	Product	Yield (%)	Ratio (α/β)	Ref
1	179	175	DMTST	CH ₂ Cl ₂	182	39	1:0	171
2	179	176	BF ₃ ·OEt ₂	THF/Et ₂ O	182	50	2.9:1	171
3	179	178	BF ₃ ·OEt ₂	THF/Et ₂ O	185	68	1:0	171, 173
4	180a	175	NIS/TfOH	CH ₂ Cl ₂	183	93	1:1	174
5	180a	174	Me ₂ S, 2-Cl-Py, Tf ₂ O	CH ₂ Cl ₂	183	83	3:1	174
6	181	174	Me ₂ S, 2-Cl-Py, Tf ₂ O	CH ₂ Cl ₂	184	nr	3:1	174
7	180b	177	Me ₂ S, 2-Cl-Py, Tf ₂ O	CH ₂ Cl ₂	186	nr	3:1	174

In the context of synthesis of α -galactosylceramide, azido-sphingosine **179**, that was obtained in nine steps from 2-deoxygalactose in an overall yield of 36%, was reacted with perbenzylated *S*-galactoside (1-thio-galactose) **175** using dimethyl(methylthio)sulfonium triflate (DMTST) as promoter affording the galactosyl

ceramide **182** in 39% yield as a pure α -isomer (entry 1, Table 1).¹⁷¹ The use of the promoter system NIS/TfOH gave complex mixtures as consequence of the addition of the electrophile to the double bond. The use of the trichloroacetimidate **176** and $\text{BF}_3 \cdot \text{Et}_2\text{O}$ as promoter allowed improving the yield to 50% but at the cost of decreasing the stereoselectivity ($\alpha/\beta=2.9:1$) (entry 2, Table 1). Schmidt¹⁷² had previously demonstrated that 4,6-benzylidene-galactosyl trichloroacetimidate **178** reacts with unprotected azido-phytosphingosine **180b** to give the α -glycosylated product in 49% yield. Interestingly, when the 2-*O*-Ms precursor of **180b** was used in the glycosylation the yield improved up to 73%, and no competition of secondary alcohols in glycosylation was observed. Thus, when the trichloroacetimidate **178** was reacted with the azido-phytosphingosine **179** using $\text{BF}_3 \cdot \text{OEt}_2$ as a promoter, galactosyl ceramide **185** was cleanly delivered in 68-70% yield.^{171,173} Hydroxyl groups were deprotected and double bond reduced by treating **185** under hydrogenolitic conditions providing α -galactosylceramide.

Coupling phytosphingosine **180a** with the galactosyl donor **175** by using NIS-TfOH as promoter system afforded **183** in 93 % yield, albeit as a 1:1 α/β mixture (entry 4, Table 1).¹⁷⁴ When a dehydrative glycosylation procedure¹⁷⁵ was used in the coupling of tetrabenzyl galactose **174** with the acceptor **180a**, compound **183** was obtained in 83% yield and improved stereoselectivity ($\alpha/\beta=3:1$) (entry 5, Table 1). α -Galactosylsphingosine **184** and α -fucosylsphingosine **186** were also synthesised in a 3:1 α/β ratio by dehydrative glycosylation of phytosphingosines **181** and **180b**, with the glycosyl donors **174** and **177** (entries 6, 7, Table 1). These compounds were transformed into the final galatosylceramides by azide reduction, amide formation, and debenzylation.

The 3-*O*-sulfo- α -galactosylceramide **189**, a stimulator of human NKT cells to secrete IL-4 and $\text{IFN-}\gamma$,¹⁷⁶ was prepared from 4,6-*O*-benzyliden-glycosyl trichloroacetimidate **187**, which has positions 2 and 3 differentially protected to facilitate selective deprotection and sulfation (Scheme 28). Donor **187** was coupled with

¹⁷¹ Plettenburg, O.; Bodmer-Narkevitch, V.; Wong, Ch-H. *J. Org. Chem.* **2002**, *67*, 4559–4564.

¹⁷² Figueroa-Pérez, S.; Schmidt, R. R. *Carbohydr. Res.* **2000**, *328*, 95–102.

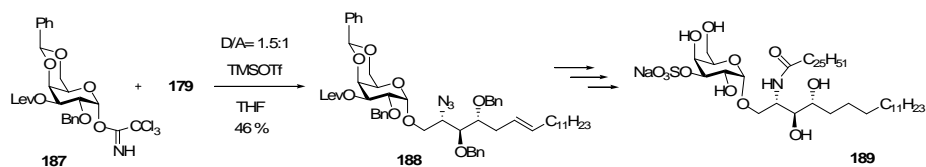
¹⁷³ Risseuw, M.D.P.; Berkens, C.R.; Ploegh, H.L.; Ovaa, H. *Tetrahedron Lett.* **2006**, *47*, 3677–3679.

¹⁷⁴ Fan, G-T.; Pan, Y-S.; Lu, -C.; Cheng, Y-P.; Lin, W-C.; Lin S.; Lin, C-H.; Wong, C-H.; Fang, J-M.; Lin C-C. *Tetrahedron* **2005**, *61*, 1855–1862.

¹⁷⁵ Nguyen, H. M.; Chen, Y.; Duron, S. G.; Gin, D. Y. *J. Am. Chem. Soc.* **2001**, *123*, 8766–8772.

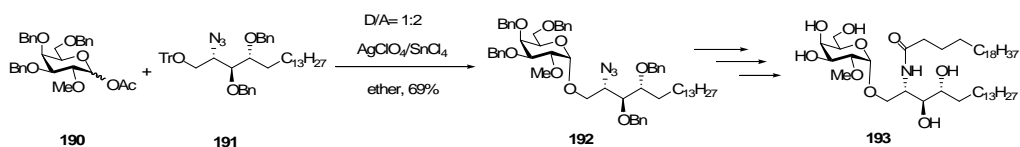
¹⁷⁶ Xing, G.-W.; Wu, D.; Poles, M.A.; Horowitz, A.; Tsuji, M.; Ho, D.D.; Wong, C.-H. *Biorg. Med. Chem.* **2005**, *13*, 2907–2916.

the azidosphingosine **179**, with a donor/acceptor ratio D/A=1.5:1, in the presence of TMSOTf to give **188** in 46% yield, exclusively as the α -anomer.



Scheme 28

Some years ago, in the course of a study concerning the immunostimulatory activity of several natural α -Gal-GSLs, it was found that the glycosylation of 2-OH group of galactose resulted in a complete loss of activity,¹⁷⁷ although the hydrolysis of the interglycosidic linkage by α -glycosidases can restore the activity. This crucial role of the galactose 2-OH group can be due to a mere steric hindrance or to the fact that the 2-OH is involved in specific interactions at the active site of the receptor. In an attempt to clarify these facts compounds **193**, **197** and **205**, in which the 2-OH of the galactose has been replaced by OMe, F, or H, were prepared. All of them showed no significant immunostimulatory activity.



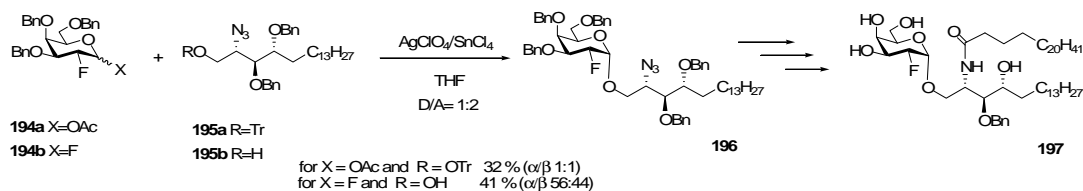
Scheme 29

The intermediate **192** was synthesised using a modification of the Mukaiyama glycosylation procedure,¹⁷⁸ which involved the use of the glycosyl acetate **190** instead of the glycosyl fluoride, and $\text{SnCl}_4\text{-AgClO}_4$, instead of $\text{SnCl}_2\text{-AgClO}_4$. In addition, the alcohol of the sphingosine moiety was activated with a trityl group.¹⁷⁹ Coupling **190** and **191** under these conditions afforded **192** in 69% yield as an essentially pure α -anomer. Then, **192** was converted into the 2-methoxy-galactoceramide **193** (Scheme 29).

¹⁷⁷ Barbieri, L.; Constantino, V.; Fattorusso, E.; Mangoni, A.; Aru, E.; Parapini, s.; Tamarelli, D. *Eur. J. Org. Chem.* **2004**, 468–473.

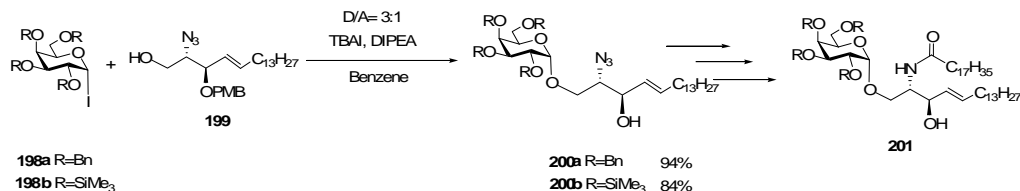
¹⁷⁸ (a) Mukaiyama, T.; Murai, Y.; Shoda, S. *Chem. Lett.* **1981**, 431-432. (b) Akimoto, K.; Natori, T.; Morita, M. *Tetrahedron Lett.* **1993**, *34*, 5593–5596. (c) Mukaiyama, T.; Takashima, T.; Katsurada, M., Aizawa, H. *Chem. Lett.* **1991**, 533–536.

¹⁷⁹ Houdier, S.; Vottéro, P. J. A. *Tetrahedron Lett.* **1993**, *34*, 3283–3284.



Scheme 30

A similar procedure was used in the synthesis of the 2-deoxy-2-fluoro-galactosylsphingosine **196** which was then converted into the 2-deoxy-2-fluoro-galactosylceramide **197** (Scheme 30).¹⁸⁰ 2-Deoxy-2-fluorogalactose **194a**, which was synthesised from tri-*O*-benzylgalactal, was reacted with the trityl derivative **195** (R=Tr) using SnCl₄-AgClO₄ as promoter affording **196** in 32% yield as 1:1 anomeric mixture. When the reaction was carried out under standard Mukaiyama conditions from glycosyl fluoride **194b** and the non tritrlated azido-sphingosine **195** (R=H) using SnCl₂-AgClO₄, the yield increased slightly but the stereoselectivity was also essentially null. Comparing Schemes 28, 29 and 30 it can be concluded that the presence of fluorine at position 2 has strong influence in the yield and stereoselectivity of glycosylation reaction.



Scheme 31

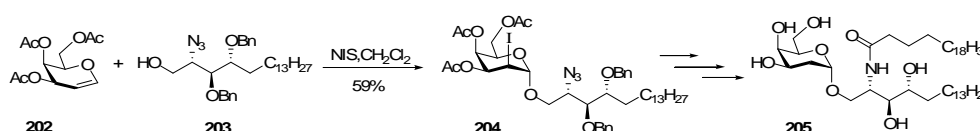
Recently, it has been shown that glycosyl iodides¹⁸¹ are excellent donors for glycosylation reactions. A high α -stereoselectivity was achieved by *in situ* anomerization of the α -iodide to the more reactive β -iodide, from which the α -glycoside was exclusively formed as a consequence of an S_N2 displacement. Recently this procedure has been used in the synthesis of α -galacto-azido-sphingolipids **200** by reacting azidosphingosine **199** with the per-*O*-benzylated **198a** and per-*O*-silylated

¹⁸⁰ Barbieri, L.; Costantino, V.; Fattorusso, E.; Mangoni, A.; Basilico, N.; Mondani, M.; Tamarelli, D. *Eur. J. Org. Chem.* **2005**, 3279–3285.

¹⁸¹ (a) Schmid, U.; Waldemann, H.; *Tetrahedron Lett.* **1996**, 37, 3837–3840. (b) Gervay, J.; Hadd, M. J. *J. Org. Chem.* **1997**, 62, 6961–6967. (c) Gervay, J.; Hadd, M. J. *Carbohydr. Res.* **1999**, 320, 61–69. (d) Lam, S. N.; Gervay-Hague, J. *Org. Lett.* **2002**, 4, 2039–2042.

iodide **198b** donors in the presence of Bu₄NI (Scheme 31).¹⁸² Compounds **200a,b** were obtained in remarkable yields, 94% and 84% respectively, exclusively as the α -anomer.

The 2-deoxy derivative **205** was synthesised by using 3,4,6-tri-*O*-acetyl-galactal **202** as the chiral starting material for synthesising phytosphingosine **203** and as starting material for glycosylation (Scheme 32).¹⁸³ Thus, stereoselective glycosylation was accomplished using **202** as glycosyl donor in an iodonium-mediated coupling with the azidosphingosine **203** to give **204**, which was converted into the 2-deoxy derivative **205**. The stereochemistry of this reaction was determined by the attack of iodine to the β -face of the double bond which controls the selective formation of the α glycosidic bond.¹⁸⁴



Scheme 32

3.2.2.2. Glycosylation of ceramides

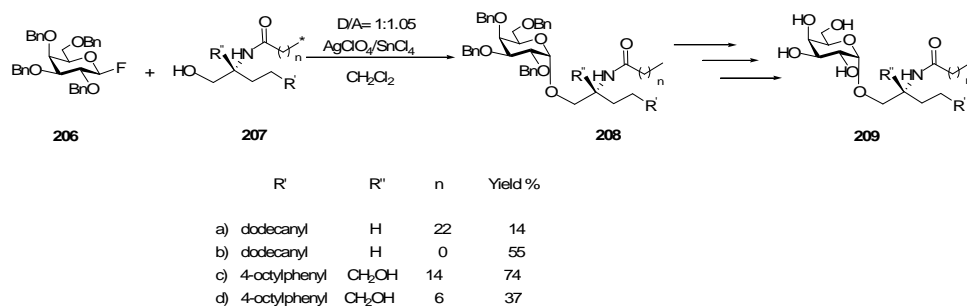
There are several examples of the use of perbenzyl-glycosyl fluorides in the glycosylation of structurally different ceramides in order to obtain α -anomers (Schemes 33-36). Using SnCl₂/AgClO₄ as a promoter system, good stereoselectivity and moderate to poor yields are usually obtained. A series of α -mannosyl and α -galactosyl ceramide analogues **209**, incorporating sphinganine **207** in place of sphingosine, were prepared from the protected derivative **208** in order to examine their effects on immune responses by V α 19 NKT cells (Scheme 33). Compound **208** was synthesized by glycosylation of ceramide **207** with β -tetrabenzylgalactosyl fluoride **206** in the presence of SnCl₂/AgClO₄. The α isomer was preferentially obtained (α/β = 9:1).¹⁸⁵

¹⁸² Du W.; Gervay-Hague J. *Org. Lett.* **2005**, *7*, 2063–2065.

¹⁸³ Constantino, V.; Fattotuddo, E.; Imperatore, C.; Mangoni, A. *Tetrahedron* **2002**, *58*, 369–375.

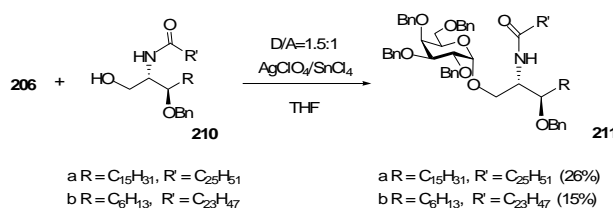
¹⁸⁴ For reviews about synthesis of 2-deoxy-glycosides see: (a) Kirschning, A.; Jesberger, M.; Schöning, K.-U. *Synthesis* **2001**, 507–540. (b) Veyrières, A. In *Carbohydrates in Chemistry and Biology*, Ernst, B.; Hart, G.W.; Sinay, P. Ed.s, Wiley, Weinheim **2000**, Part I, Vol. I, p 367. (c) Marzabadi, H.; Franck, R.W. *Tetrahedron* **2000**, *56*, 8385–8417. (d) Castro-Palomino, J.C.; Schmidt, R.R. *Synlett* **1998**, 501–503. (e) Toshima, K.; Tatsuta, K. *Chem. Rev.* **1993**, *93*, 1503–1531.

¹⁸⁵ Shimamura, M.; Okamoto, N.; Huang, Y.-Y.; Yasuoka, J.; Morita, K.; Nishiyama, A.; Amano, Y.; Mishina, T. *Eur. J. Med. Chem.* **2006**, *41*, 569–576.



Scheme 33

The α -galactosylceramide has proven to be an invaluable tool for enhancing understanding of the role of CD1d antigen presentation and NKT cell function. With the aim of elucidate this role sphinganine **211a,b**, analogues of α -GalCer, were prepared (Scheme 34). Glycosylation of ceramides **210a,b** with glycosyl fluoride **206** in the presence of SnCl₂/AgClO₄ afforded **211a,b** in low yields but with excellent α selectivity.¹⁸⁶

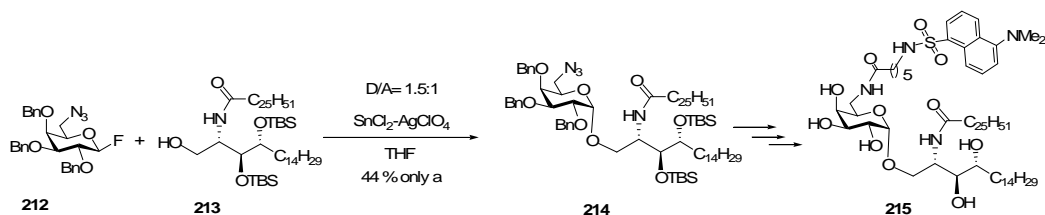


Scheme 34

Modelling of CD1d- α -GalCer complex suggested that the hydroxyl groups at C4 and C6 on galactose are not involved in complex formation. In order to quantify the association of glycolipids with CD1d and NKT cell receptors, α -galactosylceramides **215**, which have labels (fluorophores and biotin) appended at the C6 position of the sugar, were prepared. Glycosylation of ceramide **213** with 6-azido-6-deoxy- α -tribenzylgalactosyl fluoride **212** promoted by SnCl₂/AgClO₄ gave exclusively the α -

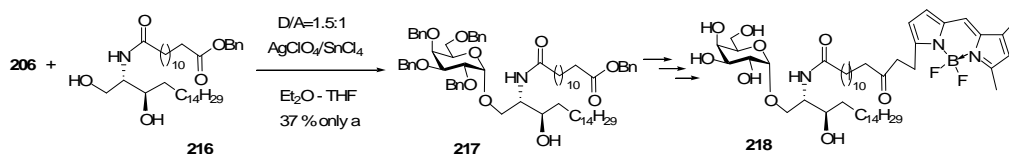
¹⁸⁶ Ndonye, R.M.; Izmirian, D.P.; Dunn, M.F.; Yu, K.O.A.; Porceli, S.A.; Khurana, A; Kronenberg, M.; Richardson, S.K.; Howell, A.R. *J. Org. Chem.* **2005**, *70*, 10260–10270.

anomer **214** in 44% yield (Scheme 35).¹⁸⁷ Compound **215** was prepared from **214** by removing the protecting groups and anchoring the label at position 6.



Scheme 35

α -Galactosylceramide **218** containing *BODIPY*, a fluorescent group, was prepared with the purpose of visualizing the behaviour of this compound *in vivo*, and how the presence of this group affects the biological activity (Scheme 36).¹⁸⁸ Ceramide **216** was glycosylated with the galactosyl fluoride **206** promoted by $\text{SnCl}_2/\text{AgClO}_4$ giving the ceramide **217** in 37% yield exclusively as the α -anomer. The lipidic chain in **217** was further elaborated and the protecting groups removed to give **218**.



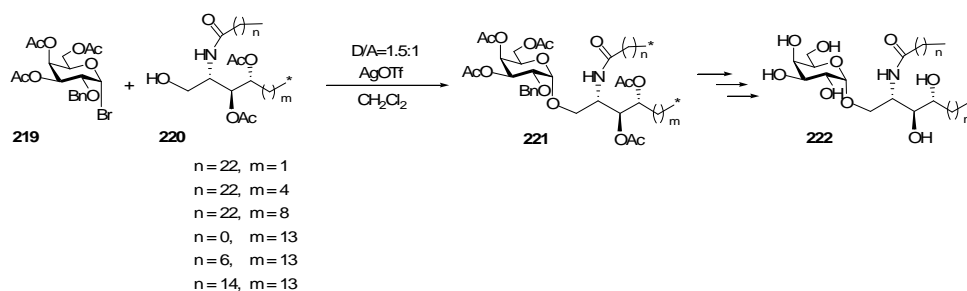
Scheme 36

A series of α -galactosylceramides **222** in which the lipid chain lengths have been incrementally varied were prepared in order to study the effects of lipid chain lengths on cytokine release by natural killer T cells (NKT cells). They concluded that truncation of the phytosphingosine lipid chain increases the IL-4 vs INF- γ bias of released cytokines and that the length of the acyl chain in α -galactosylceramides influences cytokine release profiles. With this purpose ceramides **220** were glycosylated with α -galactosyl bromide **219** in the presence of silver triflate providing the α -galactosylceramides **221** in good yield (62 %) contaminated with small amounts of the

¹⁸⁷ Zhou, X.-T.; Forestier, C.; Goff, R.D.; Li, C.; Teyton, L.; Bendelac, A.; Savage, P.B. *Org. Lett.* **2002**, *4*, 1267–1270.

¹⁸⁸ Vo-Hoang, Y.; Micouin, L.; Ronet, C.; Gachelin, G.; Bonin, M. *ChemBioChem*, **2003**, *4*, 27–33.

β -anomers (Scheme 37).¹⁸⁹ Donor **219** was used because the selective deprotection of the benzyl group allows an easier separation of the β -anomer. It is remarkable that a relatively good yield is obtained in this case from the more classical glycosyl donors. However, this glycosyl donor differentiates from **206**, apart from the halogen at the anomeric position, by the presence of the acetyl protecting groups of hydroxyls in the carbons 3, 4, and 6.



Scheme 37

Agelagalastatin¹⁹⁰ **226** is a glycolipid isolated from a marine sponge *Agelas sp.*, as other relevant glycolipids such as longiside and α -GalCer,¹⁹¹ that has shown immunomodulating activity (Scheme 38). Agelagalastatin is integrated by a trisaccharide containing two furanose and one galactose units, which is linked to phytosphingosine. In the context of the total synthesis of **226** the stereoselective construction of α -galactofuranoside and α -galactopyranoside bonds was performed by using 2'-carboxybenzyl (CB) group as leaving group.¹⁹² The synthesis of **225**, a precursor of the angelagalastatin **226**, was carried out by glycosylation of ceramide **224** with the trisaccharide **223a**, which has a 4,6-benzylidene protecting group. Using triflic anhydride as promoter, the yield of glycosylation was good (77%) but the stereoselectivity was very low ($\alpha/\beta=1.4:1$). When glycosylation was performed using the glycosyl fluoride **223b** and $\text{SnCl}_2\text{-AgClO}_4$ as promoter, the yield was also good (72%) and the α -anomer was exclusively obtained. In this case the glycosylation

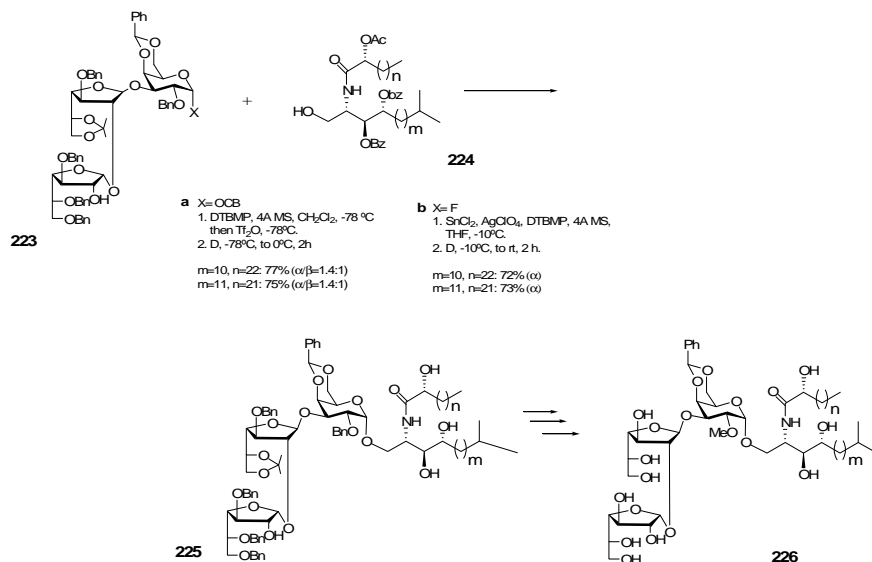
¹⁸⁹ Goff, R.D.; Gao, Y.; Mattner, J.; Zhou, D.; Yin, N.; Cantu III, C.; Teyton, L.; Bendelac, A.; Savage, P.B. *J. Am. Chem. Soc.* **2005**, *126*, 13602–13603.

¹⁹⁰ Lee, Y. J.; Lee, B. Y.; Jeon, H. B.; Kim, K. S. *Org. Lett.* **2006**, *8*, 3971–3974.

¹⁹¹ Kim, S.; Song, S.; Lee, T.; Jung, S.; Kim, D.; *Synthesis*, **2004**, *6*, 847–850.

¹⁹² (a) Kim, K.S.; Kim, J.H.; Lee, Y.J.; Park, J. *J. Am. Chem. Soc.* **2001**, *123*, 8477–8481. (b) Kim, K.S.; Park, J.; Lee, Y.J.; Seo, Y.S. *Angew. Chem. Int. Ed.* **2003**, *42*, 459–462.

reaction appears to be more dependent on the leaving group in the glycosyl donor and on the reaction conditions than on the presence of the 4,6-benzylidene group.



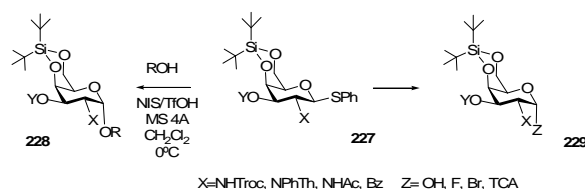
Scheme 38

A particular problem in the synthesis of glycans is the synthesis of α -2-deoxy-2-aminoglycans that usually require starting from 2-azido-derivatives in order to avoid participating groups. However, the anomeric selectivity and yield of glycosylation varies greatly depending on the structure of donors and acceptors. Alternatives to circumvent this problem include the use of 2-nitro-glycals¹⁹³ as glycosyl donors or using (1*S*)-phenyl-2-phenyl-2-(phenylsulfanyl)ethyl group at the C2- hydroxyl position.¹⁹⁴ Recently, it has been demonstrated that the presence of a 4,6-*O*-di-*tert*-butylsilylene group (DTBS) in galactosyl donors **227** allows the α -selective glycosylation of simple alcohols and carbohydrates to give **228** in excellent yields despite the presence of participating groups at the C2 position (Scheme 39).¹⁹⁵ Furthermore, the thio-glycoside **227** can be easily converted into other useful glycosyl donors **230**, all of them with α -configuration.

¹⁹³ Winterfed, G.A.; Schmidt, R.R. *Angew. Chem. Int. Ed.* **2001**, *40*, 2654–2657.

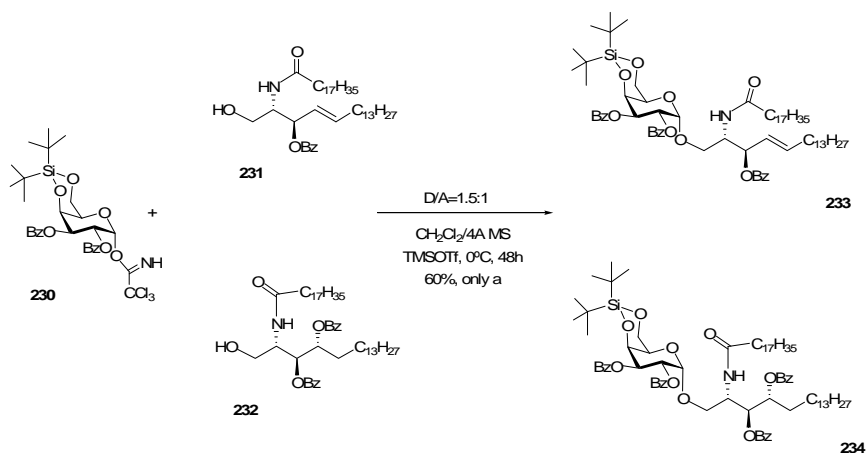
¹⁹⁴ Kim, J. H.; Yang, H.; Park, J.; Boons, *J. Am. Chem. Soc.* **2005**, *127*, 12090–12097.

¹⁹⁵ (a) Imamura, A.; Ando, H.; Korogi, S.; Tanabe, G.; Muraoka, O.; Ishida, H.; Kiso, M. *Tetrahedron Lett.* **2003**, *44*, 6725–6728. (b) Imamura, A.; Ando, H.; Ishida, H.; Kiso, M. *Org. Lett.* **2005**, *7*, 4415–4418.



Scheme 39

This discovery has been recently applied to the synthesis of α -GalCer,¹⁹⁶ and iGb₃.¹⁹⁷ Remarkably, ceramides **231** and **232** were glycosylated with the glycosyl donor **230**, which have a participating group at position 2 and trichloroacetimidate as a leaving group, to give the galactosyl ceramides **233** and **234**, respectively, in 60% yield exclusively as the α -anomers (Scheme 40). The presence of benzoate groups in the carbohydrate and in the lipidic portion facilitates the deprotection process leading to α -GalCer.



Scheme 40

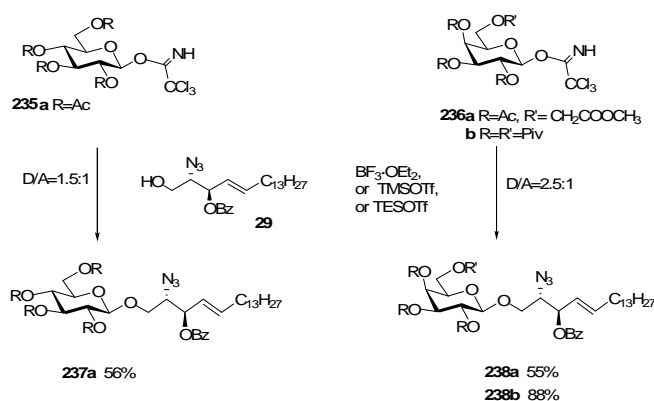
Similarly, the DTBS galactosyl donors **229** (Y=NHTroc, Z=, SPh, TCA) have also been successfully used in the synthesis of α -galactosaminyl Ser/Thr sequences, obtaining in most cases, yields higher than 88% and almost exclusively the α -isomer.¹⁹⁶

¹⁹⁶ Imamura, A.; Kimura, A.; Ando, H.; Ishida, H.; Kiso, M. *Chem. Eur. J.* **2006**, *12*, 8862–8870.
¹⁹⁷ Kimura, A.; Imamura, A.; Anfo, H.; Ishida, H.; Kiso, M. *Synlett* **2006**, 2379–2382.

3.2.3 Recent contributions in the synthesis of β -glycosyl sphingosines and ceramides reported in the literature (2000-2007)

3.2.3.1. Glycosylation of azidosphingosine

β -Glucosyl- and β -galactosyl ceramides are frequently obtained by the azidosphingosine method, from glucose and galactose trichloroacetimidates protected with participating groups, mainly Ac, Bz, Piv (Scheme 41). The glycosyl-azidosphingosines obtained are further converted into the amino derivatives, which are amidated to afford the final product.



Scheme 41

Glucosyl-sphingosine **237a** was prepared in 56% yield by reaction of **235a** with the azidosphingosine **29** in dichloromethane by using $\text{BF}_3 \cdot \text{OEt}_2$ as promoter.¹⁹⁸ β -Galactosyl-azidosphingosines **238** were prepared with the final objective of obtaining sulfated galactosyl ceramides. Thus, **238a** was synthesized in 55% yield by reaction of **236a** (6-OH was protected with CH_2COOMe in order to anchor the fluorescent dansyl group) with **29** using TESOTf as promoter.¹⁹⁹ However, when a similar reaction was carried out from the pivaloyl derivative **236b** and $\text{BF}_3 \cdot \text{OEt}_2$ as promoter **238b** was obtained in an excellent 88% yield.²⁰⁰ After deprotection of the sugar moiety and reduction of the azido group, the saturated fatty acid chains were introduced and the

¹⁹⁸ Duclos, R.I. *Chem. Phys. Lipids* **2001**, *111*, 111–138.

¹⁹⁹ Franchini, L.; Compostella, F.; Donda, A.; Mori, L.; Colombo, D.; De Libero, G.; Matto, P.; Ronchetti, F.; Panza, L. *Eur. J. Org. Chem.* **2004**, 4755–4761.

²⁰⁰ Compostella, F.; Franchini, L.; De Libero, G.; Palmisano, G.; Ronchetti, F.; Panza, L. *Tetrahedron* **2002**, *58*, 8703–8708.

resulting compound was selectively sulfated¹⁷⁶ at position 3 of the sugar moiety to afford **241a-c** (Figure 21).

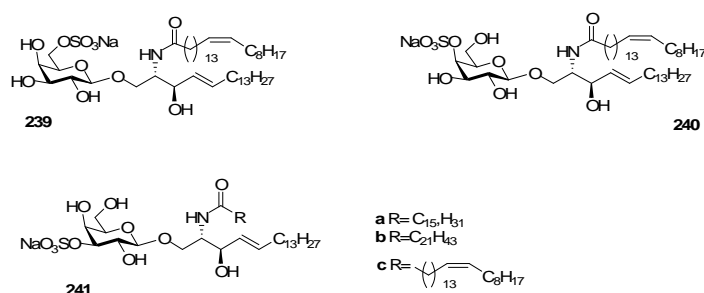
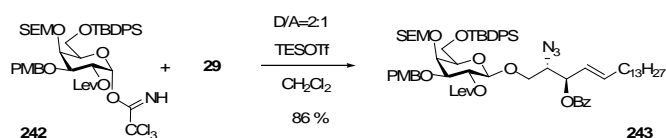


Figure 21

To assess the role of the position of the sulfate in CD1a-mediated T cell activation, the synthesis of three β -D-galactosylceramides, bearing a sulfate at position 2, 4, or 6 of galactose was carried out. Trichloroacetimidate **242**, with all the hydroxyl groups differentially protected, was reacted with **29** using TESOTf as activator to give the β -galactosyl-azidosphingosine **243** in excellent yield (86%) (Scheme 42).²⁰¹ Compound **71** was further converted into the ceramides **239**, **240** and **241c** by selective deprotection and sulfation.



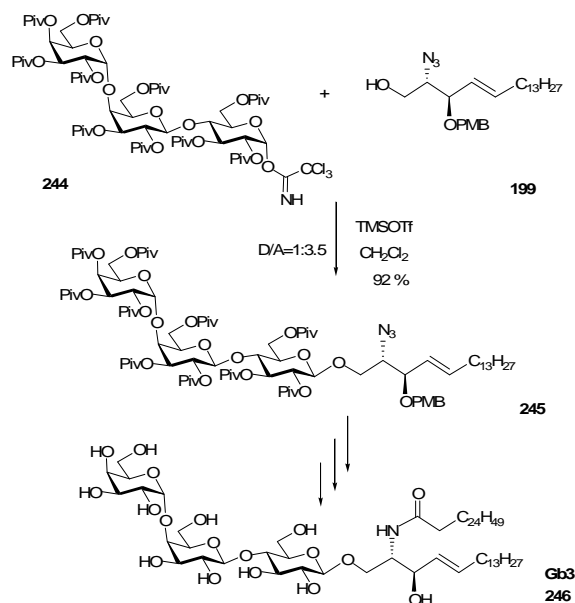
Scheme 42

Trisaccharides isoglobotrihexose, and globotrihexose, which are very difficult to obtain either from natural sources or by chemical synthesis, were synthesized by using enzymatic procedures. The suitably protected free trisaccharide was transformed into the corresponding trichloroacetimidate **242** and coupled with azido sphingosine **199** in the presence of TMSOTf to give the protected ceramides **245** in excellent yield (92%) and selectivity (Scheme 43).²⁰² When the trisaccharide was protected with benzoyl or acetyl groups yield decreased up to 75% and 48%, respectively.²⁰³ Removal of protecting groups under typical reaction conditions rendered iGb3 **3** and Gb3 **246**.

²⁰¹ Compostella, F.; Ronchi, S.; Panza, L.; Mariotti, S.; Mori, L.; De Libero, G.; Ronchetti, F. *Chem. Eur. J.* **2006**, *12*, 5587–5595.

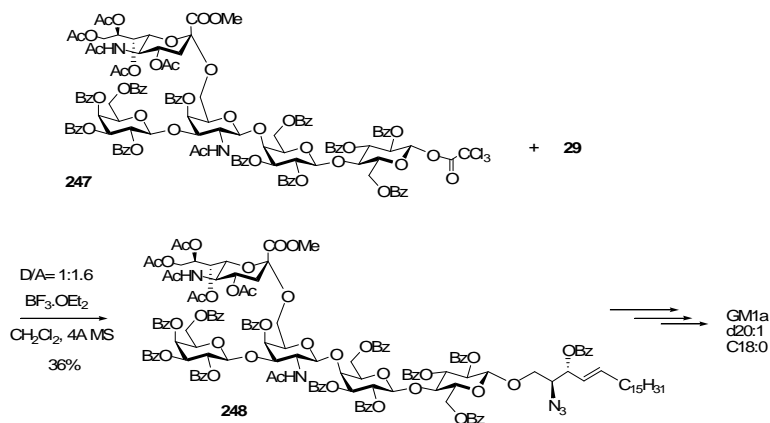
²⁰² Yao, Q.; Song, J.; Xia, C.; Zhang, W.; Wang, P.G. *Org. Lett.* **2006**, *8*, 911–914.

²⁰³ Ohtsuka, I.; Hada, N.; Sugita, M.; Takeda, T. *Carbohydr. Res.* **2002**, *337*, 2037–2047.



Scheme 43

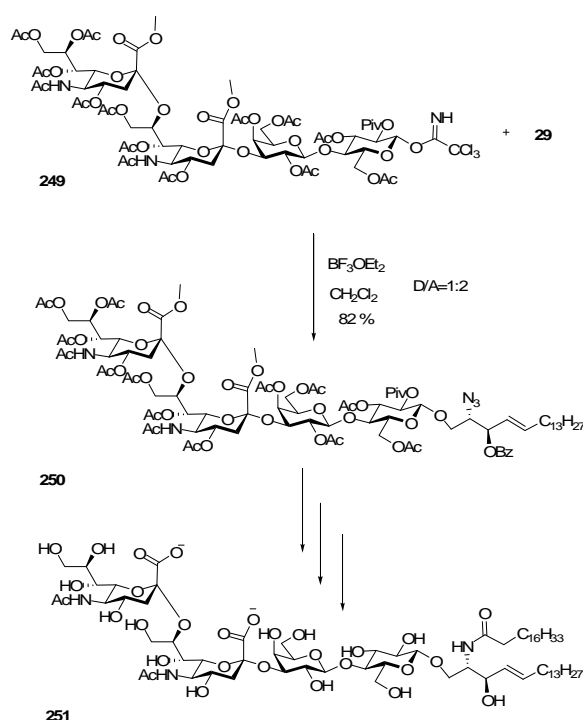
Gangliosides are ubiquitously located in vertebrate cells and are particularly abundant in the nervous system. The synthesis of the glycosyl donor **247** started from glucosamine which was further transformed into a galactosamine derivative by inverting the configuration of 4-OH. Reaction of **29** with the glycosyl donor **247** activated by BF₃·OEt₂ afforded the β-linked glycosyl sphingosine derivative **248** in 36% yield (Scheme 44).²⁰⁴ Compound **248** was then converted into GM1a by azide reduction, coupling with octadecanoic acid, methanolysis and saponification of the methyl ester.



Scheme 44

²⁰⁴ Takeda, Y.; Horito, S. *Carbohydr. Res.* **2005**, *340*, 211–220.

In the synthesis of ganglioside GF3 the coupling between the oligosaccharide and azidosphingosine **29** was also carried out by activating with $\text{BF}_3 \cdot \text{OEt}_2$ the trichloroacetimidate **249**, which is protected at positions 3 and 6 with acetate groups and at position 2 with a pivaloyl group. In this case the yield of glycosyl-sphingosine **250** was 82% and only the isomer β was obtained (Scheme 45).²⁰⁵ Compound **250** was then transformed into **251** following the standard procedure.

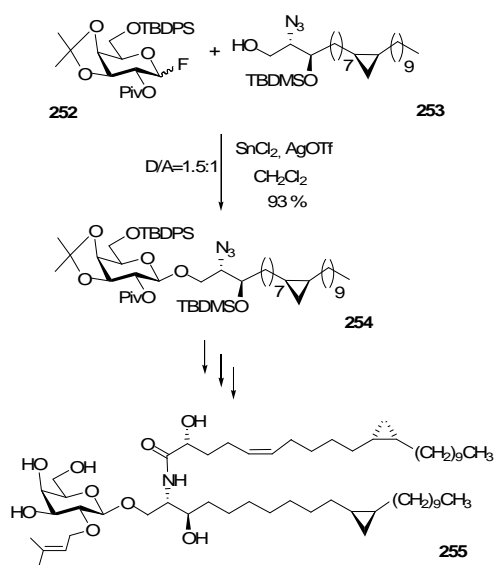


Scheme 45

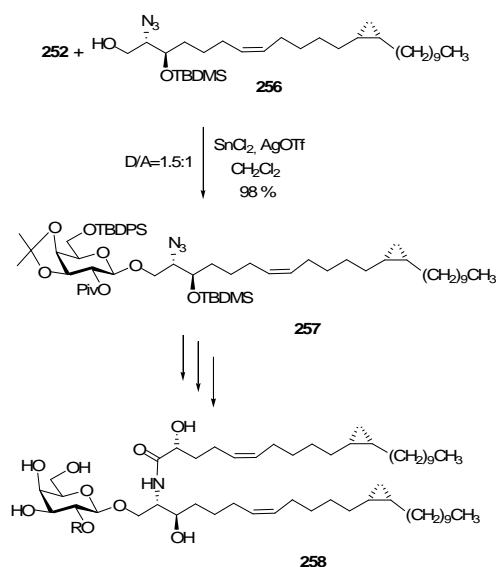
The total synthesis of plakosides A, B, **255** and **258**, which are prenylated and immunosuppressive marine galactosphingolipids, and their designed analogs was accomplished through an efficient and convergent strategy (Schemes 46 and 47). In this case the galactosyl fluoride **252** in the presence of $\text{SnCl}_2/\text{AgClO}_4$ was used for the glycosylation of sphinganine analogues **253** and **256**.²⁰⁶ Yields were practically quantitative, showing also the efficiency of galactosyl fluorides for the synthesis of β -galactosyl ceramides.

²⁰⁵ Castro-Palomino, J.C.; Simon, B.; Speer, O.; Leist, M.; Schmidt, R.R. *Chem. Eur. J.* **2001**, *7*, 2178–2184.

²⁰⁶ Nicolaou, K.C.; Li, J.; Zenke, G. *Helv. Chim. Acta* **2000**, *83*, 1977–2006.



Scheme 46

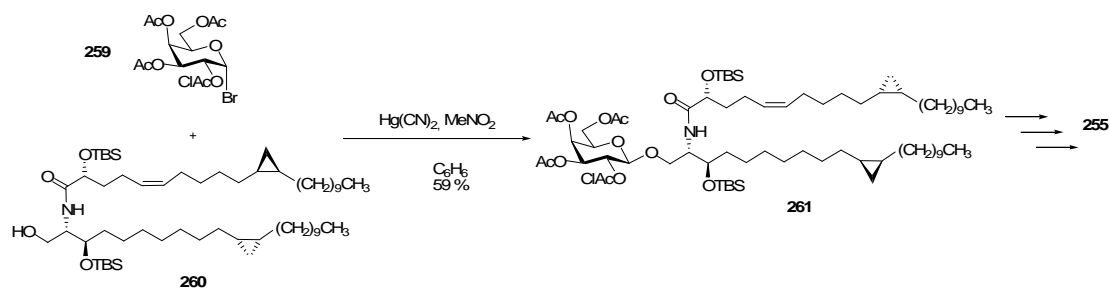


Scheme 47

It can be concluded that trichloroacetimidates and fluorides are efficient glycosyl donors for glycosylation of azidosphingosine, and that better yields are obtained when there is a pivaloyl group at 2-OH of the carbohydrate.

3.2.3.2. Glycosylation of ceramides

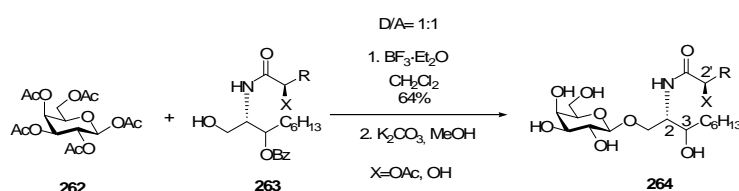
The total synthesis of plakosides A **255** was also carried out by direct glycosylation of ceramide **260** with the galactosyl bromide **259** in the presence of $\text{Hg}(\text{CN})_2$ and MeNO_2 affording the β -galactosyl ceramide **261** in 59% yield.²⁰⁷ 2-ClAcO was used in order to avoid the orthoester formation (Scheme 48).



Scheme 48

²⁰⁷ Seki, M.; Kayo, A.; Mori, K. *Tetrahedron Lett.* **2001**, 42, 2357–2360.

GalCer **264** is a water-soluble analogue of natural GalCer that contains either a hexanoic or a decanoic acyl unit and a saturated nine-carbon sphingosine moiety, and was prepared from Garner's aldehyde.²⁰⁸ These analogues were used to clearly establish the molecular basis for the selective recognition process between HIV-1 surface glycoprotein and GSL analogues within a GalCer monolayer. The authors provide evidence that this process involves conformations similar to the fundamental conformer of GalCer and demonstrate that the alkyl chains of the ceramide moiety are essential to the gp120 insertion into the monolayer. Glycosylation of ceramide **263** was carried out using penta-*O*-acetyl-galactose **262** as donor and BF₃·OEt₂ as promoter affording the glycosylated product in 64% yield, similar yields were obtained in other glycosylation procedures of ceramides (Scheme 49). The final GalCer **265** was obtained after removal of protecting groups.



Scheme 49

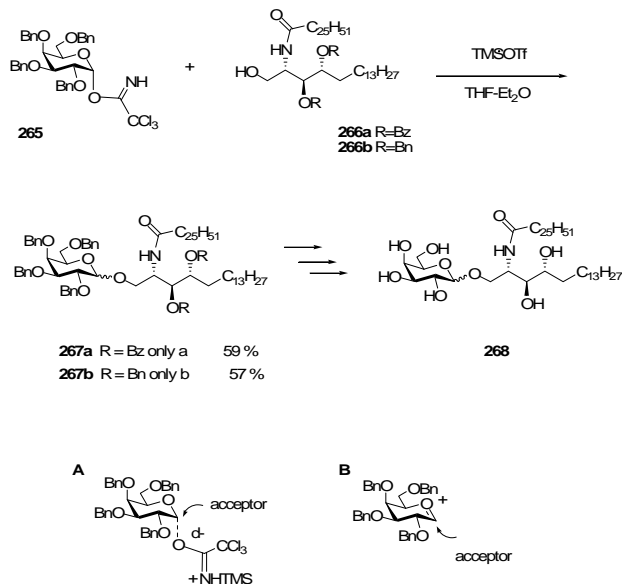
In the course of studies oriented to the synthesis of α -GalCer, the reaction of the glycosyl donor **265** with the differentially protected phytosphingosines **266a,b** was studied.^{209,210} It is well known that benzyl group is usually selected to protect the 2-OH position of glycosides to give α -glycosylation. However, unexpectedly it was observed that the stereoselectivity of the reaction depended on the protecting group at the ceramide moiety. Thus, α -anomer **267a** was exclusively obtained from ceramide **266a** with a benzoyl protecting group, while the β -anomer **267b** was obtained when ceramide **266b** (R=Bn) was used as starting material (Scheme 50). It was suggested that **266a** reacts in a S_N1 manner (intermediate **B**), while when **266b** is used an S_N2 mechanism is

²⁰⁸ Villard, R.; Hammache, D.; Delapierre, G.; Fotiadu, F.; Buono, G.; Fantini, J. *ChemBioChem* **2002**, *3*, 517–525.

²⁰⁹ Xia, C.; Yao, Q.; Schümann, J.; Rossy, E.; Chen, W.; Zhu, L.; Zhang, W.; De Libero, G.; Wang, P.G. *Borg. Med. Chem. Lett.* **2006**, *16*, 2195–2199.

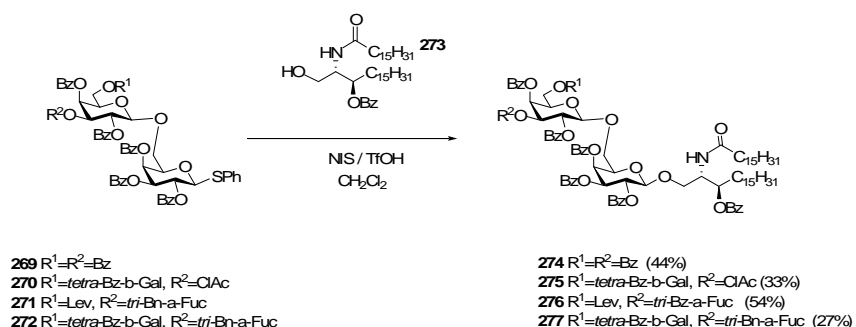
²¹⁰ The use of similar glycosyl donors for the glycosylation of azido-phytosphingosine has been recently reported. Lee, A.; Farrand, K.J.; Dickgreber, N.; Hayman, C.M.; Jürs, S.; Hermans, I.F.; Painter, G.F. *Carbohydr. Res.* **2006**, *341*, 2785–2798.

followed (intermediate **A**). An armed-disarmed effect in the ceramide moiety is suggested for explaining this behaviour.



Scheme 50

Unprotected glycosyl-ceramides **274-277** were isolated from the metacystodes of *Echinococcus multicularis* (Scheme 51).²¹¹ Coupling between benzoyl protected oligosaccharidic thioglycosides **269-272** with ceramide **273** promoted by NIS/TfOH afforded the β -glycosides **274-277** in 44%, 33%, 54%, and 27% yield, respectively. The fully protected glycosides were deprotected to give the four target glycosphingolipids.

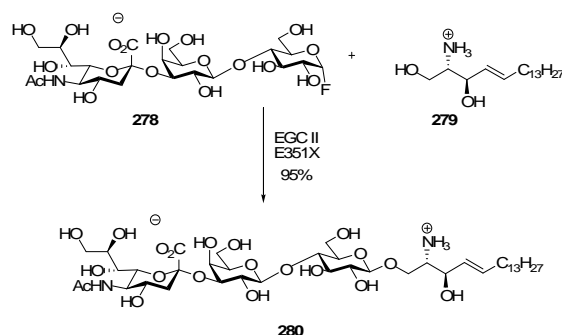


Scheme 51

²¹¹ Yamamura, T.; Hada, N.; Kaburaki, A.; Yamano, K.; Takeda, T. *Carbohydr. Res.* **2004**, *339*, 2749–2759.

3.2.3.3. Enzymatic procedures

In recent years,²¹² biocatalysis has become an established technology for synthetic production of fine chemicals. Enzymes are applied for transformations leading to complex target molecules, mainly because of their high selectivity and mild operational conditions. Novel enzymes²¹³ with improved properties are now accessible as a result of advances in high throughput screening methods, genomics, and rational protein design. Recently, GSL syntheses through enzymatic catalysis by glycosynthase, generated from endoglycoceramidase II (EGC II), has been described.²¹⁴ By utilizing specific enzymatic catalysis, GSL **280** was obtained from the fluoride **278** and the salt **279** in a high regio and stereoselective transformation (Scheme 52).



Scheme 52

The ability of glycosidases²¹⁵ to use unactivated sugars and their broad specificity for aglycones, have limited synthetic applications, since, the native enzymes perform poorly in organic media, the thermodynamic considerations require the water content to be minimized for maximal yields, and are difficult to satisfy the divergent solvent requirements of hydrophilic sugar donors and hydrophobic acceptors. However, when the reaction is carried out in plasticized glasses, high concentrations of both acceptor and sugar donor enable obtainment of glycosides **281** and **282** in good yields and high selectivity (Figure 22).²¹⁶

²¹² Panke, S.; Held, M.; Wubbolts, M. *Curr. Opin. Biotechnol.* **2004**, *15*, 272–279.

²¹³ Panke, S.; Wubbolts, M. *Curr. Opin. Chem. Biol.* **2005**, *9*, 188–194.

²¹⁴ Vaughan, M. D.; Johnson, K.; DeFrees, S.; Tang, X.; Warren, R. A. J.; Withers, S. G. *J. Am. Chem. Soc.* **2006**, *128*, 6300–6301.

²¹⁵ (a) Kren, V.; Thiem, J. *Chem. Soc. Rev.* **1997**, *26*, 463–474. (b) Drauz, K.; Waldmann, H. *Enzyme Catalysis in Organic Synthesis*, VHC, Weindmann, **1995**.

²¹⁶ Gill, I.; Valivety, R. *Angew. Chem. Int. Ed.* **2000**, *39*, 3804–3808.

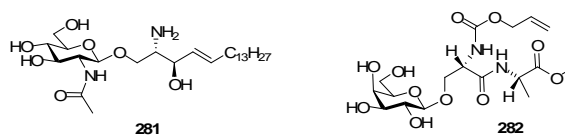
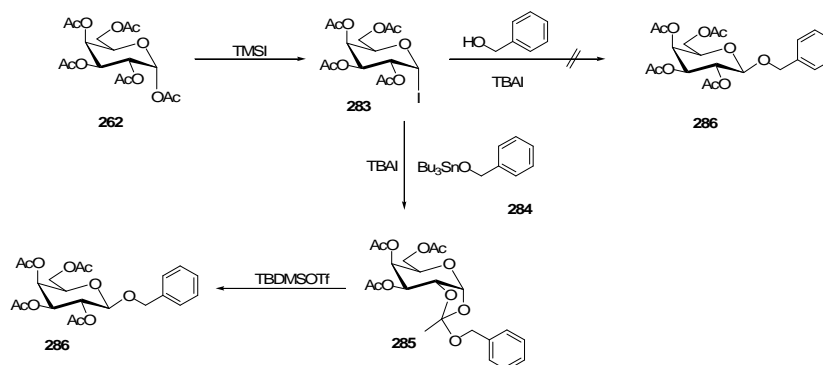


Figure 22

3.2.4. Results

3.2.4.1. Stannyl ceramides as efficient acceptors for synthesising β -galactosyl ceramides

With this back ground and with the goal to prepare β -glycosphingolipids, we glimpse a strategy involving coupling of α -galactosyl iodide and stannyl ether. The last one allows increasing the nucleophilicity of the oxygen without significant changes in the basicity. Stannyl ethers have been used in the synthesis of β -glycosides from 1,2-anhydro-glucose (1,2-oxiranes)²¹⁷ and from selenoglycosides.²¹⁸ In this context, we selected glycosyl iodides as the glycosyl donors because they can be activated by tetrabutylammonium iodide (TBAI), which can also activate the stannyl ether.



Scheme 53. Glycosylation-isomerization reaction of BnOSnBu_3 284 with the iodogalactose 283 in the presence of TBAI and TBDMSOTf to give 286

²¹⁷ (a) Danishefsky, S. J.; Gervay, J.; Peterson, J. M.; McDonald, F. E.; Koseki, K.; Griffith, D. A.; Oriyama, T.; Marsden, S. P. *J. Am. Chem. Soc.* **1995**, *117*, 1940–1953. (b) Liu, K. K.-C.; Danishefsky, S. J. *J. Org. Chem.* **1994**, *59*, 1895–1897. (c) Liu, K. K.-C.; Danishefsky, S. J. *J. Am. Chem. Soc.* **1993**, *115*, 4933–4934.

²¹⁸ (a) Yamago, S.; Yamada, T.; Ito, H.; Hara, O.; Mino, Y.; Yoshida, J.-I. *Chem. Eur. J.* **2005**, *11*, 6159–6174. (b) Yamago, S.; Yamada, T.; Nishimura, R.; Ito, H.; Mino, Y.; Yoshida, J.-I. *Chem. Lett.* **2002**, 152–153. (c) Yamago, S.; Yamada, T.; Hara, O.; Ito, H.; Mino, Y.; Yoshida, J.-I. *Org. Lett.* **2001**, *3*, 3867–3870.

Initially, we studied the reaction of tetra-*O*-acetyl- α -iodogalactose **283**, prepared by reaction of penta-*O*-acetylgalactose **262** with TMSI, with the stannyl ether **284**. We tried the reaction in toluene at 80 °C using TBAI as the catalyst, and we obtained the orthoester **285** (Scheme 53), which is the product usually obtained when the reaction is driven in neutral conditions. Treatment of **285** with tert-butyldimethylsilyl triflate (TBDMSOTf)²¹⁹⁻²²⁰ afforded the β -*O*-glycoside **286** in 90% overall yield (Table 2, entry 3). In the absence of TBAI, and in similar conditions, the reaction does not evolve (Table 2, entry 4).

Table 2. Glycosylation-isomerization reaction of BnOSnBu₃ **284** with the iodogalactose **283** in the presence of TBAI and TBDMSOTf to give **286**^a

Entry	Solvent	Bu ₄ NI	T (°C)	Time (h)	Yield ^b (%)	Ratio (α/β)
1	Toluene	10 %	rt	24	-	-
2	Toluene	-	rt	24	-	-
3	Toluene	10 %	80	18	90	0/1
4	Toluene	-	80	18	-	-
5	CH ₂ Cl ₂	10 %	reflux	18	95	0/1
6	CH ₂ Cl ₂	10 %	rt	24	96	0/1

^a Reaction conditions: **283** (1.2 mmol), **284** (1 mmol), and then TBDMSOTf (0.5 mmol), CH₂Cl₂ (20 mL), 0 °C, 30 min.

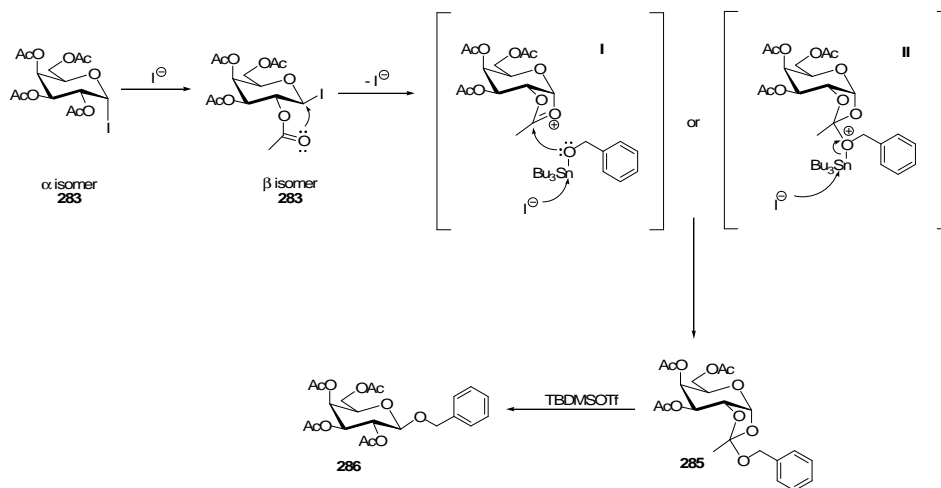
^b Yields of isolated product after chromatographic purification and for the two steps.

When the reaction was carried out in toluene at room temperature, only the starting material was recovered (Table 2, entries 1 and 2) and at 150 °C, decomposition products were observed in the crude reaction mixture. The reaction was then tried in CH₂Cl₂ at reflux in the presence of catalytic amounts of TBAI obtaining the orthoester **285**, which after treatment with TBDMSOTf gave **286** in 95% yield (Table 2, entry 5). Interestingly, the reaction also evolved at room temperature providing similar yields although in a longer reaction time (Table 2, entry 6). In both cases, the presence of TBAI was necessary for the reaction takes place. Finally, we tried the reaction with the

²¹⁹ (a) Kong, F. *Carbohydr. Res.* **2006**, *342*, 345–373. (b) López, J.C.; Agocs, A.; Uriel, C.; Gómez, A.M.; Fraser-Reid, B. *Chem. Comm.* **2005**, 5088–5090. (c) Jayaprakash K.N.; Fraser-Reid, B. *Org. Lett.* **2004**, *6*, 4211–4214.

²²⁰ For a review about the applications of sugar orthoesters in synthesis of oligosaccharies: Kong, F. *Carbohydr. Res.* **2006**, *342*, 345–373.

benzyl alcohol as the glycosyl acceptor in boiling dichloromethane and toluene, and neither the glycosylated product nor the orthoester were observed. It can be concluded that the use of TBAI and stannylether derivatives allow the efficient activation of disarmed glycosyl iodides affording the corresponding orthoester in excellent yields. This orthoester can be isomerized to the β -glycoside in excellent yields by using TBDMSOTf or $\text{BF}_3 \cdot \text{OEt}_2$.



Scheme 54. Proposed reaction mechanism

Scheme 54 shows the proposed mechanism of the reaction, which must start by the attack of iodide anion to form the β -iodo-intermediate **283**.²²¹ In principle, it would be expected, according to the well known mechanism for orthoester formation, that intermediate **I** would be formed by intramolecular attack of the acetate group. But the fact that benzyl alcohol does not react in these conditions seems to indicate that the attack of iodide is faster, thereby making the reaction reversible. Then, it is reasonable to think that iodide, removed from **283** or from TBAI, will attack the tin in **I** or **II** to form the thermodynamically stable stannyl iodide, driving the reaction to the orthoester **285** (Scheme 54). Consequently, TBAI should have two functions, to form the reactive β -iodo-glycoside and make the reaction irreversible.²²²

Next we explored the reaction of the amide **288**, a simplified model of ceramides, with the glycosyl donor **283** (Table 3). The reaction was carried out in

²²¹ Gervay, J.; Nguyen, T. N.; Hadd, M. J. *Carbohydr. Res.* **1997**, *300*, 119–125.

²²² (a) Cruzado, C.; Bernabé, M.; Martín-Lomas, M. J. *Org. Chem.* **1989**, *54*, 465–469. (b) Harpp, D. N.; Gingras, M. J. *Am. Chem. Soc.* **1988**, *110*, 7737–7745.

dichloromethane and toluene at different temperatures and in the presence or absence of TBAI. When the reaction was carried out at room temperature in dichloromethane, the orthoester **289** was obtained, and a further treatment with TBDMSOTf or $\text{BF}_3 \cdot \text{OEt}_2$ afforded **291** in 62 % yield for the two steps (Table 3, entry 1). The yield increased to 88% (entry 2) when the reaction was heated to reflux. The best result, 93% yield, was obtained performing the reaction in toluene at 80 °C (entry 3). In this case the presence of TBAI was also necessary for the reaction to evolve (entry 4). These results contrast with those obtained in the glycosylation of ceramides using other common leaving groups such as trichloroacetimidate, iodide or bromide, where yields were lower than 50%.¹⁶⁶ It has been reported that the use of pivaloyl protecting groups avoids the formation of the orthoester.²²³ However, when started from the pivaloyl protected donor **287**, a mixture of orthoester **290** and the β -glycoside **292** was obtained, similar to that reported for related glycosyl donors.²²⁴

Table 3. Synthesis of compound 291 by glycosylation of the stannyl amide 288 with the iodides 283 in the presence of TBAI followed by isomerization

Entry	Solvent	Temp. (°C)	Yield (%) ^b	Ratio (α/β)
1	CH_2Cl_2	Rt	62	0/1
2	CH_2Cl_2	Reflux	88	0/1
3	Toluene	80	93	0/1
4 ^c	Toluene	80	-	-

^a Reaction conditions: **283** (1.2 mmol), **288** (1 mmol), Bu_4NI (0.10 mmol), 18 h and then $\text{BF}_3 \cdot \text{Et}_2\text{O}$ (3 mmol), CH_2Cl_2 (20 mL), rt, 3h.

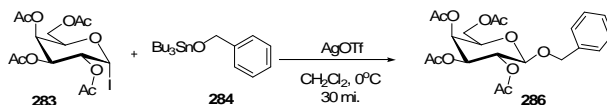
^b Yields of isolated product after chromatographic purification and for the two steps.

^c In absence of TBAI

²²³ (a) Pleuss, N.; Kunz, H. *Angew. Chem. Int. Ed.* **2003**, *42*, 3174-3176. (b) Herreus, A.; Kunz, H. *Liebigs Ann. Chem.* **1982**, 41-48.

²²⁴ Perrie, J. A.; Harding, J.R.; King, C.; Sinnott, D.; Stachulski, A. V. *Org. Lett.* **2003**, *5*, 4545-4548.

Table 4. Glycosilation of 284 with the iodide 283 in presence of AgOTf to give 286



Entry	Equi. AgOTf	Time (h)	Yield (%) ^b	Ratio α/β
1	1	0.5	63	0/1
2	1	2	63	0/1
3	2	0.5	68	0/1
4	2	2	69	0/1
5	3	0.5	89	0/1
6	3	2	90	0/1
7	4	0.5	100	0/1

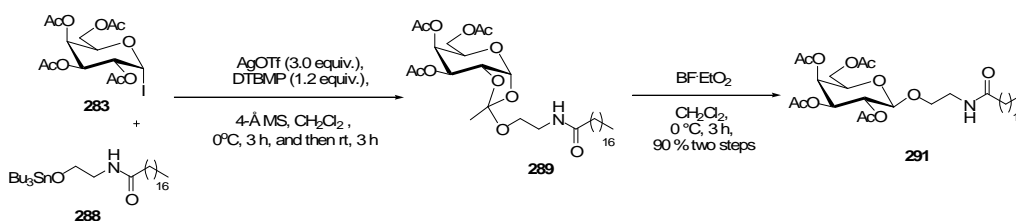
^a Reaction conditions: **283** (1.2 equiv), **284** (1 equiv), CH₂Cl₂ (15 mL), 0 °C, 30 min.

^b Yields of isolated product alter chromatographic purification.

In this point of our research, we considerate the possibility to use other promoters. Therefore, a screen of alternative activator for glycosylation reaction was conducted, focusing on replacement of the TBAI with AgOTf. Thus, when the α -iodo-galactose **263** was reacted with benzyl tributylstannyl ether **284** at 0 °C in the presence of AgOTf, the β -glycoside **286** was obtained in 63% yield after 0.5 hours (Table 4, entry 1). Longer reaction times did not affect the yield (entry 2). The equivalents of AgOTf have a strong influence in the yield and when 3 and 4 equivalents were used compound **286** was obtained in quantitative yield in a short time (Table 4, entries 3-5). The ¹H NMR spectrum of the reaction crude showed exclusively the presence of the β -

anomer, and the presence of orthoester, or elimination products was not observed. When the reaction was carried out with benzyl alcohol as glycosyl acceptor in the optimized conditions, only 42 % yield was obtained. These results indicated that stannyl ether is necessary to facilitate the reaction.

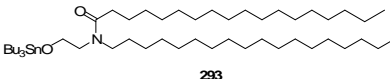
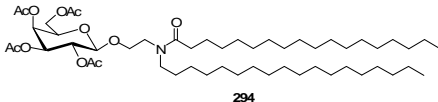
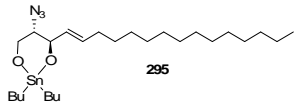
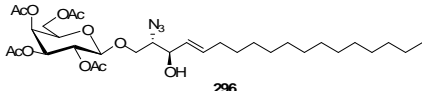
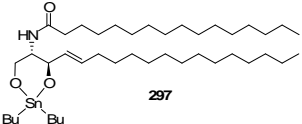
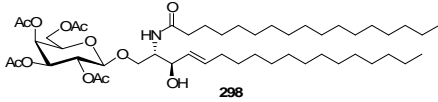
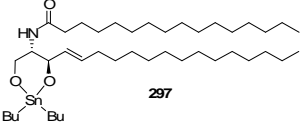
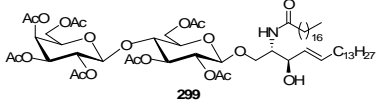
Then, we tried to glycosylate the stannyl ether **288** (Scheme 55), using AgOTf as promoter. When the galactosyl iodide **283** was reacted with **288** in the presence only of AgOTf a mixture of the orthoester **289** and the corresponding β -O-glycoside **291** (ratio 1:2) was obtained, which was deduced from the ^1H NMR of the reaction crude. The ^1H NMR spectra show in particular δ 5.79 (1H, d, $J=3.6$ Hz, 1-H) and 1.6 (3H, s, methyl group), that can be attributed to orthoester **289**. The mixture of **289** and **291** was treated with $\text{BF}_3\cdot\text{OEt}_2$ to effect the rearrangement of **289** to **291** and the β -O-glycoside was obtained in 90% of overall yield (Scheme 55). Adding of Cl_2Sn not seem to affect the ratio between **289** and **291**, and the presence of 2,6-di-tert-butyl-4-methylpyridine (DTBMP) afforded the orthoester exclusively as a consequence of the decreasing of the acidity. It should be noted that pivaloyl-protected glycosyl donor does not prevent the formation of orthoester totally.²²³



Scheme 55. Glycosylation of the stannyl ether **288 derived from β -amido alcohol**

To test the scope of these glycosylation protocols in the synthesis of biologically relevant glycolipids, glycosylation of azidosphingosine, ceramide and analogues was tested (Table 5). Thus, when the stannyl ether **293**, a ceramide analogue, was reacted with **283** following the general protocol of glycosylation employing TBAI as promoter the orthoester was exclusively obtained, which was treated with $\text{BF}_3\cdot\text{OEt}_2$ affording the glycolipid **294** in 93 % yield. Similar yields were obtained when AgOTf was used as promoter (Table 5, entry 1).

Table 5. Glycosylation of 293, 295 and 297 using 283 as glycosyl donor and TBAI or AgOTf as promoters to afford the orthoester followed by isomerization to give the glycolipids 294, 296, 298 and 299

Entry	Stannylated glycosyl acceptor	Glycolipid	Promoter	Yield (%) ^c
1	 293	 294	TBAI ^a	93
			AgOTf ^b	91
2	 295	 296	TBAI ^a	94
			AgOTf ^b	93
3	 297	 298	TBAI ^a	90
			AgOTf ^b	90
4	 297	 299	TBAI ^a	90
			AgOTf ^b	88

^a Reaction conditions: **283** (1.2 mmol), **293**, **295** or **297** (1 mmol), Bu₄NI (0.10 mmol), 18 h and then BF₃·Et₂O (3 mmol), CH₂Cl₂ (20 mL), rt, 3 h. ^b Reaction conditions: **283** (1.2 mmol), **293**, **295** or **297** (1mmol), AgOTf (3.0 mmol), DTBMP (1.2 mmol), 4-Å MS, CH₂Cl₂ (20 mL), 0°C for 3 h, after 3 h, and then BF₃·Et₂O (3 mmol), CH₂Cl₂ (15 mL), rt, 3 h.

^b Yields of isolated product after chromatographic purification and for the two steps, glycosylation and isomerization

The classical protocol for selective glycosylation of diols, require a series of programmed protection-deprotection steps to ensure that only one of the hydroxyls reacts. Azido-sphingosine has two hydroxyl functions in positions 1,3 that can be simultaneously protected as stannyl acetal. When stannyl acetal **295**, obtained from azidosphingosine by reaction with Bu₂SnO with water exclusion, was reacted with **283** in the standard conditions the β-*O*-glycoside **296** was obtained in 94 % yield after orthoester isomerization. Also in this case, the use of AgOTf as promotor afforded similar yields (Table 5, entry 2). The reaction was fully chemo and stereoselective by involving exclusively the primary hydroxyl group. Similarly, the stannyl acetal **297**, obtained by reaction of ceramide and Bu₂SnO, was also reacted with the glycosyl iodide **283** in the presence of TBAI or AgOTf, and then the corresponding reaction products were treated with BF₃·OEt₂ to obtain the galactosyl ceramide **298** in 90 % yield. Also in

this case the reaction was fully chemo and stereoselective (Table 5, entry 3). Finally, glycosilation of **297** with the corresponding hepta-*O*-acetylactosyl iodide in the presence of TBAI or AgOTf, also afforded corresponding glycolipid **299** in excellent yield (90%) after orthoester isomerization. The overall process takes place with complete chemo and stereoselectivity (Table 5, entry 4). Pleasingly, all these results are close to the obtained by enzymatic procedures by using glycosyl fluorides as glycosyl donors.²²⁵ In all cases when the reaction crudes were analyzed by ¹H NMR no α anomer or the corresponding elimination product (glycal) were observed.

Alternatively, we also investigated the reactivity of stannyl ethers with various leaving groups such as bromide, fluoride, trichloroacetimidate and acetate in the appropriate reaction conditions. This study focused in the use of stannyls ethers and **288** and **297**, which were reacted with glycosyl donors **300-302** and **262** (Table 6). It was expected that the bromo derivative **300** will behaves similarly to iodo derivative **283** when AgOTf will be used as promotor. Effectively, when **300** was reacted with the stannyl ether **288** a mixture of galactoside **291** and the orthoester **289** was obtained. Further isomerization by treatment with BF₃·OEt₂, exclusively afforded the β -galactoside **291** in yield similar to the obtained starting from α -iodo-galactose (Table 6, entry 1).

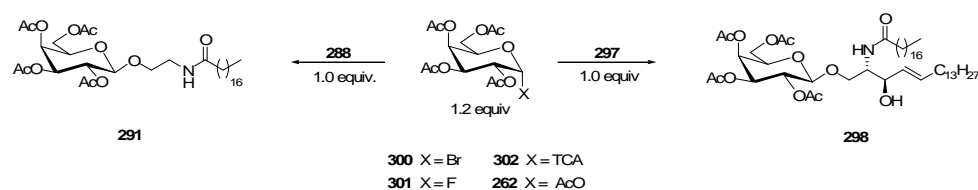
Using the glycosyl fluoride **301** as donor, the stannyl ethers **288** and **297** as acceptors and the couple SnCl₂/AgOTf as promoter β -glucosides **291** and **298** together with the respective orthoesters, were also obtained. In the presence of BF₃·OEt₂ these mixtures evolved to compounds **291** and **298**, which were obtained in high yields and exclusive as β -anomers (Table 6, entries 3 and 4.). When the trichloroacetimidate **302** was used as donor the glycosylation of **288** and **297** in the presence of BF₃·OEt₂ afforded the orthoesters as major products, in spite of the presence of substequiometric amounts of BF₃·OEt₂. The orthoester was, however, then isomerized in good yields to give the β -anomer by adding additional amounts of BF₃·OEt₂ (Table 6, entries 5 and 6.).

The reaction of penta-*O*-acetyl- β -D-galactopyranose **262**, a readily accessible glycosyl donor, was also probed with with the stannylated acceptors **288** and **297** in the presence of large excess of BF₃·OEt₂ which afforded directly the β -glycoside **291** in (76%) and **298** (70%). In this case the *O*-glycosides were obtained only in moderate yields due to the side reactions; the acetates groups are hydrolyzed to give the partially

²²⁵ Vaughan, M.D.; Johnson, K.; DeFrees, S.; Tang, X.; Warren, R.A.J.; Withers, S.G. *J. Am. Chem. Soc.* **2006**, *128*, 6300–6301.

deprotected compound (Table 6, entries 7 and 8,). These results reveal that stannyl ethers exhibit enhancement of the nucleophilicity of hydroxyl group, properties that make them react with unique selectivity with a variety of leaving groups. Despite the stannyl ethers are basic molecules with lower reactivity than the common alkoxide, no elimination product (glycal) were observed.

Table 6. Examination of various glycosyl donors-promoters pairs in glycosilation of ceramides^a



Entry	Acceptor	Donor (X)	Promoter	Time (h)	Product	Yield (%) ^a
1	288^b	300 (Br)	AgOTf (3 mmol)	5	291	88
2	2997^b	300 (Br)	AgOTf (3 mmol)	5	298	85
3	288^c	301 (F)	SnCl ₂ /AgOTf (3 mmol)	3	291	91
4	297^c	301 (F)	SnCl ₂ /AgOTf (3 mmol)	3	298	90
5	288^d	302 (TCA)	BF ₃ ·OEt ₂ (0.5 mmol)	3	291	85
6	297^d	302 (TCA)	BF ₃ ·OEt ₂ (0.5 mmol)	3	298	82
7 ^c	288^e	262 (OAc)	BF ₃ ·OEt ₂ (6 mmol)	4	291	73
8 ^c	297^e	262 (OAc)	BF ₃ ·OEt ₂ (6 mmol)	4	298	70

^aYields of isolated product after chromatographic purification and for the two steps. For conditions see:

^bRef. 226, ^cref. 227, ^dref. 228, and ^eref. 229.

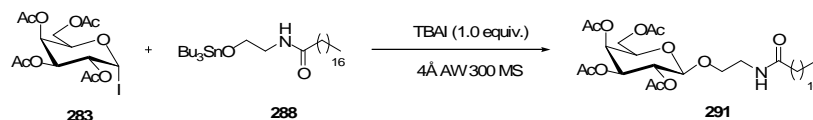
²²⁶ Hanessian, S.; Banoub, J. *Carbohydr. Res.* **1977**, *53*, C13–C16

²²⁷ (a) Mukaiyama, T.; Murai Y.; Shoda, S. *Chem. Lett.* **1981**, 431–432. (b) Ogawa T.; Takahashi, Y. *Carbohydr. Res.* **1985**, *138*, C5–C9. (c) Nicolaou, K. C.; Li J.; Zenke, G. *Helv. Chim. Acta* **2000**, *83*, 1977–2006. (d) Seki, M.; Kayo A.; Mori, K. *Tetrahedron Lett.* **2001**, *42*, 2357–2360.

²²⁸ (a) Schmidt R. R.; Michel, J. *Angew. Chem. Int. Ed. Engl.* **1980**, *19*, 731–732. (b) Compostella, F.; Franchini, L.; De Libero, G.; Palmisano, G.; Ronchetti F.; Panza, L. *Tetrahedron* **2002**, *58*, 8703–8708.

²²⁹ (a) Dahmen, J.; Frejd, T.; Magnusson G. Noori, G. *Carbohydr. Res.* **1983**, *114*, 328–330. (b) Villard, R.; Hammache, D.; Delapierre, G.; Fotiadu, F.; Buono G.; Fantini. *J. ChemBioChem.* **2002**, *3*, 517–525.

Table 7. Synthesis of compound 291 by glycosylation of stannyl amide 288 with iodide 283 in the presence of TBAI and 4Å AW 300 MS^a



Entry	AW 300MS (g)	Solvent	Temp/°C	Time (h)	Yield (%) ^b
1	0.2	Toluene	80	18	22
2	0.4	Toluene	80	18	35
3	0.6	Toluene	80	18	37
4	0.8	Toluene	80	18	42
5	1	Toluene	80	18	48
6	1.2	Toluene	80	18	64
7	1.2	Toluene	rt	18	25
8	1.2	CH ₂ Cl ₂	reflux	18	50
9	1.2	CH ₂ Cl ₂	rt	18	29
10	1.2	Et ₂ O	reflux	18	35
11	1.2	Et ₂ O	rt	18	15

^a Conditions: **283** (0.366 mmol), ratio **283/288/TBAI**=1.2:1:1

^b Yields of isolated product after chromatographic purification.

Traditionally, the rearrangement of ortho ester has been carried out by strong and moisture sensitive Lewis acids, including TMSOTf,²¹⁹⁻²²⁰ BF₃·Et₂O,²¹⁹⁻²²⁰ TBSOTf,²³⁰ Yb(OTf)₃,²³¹ and more recently AuCl₃²³² under strictly anhydrous

²³⁰ Mathew, F.; Mach, M.; Hazen, K. C.; Fraser-Reid, B. *Synlett* **2003**, 1319–1322.

²³¹ Fraser-Reid, B.; Chaudhuri, S. R.; Jayaprakash, K. N.; Lu, J.; Ramamurty, Ch. V. S. *J. Org. Chem.* **2008**, *73*, 9732–9743.

²³² Sureshkumar, G.; Hotha, S. *Chem. Comm.* **2008**, 4282–4284.

conditions. In this context, it was recently observed that activated 4 Å acid washed molecular sieves (4Å AW MS or AW 300), also catalyzed this rearrangement.²³³ Other studies indicated that AW 300 can both play the usual role of drying agents and promote²³⁴ in the synthesis of trisaccharides.²³⁵ We hence sought to exploit the application of heterogeneous solid acid promoter to tackle the direct glycosylation of ceramides. We describe here that β-*O*-galactosyl ceramides can be obtained in *one*-pot manner from 2,3,4,6-tetra-*O*-acetylgalactosyl iodide and stannyl ceramides in the presence of TBAI and AW300 MS.

The effectiveness of AW 300 as a glycosylation promoter was first tested by triggering the model experiment of donor tetra-*O*-acetyl-α-iodogalactose **283** with stannyl ceramide **288** in the presence of TBAI (1.0 equiv.) to give the glycosphingolipid **291** (Table 7). Thus, we started the screening with a relation of 0.2, 0.4, 0.6, 0.8 and 1.0 g of AW 300/1.0 mmol of stannyl ceramide **288** in toluene at 80 °C (Table 7, entries 1-5). This initial experiment gave only low yield until to our delight; we found that the corresponding β-glycoside was obtained in good yield and high stereoselective when 1.2 g of AW 300 was used (Table 7, entry 6). Encouraged by the success of this reaction, we next examined the effects of temperature and solvents. As depicted in Table 7, the reaction conducted in CH₂Cl₂ at reflux gave good yield (50%, entry 8). When the reaction was performed in Et₂O, the glycolipid **291** was obtained in 35% yield (Entry 10). The yield was dramatically decreased by lowering the reaction temperature under the same reaction conditions in CH₂Cl₂ and toluene (Table 7, entries 7 and 9). The use of AW 300 makes the workup procedure very simple; the solid was easily separated from reaction mixture by a simple filtration.

With these results in hand, we tried to extend this methodology to other acceptors and donors (Table 8). Thus, ceramide **293** could be also glycosylated with donor **283** under the same reaction conditions used for **288** giving the glycosphingolipid **294** in good yield (65 %, Table 7, entry 1). Reactions conducted with ceramide **297** provide the β-GalCer **298** in 60% yields (Table 7, entry 2). As illustrated in Table 7, reactions performed with hepta-*O*-acetylactosyl iodide as donor afforded the corresponding

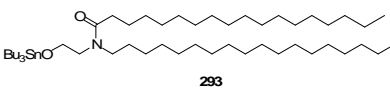
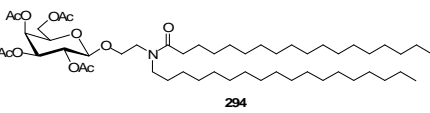
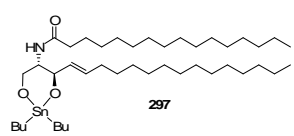
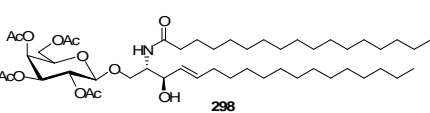
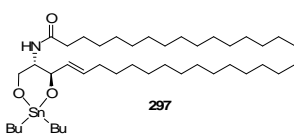
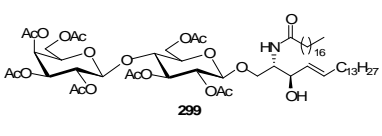
²³³ Rabiad, A.; Liu, X.; Kovacs, L.; Seeberger, P. H. *Org. Lett.* **2006**, *8*, 1815–1818.

²³⁴ Adinolfi, M.; Barone, G.; Iadonisi, A.; Schiattarella, M. *Org. Lett.* **2003**, *5*, 987–989.

²³⁵ Adinolfi, M.; Iadonisi, A.; Ravidà, A.; Schiattarella, M. *J. Org. Chem.* **2005**, *70*, 5316–5319.

glycosphingolipid **299** in moderate yield with high stereoselectivity (60 %, Table 8, entry 3).

Table 8. Glycosylation of **293, and **297** using **283** as glycosyl donor in the presence of TBAI and 4Å AW 300 MS to give the glycolipids **294**, **298** and **299**^a**

Entry	Stannylated glycosyl acceptor	Glycolipid	Ratio (α/β)	Yield ^b (%) ^c
1			0/1	65
3			0/1	60
3			0/1	60

^a Reaction conditions: **283** (1.2 mmol), **293**, or **297** (1 mmol) and 4-Å AW 300 MS (1200 mg), in toluene (10 mL), 80 °C for 18 h. ^b Yields of isolated product after chromatographic purification.

In an attempt to promote the rearrangement of ortho ester *in situ*, various acids and conditions were tested: TfOH, TMSOTf, TBSOTf, BF₃·Et₂O (Table 9). Although no glycoside with 0.2-1.0 equiv of these Lewis acids was observed, the use of BF₃·Et₂O was found successful but no equally effective than AW 300. In this case, two equiv of BF₃·Et₂O was necessary to obtain 20 % yield.

Table 9. Synthesis of compound **291 by glycosylation of stannyl amide **288** with iodide **283** in the presence of TBAI and different Lewis acids^a**

Entry	Acid	Equiv.	Product observed	Yield ^b (%)	Ratio (α/β)
1	TfOH	0.2	Orthoester 289	90	

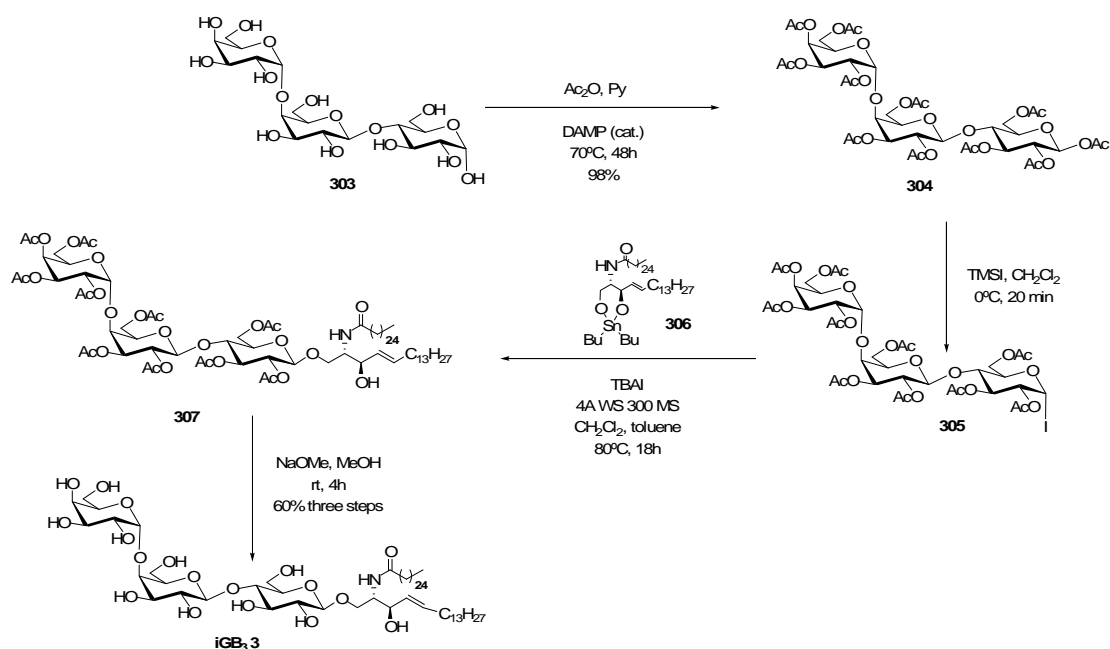
2	TfOH	0.4	Orthoester 289	90	
3	TfOH	0.8	Orthoester 289	90	
4	TfOH	1	Side products	-	
5	TMSOTf	0.2	Orthoester 289	90	
6	TMSOTf	0.4	Orthoester 289	90	
7	TMSOTf	0.8	Orthoester 289	85	
8	TMSOTf	1	Side products	-	
9	TBSOTf	0.2	Orthoester 289	90	
10	TBSOTf	0.4	Orthoester 289	80	
11	TBSOTf	0.8	Orthoester 289	75	
12	TBSOTf	1	Glycolipid 291	10	0/1
13	BF ₃ ·Et ₂ O	0.2	Orthoester 289	90	
14	BF ₃ ·Et ₂ O	0.4	Orthoester 289	90	
15	BF ₃ ·Et ₂ O	0.8	Orthoester 289	90	
16	BF ₃ ·Et ₂ O	1	Orthoester 289 and glycolipid 291	85:5	
17	BF ₃ ·Et ₂ O	1.5	Glycolipid 291	10	0/1
18	BF ₃ ·Et ₂ O	2	Glycolipid 291	15	0/1
19	BF ₃ ·Et ₂ O	3	Glycolipid 291	20	0/1

^a Reaction conditions: **283** (1.2 mmol), **288** (1 mmol) in toluene (10 mL), 80 °C for 18 h. ^b Yields was determinate by ¹H NMR.

3.2.5. Synthesis of iGb3

The synthetic utility of the new approach was further demonstrated by the rapid access to isoglobotrihexosylceramide **3** (iGb3). The donor **305** and stannyl ceramide **306** would serve as the building blocks for glycosylation. Thus, isoglobotrihexose **303** was treated with acetic anhydride and pyridine in presence of catalytic DMAP to provide the peracetylated trisaccharide **304** in 98% yield. Then, the iodide donor **305** was generated in situ from **304**. Finally, treatment of **307** with **306** in the presence of TBAI and AW 300, followed by the elimination of the acetate groups furnished iGb3 **3** in 60 % yield as unique anomer. The spectroscopic data of ¹H and ¹³C NMR for **3** were consistent with data reported for the synthetic product²³⁶ (Scheme 56).

²³⁶ Yao, Q.; Song, J.; Xia, Ch.; Zhang, W.; Wang, P. G.; *Org. Lett.* **2006**, *8*, 911–914.



Scheme 56. Synthesis of iGB3

3.2.6. Synthesis of KRN7000

Since the isolation of a group of marine galactosyl ceramides in the 1990s from *Agelas mauritanus*,²³⁷ and subsequent synthesis of analogues,²³⁸ this family has been a subject of great interest because of the potent antitumor activity found in vivo at the organism level and because the galactosyl ceramides contained α -glycosidic bonds between the sugar and ceramide, illustrated by agelasphin-9b **308** and KRN700 **309** (Figure 23), despite being naturally occurring compounds, are in general not found in higher organisms, that is, are not natural products of mammalian cells.

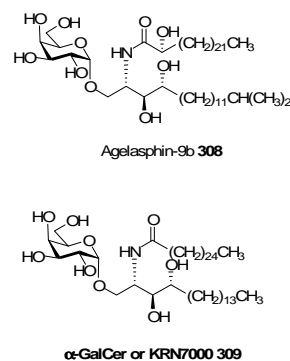


Figure 23. α -Glycosphingolipids

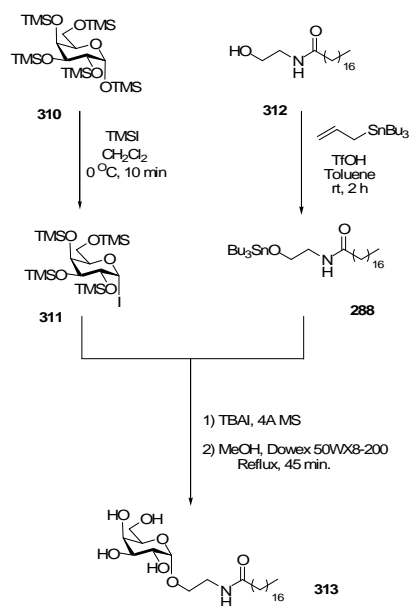
At the molecular level, glycolipid **309** has been shown to act as a connecting ligand presented by the CD1d molecule of antigen-presenting cells to the murine V α 14

²³⁷ (a) Natori, T.; Koezuka, Y.; Higa, T. *Tetrahedron Lett.* **1993**, *34*, 5591–5592. (b) Akimoto, K.; Natori, T.; Morita, M. *Tetrahedron Lett.* **1993**, *34*, 5593–5596. (c) Natori, T.; Morita, M.; Akimoto, K.; Koezuka, *Tetrahedron* **1994**, *50*, 2771–2784.

²³⁸ Franck, R.W.; Tsuji, M. *Acc. Chem. Res.* **2006**, *39*, 692–701.

receptor and the human V α 24 receptor of natural killer T (NKT) cells. Upon recognition of the galactosyl ceramide in the context of CD1d, the NKT cell then is stimulated to produce interferon- γ (IFN- γ), interleukin-4 (IL-4), and interleukin-2 (IL-2).²³⁹ Other exploration of the biological effects of KRN7000 has unveiled its remarkable activity against a group of disease, such as cancer,²⁴⁰ malaria,²⁴¹ juvenile diabetes,²⁴² hepatitis B,²⁴³ and autoimmune encephalomyelitis.²⁴⁴

Gervay-Hague recently demonstrated the effectiveness of α -galactosyl iodides in the synthesis of α -galactosyl azidosphingolipids¹⁸² and α -GalCer.²⁴⁵ In the case of α -GalCer, per-*O*-silylated galactosyl iodide donor **311** and an unprotected ceramide acceptor were used under microwave conditions. The reaction proceeded with complete stereoselectivity and a remarkable 67% yield for the synthesis of KRN7000 **309**. However, in our hands, this procedure (TBAI, DIPEA, CH₂Cl₂, 120 °C, 300 W, 2 h) proved ineffective for the preparation of simple α -GalCer analogues such as **313** starting from per-*O*-silylated galactosyl iodide **311** and acceptor **288** (Scheme 57). Under these conditions, the expected product was obtained in only 10% yield (α/β ratio 87:13).



Scheme 57. Glycosylation reaction of 42 with the iodogalactose 62 in the presence of TBAI

²³⁹ (a) Brigl, M.; Brenner, M. B. *Annu. Rev. Immunol.* **2004**, *23*, 817–890. (b) Zhou, D.; Mattner, J.; Cantu, C., 3rd; Schrantz, N.; Yin, N.; Gao, Y.; Sagiv, Y.; Hudspeth, K.; Wu, Y. P.; Yamashita, T.; Teneberg, S.; Wang, D.; Proia, R. L.; Lavery, S. B.; Savage, P. B.; Teyton, L. *Science* **2004**, *306*, 1786–1789.

²⁴⁰ (a) Kikuchi, A.; Nieda, M.; Schmidt, C.; Koezuka, Y.; Ishihara, S.; Ishikawa, Y.; Tadokoro, K.; Durrant, S.; Boyd, A.; Juji, T.; Nicol, A. *Br. J. Cancer* **2001**, *85*, 741–746.

²⁴¹ Gonzalez-Aseguinolaza, G.; de Oliveira, C.; Tomaska, M.; Hong, S.; Bruna-Romero, O.; Nakayama, T.; Taniguchi, M.; Bendelac, A.; Van Kaer, L.; Koezuka, Y.; Tsuji, M. *Proc. Natl. Acad. Sci. USA* **2000**, *97*, 8461–8466.

²⁴² (a) Hong, S.; Wilson, M. T.; Serizawa, I.; Wu, L.; Singh, N.; Naidenko, O. V.; Miura, T.; Haba, T.; Scherer, D. C.; Wei, J.; Kronenberg, M.; Koezuka, Y.; Van Kaer, L. *Nat. Med.* **2001**, *7*, 1052–1056.

²⁴³ Kakimi, K.; Guidotti, L. G.; Koezuka, Y.; Chisari, F. V. *J. Exp. Med.* **2000**, *192*, 921–930.

²⁴⁴ Miyamoto, K.; Miyake, S.; Yamamura, T. *Nature* **2001**, *413*, 531–534.

²⁴⁵ Du, W.; Kulkarni, S.S.; Gervay-Hague, J. *Chem. Commun.* **2007**, 2336–2338.

In an effort to improve the yield of the direct glycosylation reaction, we applied our experience with stannyl ethers in the glycosylation of ceramides to give β -glycolipids in the synthesis of α -glycolipids. This procedure involves the reaction of tetra-*O*-acetyl- α -galactosyl iodide with stannyl ceramides in the presence of TBAI as activator to give β -GalCer analogues in high yield with complete stereoselectivity. TBAI inverts the configuration of the anomeric iodine to afford the highly reactive β -glycosyl iodide. We show herein a new glycosylation protocol providing α -GalCer analogues, and particularly KRN7000 **309**. This method activates classically reluctant acceptors such as amido alcohols and ceramides as stannyl derivatives in the TBAI-promoted glycosylation with glycosyl iodides **311**.

Table 10. Synthesis of compound 313 by glycosylation of stannyl amide 288 with iodides

Entry	Reaction conditions ^a (eq)	Yield%	α/β^b ratio
1	TBAI (2), 4Å MS, CH ₂ Cl ₂ , rt, 48 h	25	92:8
2 ^c	TBAI (2), 4Å MS, toluene, 110 °C, 5 h	47	89:11
3 ^{d,e}	TBAI (2), 4Å MS, toluene, 110 °C, 18 h	95	88:12
4	TBAI (2), 4Å MS, toluene, 80 °C, 18 h	98	97:3

^a α -Galactosyl iodide: TMSO-Gal (1eq), TMSI (1eq), CH₂Cl₂, 0 °C, 10 min; Stannyl ether: amide (1eq), Bu₃SnCH₂CH=CH₂ (1.3eq), TfOH (0.3eq), rt, 2 h.

^b Determined by integration of the anomeric proton signals in the ¹H NMR spectrum of the crude reaction mixture.

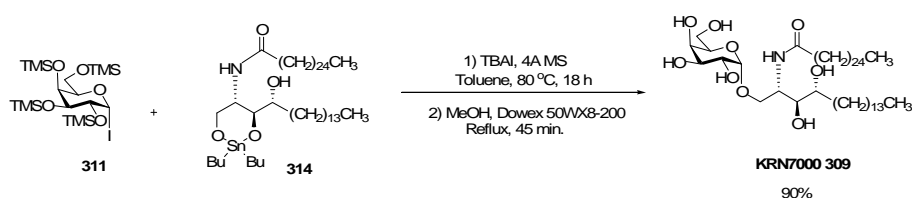
^c Addition of the α -Galactosyl iodide over the stannyl ether for 3 h.

^d Addition of the stannyl ether over the α -Galactosyl iodide for 3 h. ^e Dowex 50WX8-200, MeOH, rt, 4 h.

The glycosylation reaction conditions were optimized by starting from amido alcohol **312** (Scheme 57), which was converted into stannyl ether **288** to increase the nucleophilicity of the oxygen atom without significantly changing the basicity.²¹⁸ Initially, the reaction of **288** with α -iodogalactose **311** in the presence of TBAI was carried out in CH₂Cl₂ at room temperature (Table 10, entry 1). After hydrolysis by using Dowex 50WX8–200, isomer **313a** was obtained as the major product in a modest 25% yield. Next, we tried the reaction in toluene at 110 °C for 5 h in the presence of TBAI, but unexpectedly, the yield remained moderate (Table 10, entry 2). To our delight, however, we found that the order of addition of the reagents was important; specifically, we found that by adding the galactosyl iodide over the stannyl ether in toluene at 110 °C afforded the expected glycoside in an excellent overall yield of 95% and 88:12 α/β ratio

(Table 10, entry 3). Moreover, when the reaction was performed at 80 °C, the glycoside was obtained in almost quantitative yield with excellent selectivity (α/β ratio 97:3; Table 9, entry 4).

The highly stereoselective glycosylation method described above offers a very efficient and direct synthesis of unprotected α -glycolipids. To further demonstrate its synthetic value, we showed that the method can be used to rapidly prepare the biologically active compound KRN7000 **309** (Scheme 58). The reaction of the stannyl derivative of ceramide **314** with donor **311** was performed under optimized reaction conditions. After hydrolysis of protecting groups by using acidic resin, final product **309** was obtained in 90% yield with complete α -selectivity. The overall process takes place with complete chemoselectivity (differentiation of the primary and secondary OH at the lipid moiety) and stereoselectivity (α -anomer only).



Scheme 58. Direct glycosylation of phitosphingosine to obtain KRN7000

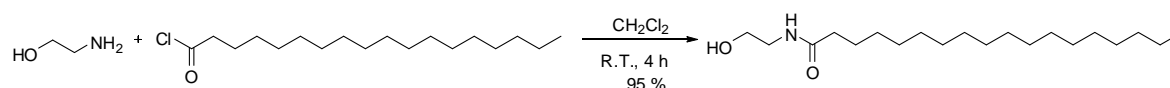
3.2.5. Experimental Part

General methods

All reactions were conducted under a dried argon stream. Solvents (CH_2Cl_2 99.9%, toluene 99.9%) were purchased in capped Pure Solv System-4[®] bottles and used without further purification and stored under argon. Yields refer to the chromatographically and spectroscopically (^1H and ^{13}C) homogeneous materials, unless otherwise stated. TMSI was stored at -15°C under desiccated atmosphere. All other solvents and reagents were used without further purification. All glassware utilized was flame-dried before use. Reactions were monitored by TLC carried out on 0.25 mm E. Merck silica gel plates. Developed TLC plates were visualized under a short-wave UV lamp and by heating plates that were dipped in ethanol/ H_2SO_4 (15:1). Flash column chromatography (FCC) was performed using flash silica gel (32–63 μm) and employed a solvent polarity correlated with TLC mobility. Melting points, determined with Reichert apparatus, are uncorrected. Optical rotations were measured at 598 nm on a Jasco DIP-370 digital polarimeter using a 100 mm cell. NMR experiments were conducted on a Varian 400 MHz instrument using CDCl_3 (99.9% D) as the solvent, with chemical shifts (δ) reference to internal standards CDCl_3 (7.26 ppm ^1H , 77.23 ppm ^{13}C) or Me_4Si as an internal reference (0.00 ppm) Chemical shifts are relative to the deuterated solvent peak and are in parts per million (ppm).

Experimental Procedures

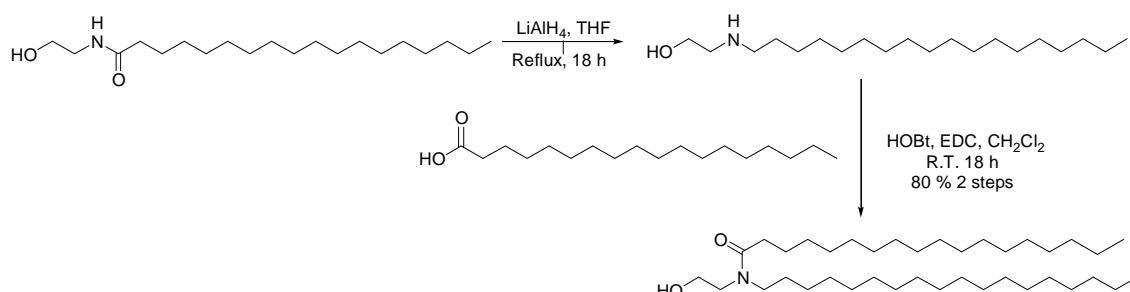
Synthesis of *N*-(2-hydroxyethyl)stearamide



A solution of stearoyl chloride (50 g 0.165 mol) in 250 mL of dry CH_2Cl_2 was cooled to 0°C . To this solution 2-amino ethanol (100.78 g, 1.65 mol) was added in a slow drop-wise manner over a period of 30 min, resulting in the precipitation of a white solid. The reaction was stirred for 4 h at room temperature and then the mixture was

filtered. The solid was washed with hexane and diethyl ether and dried *in vacuo*. The resulting crystalline material was recrystallized from CH_2Cl_2 to give 51.26 g of pure *N*-(2-hydroxyethyl)stearamide (95%) as a white solid²⁴⁶ that was homogeneous. TLC (Hexane-AcOEt-MeOH 60:30:10) R_f 0.25; m.p. 53–55 °C; ^1H NMR (400 MHz, CDCl_3): δ 5.94 (1H, br. s), 3.72 (2H, t, $J=5.2$ Hz), 3.42 (2H, td, $J=5.2, 1$ Hz), 2.18 (2H, t, $J=7.2$ Hz), 1.62 (2H, quint, $J=7.2$ Hz), 1.28 (28H, m), 0.87 (3H, t, $J=6.8$ Hz); ^{13}C NMR (100.6 MHz, CDCl_3): δ 172.6, 61.0, 41.6, 36.5, 31.8, 29.5, 28.6, 25.6, 22.7, 14.1. Anal. Calcd. for $\text{C}_{20}\text{H}_{41}\text{NO}_2$: C, 73.34; H, 12.62; N, 4.28. Found: C, 73.30; H, 12.69; N, 4.20.

Synthesis of *N*-(2-hydroxyethyl)-*N*-octadecylstearamide



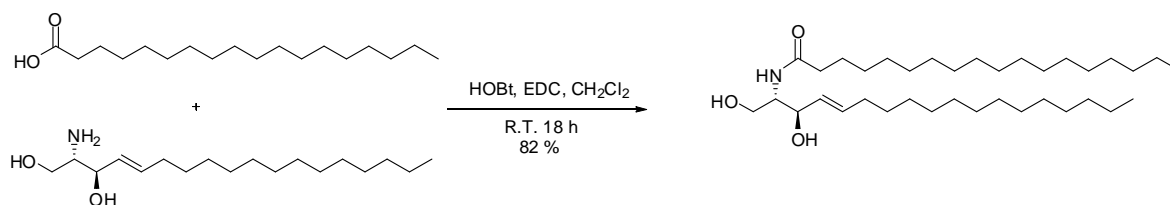
A 250 mL, three-necked, roundbottomed flask was fitted with a heating bath, mechanical stirrer, reflux condenser with drying tube, and a stoppered, pressure-equalizing dropping funnel, flushed with nitrogen or argon, and charged with 75 mL of dry THF, and LiAlH_4 (1.45 g, 38.22 mmol). A mixture of 75 mL of THF and *N*-(2-hydroxyethyl)stearamide (10 g, 30.58 mmol) was added, with stirring, at a rate sufficient to reach and maintain refluxing. After the addition was completed, the reaction mixture was kept boiling for 18 h. The flask was immersed in an ice bath, and 30 mL of water, 15 mL of 10% aqueous potassium hydroxide, and again 30 mL of water were added cautiously with very vigorous stirring. The reaction mixture was stirred for an additional 1h, filtered with suction, and the solid was washed with several 100-mL portions of ethyl acetate. The two layers were separated, and the aqueous phase was extracted with ethyl acetate (3 x 100 mL). The combined organic layers were dried

²⁴⁶ Eliash, R.; Weissbuch, I.; Weygand, M.J.; Kjaer, K.; Leiserowitz, L.; Lahav, M. *J. Phys. Chem. B*, **2004**, *108*, 7228–7240.

over anhydrous sodium sulphate and concentrated *in vacuo* to get crude residue of 2-(ocatadecylamino) ethanol as a white solid (6.7 g, 70%).²⁴⁷

A solution of 2-(octadecylamino) ethanol (1 g, 3.194 mmol), HOBt (586 mg, 3.832 mmol), EDC (734 mg, 3.832 mmol) and DIPEA (494 mg, 3.832 mmol) in 30 mL of dry CH₂Cl₂ was cooled to 0 °C. Stearic acid (908 mg, 3.194 mmol) in 20 mL of dry CH₂Cl₂ was added drop wise over 6 h at 0 °C, and then the reaction was stirred under argon for 18 h at room temperature. The mixture was diluted with ethyl acetate (75 mL) and washed successively with HCl (10 % aqueous, 2 x 30 mL), NaHCO₃ (7 % aqueous, 2 x 30 mL), K₂CO₃ (7% aqueous, 2 x 30 mL), and brine (3 x 30 mL). The organic layer was dried over MgSO₄ and concentrated *in vacuo*. The residue was purified by flash column chromatography on silica gel using hexane/AcOEt/MeOH (85:10:5) as the eluent to give 1.67 g of pure *N*-(2-hydroxyethyl)-*N*-octadecylstearamide (90 %). TLC (Hexane/AcOEt/MeOH 60:30:10) *R*_f 0.70; m.p. 50–52 °C; ¹H NMR (400 MHz, CDCl₃): δ 3.75 (2H, t, *J*=5.2 Hz), 3.52 (2H, t, *J*=5.2 Hz), 3.26 (2H, t, *J*=7.6 Hz), 2.32 (2H, t, *J*=7.6 Hz), 1.62-1.54 (4H, m), 1.25 (58H, m), 0.87 (6H, t, *J*=6.5 Hz); ¹³C NMR (100.6 MHz, CDCl₃): δ 173.0, 58.9, 50.2, 47.3, 34.3, 31.8, 30.4, 29.6, 29.3, 28.9, 28.6, 27.7, 22.7, 14.1. Anal. Calcd. for C₃₈H₇₇NO₂: C, 78.69; H, 13.38; N, 2.41. Found: C, 78.73; H, 12.98, N, 2.45.

Synthesis of *N*-((2*S*,3*R*,4*E*)-1,3-dihydroxyoctadec-4-en-2-yl)stearamide



A solution of sphingosine (100 mg, 0.333 mmol), HOBt (61 mg, 0.4 mmol), EDC (76 mg, 0.4 mmol) and DIPEA (77 mg, 0.6 mmol) in 20 mL of dry CH₂Cl₂ was cooled to 0 °C. Under stirring, stearic acid (94 mg, 0.333 mmol in 20 mL of dry CH₂Cl₂) was added drop wise over 6 h at 0 °C, and then the reaction was stirred under argon for 18 h at room temperature. The mixture was diluted with ethyl acetate (75 mL) and washed

²⁴⁷ Wilson, C.V.; Stenberg, J.F. *Org. Synth. Coll. Vol. 4*, 564–565.

successively with HCl (10% aqueous, 2 x 30 mL), NaHCO₃ (7% aqueous, 2 x 30 mL), K₂CO₃ (7% aqueous, 2 x 30 mL), and brine (3 x 30 mL). The organic layer was dried over MgSO₄ and concentrated *in vacuo*. The residue was purified by flash column chromatography on silica gel using hexane-AcOEt-MeOH (85:10:5) as the eluent to give 154 mg of pure *N*-((2*S*,3*R*,*E*)-1,3-dihydroxyoctadec-4-en-2-yl)stearamide (82 %). TLC (Hexane-AcOEt-MeOH 60:30:10) *R*_f 0.70; m.p. 104–106 °C; ¹H NMR (400 MHz, CDCl₃): δ 6.23 (1H, d, *J*=7.3 Hz), 5.77 (1H, dt, *J*=15.4, 6.7 Hz), 5.51 (1H, dd, *J*=15.4, 6.4 Hz), 4.3 (1H, dd, *J*=6.4, 3.4 Hz), 3.94 (1H, dd, *J*=11.3, 3.7 Hz), 3.89 (1H, dddd, *J*=7.3, 3.7, 3.4, 3.2 Hz), 3.69 (1H, dd, *J*=11.3, 3.2 Hz), 2.21 (2H, t, *J*=7.5 Hz), 2.03 (2H, dt, *J*=7.2, 6.7 Hz), 1.62 (2H, quint, *J*=7.5 Hz), 1.35 (2H, m), 1.34-1.20 (48H, m), 0.86 (6H, t, *J*=6.9 Hz); ¹³C NMR (100.6 MHz, CDCl₃): δ 174.2, 134.6, 129, 74.9, 62.8, 54.7, 36.92, 32.2, 31.98, 29.9, 29.8, 29.7, 29.6, 29.5, 29.4, 26, 22.9, 14.3. Anal. Calcd. for C₃₆H₇₁NO₃: C, 76.40; H, 12.64; N, 2.47. Found: C, 76.59; H, 12.47, N, 2.59.

General procedures for the preparation of amide-derivative of stannyl ethers

Preparation of 284, 288 and 293: A mixture of alcohol (0.305 mmol) and bis-(tributyltin) oxide (30 mg, 0.152 mmol) in 15 ml of dry toluene, was heated to reflux and was subjected to azeotropic dehydration using a Dean-Stark system or 4 Å molecular sieves overnight. Removal of solvent under reduced pressure afforded the stannyl ethers **284**, **288**, and **293** which were used for the glycosylation reaction without further purification.

Preparation of 295, 297, 306 and 34: A mixture of sphingosine or ceramide (0.176 mmol) and dibutyltin oxide (0.176 mmol) in dry toluene (15 mL), was heated to reflux and was subjected to azeotropic dehydration using a Dean-Stark system or 4 Å molecular sieves overnight. Removal of solvent under reduced pressure afforded the stannyl acetals **295**, **297**, **306** and **34**, which was used for the glycosylation reaction without further purification.

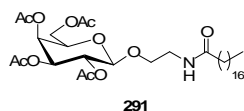
General procedure for glycosylation employing TBAI as promoter

The following protocol was followed prior to the glycosylation reaction: 1,2,3,4,6-penta-*O*-acetyl- β -D-galactopyranose and donor alcohol were separately dried by co-distillation with toluene (3 x 5 mL) in dried flasks and then were placed under vacuum for 1 h. TBAI was added to a dried flask with a magnetic stirring bar and was co-distilled with dry toluene (2 x 5 mL) in the dark. Activated 4 Å molecular sieves were added to the flask, and the mixture was co-distilled with toluene once more (5 mL) before being placed under vacuum for 1 h. Complete water exclusion is crucial to achieve good yields.

A solution of 1,2,3,4,6-penta-*O*-acetyl- β -D-galactopyranose previously dried (0.366 mmol) in CH₂Cl₂ (3 mL) was cooled to 0 °C under argon atmosphere in the dark and TMSI (0.439 mmol) was added to the stirring mixture. The reaction was stirred for 20 min at 0 °C. The reaction was stopped by adding 3 mL of dry toluene and co-distilling three times with dry toluene to obtain compound **283** as a slightly yellow oil, which was then dissolved in anhydrous toluene (5 mL) and kept under argon.

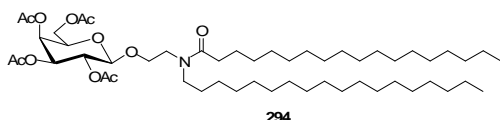
To a stirred mixture of TBAI (0.030 mmol) and 4Å molecular sieves (300 mg) in anhydrous toluene (5 mL) under argon at room temperature was added a solution of stannyl derivative (0.305 mmol) in dry toluene (5 mL) and a solution of **283** (0.366 mmol) in dry toluene (5 mL) *via* syringe. The reaction mixture was stirred at 80 °C in the dark for 18 h and then diluted with AcOEt (15 mL) and cooled to 0 °C. The white precipitate was removed by filtration through a pad of Celite. The organic layer was concentrated *in vacuo* to get the orthoester, which was co-distilled with dry toluene (3 x 5 mL) and placed under vacuum for 1 h before the next reaction.

A solution containing the orthoester in anhydrous CH₂Cl₂ (5 mL) was cooled to 0 °C under argon atmosphere, and freshly distilled BF₃·EtO₂ (0.915 mmol) was added to the stirring mixture. After, the resulting reaction mixture was stirred for 3 h at room temperature, it was quenched with saturated aqueous NaHCO₃ solution and 25 mL of AcOEt was added. The aqueous phase was extracted with AcOEt (2 x 15 mL), and the combined organic extract was washed with saturated aqueous Na₂S₂O₃ solution (2 x 10 mL) and brine (3 x 10 mL), dried with anhydrous Na₂SO₄, and concentrated *in vacuo*. The resulting residue was purified by flash column chromatography on silica gel using hexane/AcOEt/MeOH as eluent to give the product.



Synthesis of 291. Following the general procedure, the reaction was carried out starting from penta-*O*-acetyl-galactopyranose (142 mg, 0.366 mmol), TMSI (88 mg, 0.839 mmol), TBAI (11 mg, 0.030 mmol) and **288** (188

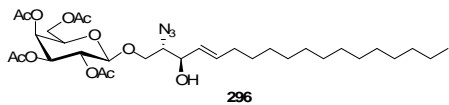
mg, 0.305 mmol). When the reaction was finished the reaction crude was purified by flash column chromatography on silica gel using hexane-AcOEt-MeOH (85:10:5) as eluent to give 186 mg (93%) of **291** as a unique anomer. TLC (hexane/AcOEt/MeOH 60:30:10) R_f 0.40; m.p. 136–138 °C; $[\alpha]_D^{25}$ -5 ($c = 1.0$, CHCl_3). ^1H NMR (400 MHz, CDCl_3): δ 5.85 (1H, t, $J=5.2$ Hz), 5.34 (1H, d, $J=3.2$ Hz), 5.13 (1H, dd, $J=10.8$, 7.6 Hz), 4.97 (1H, dd, $J=10.8$, 3.6 Hz), 4.43 (1H, d, $J=7.6$ Hz), 4.13-4.05 (2H, m), 3.88 (1H, t, $J=6.4$ Hz), 3.82 (1H, ddd, $J=10.4$, 6.4, 4.0 Hz), 3.63 (1H, ddd, $J=10.4$, 6.8, 3.6 Hz), 3.48-3.41 (1H, m) 3.39-3.32 (1H, m), 2.12 (2H, t, $J=7.2$ Hz), 2.11 (3H, s), 2.02 (3H, s), 2.01 (3H, s), 1.94 (3H, s), 1.58-1.52 (2H, m), 1.25-1.20 (28H, m), 0.82 (3H, t, $J=7.2$ Hz); ^{13}C NMR (100.6 MHz, CDCl_3): δ 172.0, 170.2, 170.0, 169.9, 168.8, 100.0, 71.8, 70.9, 68.2, 67.0, 61.2, 61.0, 41.6, 36.5, 31.8, 29.5, 28.6, 25.6, 22.7, 20.7, 20.5 14.1. Anal. Calcd. for $\text{C}_{34}\text{H}_{59}\text{NO}_{11}$: C, 62.08; H, 9.04; N, 2.11. Found: C, 62.02; H, 9.08; N, 2.21.



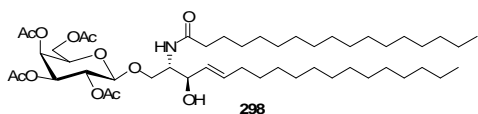
Synthesis of 294. Following the general procedure, the reaction was carried out starting from penta-*O*-acetyl-galactopyranose (80 mg, 0.206 mmol), TMSI (49 mg, 0.247

mmol), TBAI (6 mg, 0.017 mmol) and **293** (149 mg, 0.172 mmol). When the reaction was finished the reaction crude was purified by flash column chromatography on silica gel using hexane-AcOEt-MeOH (85:10:5) as eluent to give 145 mg (93%) of **294** as a unique anomer. TLC (Hexane/AcOEt/MeOH 60:30:10) R_f 0.50; m.p. 136–138 °C; $[\alpha]_D^{25}$ -11 ($c = 1.0$, CHCl_3). ^1H NMR (400 MHz CDCl_3): δ 5.37 (1H, d, $J=3.2$ Hz), 5.17 (1H, dd, $J=10.4$, 8.0 Hz), 5.0 (1H, dd, $J=10.4$, 3.2 Hz), 4.47 (1H, d, $J=8.0$ Hz), 4.17-4.03 (2H, m), 3.88 (1H, t, $J=6.4$ Hz), 3.83 (1H, ddd, $J=10.0$, 6.0, 4.0 Hz), 3.64 (1H, ddd, $J=10.0$, 6.4, 3.6 Hz), 3.47-3.41 (1H, m) 3.39-3.33 (1H, m), 2.27 (2H, t, $J=7.2$ Hz), 2.12 (2H, t, $J=7.2$ Hz), 2.11 (3H, s), 2.02 (3H, s), 2.01 (3H, s), 1.94 (3H, s), 1.57-1.50 (4H, m), 1.25 (58H, m), 0.87 (6H, t, $J=7.2$ Hz); ^{13}C NMR (100.6 MHz, CDCl_3): δ 172.0, 170.2, 170.0, 169.9, 168.8, 100.0, 71.8, 70.9, 68.2, 67.0, 61.2, 61.0, 41.6, 36.5, 31.8,

29.5, 28.6, 25.6, 22.7, 20.7, 20.5 14.1. Anal. Calcd. for C₅₂H₉₅NO₁₁: C, 68.61; H, 10.52; N, 1.54. Found: C, 68.59; H, 10.55, N, 1.49.

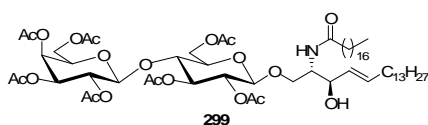


Synthesis of 296. Following the general procedure, the reaction was carried out starting from penta-*O*-acetyl-galactopyranose (143 mg, 0.368 mmol), TMSI (88 mg, 0.441 mmol), TBAI (11 mg, 0.030 mmol) and **295** (171 mg, 0.307 mmol). When the reaction was finished the reaction crude was purified by flash column chromatography on silica gel using hexane-AcOEt-MeOH (85:10:5) as eluent to give 188 mg (94%) of **296** as a unique anomer. TLC (Hexane/AcOEt/MeOH 60:30:10) *R_f* 0.60; m.p. 50–52 °C; [α]_D²⁵ -21 (c = 1.0, CHCl₃). ¹H NMR (400 MHz, CDCl₃): δ 5.8 (1H, dt, *J*=15.6, 6.4 Hz), 5.48 (1H, dd, *J*=15.6, 7.2 Hz), 5.37 (1H, d, *J*=3.2 Hz), 5.19 (1H, dd, *J*=10.5, 7.5 Hz), 5.0 (1H, dd, *J*=10.5, 3.2 Hz), 4.5 (1H, d, *J*=8.0 Hz), 4.25 (1H, dd, *J*=6.8, 6.0 Hz), 4.2-4.06 (2H, m), 3.96 (1H, t, *J*=6.4 Hz), 3.93 (1H, dd, *J*=12.8, 6.0 Hz), 3.69 (1H, dd, *J*=10.4, 4.4 Hz), 3.45 (1H, m), 2.06 (2H, q, *J*=7.2 Hz), 2.05 (3H, s), 2.04 (3H, s), 2.03 (3H, s), 1.96 (3H, s), 1.36 (2H, m), 1.25 (20H, m), 0.87 (3H, t, *J*=7.2 Hz); ¹³C NMR (100.6 MHz, CDCl₃): δ 170.2, 169.3, 169.2, 165.0, 139.0, 122.7, 100.5, 72.8, 72.5, 72.0, 71.0, 68.3, 68.1, 63.5, 61.8, 32.4, 31.9, 29.6-28.7, 22.7, 20.6, 20.5, 14.0. Anal. Calcd. for C₃₂H₅₃N₃O₁₁: C, 58.61; H, 8.15; N, 6.41. Found: C, 58.80; H, 8.17; N, 6.28.



Synthesis of 298. Following the general procedure, the reaction was carried out starting from penta-*O*-acetyl-galactopyranose (82 mg, 0.211 mmol), TMSI (50 mg, 0.253 mmol), TBAI (6 mg, 0.017 mmol) and **297** (140 mg, 0.176 mmol). When the reaction was finished the reaction crude was purified by flash column chromatography on silica gel using hexane-AcOEt-MeOH (85:10:5) as eluent to give 139 mg (90%) of **298** as a unique anomer. TLC (Hexane/AcOEt/MeOH 60:30:10) *R_f* 0.60; m.p. 50–52 °C; [α]_D²⁵ -13.5 (c = 1.0, CHCl₃). ¹H NMR (400, MHz CDCl₃): δ 5.94 (1H, t, *J*=7.0 Hz), 5.75 (1H, dt, *J*=15.3, 6.7 Hz), 5.49 (1H, dd, *J*=15.3, 7.5 Hz), 5.38 (1H, d, *J*=3.2 Hz), 5.17 (1H, dd, *J*=10.6, 8.0 Hz), 5.0 (1H, dd, *J*=10.6, 3.6 Hz), 4.47 (1H, d, *J*=8.0 Hz), 4.25

(1H, dd, $J=7.5$, 3.4 Hz), 4.16 (1H, dd, $J=10.0$, 4.6 Hz), 4.15-3.99 (3H, m), 3.92 (1H, t, $J=6.4$ Hz), 3.65 (1H, dd, $J=10.0$, 3.2 Hz), 2.20 (2H, t, $J=7.5$ Hz), 2.05 (3H, s), 2.04 (3H, s), 2.03 (2H, dt, $J=7.2$, 6.7 Hz), 2.03 (3H, s), 1.99 (3H, s), 1.61 (2H, m), 1.35 (2H, m), 1.34-1.20 (48H, m), 0.87 (6H, t, $J=6.9$ Hz); ^{13}C NMR (100.6 MHz, CDCl_3): δ 174.3, 170.2, 170.1, 169.9, 168.8, 133.9, 128.8, 101.0, 71.9, 71.7, 71.0, 68.2, 68.1, 67.1, 61.3, 53.0, 36.0, 31.9, 31.5, 29-28.8, 25.5, 21.2, 20.6, 20.5, 13.4. Anal. Calcd. for $\text{C}_{49}\text{H}_{87}\text{NO}_{12}$: C, 66.7; H, 9.94; N, 1.59. Found: C, 66.97; H, 9.63, N, 1.38.



Synthesis of 299. Following the general procedure, the reaction was carried out starting from octa-*O*-acetyl-lactose (143 mg, 0.211 mmol), TMSI (50 mg, 0.253 mmol), TBAI (6 mg, 0.017 mmol) and **297** (140 mg, 0.176 mmol). When the reaction was finished the reaction crude was purified by flash column chromatography on silica gel using hexane-AcOEt-MeOH (85:10:5) as eluent to give 184 mg (90%) of **299** as a unique anomer.

TLC (Hexane/AcOEt/MeOH 60:30:10) R_f 0.35; m.p. 50–52 °C; $[\alpha]_D^{25}$ -12.2 ($c = 1.0$, CHCl_3). ^1H NMR (400 MHz, CDCl_3): δ 5.97 (1H, d, $J=7.0$ Hz), 5.76 (1H, dt, $J=15.3$, 6.7 Hz), 5.50 (1H, dd, $J=15.3$, 7.5 Hz), 5.33 (1H, d, $J=2.6$ Hz), 5.10 (1H, dd, $J=10.4$, 9.2 Hz), 5.08 (1H, dd, $J=10.4$, 8.0 Hz), 4.94 (1H, dd, $J=10.4$, 3.4 Hz), 4.87 (1H, dd $J=9.6$, 8.0 Hz), 4.49 (1H, d, $J=8.0$ Hz), 4.48 (1H, d, $J=8.0$ Hz), 4.35 (1H, dd, $J=9.6$, 1.0 Hz), 4.16-4.01 (2H, m), 4.02-3.93 (3H, m), 3.88 (1H, t, $J=6.4$ Hz), 3.81 (1H, t, $J=9.6$ Hz), 3.62 (1H, dd, $J=10.0$, 3.2 Hz), 3.55 (1H, m), 2.20 (2H, t, $J=7.5$ Hz), 2.14 (3H, s), 2.07 (3H, s), 2.05 (3H, s), 2.03 (2H, dt, $J=7.2$, 6.7, Hz), 2.02 (3H, s), 2.01 (3H, s), 1.96 (3H, s), 1.95 (3H, s), 1.61 (2H, m), 1.35 (2H, m), 1.34-1.20 (48H, m), 0.87 (6H, t, $J=6.9$ Hz); ^{13}C NMR (100.6 MHz, CDCl_3): δ 173.1, 170.7, 170.6, 170.5, 170.2, 170.1, 169.9, 169.6, 133.5, 128.8, 101.0, 100.7, 76.5, 74.5, 73.1, 73.0, 72.2, 71.4, 71.1, 69.4, 67.9, 67.0, 62.3, 61.2, 52.2, 36.1, 31.9, 31.6, 21.2-21.0, 14.1. Anal. Calcd. for $\text{C}_{61}\text{H}_{103}\text{NO}_{20}$: C, 62.59; H, 8.87; N, 1.2. Found: C, 62.87; H, 8.29, N, 1.39.

General procedure for glycosylation employing AgOTf as promoter

The following protocol was followed prior to the glycosylation reaction. The acceptor 1,2,3,4,6-penta-*O*-acetyl- β -D-galactopyranose and donor were azeotroped with dry toluene (3 x 5 mL) in a dried flask and placed under vacuum for 1 h before the

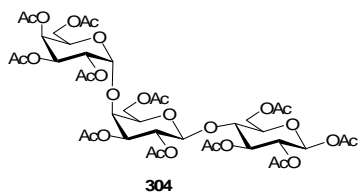
reaction. The AgOTf was added to a dried flask with a magnetic stirring bar. The flask wrapped in Al foil was azeotroped with dry toluene (2 x 5 mL) in the dark. Activated 4 Å molecular sieves were added to the flask, and the mixture was azeotroped with benzene once more (5 mL) before being placed under vacuum for 1 h.

A solution of 1,2,3,4,6-penta-*O*-acetyl- β -D-galactopyranose (286 mg, 0.733 mmol) in CH₂Cl₂ (3 mL) was cooled to 0 °C under argon atmosphere in the dark and TMSI (176 mg, 0.879 mmol) was added to the stirring mixture. The reaction was stirred for 20 min at 0 °C. The reaction was stopped by adding 3 mL of dry toluene and azeotroped three times with dry toluene. The slightly yellow oil **283** was dissolved in CH₂Cl₂ (5 mL) and kept under argon.

To a stirred mixture of AgOTf (1.83 mmol) and 4 Å molecular sieves (600 mg) in dry CH₂Cl₂ (5 mL) under argon at room temperature was added a solution of stannyl derivative (0.611 mmol) in dry CH₂Cl₂ (5 mL) and a solution of **283** (0.733 mmol) in dry CH₂Cl₂ (5 mL) via syringe. The reaction mixture was stirred at 0 °C in the dark for 3 h before it was allowed to warm to 25 °C and stirred further for 3 h. The mixture was diluted with AcOEt (15 mL) and cooled to 0 °C. The white precipitate was removed by filtration through a pad of Celite. The organic layer was concentrated *in vacuo* to get crude residue, which mainly consisted of orthoester. This crude product was azeotroped with dry toluene (3 x 5 mL) and placed under vacuum for 1 h before the next reaction.

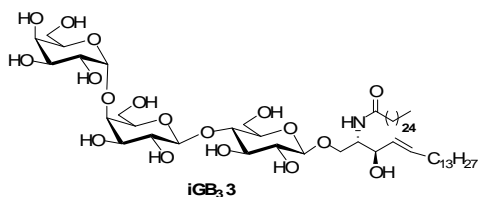
A solution containing the orthoester in CH₂Cl₂ (10 mL) was cooled to 0 °C under argon atmosphere, and freshly distilled BF₃·EtO₂ (1.833 mmol) was added to the stirring mixture. After, the resulting reaction mixture was stirred for 3 h at room temperature, it was quenched with saturated aqueous NaHCO₃ solution and 25 mL of AcOEt was added. The aqueous phase was extracted with AcOEt (2 X 20 mL), and the combined organic extract was washed with saturated aqueous Na₂S₂O₃ solution (2 x 20 mL) and brine (3 x 20 mL), dried with anhydrous Na₂SO₄, and concentrated *in vacuo*. The resulting residue was purified by flash column chromatography on silica gel using hexane-AcOEt-MeOH (85:10:5) as eluent to give the product.

Activation of MSAW3000. Molecular sieves AW-300 (MSAW300) purchased from Aldrich (lot no. 04024CI) were ground and activated by heating over 200 °C under reduced pressure 12 h.



Synthesis of 304: Isoglobotrihexose **303** (50 mg, 0.099 mmol) was dissolved in 10 ml of pyridine followed by addition of acetic anhydride (0.556 mg, 5.45 mmol) and DMAP (65 mg, 0.54 mmol).

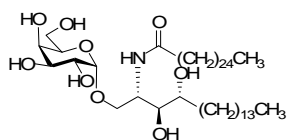
The mixture was stirred for 48 h at 70 °C and then concentrated *in vacuo*. The residue was dissolved in EtOAc (15 mL) and washed with HCl (10% aqueous, 3 x 10 mL), NaHCO₃ (7% aqueous, 3 x 30 mL), and brine (3 x 30 mL) successively, The organic layer was dried over MgSO₄ and concentrated *in vacuo*. The residue was purified by flash column chromatography on silica gel using hexane-AcOEt (85:15) as the eluent to give 94 mg of **304** as syrup in 98 %. ¹H NMR (400 MHz, CDCl₃): δ 5.68 (1H, d, *J*=8.4 Hz), 5.43-5.37 (2H, m), 5.26-5.21 (3H, m), 5.14 (1H, m), 5.0 (1H, m), 4.93 (1H, t, *J*=8.4 Hz), 4.47-4.40 (2H, m), 4.31 (1H, dd, *J*=12, 4.0 Hz), 4.14-3.99 (5H, m), 3.91 (1H, m), 3.81 (1H, dd, *J*=15, 6.4 Hz), 3.77 (1H, m), 3.68 (1H, m), 2.2 (3H, s), 2.18 (3H, s), 2.16 (3H, s), 2.15 (3H, s), 2.14 (3H, s), 2.13 (3H, s), 2.12 (3H, s), 2.11 (3H, s), 2.04 (3H, s), 1.99 (3H, s), 1.95 (3H, s); ¹³C NMR (100.6 MHz, CDCl₃): δ 170.5, 170.4, 170.3, 170.2, 170.0, 169.8, 169.7, 169.5, 169.3, 168.7, 96.9, 95.0, 91.7, 75, 73.3, 72.8, 72.3, 71.5, 70.8, 70.3, 69.9, 69.2, 68.9, 68.4, 67.7, 62.5, 62.1, 61.2, 22, 20.9, 20.8, 20.7, 20.5, 20.3. Anal. Calcd. for C₄₀H₅₄O₂₇: C, 49.69; H, 5.63. Found: C, 49.63; H, 5.65.



Synthesis of iGB3: Following the general procedure, the reaction was carried out starting from peracetylated trisaccharide **304** (50 mg, 0.051 mmol), TMSI (12 mg, 0.061 mmol), TBAI (13 mg, 0.051 mmol), **306** (46

mg, 0.051 mmol) and 4Å acid washed molecular sieves (200 mg). When the reaction was finished the solvent was evaporated and then, MeOH (15 mL) and Dowex 50WX8–200 ion-exchange resin (1 g) were added and the reaction was stirred at room temperature for 4 h. The resin was then removed by filtration. The solvent was removed *in vacuo*, and the resulting residue was purified by flash column chromatography on silica gel using CHCl₃-MeOH (85:15) as eluent to give 32 mg (60%) of **3** as a unique anomer. ¹H NMR (Py-*d*₅, 400 MHz): δ 8.31 (1H, d, *J*=8.0 Hz), 7.53 (1H, br s), 7.32 (1H, br s), 6.98 (1H, br s), 6.66 (1H, br s), 6.58 (1H, br s), 6.52 (1H, br s), 6.42 (1H br s), 6.38 (1H, br s), 6.36 (1H, br s), 6.09 (1H, br s), 6.01 (1H dd, *J*=15.5 Hz, 6.0 Hz),

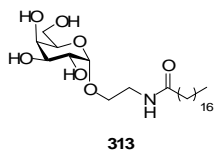
5.91 (1H, dt, $J=15.5, 6.5$ Hz), 5.76 (1H, br s), 5.64 (1H, d, $J=3.8$ Hz), 5.05-5.00 (2H, m), 4.87 (1H, d, $J=12.0$ Hz), 4.81-4.75 (3H, m), 4.72-4.69 (1H, m), 4.65 (1H, m), 4.56 (1H, m), 4.54-4.49 (3H, m), 4.47-4.39 (4H, m), 4.32-4.29 (1H, m), 4.24-4.20 (3H, m), 4.15 (1H, dd, $J=9.5, 2.5$ Hz), 4.05-4.00 (2H, m), 3.86-3.84 (1H, m), 2.42 (2H, t, $J=7.0$ Hz) 2.06 (2H, q, $J=6.5$ Hz), 1.82 (2H, m), 1.39-1.21 (66H, m), 0.87 (3H, t, $J=6.5$ Hz), 0.86 (3H, t, $J=7.0$ Hz); ^{13}C NMR (Py- d_5 , 100.6 MHz): δ 174.2, 133.5, 133.2, 106.4, 98.6, 83.0, 81.0, 77.6, 77.5, 77.4, 75.7, 73.7, 73.6, 72.5, 71.7, 71.4, 71.3, 66.9, 63.1, 62.9, 62.7, 55.8, 37.8, 33.6, 33.0, 31.4, 31.0, 30.9, 30.8, 30.7, 30.6, 30.5, 27.3, 23.3, 15.1. Anal. Calcd. for $\text{C}_{62}\text{H}_{117}\text{NO}_{18}$: C, 63.94; H, 10.13; N, 1.20. Found: C, 63.90; H, 10.11; N, 1.18.



KRN7000 309

Synthesis of KRN7000 309: To a solution of 1,2,3,4,6-penta-*O*-trimethylsilyl-D-galactopyranose **310** (38 mg, 0.071 mmol) in CH_2Cl_2 (5 mL) at 0 °C was added TMSI (14 mg, 0.071 mmol). The reaction was stirred under argon at 0 °C for 20 min. The reaction was stopped by adding 15 mL of anhydrous benzene and solvent was

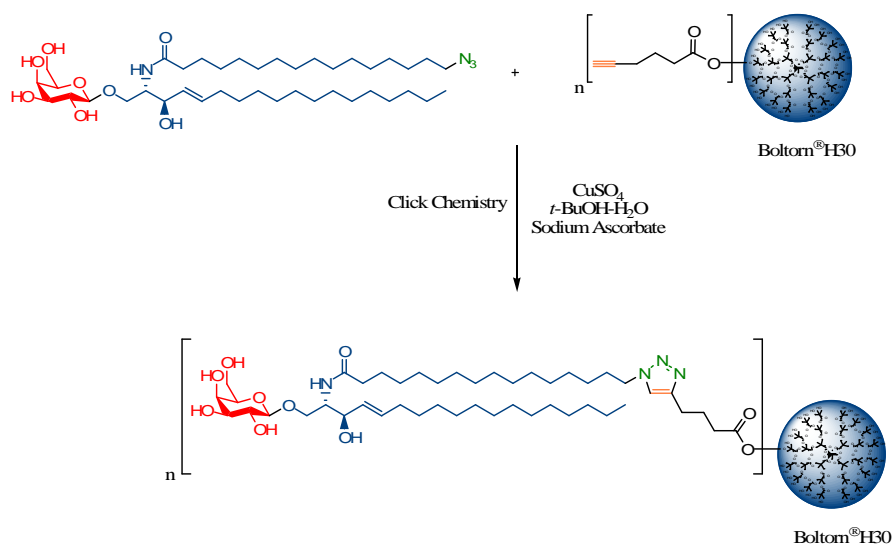
evaporated under reduced pressure. The slightly yellow oil **311** was dissolved in toluene (3 mL) and kept under argon. In a separate flask, molecular sieves (MS, 4 Å, 50 mg), TBAI (53 mg, 0.143 mmol), and **314** (66 mg, 0.071 mmol) were added into toluene (5 mL). The mixture was stirred under argon and the glycosyl iodide **311** was added dropwise. The reaction mixture was stirred at 80 °C for 18 h and then the solvent was evaporated. MeOH (15 mL) and Dowex® 50WX8-200 ion exchange resin (0.5 g) were added and the reaction was stirred at rt for 4 h. Resin was removed by filtration. The solvent was removed in vacuo and the resulting residue was purified by silica gel chromatography. The ^1H and ^{13}C NMR spectral data of **309** corroborated well with the literature report. ^1H NMR (400 MHz, pyridine- d_5) δ 8.43 (1H, d, $J=8.6$ Hz), 5.55 (1H, d, $J=3.5$ Hz), 5.25–5.21 (1H, m), 4.66–4.61 (2H, m), 4.53 (1H, m), 4.49 (1H, t, $J=5.8$ Hz), 4.42–4.36 (4H, m), 4.31–4.29 (1H, m), 2.43 (2H, t, $J=7.4$ Hz), 2.23 (1H, m), 1.92–1.86 (2H, m), 1.82–1.77 (2H, m), 1.63 (1H, m), 1.44–1.18 (66H, m), 0.88–0.83 (6H, m); ^{13}C NMR (125 MHz, pyridine- d_5) δ 174.6, 102.8, 78.0, 74.3, 72.98, 72.3, 71.6, 69.90, 63.90, 52.8, 38.1, 35.60, 33.4, 31.6, 31.4, 31.3, 31.3, 31.2, 31.1, 31.1, 30.9, 27.8, 27.6, 24.2, 15.5.



Glycolipid 313. The general procedure as reported for the preparation of **309** was followed. ^1H NMR (400 MHz, $\text{CDCl}_3/\text{CD}_3\text{OD}$, 4:1): δ 7.52 (1H, s), 4.87 (1H, d, $J=3.2$ Hz), 3.93 (1H, m), 3.80–3.72 (6H, m), 3.49 (1H, m), 3.32 (2H, m) 2.20 (2H, t, $J=8.0$ Hz), 1.62 (2H, m), 1.27 (28H, m), 0.89 (3H, t, $J=7.2$ Hz); ^{13}C NMR (100.6 MHz, 4:1 $\text{CDCl}_3/\text{CD}_3\text{OD}$): δ 174.9, 98.8, 70.6, 69.9, 69.5, 68.7, 66.7, 61.4, 41.5, 36.0, 29.3–28.9, 25.6, 22.3, 13.5.

3.3. Synthesis of novel glycodendritic polymer of β -Galcer that bind HIV-1 gp 120

Glycodendrimers have been employed as useful tools to investigate carbohydrate recognition processes. Now, we present new water-soluble hyperbranched glycodendritic polymers for the study of carbohydrate interactions. These glycoconjugate consists of Boltorn H30 hyperbranched polymers, based on the monomer 2,2-bis(hydroxymethyl)propionic acid, functionalized with naturally occurring β -Galceramide. Click chemistry permits functional group tolerance during the derivatization of Boltorn H30. Their ability to bind HIV-1 gp 120 was demonstrated using surface plasmon resonance (SPR).



3.3.1. The HIV process

HIV-1 infects susceptible cells by fusion of viral membrane with the plasma membrane. The HIV entry process is understood in some detail at the molecular level,²⁴⁸ it is coordinated by the HIV envelope glycoprotein complex, a trimer of gp120 surface glycoproteins, each noncovalently attached to three gp41 membrane glycoprotein subunits. HIV must first engage CD4, a host cell surface protein, via the CD4 binding site on gp120. Interaction between gp120 and CD4 induces a significant conformational change in the envelope glycoprotein, exposing a previously hidden site that, together with the V3 region, is necessary for coreceptor engagement.²⁴⁹ Binding to the coreceptor induces the insertion of gp41 into the host cell membrane, forming a molecular bridge between the virus and the host cell leading to the formation of a prefusion complex, which undergoes further conformational rearrangement that is sufficient to drive membrane fusion, allowing the contents of the virion to be ejected into the host cell.²⁵⁰ Several viral envelope glycoprotein oligomers then assemble into a viral fusion machine, forming a molecular scaffold that brings the viral and target cell membranes into close apposition and allow the subsequent fusion events.²⁵¹ The fusion pore formation and its sequential expansion are orchestrated by viral and cellular lipids and proteins.

Recently works has shown that changes in GSLs expression in target membranes can modulate viral fusion and entry. These studies on structure–function relationship of target membrane GSLs, the gp120-gp41 and the viral receptors suggest that plasma membrane GSLs support HIV-1 entry by stabilizing the intermediate steps in the fusion cascade.²⁵² These observations, led it to hypothesize that upregulation of GSL metabolites

²⁴⁸ Gallo, S. A.; Finnegan, G. M.; Viard, M.; Raviv, Y.; Dimitrov, A.; Rawat, S. S.; Puri, A.; Durell, S. *Biochim. Biophys. Acta* **2003**, *1614*, 36–50

²⁴⁹ (a) Huang, C. C.; Thang, M.; Zhang, M. Y.; Majeed, S.; Montabana, E.; Stanfield, R. L.; Dimitrov, D. S.; Krober, B.; Sodroski, J.; Wilson, I. A.; Wyatt, R.; Kwong, P. D. *Science* **2005**, *310*, 1025–1028. (b) Chen, B.; Vogan, E. M.; Gong, H.; Skehel, J. J.; Wiley, D. C.; Harrison, S. C. *Nature* **2005**, *433*, 834–841. (c) Rizzuto, C. D.; Wyatt, R.; Hernandez-Ramos N.; Sun, Y.; Kwong, P. D.; Hendrickos, W. A.; Sodroski, J. *Science* **1998**, *280*, 1949–1953. (c) Cocchi, F.; DeVico, A. L.; Garzino-Demo, A.; Cara, A.; Gallo, R. C.; Lusso, P. *Nat. Med.* **1996**, *2*, 1244–1247.

²⁵⁰ Weiss, C. D. *AIDS Rev.* **2003**, *5*, 214–221.

²⁵¹ Jones, P. L.; Korte, T.; Blumenthal, R. *J. Biol. Chem.* **1998**, *273*, 404–409.

²⁵² (a) Rawat, S. S.; Eaton, J.; Gallo, S. A.; Martin, T. D.; Ablan Ratnayake, S.; Viard, M.; KewalRamani, V. N.; Wang, J. M.; Blumenthal, R.; Puri, A. *Virology* **2004**, *318*, 55–65. (b) Rawat, S. S.; Gallo, S. A.; Eaton,

(such as ceramide) and/or modulation of GSLs, which preferentially partition in the plasma membrane microdomains, could have a significant influence on HIV-1 entry.²⁵³ Based on these findings, other researchers have attempted to develop strategies to synthesize glycoconjugate derivatives, GSL analogs, polymers and/or hybrids as new agents to inhibit HIV-1 entry.

3.3.2. Hyperbranched polymers

In the last decade, a new promising class of drug carriers, the dendritic polymers, has attracted increasing attention. A large number of interdisciplinary research activities on dendritic polymers, i.e., dendrimers and hyperbranched polymers, that explored a wide variety of new applications have emerged (Figure 24).²⁵⁴ At the end of the 1990s an increasing number of research groups focused on the potential of dendrimers in the field of life science; they were fascinated by their unique features such as monodispersity, a well-defined globular architecture, and the possibility of tailoring their physical and chemical properties. Since several dendrimers exhibit a low in vivo toxicity, their applications as diagnostic imaging agents, gene-therapy vectors, vaccines, drugs, and boron neutron capture therapy agents were examined intensively.²⁵⁵ Dendrimers offer many

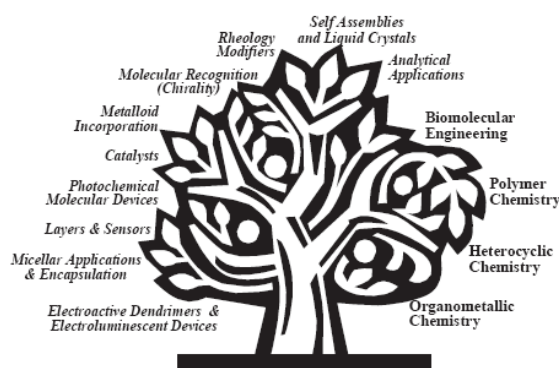


Figure 24. Dendritic polymer chemistry

J.; Martin, T. D.; Ablan, S.; KewalRamani, V. N.; Wang, J. M.; Blumenthal, R.; Puri, A. *J. Virol.* **2004**, *65*, 7360–7368.

²⁵³ Rawat, S. S.; Benitra, T. J.; Puri, A. *Biosci. Rep.* **2005**, *25*, 329–343.

²⁵⁴ (a) Seiler, M.; Jork, C.; Kavarnou, A.; Arlt, W.; Hirsch, R. *Aiche J.* **2004**, *50*, 2439–2454. (b) Inoue, K. *Prog. Polym. Sci.* **2000**, *25*, 453–571. (c) Sunder, A.; Heinemann, J.; Frey, H. *Chem. Eur. J.* **2000**, *6*, 2499–2506. (d) Hult, A.; Johansson, M.; Malmstrom, E. *Adv. Polym. Sci.* **1999**, *143*, 1–34. (e) Matthews, O. A.; Shipway, A. N.; Stoddart, J. F. *Prog. Polym. Sci.* **1998**, *23*, 1–56.

²⁵⁵ (a) Malik, N.; Wiwattanapatapee, R.; Klopsch, R.; Lorenz, K.; Frey, H.; Weener, J. W.; Meijer, E. W.; Paulus, W.; Duncan, R. *J. Control. Release* **2000**, *68*, 299–302. (b) Eichman, J. D.; Bielinska, A. U.; Kukowska-Latallo, J. F.; Baker, J. R., Jr. *Pharm. Sci. Technol. Today* **2000**, *3*, 232–245. (c) Kawaguchi, H.

outstanding advantages as a versatile strategy for a more effective delivery of therapeutic drugs to disease sites. Their size and structure can be controlled by synthetic means and further modifications can ensure biocompatibility and biodegradability. Dendrimers are also considered to function as analogs of enzymes, proteins, viruses, and antibodies.^{255a,b,c} Thus, it seems certain that dendrimers will play a significant role in the future development of new biomedical devices for the treatment of human diseases.²⁵⁶

Hyperbranched polymers represent an important part of the family of dendritic and multibranching polymers.²⁵⁷ While dendrimers have perfect, monodisperse structures built around a core moiety with a branching point in every repeating unit, hyperbranched polymers are polydisperse and include some linear units in their molecular structure (Figure 25a). However, these differences are not large enough to suppress some of their typical dendritic polymer characteristics. Similarly to dendrimers (Figure 25b), hyperbranched polymers were shown to exhibit much lower solution viscosities than linear polymers due to the lack of entanglements and to their very low intrinsic viscosities, which result from their packed structure.²⁵⁸ The properties of hyperbranched

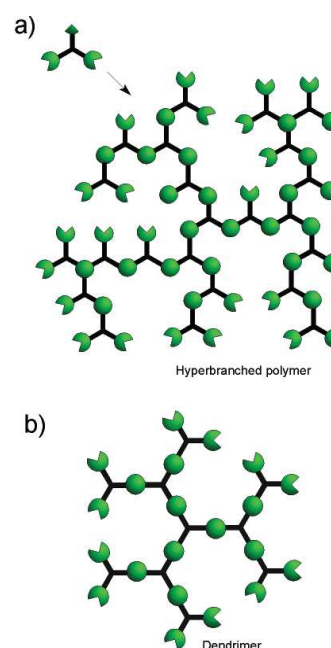


Figure 25

Prog. Polym. Sci. **2000**, *25*, 1171–1210. (c) Hudde, T.; Rayner, S. A.; Comer, R. M.; Weber, M.; Isaacs, J. D.; Waldmann, H.; Larkin, D. P. F.; George, A. J. T. *Gene Ther.* **1999**, *6*, 939–943. (d) Langer, R. *Nature* **1998**, *392*, 5–10.

²⁵⁶ (a) Maksimenko, A. V.; Mandrouguine, V.; Gottikh, M. B.; Bertrand, J. R.; Majoral, J. P.; Malvy, C. J. *Gene Med.* **2003**, *5*, 61–71. (b) Esfand, R.; Tomalia, D. A. *Drug Discov. Today* **2001**, *6*, 427–436.

²⁵⁷ For reviews about hyperbranched polymers see: (a) Voit, B. *J. Pol. Sc. Part A: Polym. Chem.* **2005**, *43*, 2679–2699. (b) Gao, C.; Yan, D. *Prog. Polym. Sci.* **2004**, *29*, 183–275. (c) Voit, B. *I. C. R. Chimie*, **2003**, *6*, 821–832. (d) Seiler, M. *Chem. Eng. Technol.* **2002**, *25*, 237–253. (e) Jikei, M.; Kakimoto, M. *Prog. Polym. Sci.* **2001**, *26*, 1233–1285. (f) Voit, B. *J. Pol. Sc. Part A: Polym. Chem.* **2000**, *38*, 2505–2525. (g) Kim, Y. H. *J. Pol. Sc. Part A: Polym. Chem.* **1998**, *36*, 1685–1698. (h) Zeng, F.; Zimmerman, S. C. *Chem. Rev.* **1997**, *97*, 1681–1712. (i) Tomalia, D.; Naylor, A. M.; Goddard III, W. A. *Angew. Chem. Int. Ed. Engl.* **1990**, *29*, 138–175.

²⁵⁸ (a) Hsieh, T. T.; Tiu, C.; Simon, G. P. *Polymer* **2001**, *42*, 1931–1939. (b) Nunez, C. M.; Chiou, B. S.; Andrady, A. L.; Khan, S. A. *Macromolecules* **2000**, *33*, 1720–1726. (c) Sendjarevic, I.; McHugh, A. J. *Macromolecules* **2000**, *33*, 590–596. (d) Wooley, K. L.; Frechet, J. M.; Hawker, C. J. *Polymer* **1994**, *35*, 4489–4495.

polymers in blends are indeed strongly determined by the nature of their terminal groups.²⁵⁹ For example, solubility, which mainly depends on the end group structure, may be regulated by the partial or total chemical modification of the “terminal” groups. Due to the irregularities of hyperbranched polymers in their molecular architecture, these functional groups can be located not only in the periphery, as in perfect dendrimers, but also inside the globular branched structure; even the terminal functional groups of dendritic macromolecules can fold back to the inside.²⁶⁰

In this context, a promising idea is the replacement of dendrimers by hyperbranched polymers.²⁶¹ The tedious and complex multi step synthesis of dendrimers results in expensive products with a limited use for large-scale industrial applications.^{257d} For many applications, which do not require structural perfection, hyperbranched polymers can circumvent this major drawback of dendrimers.^{257d,f,256a} Unlike dendrimers, randomly branched hyperbranched polymers with similar properties can be easily synthesized via one-step reactions and, therefore, represent economically promising products for both small-scale and large-scale industrial applications. Several hyperbranched polymers have been commercialised e.g. by Dendritech®, Inc. (Starburst®), Qiagen (SuperFect®), DSM (Astramol, Hybrane™) and Perstorp (Boltorn®). Therefore, during the last years, a wide variety of applications, which originally only seemed conceivable for dendrimers, were investigated for the statistically branched hyperbranched polymers.^{257b,261f,262} Among these

²⁵⁹ (a) Voit, B. I. *Acta Polym.* **1995**, *46*, 87–99. (b) Turner, S. R.; Walter, F.; Voit, B. I.; Mourey, T. H. *Macromolecules* **1994**, *27*, 1611–1616. (c) Turner, S. R.; Voit, B. I.; Mourey, T. H. *Macromolecules* **1993**, *26*, 4617–4623.

²⁶⁰ Scherrenberg, R.; Coussens, B.; van Vliet, P.; Edouard, G.; Brackman, J.; de Brabander, E. *Macromolecules* **1998**, *31*, 456–461.

²⁶¹ (a) Twyman, L. J.; King, A. S. H.; Burnett, J.; Martin, I. K. *Tetrahedron Lett.* **2004**, *45*, 433–435. (b) Haag, R. *Angew. Chem. Int. Ed.* **2004**, *43*, 278–282. (c) Gao, C.; Xu, Y. M.; Yan, D. Y.; Chen, W. *Biomacromolecules* **2003**, *4*, 704–712. (d) Kolhe, P.; Misra, E.; Kannan, R. M.; Kannan, S.; Lieh-Lai, M. *Int. J. Pharm.* **2003**, *259*, 143–160. (e) Moorefield, C. N.; Newkome, G. R. *C. R. Chimie* **2003**, *6*, 715–724. (d) Ooya, T.; Lee, J.; Park, K. *J. Control. Release* **2003**, *93*, 121–127. (e) Frey, H.; Haag, R. *Rev. Mol. Biotechnol.* **2002**, *90*, 257–267. (f) Crooks, R. M. *Chemphyschem.* **2001**, *2*, 644–654. (g) Breitenbach, A.; Li, Y. X.; Kissel, T. *J. Control Release*, **2000**, *64*, 167–178. (h) Franchina, J. G.; Lackowski, W. M.; Dermody, D. L.; Crooks, R. M.; Bergbreiter, D. E.; Sirkar, K.; Russell, R. J.; Pishko, M. V. *Anal. Chem.* **1999**, *71*, 3133–3139. (i) Peez, R. F.; Dermody, D. L.; Franchina, J. G.; Jones, S. J.; Bruening, M. L.; Bergbreiter, D. E.; Crooks, R. M. *Langmuir* **1998**, *14*, 4232–4237. (j) Uhrich, K. *Trends Polym. Sci.* **1997**, *5*, 388–393.

²⁶² (a) Voit, B.; Eigner, M.; Estel, K.; Wenzel, C.; Bartha, J. W. *Macromol. Symp.* **2002**, *177*, 147–154. (b) Klee, J. E.; Schneider, C.; Holter, D.; Burgath, A.; Frey, H.; Mulhaupt, R. *Polym. Adv. Technol.* **2001**, *12*, 346–354. (c) Haag, R. *Chem. Eur. J.* **2001**, *7*, 327–335. (d) Pitois, C.; Wiesmann, D.; Lindgren, M.; Hult, A. *Adv. Mater.* **2001**, *13*, 1483–1487. (e) Duan, L.; Qiu, Y.; He, Q. G.; Bai, F. L.; Wang, L. D.; Hong, X. Y. *Synthetic Met.* **2001**, *124*, 373–377. (f) van Benthem, R. A. T. M. *Prog. Org. Coat.* **2000**, *40*, 203–214. (g)

new potential applications for hyperbranched polymers, the applications in the field of life science seem to be one of the most challenging goals.

The synthesis of multivalent neoglycoconjugates is currently promoted by the extensive findings of multiple ligand-receptor interactions that occur in nature and by the phenomenon generally referred to as the glycoside cluster effect.^{263,264} Glycodendritic structures are particularly effective due to their propensity to form spherical nano-cellular decoys.²⁶⁵ Boltorn H30 hyperbranched dendritic polymer **315** (Figure 26) functionalized with mannose has been used to interactions studies with *Lens culinaris* lectin²⁶⁶ and to inhibit DC-SIGN-mediated infection in an Ebola-pseudotyped viral model.²⁶⁷ Thus, to study the interaction of HIV-1 rgp 120 with β -GalCer, and to develop potential carbohydrate-based inhibitors of this interaction, multivalent scaffolds bearing carbohydrates have been prepared. These systems consist of dendritic structures based on Boltorn H30 hyperbranched dendritic polymer **315** to which the glycosphingolipids are linked through click chemistry. NMR was used to confirm synthesis, and the average molecular weights of glycodendrimers were determined by MALDI-TOF MS. Surface plasmon resonance (SPR) was used for kinetic analysis of the interaction of HIV-1 rgp 120 IIIB with the glycodendritic compounds.

For the preparation of glycodendritic structure three general synthetic approaches were considered:

- Synthesis of β -GalCer containing a hydrophobic chain with azide group.
- Introduction of acetylene group on the dendritic core surface.
- Finally, the cycloaddition reaction of azide groups with terminal acetylenes.

Tao, X. T.; Zhang, Y. D.; Wada, T.; Sasabe, H.; Suzuki, H.; Watanabe, T.; Miyata, S. *Adv. Mater.* **1998**, *10*, 226–230.

²⁶³ A simple definition of this effect is: “affinity enhancement achieved by multivalent ligands over monovalent ones that is greater than expected from a simple effect of concentration increase”; see: Quesenberry, M. S.; Lee, R. T.; Lee, Y. C. *Biochemistry*, **1997**, *36*, 2724–2732.

²⁶⁴ For reviews, see: a) Lundquist, J. J.; Toone, E. J. *Chem. Rev.* **2002**, *102*, 555–578. b) Mammen, M.; Choi, S. K.; Whitesides, G. M. *Angew. Chem. Int. Ed.* **1998**, *37*, 2754–2794

²⁶⁵ a) Borman, S. *C&EN* **2000**, *78*, 48–53. b) Reuter, J. D.; Myc, A.; Hayes, M. M.; Gan, Z.; Roy, R.; Qin, D.; Yin, R.; Piehler, L. T.; Esfand, R.; Tomalia, D. A.; Baker, J. R. Jr. *Bioconjugate Chem.* **1999**, *10*, 271–278.

²⁶⁶ Arce, E.; Nieto, P. M.; Díaz, V.; Castro, R. G.; Bernad, A.; Rojo, J. *Bioconjug. Chem.* **2003**, *14*, 817–823.

²⁶⁷ a) Rojo, J.; Delgado, R. *Antimicrob. Agents Chemothe.* **2004**, *54*, 579–581. b) Lasala, F.; Arce, E.; Otero, J. R.; Rojo, J.; Delgado, R. *Antimicrob. Agents Chemothe.* **2003**, *47*, 3970–3972.

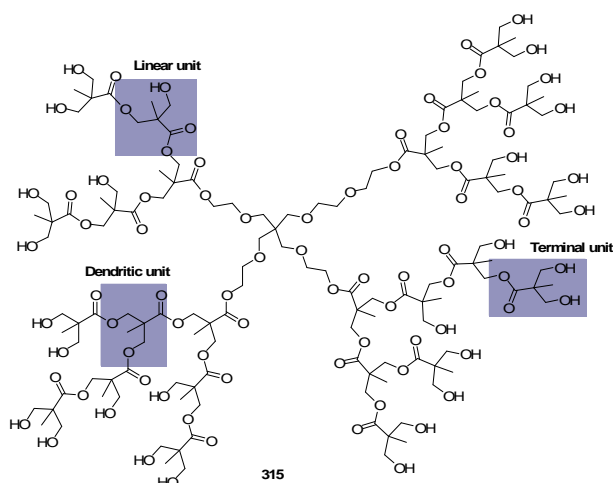
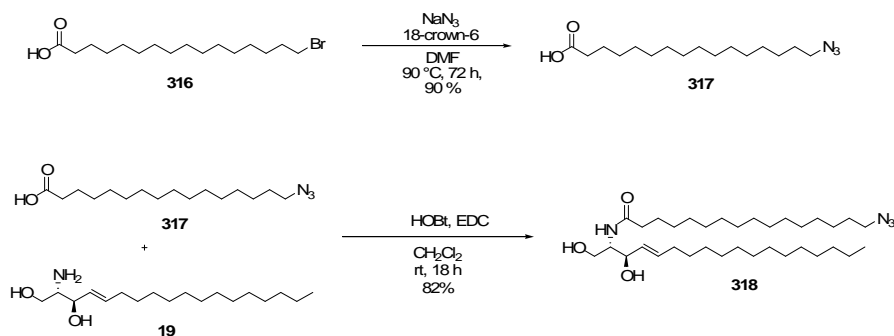


Figure 26. Idealized chemical structure of the commercial hyperbranched polymer Boltorn H30

3.3.3 Results

3.3.3.1. Synthesis of modified β -glycosphingolipid

The initial efforts were directed toward the synthesis of compound **318** (Scheme 59) from the 16-Bromohexadecanoic acid **316** following a standard literature procedure.²⁶⁸

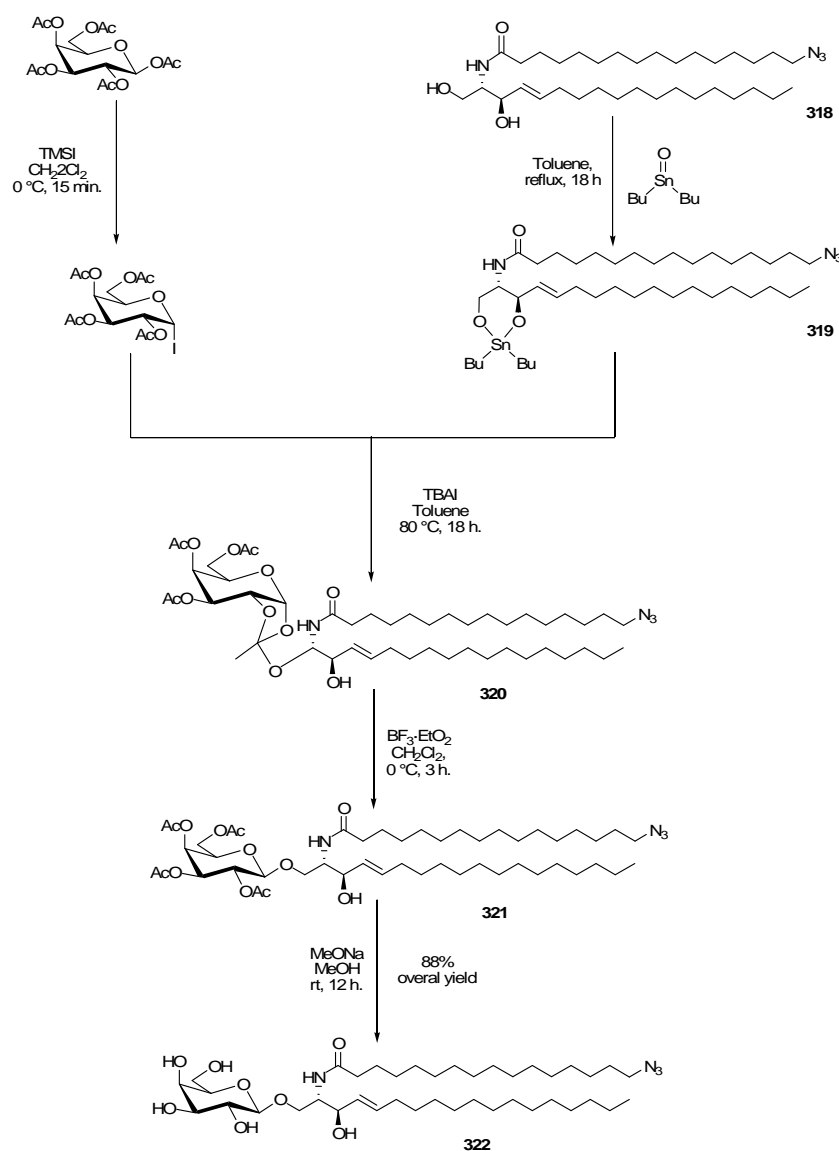


Scheme 59. Synthesis of azido ceramide **318**

The 16-Bromohexadecanoic acid **316** was transformed into the corresponding azide derivative **317** in 90% yield by treatment with NaN_3 in DMF at 90 °C. As depicted in

²⁶⁸ Ohlsson, J.; Magnusson, G. *Carbohydr. Res.* **2001**, *331*, 91–94

Scheme 59, the sphingosine **19**, was acylated overnight with the carboxylic acid derivative **317** in CH_2Cl_2 to give the ceramide **318** in 88% yield. A mixture of the tetra-*O*-acetyl- α -iodogalactose **283** and the stannyl ceramide **319**, prepared in situ from **318**, in toluene at 80 °C was treated for 18 h with TBAI in the presence of molecular sieves (MS 300) to afford first the orthoester **320**, which was further isomerized to the β -anomer **321** with $\text{BF}_3 \cdot \text{OEt}_2$. Removal of the acetyl protecting groups by treatment with methanolic sodium methoxide, followed by chromatography, provided the glycosphingolipid **322** in high yields (88% three steps, Scheme 60).



Scheme 60. Síntesis of β -glycosphingolipid **322**

3.3.3.2. A click approach to unprotected glycodendritic structure

The copper(I)-catalyzed regiospecific formation of 1,2,3-triazoles from azides and terminal acetylenes (click chemistry), has been used as key step for the efficient functionalization of dendrimers.²⁶⁹ Click chemistry serves as a powerful strategy in the quest for function, and can be summarised neatly in one sentence: “all searches must be restricted to molecules that are easy to make”.²⁷⁰ These reactions are governed by kinetic control and are highly reliable and selective processes. A set of stringent criteria that a process must meet to be useful in the context of click chemistry has been defined by Sharpless as reactions that: “are modular, wide in scope, high yielding, create only inoffensive by-products (that can be removed without chromatography), are stereospecific, simple to perform and that require benign or easily removed solvent”. Ideally, starting materials and reagents for ‘click’ reactions should be readily available, and it is a convenient coincidence that unsaturated-hydrocarbon based organic synthesis is currently at the heart of this powerful approach, since these materials are readily available from nature or can be obtained by steam cracking of alkanes in the petrochemical industry.²⁷⁰

This concept and associated set of reactions have garnered a significant amount of attention due to its complete specificity, quantitative yields, and almost perfect fidelity in the presence of a wide variety of other functional groups.²⁷¹ This unprecedented degree of control is perfectly suited to polymeric materials. In direct contrast with small molecule chemistry, one of the greatest challenges in polymer chemistry is the ability to perform multiple functionalization reactions without cross-linking (side reactions) or incomplete

²⁶⁹ a) Fernandez-Megia, E.; Correa, J.; Rodríguez-Meizoso, I.; Riguera, R. *Macromolecules* **2006**, *39*, 2113–2120. b) Malkoch, M.; Schleicher, K.; Drockenmuller, E.; Hawker, C. J.; Russell, T. P.; Wu, P.; Fokin V. V. *Macromolecules* **2005**, *38*, 3663–3678.

²⁷⁰ Kolb, H. C.; Finn, M. G.; Sharpless, K. B. *Anew. Chem. Int. Ed.* **2001**, *40*, 20004–2021.

²⁷¹ a) Speers, A. E.; Adam, G. C.; Cravatt, B. F. *J. Am. Chem. Soc.* **2003**, *125*, 4686–4687. b) Deiters, A.; Cropp, T. A.; Mukherji, M.; Chin, J. W.; Anderson, J. C.; Schultz, P. G. *J. Am. Chem. Soc.* **2003**, *125*, 11782–11783. c) Wang, Q.; Chan, T. R.; Hilgraf, R.; Fokin, V. V.; Sharpless, K. B.; Finn, M. G. *J. Am. Chem. Soc.* **2003**, *125*, 3192–3193. d) Rostovtsev, V. V.; Green, L. G.; Fokin, V. V.; Sharpless, K. B. *Angew. Chem., Int. Ed.* **2002**, *41*, 2596–2599. e) Lewis, W. G.; Green, L. G.; Grynszpan, F.; Radic, Z.; Carlier, P. R.; Taylor, P.; Finn, M. G.; Sharpless, K. B. *Angew. Chem., Int. Ed.* **2002**, *41*, 1053–1055. f) Fazio, F.; Bryan, M. C.; Blixt, O.; Paulson, J. C.; Wong, C. H. *J. Am. Chem. Soc.* **2002**, *124*, 14397–14402. g) Shintani, R.; Fu, G. C. *J. Am. Chem. Soc.* **2002**, *124*, 10778–10779.

functionalization occurring.²⁷² The occurrence of even minor amounts of cross-linking can lead to gelation due to the numerous functional groups along the backbone, while the inability to separate unreacted functional groups is a significant issue. Hyperbranched polymers, due to their high functionality, are perfect test vehicles to probe the fidelity of click chemistry as a functionalization tool in polymeric systems since crosslinking reactions or unreacted starting groups can be detected.

In this context, click chemistry applications are increasingly found in all aspects of drug discovery,²⁷³ ranging from lead finding through combinatorial chemistry and target-templated *in situ* chemistry, to proteomics and DNA research, using bioconjugation reactions. The copper(I)-catalyzed 1,2,3-triazole formation from azides and terminal acetylenes is a particularly powerful linking reaction, due to its high degree of dependability, complete specificity, and the bio-compatibility of the reactants. The triazole products are more than just passive linkers; they readily associate with biological targets, through hydrogen bonding and dipole interactions.²⁷⁴

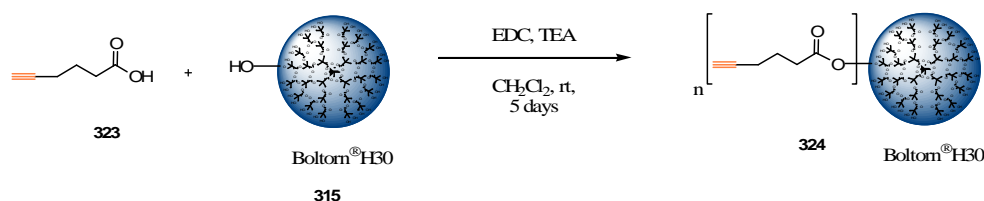
3.3.3.3. Functionalization of Boltorn H30 hyperbranched dendritic polymer

With this background and with the goal to prepare the glycocluster of β -Galcer **319** that bind HIV-1 rgp120 IIIB, it was glimpsed a strategy involving coupling of glycosphingolipid **322** and the hyperbranched dendritic polymer **315**, based on the monomer 2,2-bis(hydroxymethyl)propionic acid. The first step of the synthesis was the introduction of acetylene groups on the dendritic core surface. This was achieved by mixing Boltorn H30 hyperbranched dendritic polymer **315** and 5-hexynoic acid **323** in the presence of EDC and TEA (Scheme 61). After, the mixture was stirred for five days at room temperature. Thus, the functionalized hyperbranched **324** was obtained, as demonstrated by NMR and MALDI-TOF MS analysis.

²⁷² For review about the growing applications of click chemistry see: a) Moses, J. E.; Moorhouse, D. A. *Chem. Soc. Rev.* **2007**, *36*, 1249–1262. b) Nandivada, H.; Jiang, X.; Lahann, J. *Adv. Mater.* **2007**, *19*, 2197–2208. c) Dondoni, A. *Chem. Asian J.* **2007**, *2*, 700–708. d) Lutz, J.-F. *Angew. Chem. Int. Ed.* **2007**, *46*, 1018–1025. e) Binder, W. H.; Sachsenhofer, R. *Macromol. Rapid Commun.* **2007**, *28*, 15–54.

²⁷³ Kolb, H. C.; Sharpless, K. B. *DDT*, **2003**, *8*, 1128–1136.

²⁷⁴ a) Lutz, J.-F.; Börner, H. G.; *Prog. Polym. Sci.* **2008**, *31*, 1–39 b) Lutz, J.-F. *Angew. Chem. Int. Ed.* **2007**, *46*, 2182–2184. c) Foking, V. V. *ACS Chem. Biol.* **2007**, *2*, 775–778. d) Fokin, V. V.; Wu, P. *AldrichimicaActa*, **2007**, *40*, 7–17.



Scheme 61. Functionalization of Boltorn H30

Commercial Boltorn H30 **315** from Prestorp have already been used in several studies for which that was quite completely characterized, especially recently by Žagar.²⁷⁵ A good knowledge of the chemical microstructure of Boltorn H30 **315** was indeed particularly important in order to understand how it could be influenced by its chemical modification. To illustrate the possible defects in the molecular architecture, a typical chemical structure of a third-generation is shown in figure 26. To the commercial Boltorn H30 **315**, Dendritic **D**, Linear **L**, and terminal **T** units can be distinguished both by ¹H NMR using the methyl signal at 1.4-1.0 ppm and ¹³C NMR using either the carbonyl peaks at 175-171 ppm or that of the quaternary carbons at 50.25-46.25 ppm. After modification of part of the OH groups by 5-hexynoic acid **323**, new pseudo-dendritic and pseudo-linear units are generated and ¹H NMR and ¹³C NMR can be as useful in detecting these units as in the case of the commercial Boltorn H30. All the units that can be found in a partially modified Boltorn H30 are depicted in figure 28. **D_i**, **L_i** and **T_i** are the initial dendritic, linear and terminal units, respectively; whereas **L_u** is a new linear unit created by the reaction of a **T_i** unit with one hexynoic acid; **D_{1u}** and **D_{2u}** arise from the reaction of one hexynoic acid with **L_i**, or of two hexynoic acid with **T_i**, respectively (Figure 27).

Thus, the ¹H NMR spectrum of **324** indicated the presence of methyl groups at 1.26 ppm, acetylenic protons at 1.99 ppm, and methylene groups at 1.82 ppm, 2.24 ppm, and 2.48 ppm, which corresponding to protons β, α and γ to acetylene group. The protons of Boltorn core appeared at 3.68 ppm to CH₂ of alcohol and 4.24 ppm to CH₂ of ester (Figure 28), but from these spectra it is not possible to tell whether hexynoic acid has reacted with Boltorn H30.

²⁷⁵ Žagar, E.; Žigon, M.; Podzimek, S. *Polymer*, **2006**, *47*, 166–175.

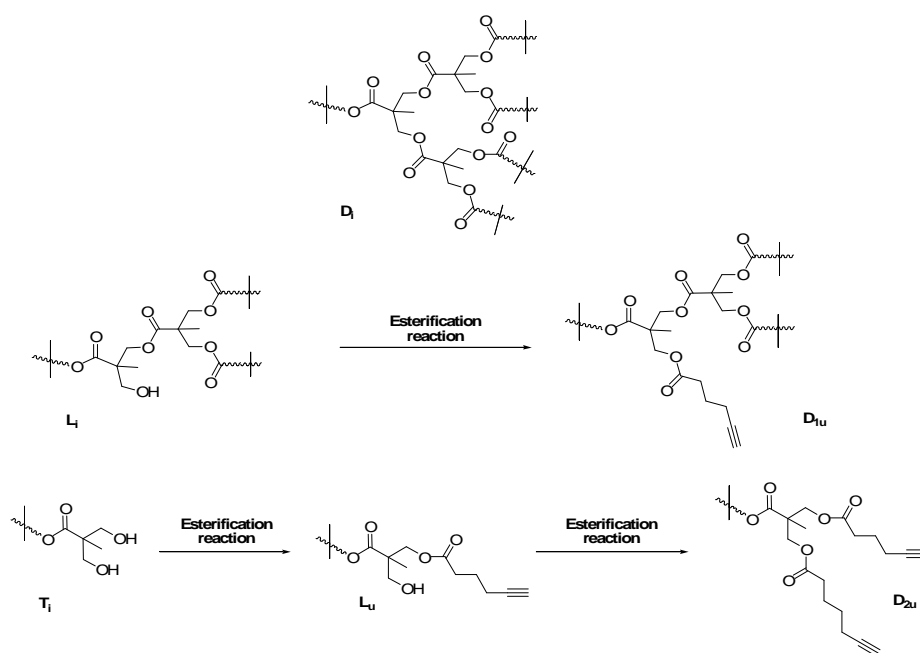


Figure 27. Various D, L, and T units in a partially modified Bolton H30

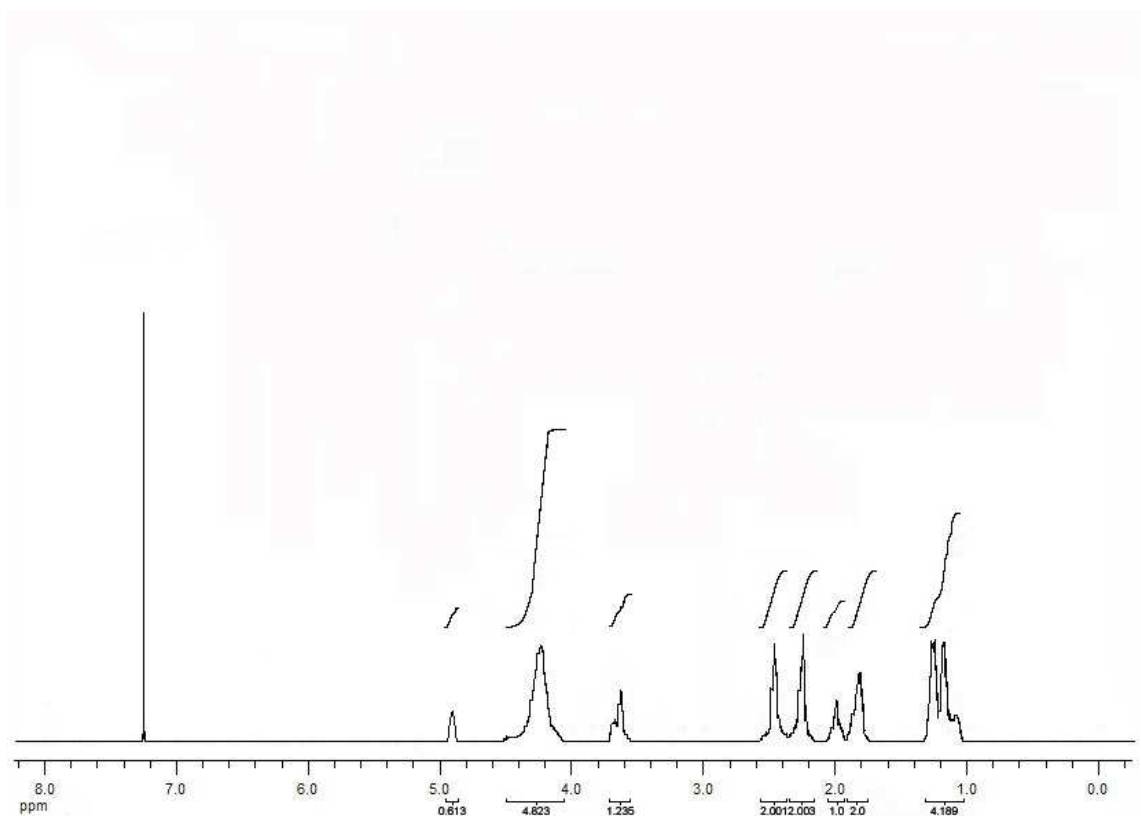


Figure 28. ¹H NMR of 324 in CD₃Cl

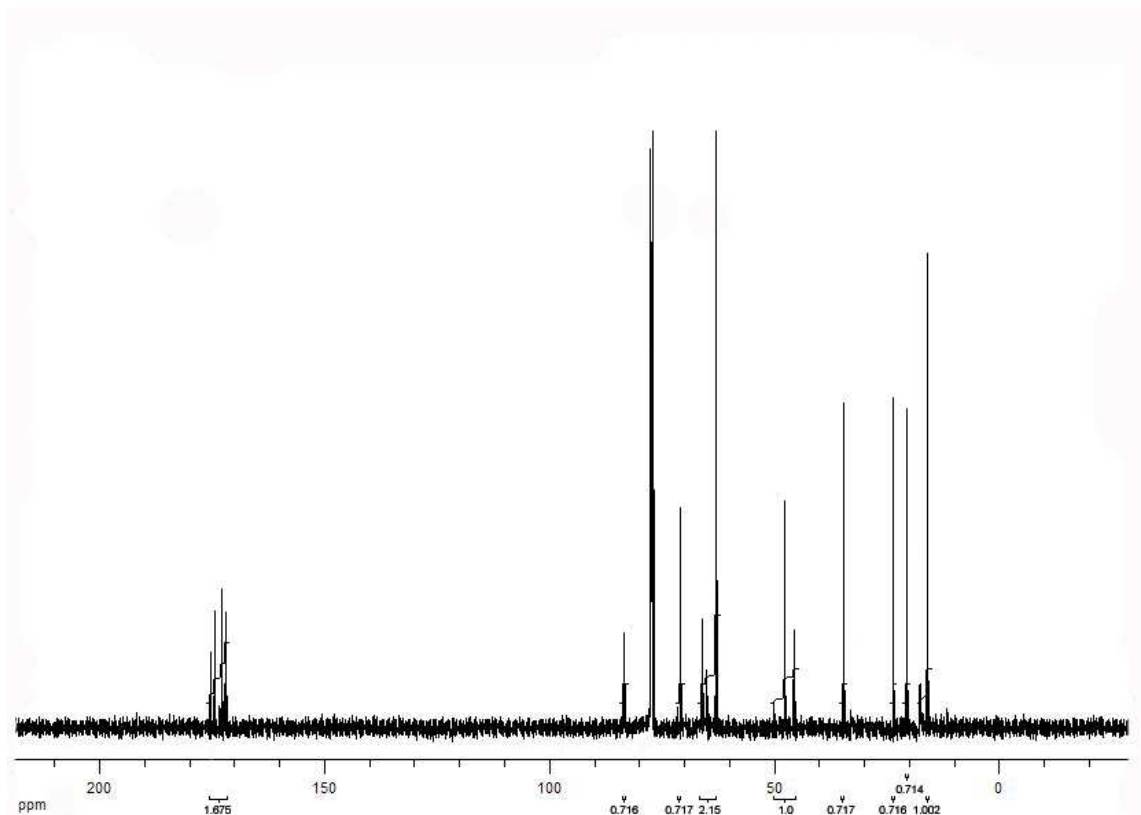


Figure 29. ^{13}C NMR of 324 in CD_3Cl

The ^{13}C spectrum of the same sample is shown in figure 29. The modified Boltorn displays C=O peaks between 175-172 ppm than can be attributed to ester groups. Acetylenic carbons appear at 84.6 ppm and 71.3 ppm, whereas the methylene groups from Boltorn core can be found at 66-63 ppm and the methyl group can be found at 17 ppm. The signals at 34.9 ppm, 23.6 ppm and 20.7 ppm corresponding to methylene γ , β and α to triple bond. The chemical modification of Boltorn H30 induces a change in the peaks associated with quaternary carbons (Figure 30), this evolution is visible with a decrease in the intensity of **T** signals at 50.25 ppm, as well as the

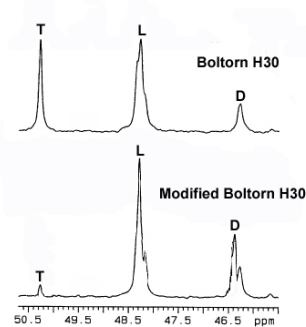
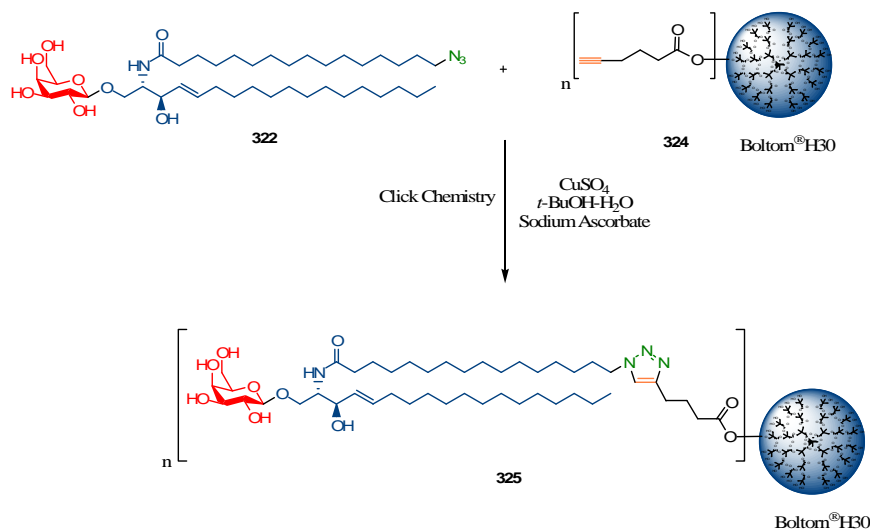


Figure 30. Cq area in the ^{13}C NMR spectra

appearance of news peaks in the **L** and **D** areas between 48.5 ppm and 46.2 ppm. A quantitative analysis of this resonance allows calculating the total amount of hexynoic acid that was initially added to Boltorn H30 from the integration of the quaternary carbons from Boltorn H30²⁷⁵ and an acetylenic carbon from modified Boltorn H30 (62%, Equation 1).

$$\begin{aligned} [\text{hexynoic acid}]_0/[\text{OH}]_0 &= (\text{acetylenic carbon})/(\text{LC}_q+2\text{TC}_q)_{\text{HB30}} & (1) \\ &= (0.716)/(0.570+0.580) \end{aligned}$$

Next a mixture of β -Galceramide **322** and Boltorn hyperbranched polymer **324** was treated for 72 h with sodium ascorbate²⁷⁶ and CuSO₄ in *t*-BuOH/H₂O (Scheme 62). Dialysis purification afforded the corresponding glycodendritic polymer **325** containing β -Galceramide. The process has allowed to anchor unprotected β -GalCer to the dendritic polymer. The efficiency of this coupling reaction was proved by NMR and MALDI-TOF MS analysis (see below).



Scheme 62. A click approach to unprotected glycodendritic structure

²⁷⁶ Rostovtsev, V. V.; Green, L. G.; Fokin, V. V.; Sharpless, K. B. *Angew. Chem. Int. Ed.* **2002**, *41*, 2596–2599.

The analysis of the ^1H NMR spectra of glycodendritic polymer of β -GalCer **325** revealed the presence of the triazole protons at 7.79 ppm, the presence of vinylic protons at 5.60 ppm, and complete disappearance of the acetylenic signal at 1.99 ppm. The ^1H NMR spectroscopic data also showed the presence of aliphatic chains at 1.2 ppm. The protons of galactose and Boltorn core showed broad and overlapping peaks between 4.57 ppm and 3.25 ppm (Figure 31). In ^{13}C NMR spectra carbonyl groups can be seen between 175 and 172 ppm, methylene groups between 66 and 63 ppm and quaternary carbons between 49 and 46 ppm. In the same spectra it is possible to find signals of 4- and 5-position of 1,2,3-triazol, these signals appeared at 145 ppm and 126.1 ppm. The signals to double bond can be found at 134.6 ppm and 130.2 ppm, whereas the anomeric carbon from galactose appear at 105 ppm (Figure 32).

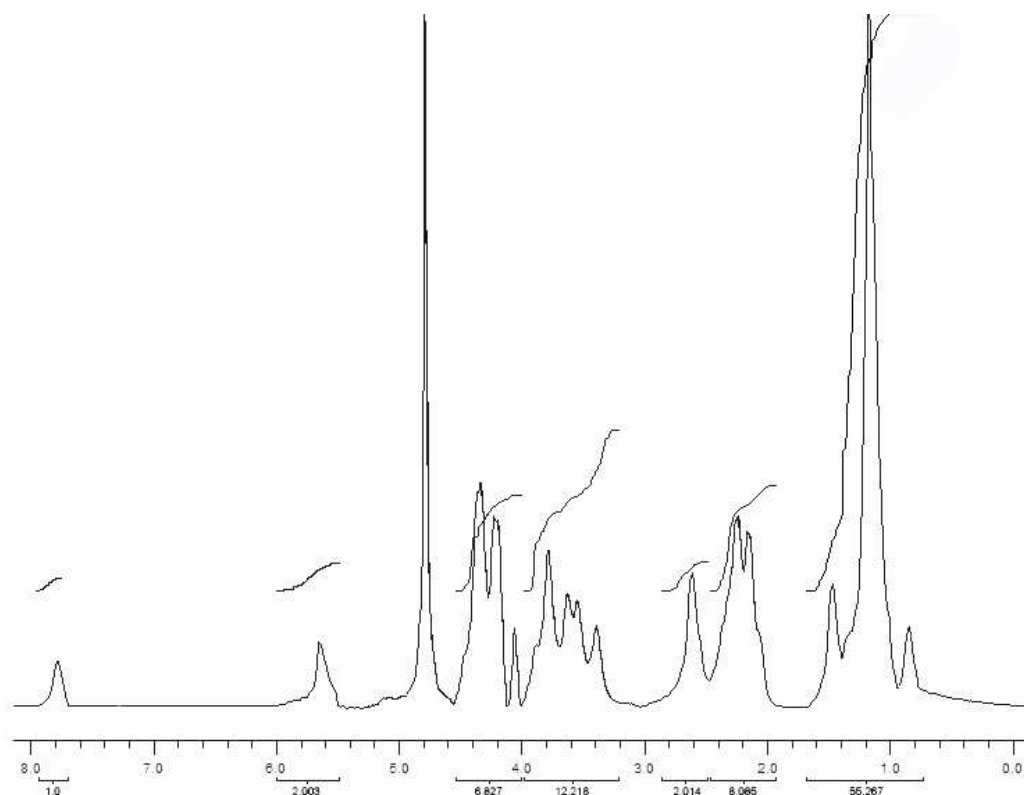


Figure 31. ^1H NMR of **325** in D_2O

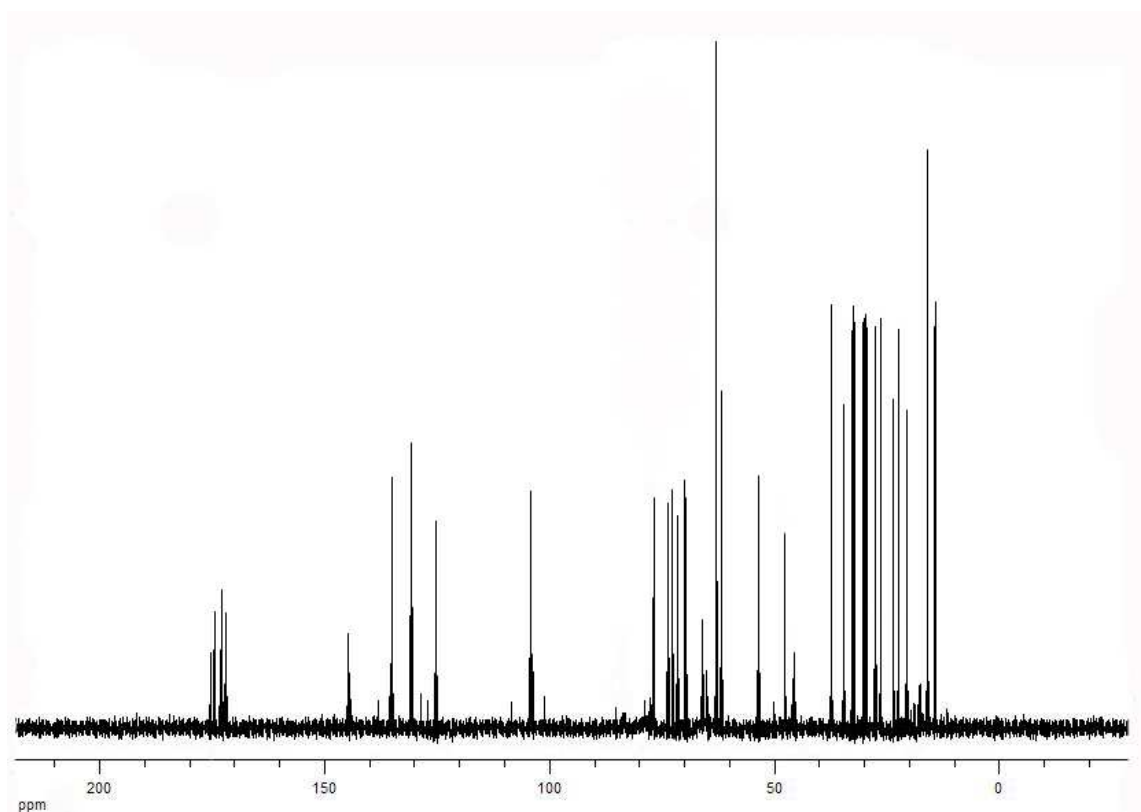


Figure 32. ^{13}C NMR of 325 in D_2O

3.3.3.4. Sulfation of glycodendritic polymer of β -GalCer

The findings of the past decade relating to the determination that CD4 alone is not sufficient for allowing HIV entry into host cells and that coreceptors and heparan sulphate proteoglycans (HSPGs) on the host cell are utilized for viral fusion, highlights the importance of electrostatic interactions between gp120, and the host cell surface. Gp120 has several highly basic regions, most notably, the V3 loop, while host cell surface structures are now known to have polyanionic regions that can interact with the basic regions of

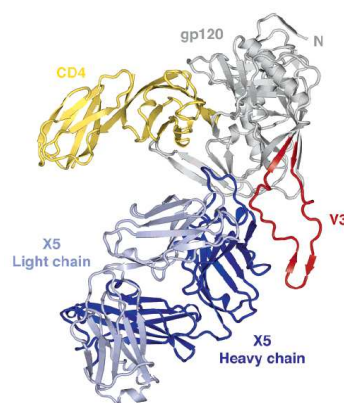


Fig. 33. Structure of an HIV-1 gp120 core with V3

gp120. It should therefore not be a surprise that there have been a large number of anionic polysaccharides of both natural and semisynthetic nature reported to have anti-HIV activities relating to early stages of infection, namely viral fusion and entry.²⁷⁷ The figure 33 shows the structure of an HIV-1 gp120 core with V3. The crystal structure of core gp120 (gray) with an intact V3 (red) is shown bound to the membrane-distal two domains of the CD4 receptor (yellow) and the portion of the X5 antibody (dark and light blue). In this orientation, the viral membrane would be positioned toward the top of the page and the target cell toward the bottom.²⁷⁸

Recently, it was noted that the binding of HSPG to recombinant monovalent gp120 (rgp120) was enhanced if CD4 had bound to gp120 prior to HSPG, compared to free gp120 binding HSPG.²⁷⁹ Further studies highlighted a single highly conserved amino acid in the V3 loop, Arg 298, and its importance in binding to both HSPGs and CCR5 (Figure 34). This study involved the use of whole virus with trimeric

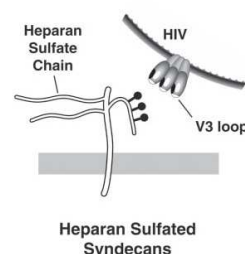


Figure 34. Schematic of HIV-1/syndecan

gp120, which is important given that carbohydrate interactions within biological systems are typically multivalent in nature. The interesting, and perhaps most significant, aspect of the findings in this study was that a specific sulfation motif was preferred by the virus, 6-*O*-sulfation, indicating that random sulfation or negative charges were not sufficient to yield a strong binding event between the virus and the host cell.²⁸⁰

In this context, recently galactose- and sulphated galactose-derived dendrimers were synthesized. By means of surface plasmon resonance studies has been demonstrated that the randomly sulphated galactose-derivatized dendrimers are better ligands for rgp120 IIIB than nonsulfated glycodendrimers. With this background and the hyperbranched glycodendritic polymer to hand, the desired sulfatide were prepared following reported

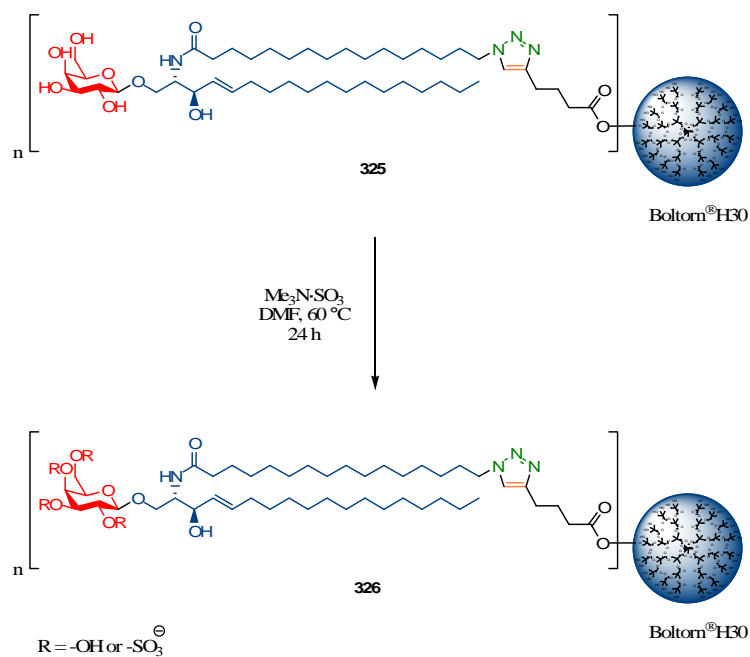
²⁷⁷ McReynolds, K. D.; Gervay-Hague, J. *Chem. Rev.* **2007**, *107*, 1533–1552.

²⁷⁸ Huang, C.-C.; Tang, M.; Zhang, M.-Y.; Majeed, S.; Mantabana, E.; Stanfield, R. L.; Dimitrov, D. S.; Korber, B.; Sodroski, J.; Wilson, A.; Wyatt, R.; Kwong, P. D. *Science* **2005**, *310*, 1025–1928.

²⁷⁹ Vives, R. R.; Invertí, A.; Sattentau, Q. J.; Lortat-Jacob, H. *J. Biol. Chem.* **2005**, *280*, 21353–21357.

²⁸⁰ de Parseval, A.; Bobardt, M. D.; Chatterji, A.; Chatterji, U.; Elder, J. H.; David, G.; Zolla-Pazner, S.; Farzan, M.; Lee, T.-H.; Galloway, P. A. *J. Biol. Chem.* **2005**, *280*, 39493–39504.

procedures²⁸¹ as it is shown in Scheme 63. Thus, the glycodendritic compound **325** was subjected to sulfation by treatment with an excess of sulphur trioxide/trimethylamine in DMF. After the dialysis purification and lyophilization, the sulphated glycodendritic compound **326** was obtained. The structure of this compound was confirmed by NMR and MALDI-TOF MS analysis. The most relevant data of ¹H NMR to **326** indicate the presence of aromatic proton at 7.79 ppm, vinylic protons at 5.61 ppm, aliphatic chains at 1.2 ppm and protons from galactose and Boltorn core between 4.55 ppm and 3.39 ppm (Figure 35). In ¹³C NMR the modified hyperbranched displays a new peak at 81.6 ppm, which can be attributed to sulphated carbon of galactose (Figure 36).



Scheme 63. Sulfation of glycodendritic polymer of β -GalCer

²⁸¹ Gilbert, B.; Davis, N. J.; Pearce, M.; Aplin, R. T.; Flitsch, S. L. *Tetrahedron:Asymmetry*, **1994**, 5, 2163–2178.

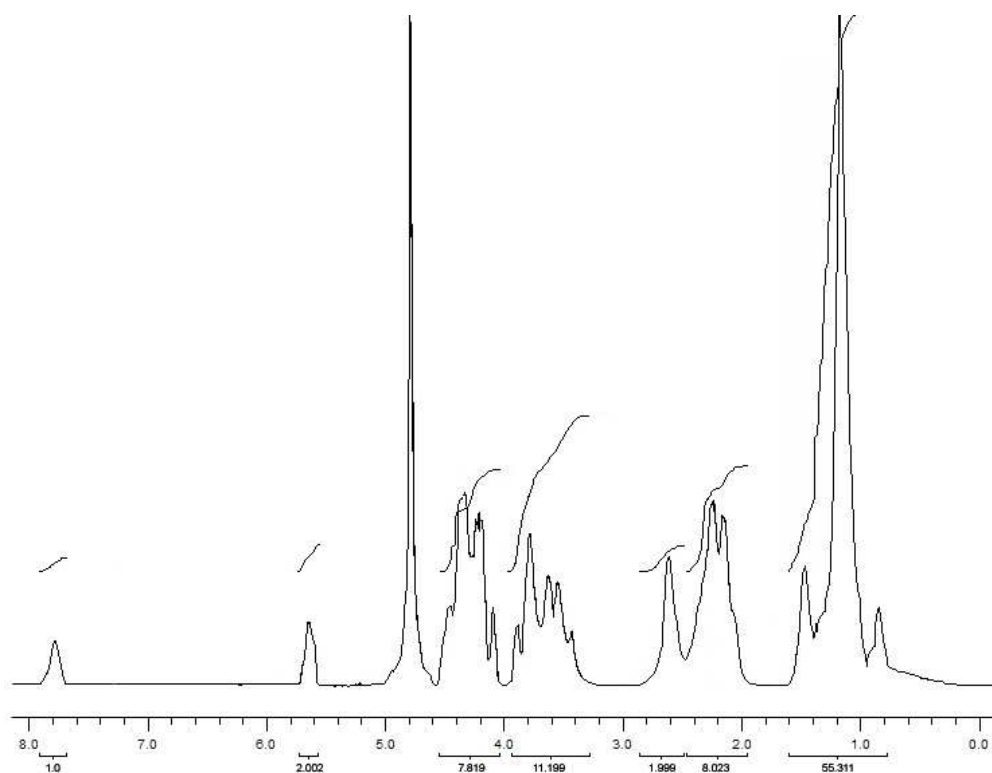


Figure 35. ^1H NMR of 324 in D_2O

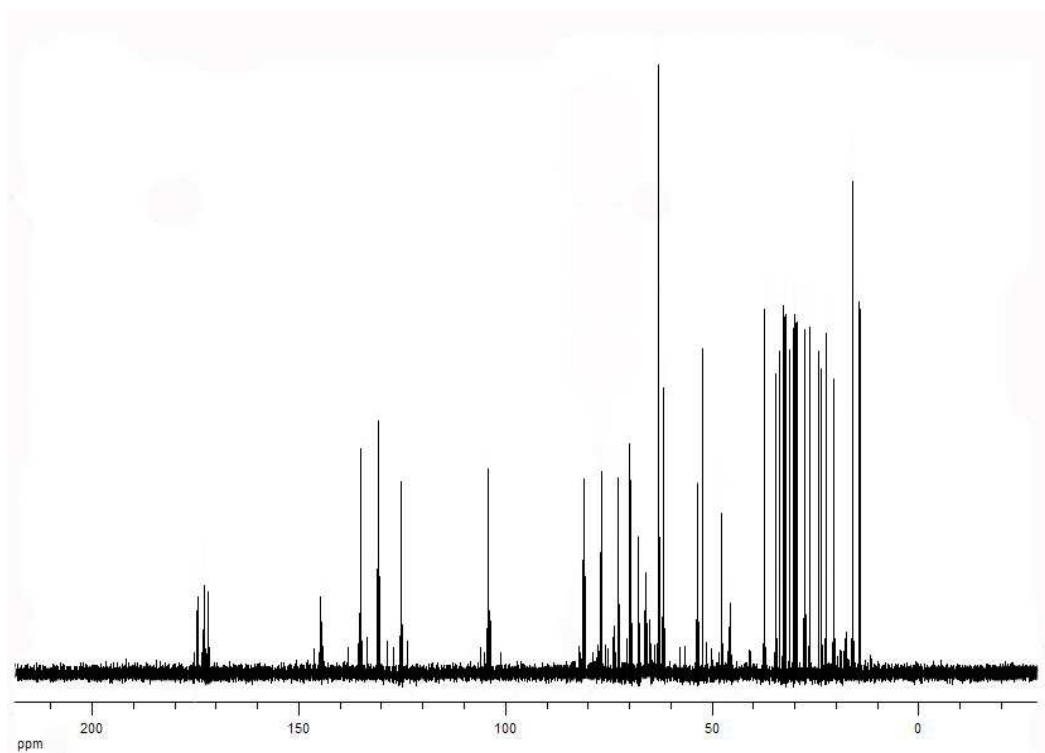


Figure 36. ^{13}C NMR of 324 in D_2O

MALDI-TOF MS analysis of the hyperbranched polymers revealed that 62.84% of the Boltorn H30 **315** was derivatized with **323** to give **324**. To calculate the average number of residues incorporated, the theoretical molecular weight of the starting Boltorn H30 **315** was subtracted from the M_w of the functionalized dendrimer and the difference divided by the weight of one hexynoic acid **323**, minus 18 to account for the loss of a H₂O molecule during formation of the ester bond. In the case of **325**, on average 95.47% of β -GalCer residues were incorporated onto the dendritic polymer **324**. Finally, these same analyses indicated that on average 20.4 sulfate groups were added to the glycodendritic polymer **325** to afford **326** (Table 11).

Table 11. MALDI-TOF MS Analysis of the hyperbranched polymers 324, 325 and 326

Entry	Compound	Theoretical molecular wt	Observed molecular wt	Average of residues incorporated	Theoretical % incorporation
1	324	6392	5275.9	20.11	62.84
2	325	20064	20033.9	19.92	95.47
3 ^a	326	21644	21617.1	20.04	100.60

3.3.3.5. Biological Evaluation

To demonstrate the binding ability the hyperbranched glycodendritic polymers toward HIV-1 rgp120 IIIB, the kinetic analysis was performed using surface plasmon resonance (SPR). The application of surface plasmon resonance (SPR)²⁸² based on optical biosensors have contributed extensively to understanding of the functional aspects of HIV. SPR biosensors allow the analysis of real-time interactions of any biomolecule, be it protein, nucleic acid, lipid, carbohydrate or small molecule, without the need for intrinsic or extrinsic probes. As such, the technology has been used to analyze molecular interactions associated with every aspect of the viral life cycle, from basic studies of binding events occurring during docking, replication, budding and maturation to applied research related to vaccine and inhibitory drug development. Along the way, SPR biosensors have provided a unique and detailed view into the inner works of HIV.

²⁸² Rich, R. L.; Myszka, D. G. *Trends Microbiol.* **2003**, *11*, 124–133

The ability to measure binding interactions in real time is the hallmark of SPR biosensors. Kinetic association and dissociation rates can be extracted from the binding responses to provide high-resolution information about complex formation and stability. By measuring binding constants over a range of temperatures, it is possible to determine the change in enthalpy and entropy associated with complex formation, as well as the transition-state energetic.

When polarized light is shone through a prism on a sensor chip with a thin metal film on top, the light will be reflected by the metal film acting as a mirror. On changing the angle of incidence, and monitoring the intensity of the reflected light, the intensity of the reflected light passes through a minimum (Figure 37, line A).

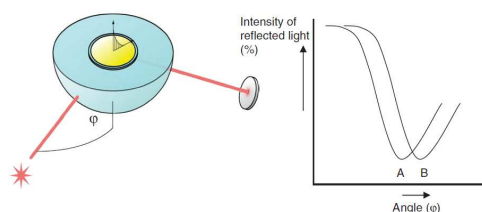


Figure 37. Schematic experimental set-up of surface plasmon resonance excitation

At this angle of incidence, the light will excite surface plasmons, inducing surface plasmon resonance, causing a dip in the intensity of the reflected light. Photons of p-polarized light can interact with the free electrons of the metal layer, inducing a wave-like oscillation of the free electrons and thereby reducing the reflected light intensity. The angle at which the maximum loss of the reflected light intensity occurs is called resonance angle or SPR angle. The SPR angle is dependent on the optical characteristics of the system, *e.g.* on the refractive indices of the media at both sides of the metal, usually gold. While the refractive index at the prism side is not changing, the refractive index in the immediate vicinity of the metal surface will change when accumulated mass (*e.g.* proteins) adsorb on it. Hence the surface plasmon resonance conditions are changing and the shift of the SPR angle is suited to provide information on the kinetics of *e.g.* protein adsorption on the surface.

When the refractive index changes, the angle at which the intensity minimum is observed will shift as indicated in figure 37, where **A** depicts the original plot of reflected light intensity vs. incident angle and **B** indicates the plot after the change in refractive index. Surface plasmon

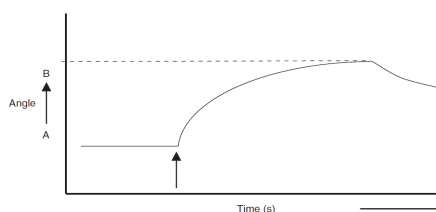


Figure 38. A sensorgram: the angle at which the dip is observed vs. time

resonance is not only suited to measure the difference between these two states, but can also monitor the change in time, if one follows in time the shift of the resonance angle at which the dip is observed. Figure 38 depicts the shift of the dip in time, a so-called sensorgram. If this change is due to a biomolecular interaction, the kinetics of the interaction can be studied in real time.

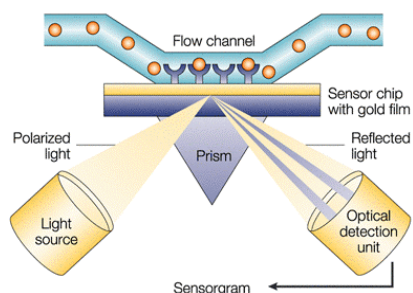


Figure 39. Schematic representation of direct detection

In the simplest case of an SPR measurement,²⁸³ a target component or *analyte* is captured by the capturing element or so-called *ligand*. The *ligand* is permanently immobilized on the sensor surface previous to the measurement. The event of capturing the *analyte* by the *ligand* gives rise to a measurable signal; this is called direct detection (Figure 39). Each measurement starts with conditioning the sensor surface with a suitable buffer solution (Figure 40, base line step). At this point, the sensor surface contains the active *ligands*, ready to capture the target *analytes*. On injecting the solution containing the *analytes* (Figure 40, association step), they are captured on the surface. At this step, adsorption kinetics of the *analyte* molecule can be determined in a real-time measurement. Next, buffer is injected on to the sensor and the non-specifically bound components are flushed off (Figure 40, dissociation step). As indicated in the figure, the accumulated mass can be obtained from the SPR response (ΔR). Also in this step, dissociation of the *analyte* starts, enabling the kinetics of the dissociation process to be studied. Finally, a regeneration solution is injected, which breaks the specific binding between *analyte* and *ligand* (Figure 40, regeneration step).

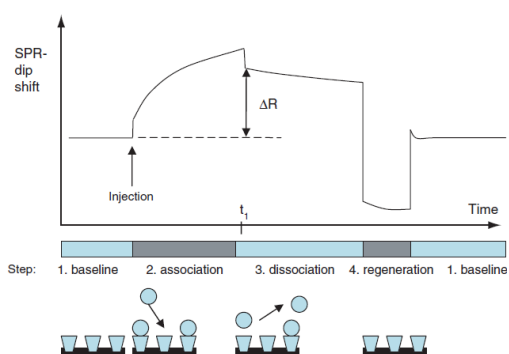


Figure 40. Sensorgram showing the steps of an analysis cycle

²⁸³ Schasfoort, R. B. M.; Tudos, A. J. *Handbook of Surface Plasmon Resonance*, RSC Publishing, 2008.

The most prominent benefit of direct detection using SPR biosensor technology is the determination of kinetics of biomolecular interactions. Reaction rate and equilibrium constants of interactions can be determined, *e.g.* the interaction $\mathbf{A} + \mathbf{B} \rightarrow \mathbf{AB}$ can be followed in real time with SPR technology, where **A** is the *analyte* (in this work: rgp 120 IIIB protein) and **B** is the *ligand* immobilized (in this work: polymer dendrimeric **345** and **324**) on the sensor surface. The association constant (k_a) is the reaction rate of complex (**AB**) formation, giving the number of complexes formed per time at unit concentration of **A** and **B** (Figure 41). As soon as the complex **AB** is formed, its dissociation can commence. The dissociation rate constant (k_d) describing this process expresses the number of **AB** complexes dissociating per unit time (Figure 41). When association of **A** and **B** starts, no product is yet present at the sensing surface. At this point, the rate of the association reaction is the highest and that of the dissociation reaction is the lowest. As the process progresses, more and more of the **AB** complex is produced, enhancing the rate of dissociation (Figure 41). Due to decreasing **A** and **B** concentration, the rate of association might decrease. Equilibrium is reached when the rates of the association and dissociation reactions are equal. Thus, the equilibrium association (K_A) and dissociation (K_D) constants, which represent the affinity of an interaction and stability of **AB**, are given by the equations 2 and 3:

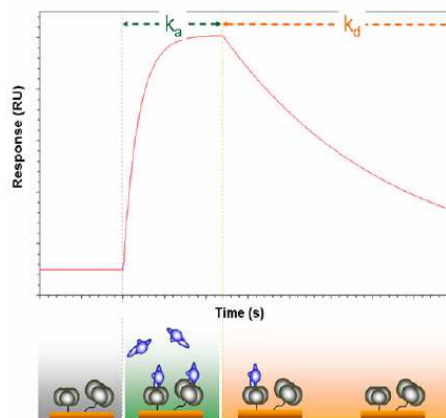


Figure 41. Interpretation of binding response curves

$$K_A \qquad \qquad \qquad K_D$$

$$(2) \quad [\mathbf{AB}]/[\mathbf{A}][\mathbf{B}] = k_a/k_d \quad \text{and} \quad (3) \quad [\mathbf{A}][\mathbf{B}]/[\mathbf{AB}] = k_d/k_a$$

Thus, sensorgrams (Figure 42 and 43) were analyzed by fitting the data to a 1:1 (Langmuir) binding model and kinetic constants determined using the BiaE-valuation 3.2

software. The rate constants and affinity constants for hyperbranched-rgp120 IIB interactions are shown in Table 12. These data suggest that rgp120 IIB exhibits similar binding to hyperbranched glycodendritic polymers **325** and **326**, and appreciably lower affinity that reported by Schengrund²⁸⁴ to Dextran sulphate **327** (DxS, Figuer 44), which is a potent binding antagonist of HIV infection in vitro.²⁸⁵

Table 12. Rate and Equilibrium Constants for the Interaction of Rgp120 IIB with hyperbranched glycodendritic polymers 325 and 326

Entry	Compound	k_a	k_d	K_D (M)
1	325	6.4×10^5	5.9×10^{-3}	9.14×10^{-8}
2	326	3.6×10^4	4.6×10^{-3}	1.28×10^{-8}
3 ^a	DxS (50 kDa) 327	2.8×10^6	6.4×10^{-5}	2.29×10^{-11}

^aValue reported by Schengrund and co-workers.

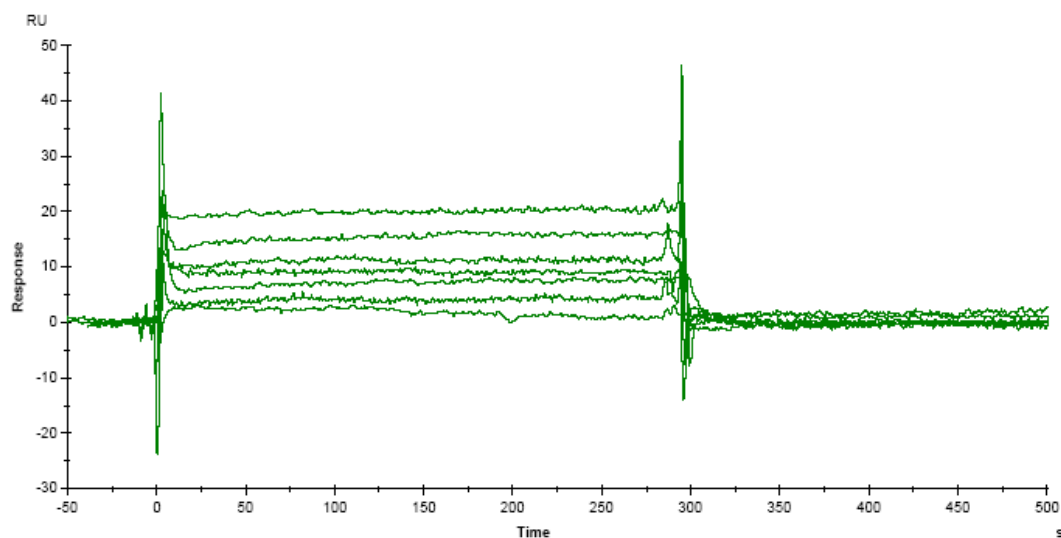


Figure 42. Sensogram to glycodendritic compound 325

²⁸⁴ Kensinger, R. K.; Yowler, B. C.; Benesi, A. J.; Schengrund, C.-L. *Bioconjugate Chem.* **2004**, *15*, 349–358.

²⁸⁵ Callahan, L. N.; Phelan, M.; Mallinson, M.; Norcross, M. A. *J. Virol.* **1991**, 1543–1550.

The response sensograms were obtained with increasing concentration of glycodendritic compound **325** and sulphated glycodendritic compound **326**: 10, 20, 50, 100, 250, 500 nM, and 1 μ M as show in Figure 43 and 44 respectively. That **325** and **326** bind HIV rgp120 IIIB with comparable affinity suggests the importance of multivalent presentation of carbohydrates and how this contributes to the binding affinity, which it may be possible by cluster effect.

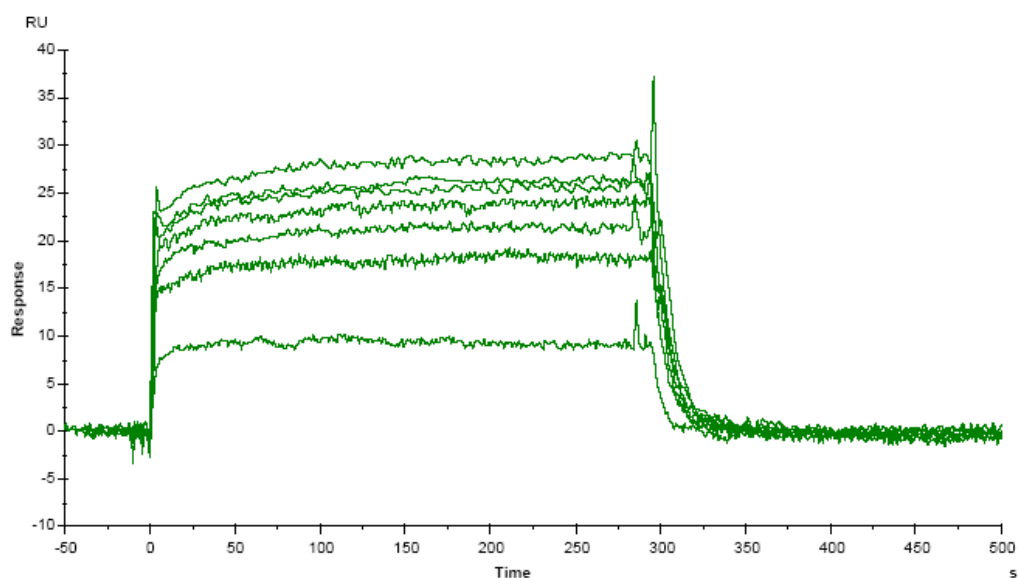


Figure 43. Sensogram to sulphated glycodendritic compound **326**

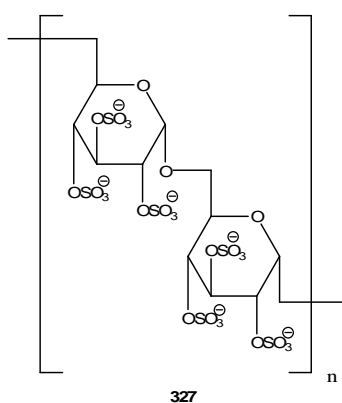


Figure 44. Structure of DxS **327**

In the other hand, the efficiency of hyperbranched glycodendritic polymers was tested for their ability to inhibit HIV-1 BaL (R5-tropic) infection of U373-MAGI-CCR5 cells and their effect on cell viability. The observed EC_{50} for the compound **328** was $80 \mu\text{M}$ (Figure 45). This observed efficiency in the micromolar range is consistent with observations recently reported to similar structures, however is lower than EC_{50} of DxS ($<1.0 \mu\text{M}$).²⁸⁴ In contrast, no inhibition was observed when the glycodendritic polymer **327** was tested. The fact that **327** and **328** have different behaviour in the inhibition suggests that it may be possible by presence of sulphate groups in these compounds. Finally, neither hyperbranched glycodendritic polymers **327** nor DxS were cytotoxic to the cultured indicator cells at the highest concentrations tested (2.5 mg/mL).

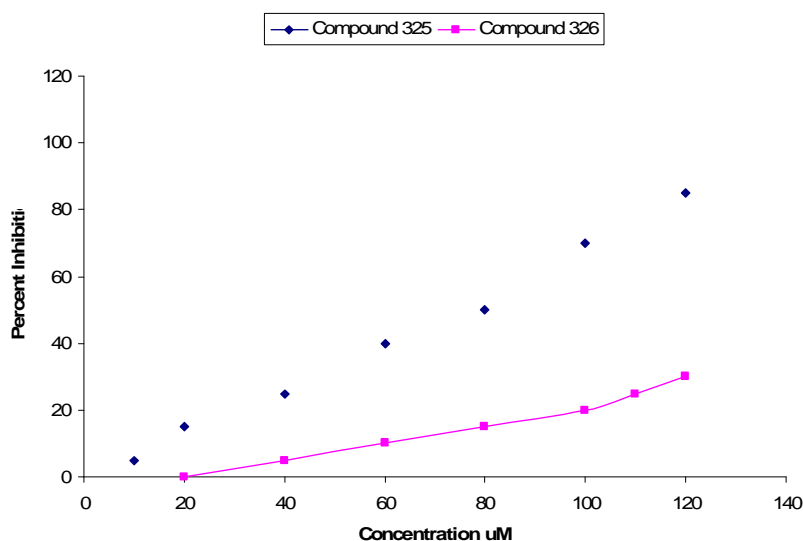


Figure 45. Inhibition of HIV-1 BaL (R5-tropic) infection of U373-MAGI-CCR5 cells

3.3.4. Experimental Part

General methods

All reactions were conducted under a dried argon stream. Solvents (CH₂Cl₂ 99.9%, toluene 99.9%) were purchased in capped Pure Solv System-4[®] bottles and used without further purification and stored under argon. Yields refer to the chromatographically and spectroscopically (¹H and ¹³C) homogeneous materials, unless otherwise stated. TMSI was stored at -15°C under desiccated atmosphere. All other solvents and reagents were used without further purification. The sphingosine was purchased from Avanti Polar Lipids Inc (Alabaster, AL). All glassware utilized was flame-dried before use. Reactions were monitored by TLC carried out on 0.25 mm E. Merck silica gel plates. Developed TLC plates were visualized under a short-wave UV lamp and by heating plates that were dipped in ethanol/H₂SO₄ (15:1). Flash column chromatography (FCC) was performed using flash silica gel (32–63 μm) and employed a solvent polarity correlated with TLC mobility. Melting points, determined with Reichert apparatus, are uncorrected. Optical rotations were measured at 598 nm on a Jasco DIP-370 digital polarimeter using a 100 mm cell. NMR experiments were conducted on a Varian 400 MHz instrument using CDCl₃ and D₂O (99.9% D) as the solvents. Chemical shift are in ppm with respect to TMS (Tetramethylsilane). Integrals in the ¹³C NMR spectra were obtained from 10% solutions using an inverse gated decoupling mode with a suppressed NOE effect, a relaxation delay of 20 s, an acq. time of 5 s and up to 20,000 repetitions.

Mass Spectrometry MALDI-TOF MS was done on a Perseptive Biosystems Voyager DE-PRO spectrometer. Spectra of negatively charged sugars were generated in linear, negative ion mode using THAP matrix, or in linear, positive ion mode using IAA. Glycodendrimer spectra were generated in linear, positive ion mode using an IAA matrix (20 mg/mL in DMF, diluted 11:1 with a 1 mM aqueous solution of glycodendrimer to yield a matrix-to analyte ratio of 1000:1).

Surface Plasmon Resonance experiments were done at 25 °C using a Biacore 3000 system and CM5 sensor chips (Biacore, Uppsala, Sweden). Glycodendrimers were amine-coupled to the sensor chip according to the manufacturer's protocol. To obtain a low-

density surface suitable for affinity analysis, 350-500 RUs of each glycodendrimer were immobilized. Varying concentrations of rgp120 were injected simultaneously over a blank control surface and the immobilized glycodendrimers at a flow rate of 30 mL/min for 3 min in HBS-EP buffer (10 mM HEPES, 150 mM NaCl, 3 mM EDTA, 0.005% P-20 surfactant, pH 7.4). Following the injection, the dissociation of the rgp120-glycodendrimer complex was measured for 10 min. Any remaining bound rgp120 was removed by 1 min injection of 4 M KCl. This regeneration step prepared the surface for the next injection of rgp120. Each concentration of rgp120 was injected in duplicate over the immobilized glycodendrimer, with a representative sensorgram chosen for analysis.

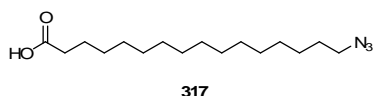
U373-MAGI-CCR5 cells were obtained from the AIDS Reagent Program. Cells were propagated in 'Selection Media' consisting of DMEM supplemented with 10% FCS, 0.4 mg/mL L-glutamine, penicillin and streptomycin (0.08 mg/mL each), 0.05% sodium bicarbonate, 0.2 mg/mL G418, 0.1 mg/mL hygromycin B, and 1.0 ug/mL puromycin. 'Culture Media' for virus inhibition assays consisted of DMEM with 10% FCS and 0.05% sodium bicarbonate. Cells were grown at 37 °C in an atmosphere of 95% air and 5% CO₂.

To viral inhibition assays, cells, were plated in 96-well tissue culture plates at a density of 1.0×10^4 cells per well. One day later, commercially available (Advanced Biotechnologies, Columbia, MD), concentrated cell-free viral preparations of HIV-1 Ba-L (R5) were diluted 1:400 in 'Culture Media'. Glycodendrimers solutions were made up in culture media and serially diluted with culture media in separate sterile V-bottom 96-well microliter plates, to a final volume of 30 mL per well. This was followed by the addition of 30 mL of the diluted virus and incubation at 37 °C for 20 min. Selection Media was then removed from the plated cells, and 50 mL of virus or virus plus potential inhibitor was added to the plated cells. The virus- or virus plus inhibitor-exposed cells were then incubated at 37 °C in an atmosphere of 95% air/5% CO₂ for 2 h. After the absorption period, 200 mL of Culture Media was added to the wells, and the cells were allowed to grow for an additional 40-48 h. Cells treated with culture media served as negative controls, and cells treated with virus only were positive controls. All measurements were done in quadruplicate.

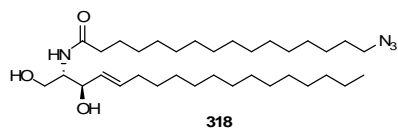
After the 48 h incubation, culture media was removed from the wells, the cells were washed with 200 mL of PBS, and β -galactosidase activity was measured using the Galacto-

Star β -Galactosidase Reporter Gene Assay System from Applied Biosystems (Foster City, CA), according to the manufacturer's instructions. Briefly, after the cells were washed with PBS, 10 mL of lysis solution was added to each well and the plate incubated for 10 min at 37 °C. The Galacto-Star substrate was diluted 1:50 and 100 μ L added to each well containing cell lysate. Well contents were mixed and 90 μ L were removed and added to a 96-well opaque luminometer plate. One hour after the Galacto-Star substrate was added, luminescence was determined using a luminometer. Percent inhibition was determined as $[(L_{\text{no inhibitor}} - L_{\text{inhibitor}})/L_{\text{no inhibitor}}] \times 100$. The effective concentration that inhibited 50% of viral infectivity (EC50) was determined by plotting the percent inhibition versus the log of the concentration of the potential inhibitor.

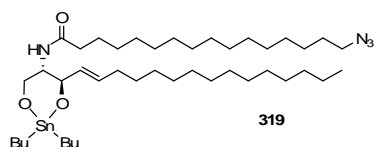
Experimental Procedures



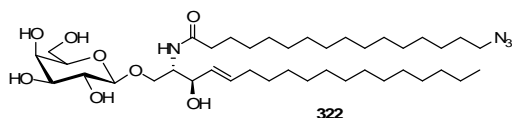
16-azidohexadecanoic acid 317. To a solution of 16-Bromohexadecanoic acid **316** (1 g, 2.99 mmol) in freshly distilled DMF (50 mL) was added NaN_3 (1.94 g, 29.9 mmol) and a catalytic amount of 18-crown-6, and the mixture was stirred at 90 °C for 72 h. The reaction mixture was poured into 1:1 AcOEt-water (80 mL) and the aqueous phase was extracted with AcOEt (3 x 20 mL). The organic phases were combined, washed with brine (3 x 20 mL), dried over MgSO_4 and concentrated in *vacuo*. The residue was purified by flash column chromatography on silica gel using hexane/AcOEt (95:5) as the eluent to give 799 mg of **317** (90 %). TLC (Hexane/AcOEt 90:10) R_f 0.70; ^1H NMR (400 MHz, CDCl_3): δ 3.27 (t, 2H, $J=7.2$ Hz), 2.37 (t, 2H, $J=7.5$ Hz), 1.62 (m, 4H), 1.40–1.20 (m, 22H); ^{13}C NMR (100.6 MHz, CDCl_3): δ 177.0, 51.4, 34.0, 29.6, 29.5, 29.4, 29.2, 29.1, 29.0, 26.7, 24.6. Anal. Calcd. for $\text{C}_{16}\text{H}_{31}\text{N}_3\text{O}_2$: C, 64.61; H, 10.51; N, 14.13. Found: C, 64.68; H, 10.52, N, 14.10.



Synthesis of ceramide 318. A solution of sphingosine **19** (100 mg, 0.333 mmol), HOBt (61 mg, 0.4 mmol), EDC (76 mg, 0.4 mmol) and DIPEA (77 mg, 0.6 mmol) in 20 mL of dry CH₂Cl₂ was cooled to 0 °C. Under stirring, stearic acid (98 mg, 0.333 mmol in 20 mL of dry CH₂Cl₂) was added drop wise over 6 h at 0 °C, and then the reaction was stirred under argon for 18 h at room temperature. The mixture was diluted with ethyl acetate (75 mL) and washed successively with HCl (10% aqueous, 2 x 30 mL), NaHCO₃ (7% aqueous, 2 x 30 mL), K₂CO₃ (7% aqueous, 2 x 30 mL), and brine (3 x 30 mL). The organic layer was dried over MgSO₄ and concentrated *in vacuo*. The residue was purified by flash column chromatography on silica gel using hexane-AcOEt-MeOH (85:10:5) as the eluent to give 162 mg of pure cearamide **318** (85 %). TLC (Hexane-AcOEt-MeOH 60:30:10); ¹H NMR (400 MHz, CDCl₃): δ 6.23 (1H, d, *J*=7.3 Hz), 5.77 (1H, dt, *J*=15.4, 6.7 Hz), 5.51 (1H, dd, *J*=15.4, 6.4 Hz), 4.3 (1H, dd, *J*=6.4, 3.4 Hz), 3.94 (1H, dd, *J*=11.3, 3.7 Hz), 3.89 (1H, dddd, *J*=7.3, 3.7, 3.4, 3.2 Hz), 3.69 (1H, dd, *J*=11.3, 3.2 Hz), 3.27 (t, 2H, *J*=7.2 Hz), 2.21 (2H, t, *J*=7.5 Hz), 2.03 (2H, dt, *J*=7.2, 6.7 Hz), 1.62 (m, 4H), 1.40–1.20 (m, 44H), 0.86 (t, 3H, *J*=7.5 Hz); ¹³C NMR (100.6 MHz, CDCl₃): δ 174.2, 134.6, 129, 74.9, 62.8, 54.7, 51.4, 36.92, 32.2, 31.98, 29.9, 29.8, 29.7, 29.6, 29.5, 29.4, 26, 22.9, 14.3. Anal. Calcd. for C₃₄H₆₆N₄O₃: C, 70.54; H, 11.49; N, 9.68. Found: C, 70.52; H, 11.47, N, 9.69.



Preparation of stannyl acetal 319: A mixture of cearamide (101 mg, 0.176 mmol) and dibutyltin oxide (44 mg, 0.176 mmol) in dry toluene (20 mL), was heated to reflux and was subjected to azeotropic dehydration using a Dean-Stark system or 4 Å molecular sieves overnight. Removal of solvent under reduced pressure afforded the stannyl ether **319**, which was used for the glycosylation without further purification.



Synthesis of β -GalCer 322. The following protocol was followed prior to the glycosylation reaction: 1,2,3,4,6-penta-*O*-acetyl- β -D-galactopyranose and stannyl ether

319 were separately dried by co-distillation with toluene (3 x 5 mL) in dried flasks and then were placed under vacuum for 1 h.

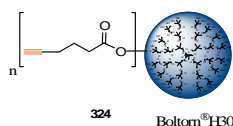
TBAI was added to a dried flask with a magnetic stirring bar and was co-distilled with dry toluene (2 x 5 mL) in the dark. Activated 4 Å molecular sieves were added, and the mixture was co-distilled with toluene once more (5 mL) before being placed under vacuum for 1 h. Complete water exclusion is crucial to achieve good yields.

A solution of previously dried 1,2,3,4,6-penta-*O*-acetyl- β -D-galactopyranose **262** (82 mg, 0.211 mmol) in CH_2Cl_2 (3 mL) was cooled to 0°C under argon atmosphere in the dark and TMSI (50 mg, 0.253 mmol) was added to the stirring mixture. The reaction was stirred for 20 min at 0°C. The reaction was stopped by adding 3 mL of dry toluene and co-distilling three times with dry toluene to obtain compound **283** as a slightly yellow oil, which was then dissolved in anhydrous toluene (5 mL) and kept under argon.

To a stirred mixture of TBAI (6 mg, 0.017 mmol) and 4Å acid washed molecular sieves (1.2 g) in anhydrous toluene (5 mL) under argon at room temperature was added a solution of stannyl derivative **319** (101 mg, 0.176 mmol) in dry toluene (5 mL) and a solution of **283** (0.211 mmol) in dry toluene (5 mL) via syringe. The reaction mixture was stirred at 80°C in the dark for 18 h and then diluted with AcOEt (15 mL) and cooled to 0°C. The white precipitate was removed by filtration through a pad of Celite. The organic layer was concentrated *in vacuo* to get the orthoester **320**, which was co-distilled with dry toluene (3 x 5 mL) and placed under vacuum for 1 h before the next reaction.

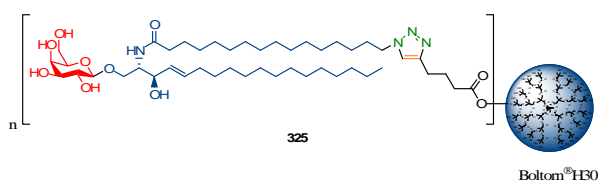
A solution containing the orthoester in anhydrous CH_2Cl_2 (5 mL) was cooled to 0°C under argon atmosphere, and freshly distilled $\text{BF}_3 \cdot \text{Et}_2\text{O}$ (0.528 mmol) was added to the stirring mixture. After, the resulting reaction mixture was stirred for 3 h at room temperature, it was quenched with saturated aqueous NaHCO_3 solution and 25 mL of AcOEt was added. The aqueous phase was extracted with AcOEt (2 x 15 mL), and the combined organic extract was washed with saturated aqueous $\text{Na}_2\text{S}_2\text{O}_3$ solution (2 x 10 mL) and brine (3 x 10 mL), dried with anhydrous Na_2SO_4 , and concentrated *in vacuo*.

Then, MeOH (15 mL) and Dowex 50WX8–200 ion-exchange resin (1.5 g) were added and the reaction was stirred at room temperature for 4 h. The resin was then removed by filtration. The solvent was removed *in vacuo*, and the resulting residue was purified by flash column chromatography on silica gel using CHCl₃-MeOH (85:15) as eluent to give 114 mg (88%) of **322** as a unique anomer. $[\alpha]_D^{25} -5$ (c=1.0, Py). ¹H NMR (400 MHz, CDCl₃/CD₃OD, 1:1): δ 7.57 (d, 1H, *J*=9.0 Hz), 5.66 (dt, 1H, *J*=15.5, 7.0 Hz), 5.42 (ddt, 1H, *J*=15.5, 7.5, 1.0 Hz), 4.19 (d, 1H, *J*=7.5 Hz), 4.17 (dd, 1H, *J*=10.0, 4.3 Hz), 4.08 (dd, 1H, *J*=7.5 Hz), 3.99-3.93 (m, 1H), 3.84 (d, 1H, *J*=3.0 Hz), 3.78 (dd, 1H, *J*=11.5, 6.6 Hz), 3.71 (dd, 1H, *J*=11.5, 5.0 Hz), 3.56 (dd, 1H, *J*=10.0, 3.0 Hz), 3.53 (dd, 1H, *J*=9., 7.5 Hz), 3.50-3.44 (m, 2H), 3.26 (t, 2H, *J*=7.2 Hz), 2.14 (t, 2H, *J*=7.5 Hz), 2.02 (dt, 2H, *J*=7.2, 6.7 Hz), 1.62 (m, 4H), 1.40–1.20 (m, 44H), 0.86 (t, 3H, *J*=7.5 Hz); ¹³C NMR (100.6 MHz, CDCl₃/CD₃OD, 1:1): δ 176.0, 135.5, 130.8, 105.1, 76.5, 74.8, 73.2, 72.7, 70.3, 70.0, 62.7, 54.7, 51.3, 37.7, 33.6, 33.2, 30.9-30.6, 27.3, 26.3, 23.9, 15.0. Anal. Calcd. for C₄₀H₇₆N₄O₈: C, 64.83; H, 10.34; N, 7.56. Found: C, 64.80; H, 10.32, N, 7.53.



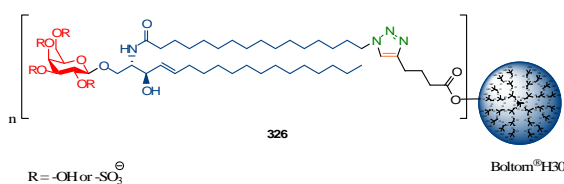
Synthesis of dendritic polymer 324. To a solution of 5-hexynoic acid **323** (2.115 g, 18.88 mmol, 2 equiv per OH) and Boltorn H30 **315** (1 g, 0.295 mmol) in DMF:CH₂Cl₂ 1:1 (100 mL) were added HOBt (2.879 g, 18.88 mmol), EDC (3.587 g, 18.88 mmol) and DIPEA (2.422 g, 18.88 mmol). The reaction

mixture was stirred at room temperature for five days and then concentrated *in vacuo*. The residue was purified by dialysis to obtain compound **324** (1.245 g, 80%) as a slightly yellow oil. ¹H NMR (400 MHz, CDCl₃): δ 4.918 (s, br, 12H) 4.24 (m, 96H), 3.62 (m, 24H), 2.48 (m, 40H), 2.24 (m, 40H), 1.99 (m, 20H), 1.82 (m, 40H), 1.26 (m, 84H); ¹³C NMR (100.6 MHz, CDCl₃): δ 175-172, 84.6, 71.3, 71, 66-63, 51-46, 34.9, 23.6, 20.7, 17. MALDI-TOF MS: 5275.9



Synthesis of glycodendritic polymer of β -GalCer 325.

To a solution of dendritic polymer **324** (17 mg, 0.0032 mmol) in a 1:1 mixture of *t*-BuOH- H_2O , were added β -GalCer **322** (95 mg, 0.128 mmol), $CuSO_4 \cdot 5H_2O$ (0.3 eq. per propargyl) and sodium ascorbate (0.3 eq. per propargyl). The reaction mixture was stirred at room temperature for 72 h and then purified by dialysis to obtain compound **325** (58 mg, 90%) as a white lyophilizate. 1H NMR (400 MHz, D_2O): δ 7.8 (m, 20H), 5.6 (m, 40H), 4.4-4.1 (m, 136H), 3.88-3.4 (m, 244H), 2.6 (m, 40H), 2.36-2.05 (m, 160H), 1.42-0.8 (m, 1104H); ^{13}C NMR (100.6 MHz, D_2O): δ 175-172, 145, 134.6, 130.2, 126.1, 105, 76.5, 74.8, 73.3, 72.6, 70.4, 70.1, 65.7-63.1, 54.7, 49-46, 37.7, 34.9, 33.8, 33.4, 30.8-30.5, 27.4, 26.3, 23.8, 23.6, 20.7, 17, 15. MALDI-TOF MS: 20033.9



Sulfation of glycodendritic polymer of β -GalCer.

To a solution of glycodendritic polymer of β -GalCer **325** (25 mg, 0.0012 mmol) was added SO_3NMe_3 (2 equiv per hydroxyl group). The reaction mixture was refluxed with stirring at 60 °C for 48 h and then dried by rotary evaporation under reduced pressure supplied by an oil vacuum pump and then purified by dialysis to obtain compound **326** (23 mg, 88%) as a white solid. 1H NMR (400 MHz, D_2O): δ 7.85 (m, 20H), 5.6 (m, 40H), 4.5-4.1 (m, 156H), 3.9-3.4 (m, 224H), 2.6 (m, 40H), 2.39-2.1 (m, 160H), 1.58-0.83 (m, 1104H); ^{13}C NMR (100.6 MHz, D_2O): δ 175-172, 145.1, 135.6, 130.7, 126.4, 105.5, 81.6, 76.1, 73.1, 70.9, 70.2, 68.7, 65.7-63.1, 54.7, 52.6, 51-46, 37.7, 33.8, 33.2, 32.4, 31, 30.8-30.5, 28.5, 27.3, 25.3, 23.8, 23.6, 20.7, 17.1, 15. MALDI-TOF MS: 21617.1

4. CONCLUSIONS

1. D/L-erythro-sphingosine **11** has been synthesised in 8 steps and 33% overall yield from alcohol **17** using a tethered aminohydroxylation (TA) as key step, which allowed to introduce the 2-amino and 3-hydroxylic groups with complete region- and stereoselectivity (Figure 33).

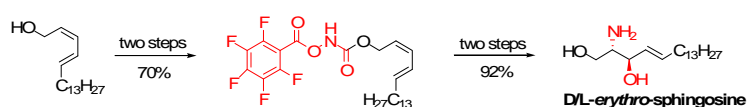


Figure 33

2. Also, we have reported a very efficient 5-step synthesis of D-erythro-sphingosine **11** in 60% overall isolated yield and high enantioselectivity and diastereoselectivity by an asymmetric sulfur ylide reaction between the allyl bromide of dodecane **23** and the appropriate aldehyde **22** in presencia the EtP₂ as base (Figure 34).

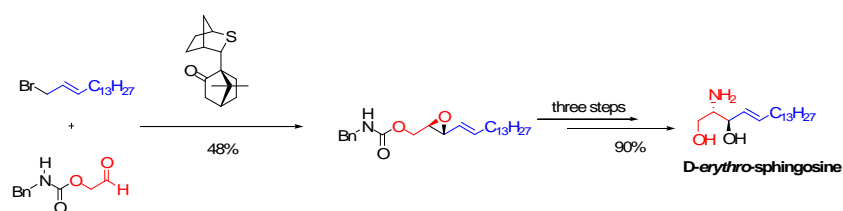


Figure 34

3. It has developed a process for the synthesis of glycosphingolipids based on a complete chemo and stereoselective reaction of α -glycosyl iodides with stannyl ceramides in the presence of TBAI (Figure 35). The synthetic scope was established by the use of a disaccharide and trisaccharide as donors. Moreover, it provides a solution for synthesising glycolipids via the direct glycosylation of ceramides. We believe that this methodology will find use in the efficient assembly of glycosphingolipids, which should provide avenues for the synthesis of these therapeutically valuable compounds.

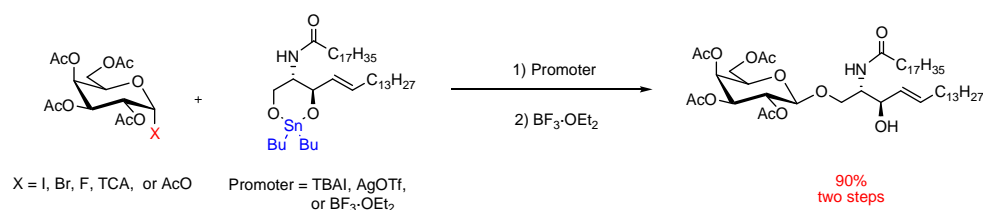


Figure 35

4. The copper(I)-catalyzed azide-alkene cycloaddition has proven to be a powerful tool for the preparation of water-soluble glycoconjugates, which consists of Boltorn H30 hyperbranched polymers and the naturally occurring β -Galceramide. The hyperbranched glycodendritic polymers have been used as models to mimic GSLs clustering at the cell surface demonstrating an excellent cluster effect. This is in agreement with the current hypothesis that the assembly of the HIV-1 fusion complex requires, in addition to CD4 and a coreceptor, specific glycolipids which are present in restricted areas of the plasma membrane. This approach opens the way to the development of novel class of HIV-1 binding antagonists employing hyperbranched dendritic polymers (Figure 36).

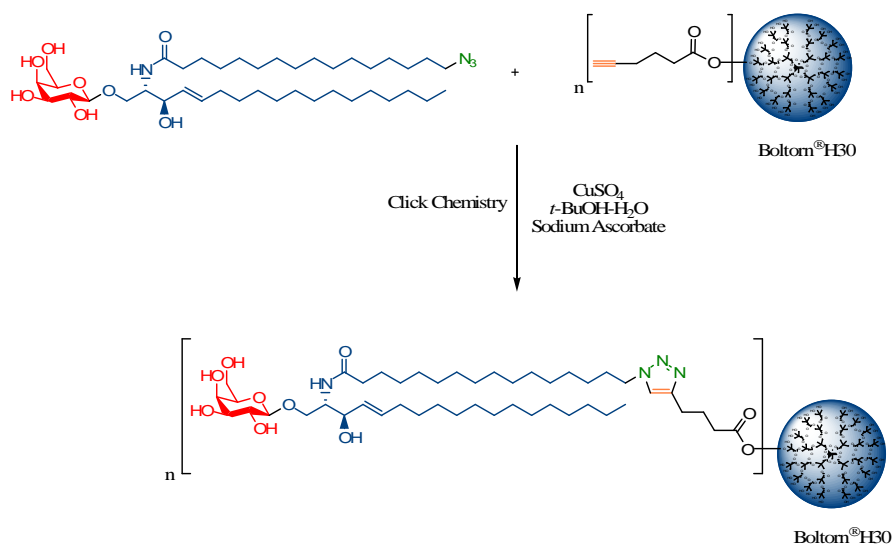
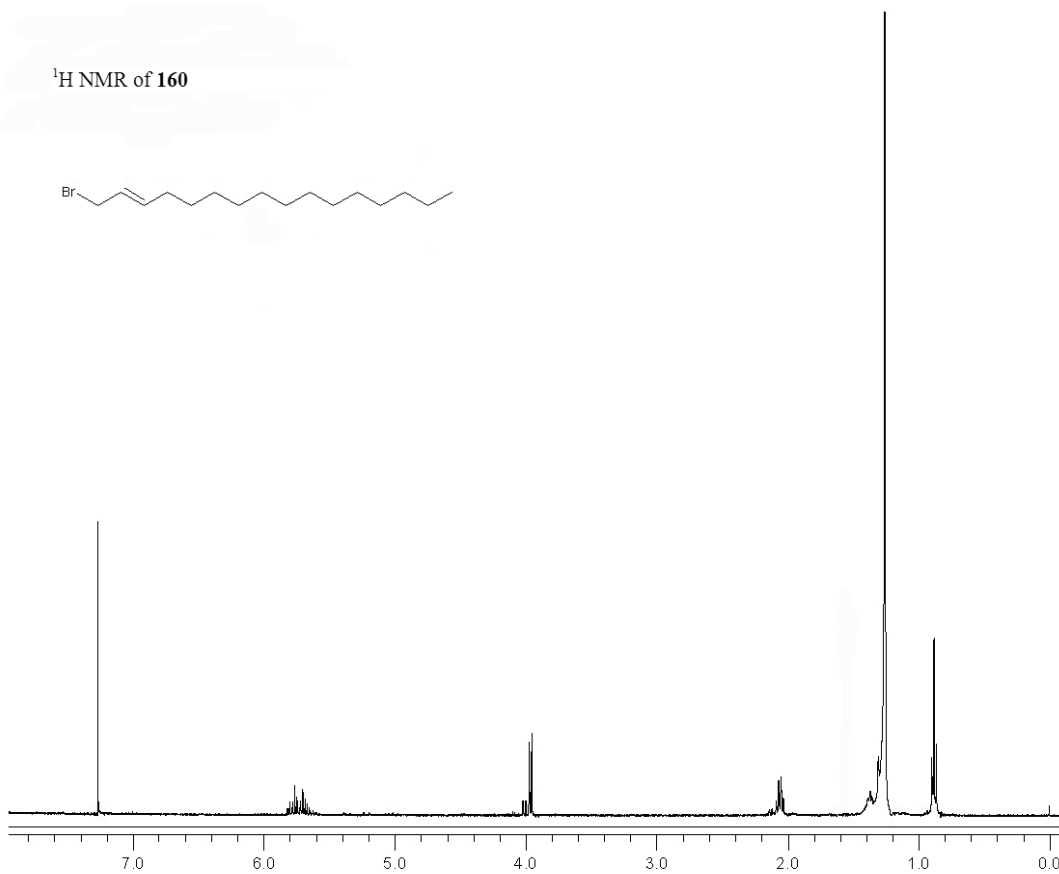


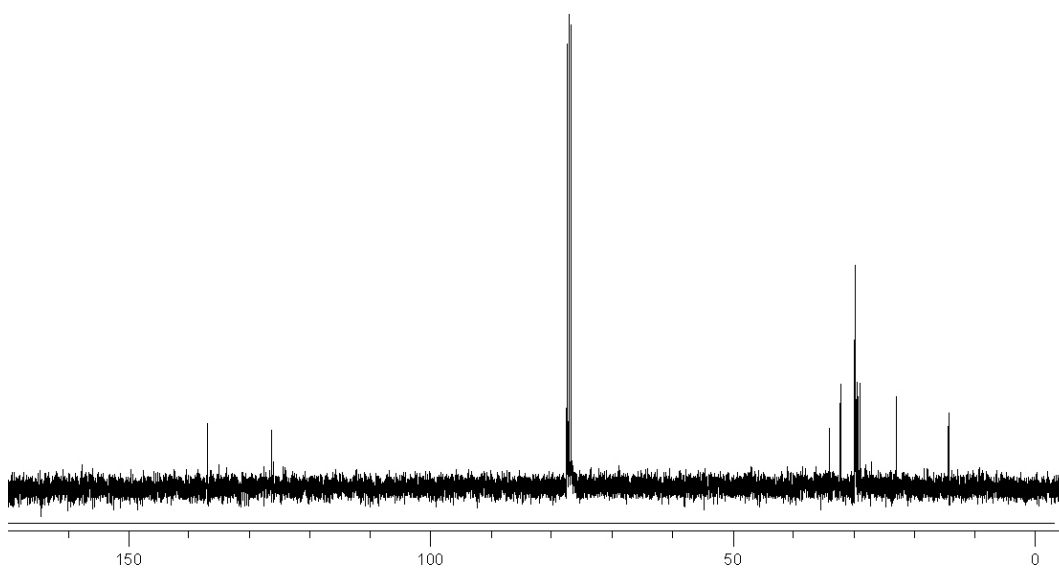
Figure 36

4. ANNEX

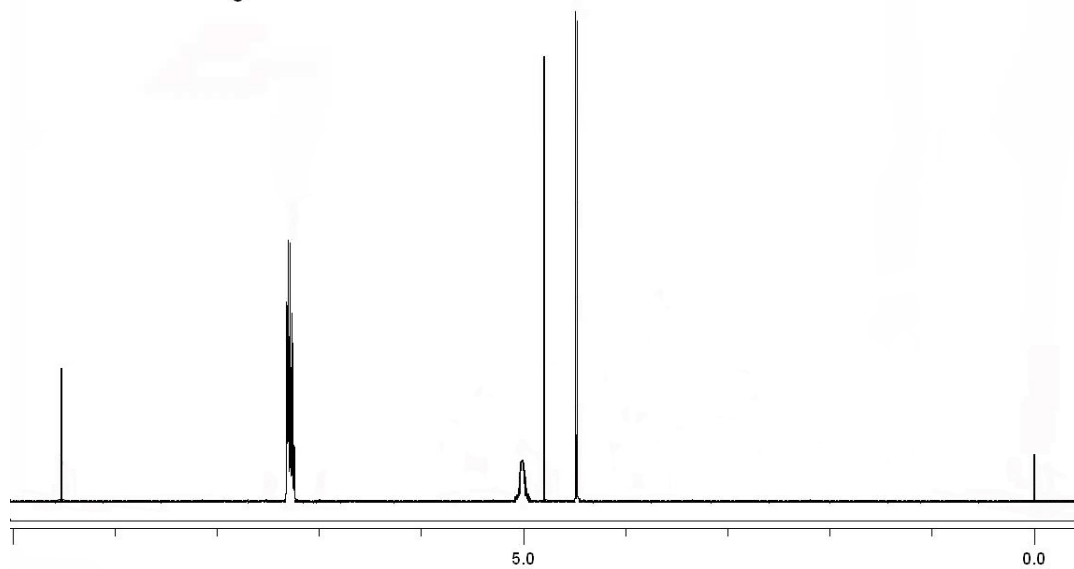
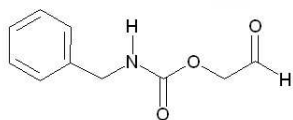
¹H NMR of **160**



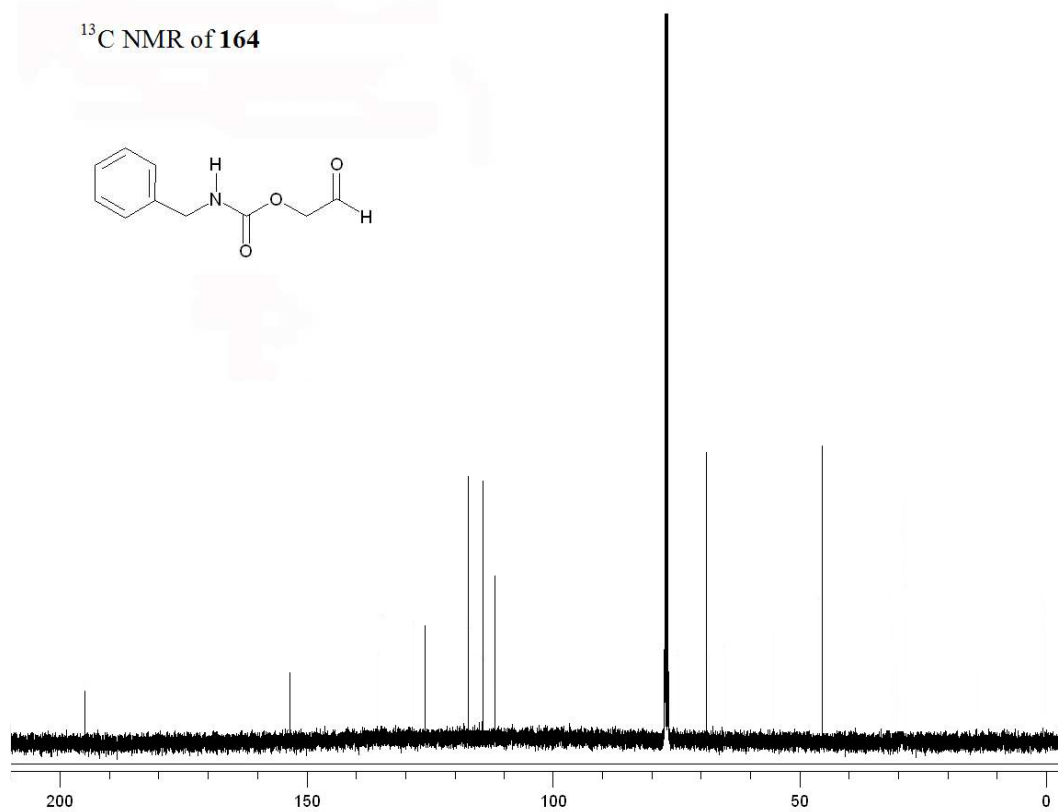
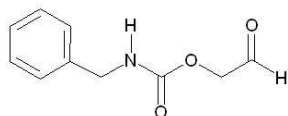
¹³C NMR of **160**



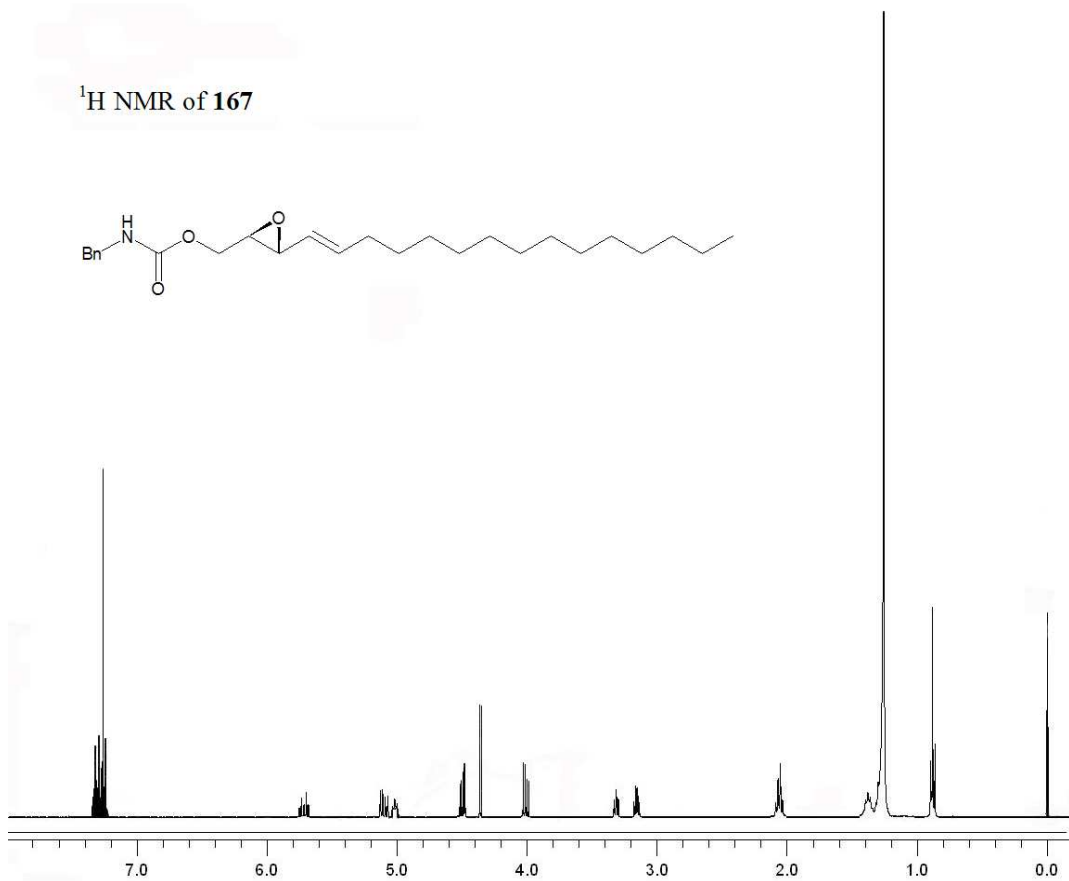
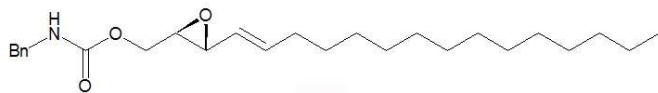
¹H NMR of 164



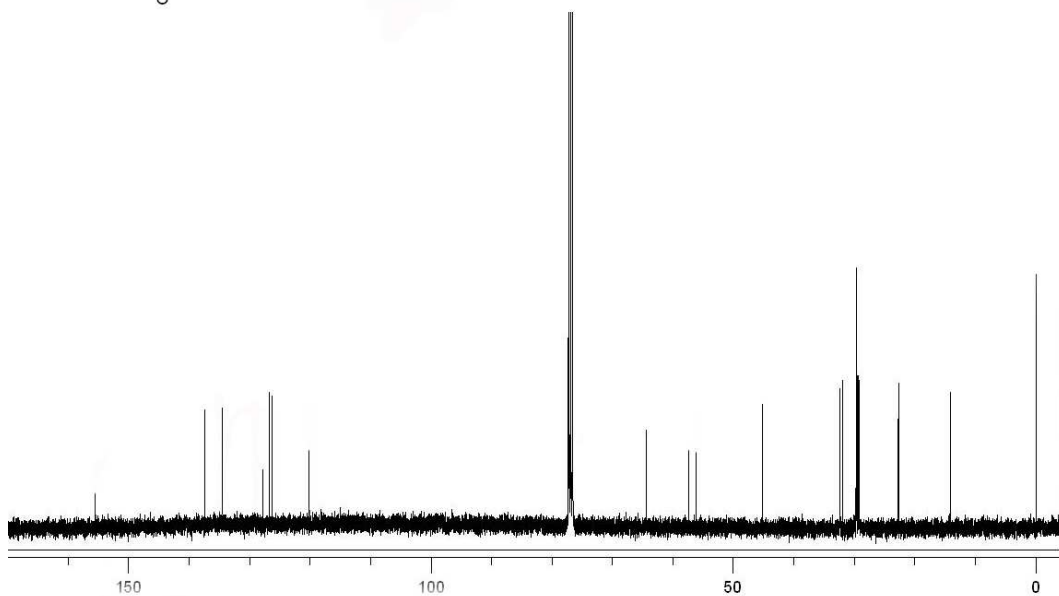
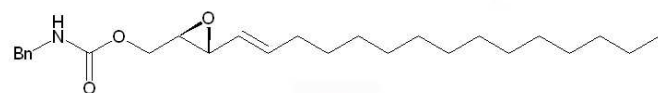
¹³C NMR of 164



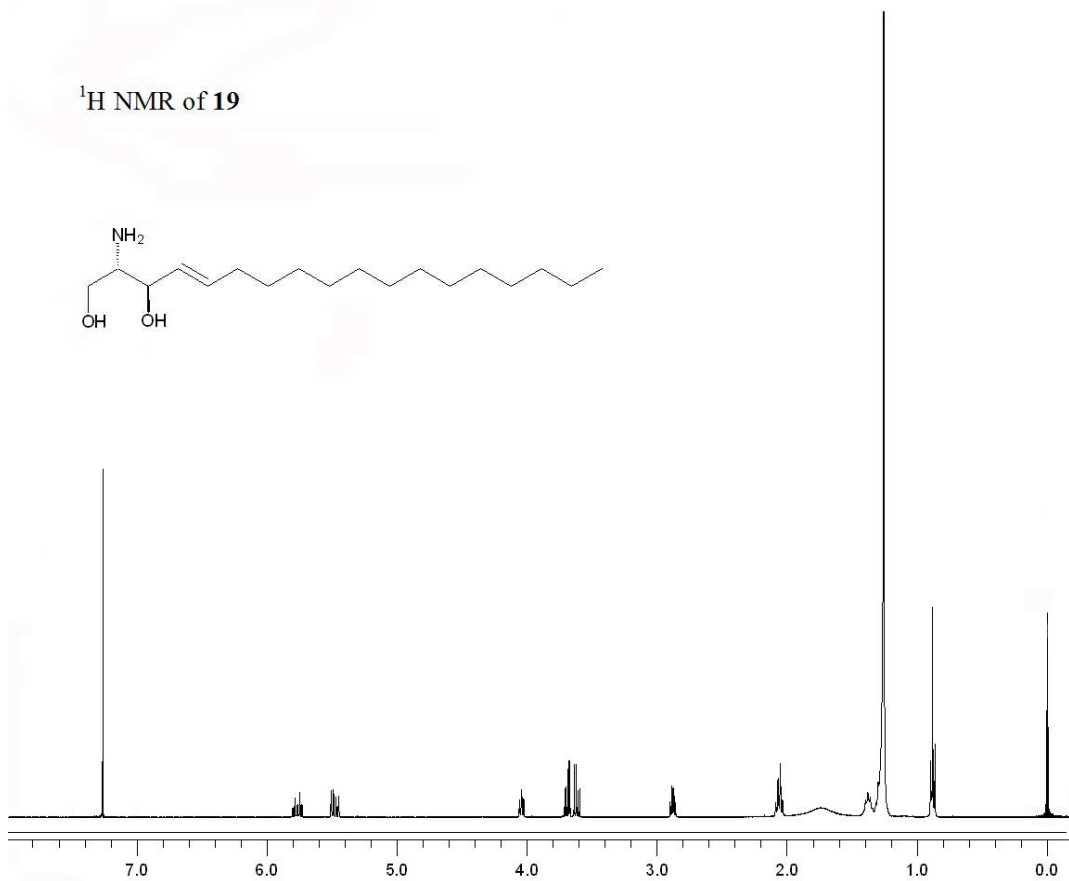
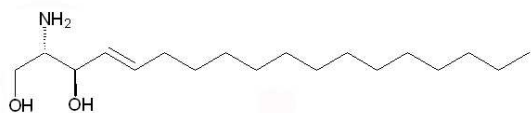
^1H NMR of **167**



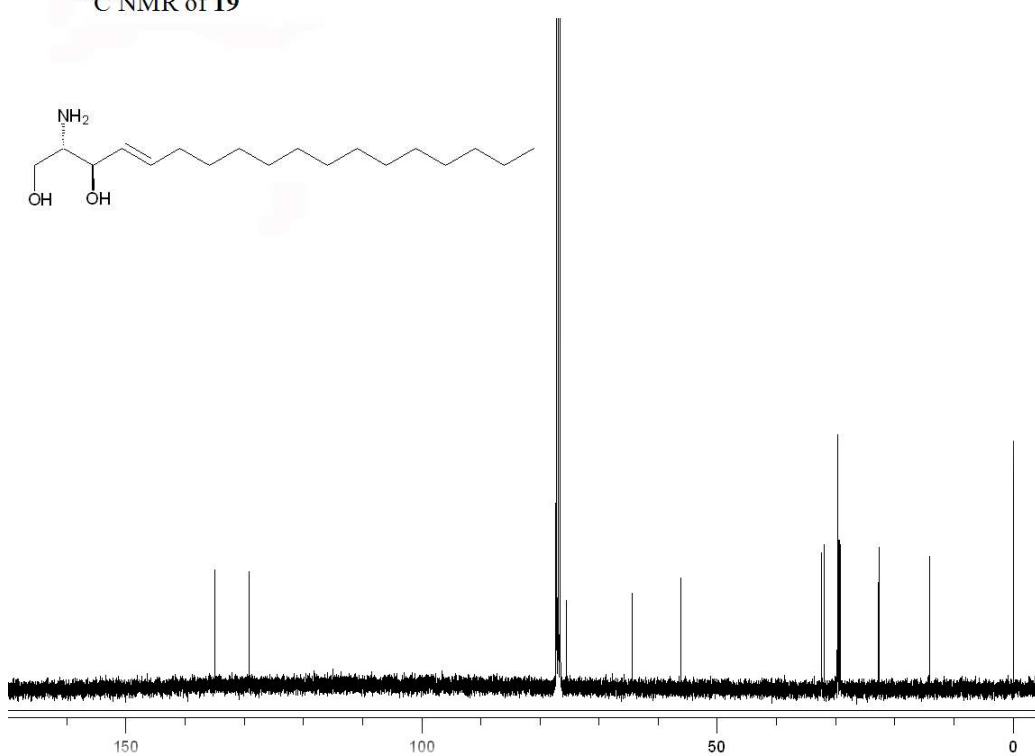
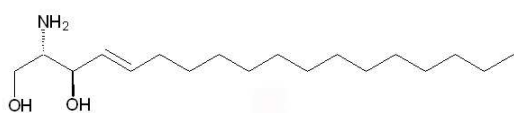
^{13}C NMR of **167**



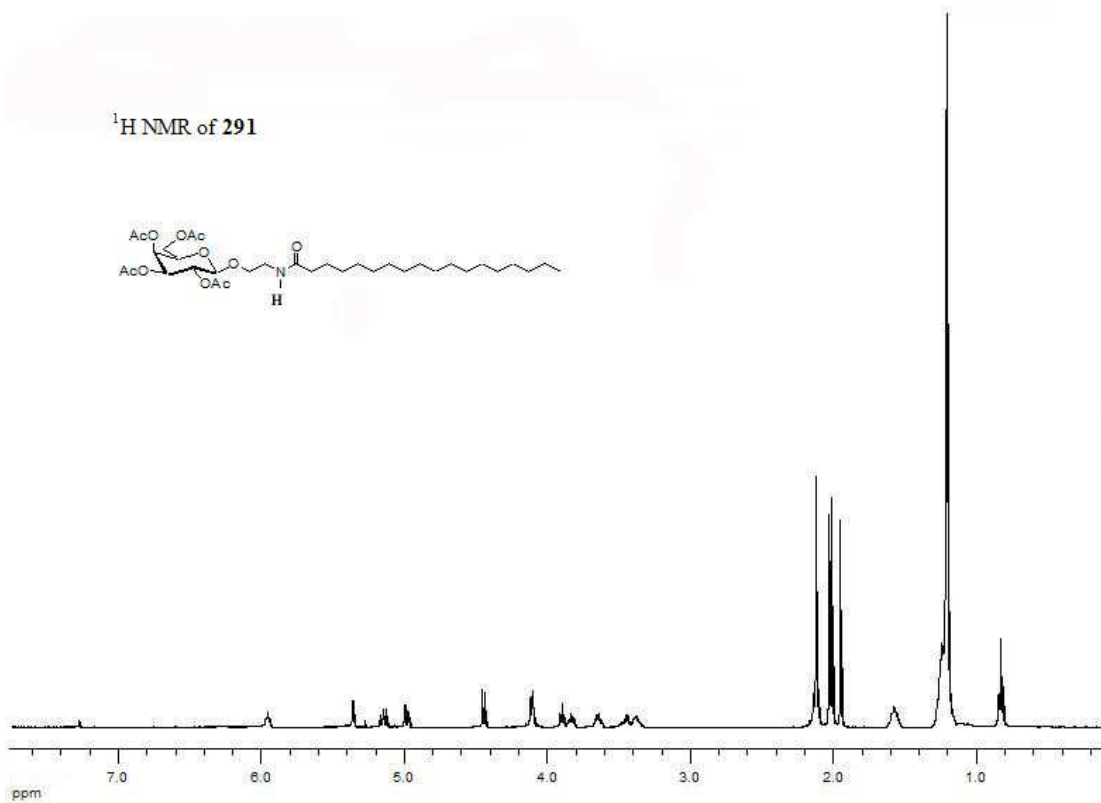
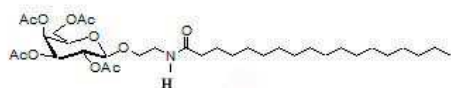
^1H NMR of **19**



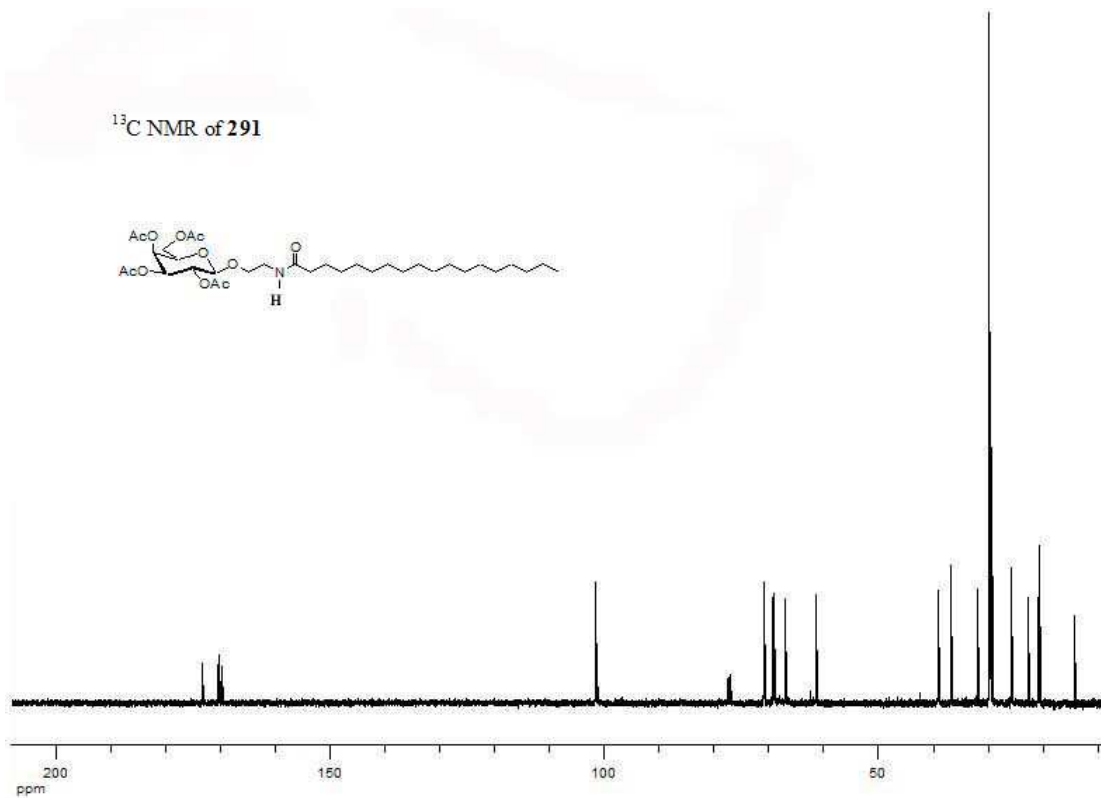
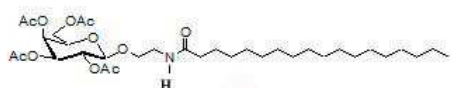
^{13}C NMR of **19**



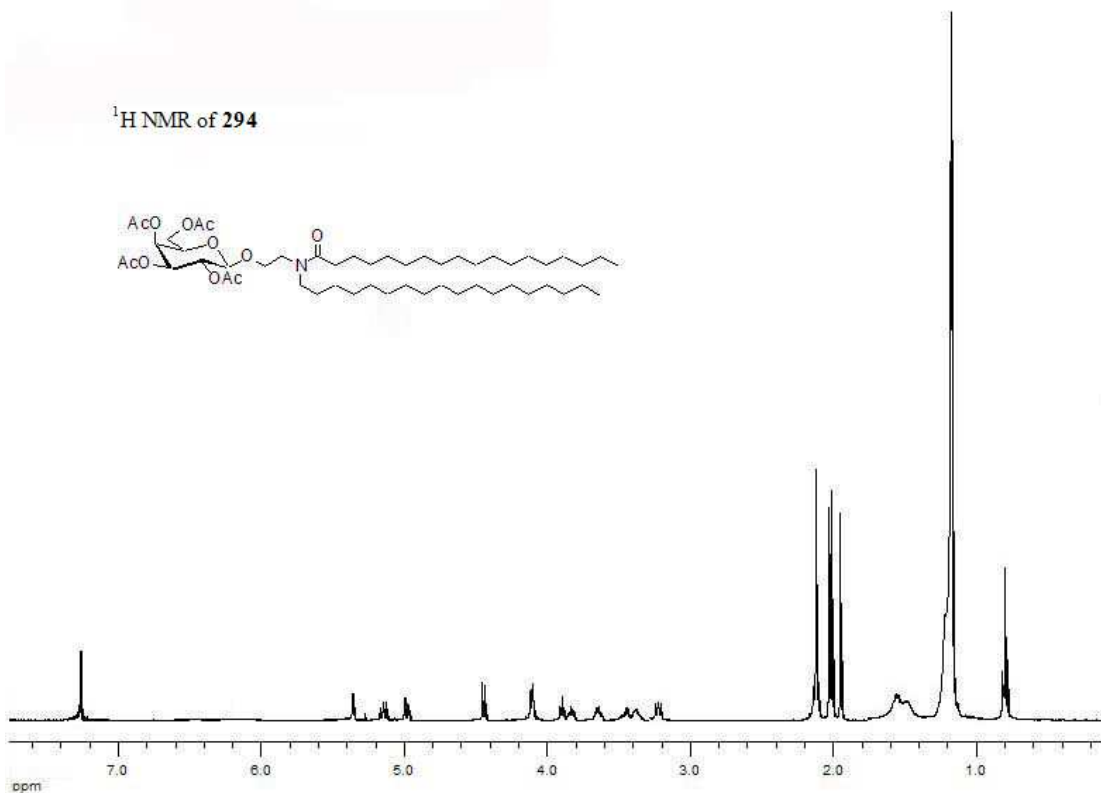
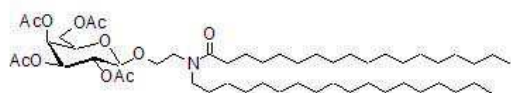
¹H NMR of 291



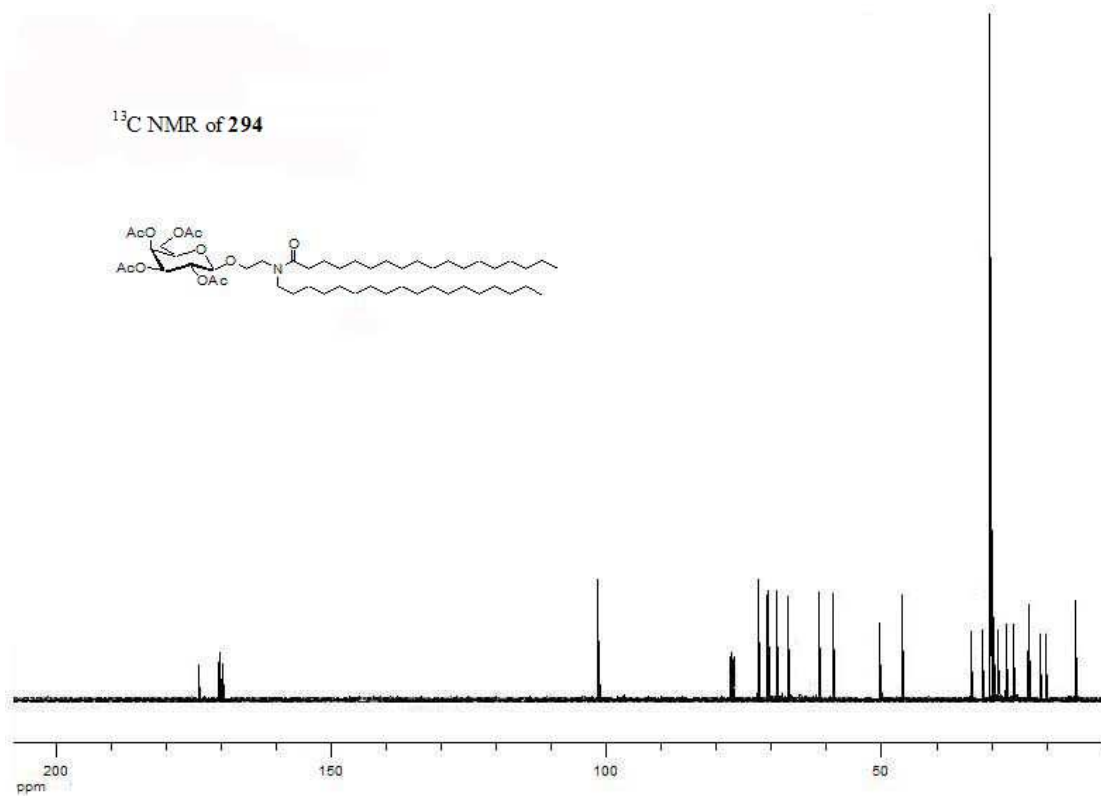
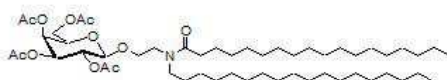
¹³C NMR of 291



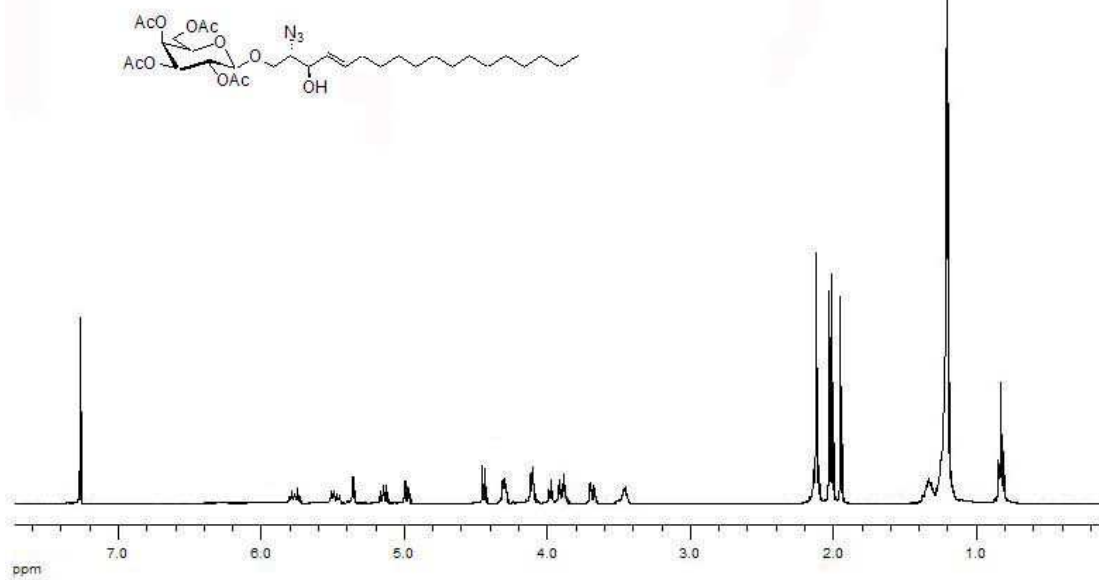
^1H NMR of 294



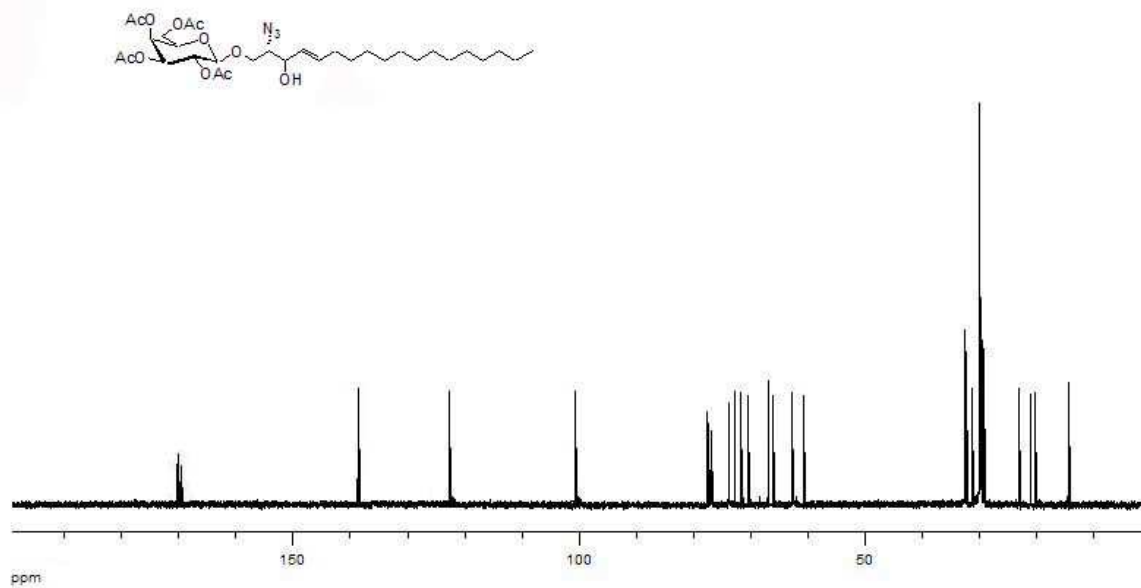
^{13}C NMR of 294



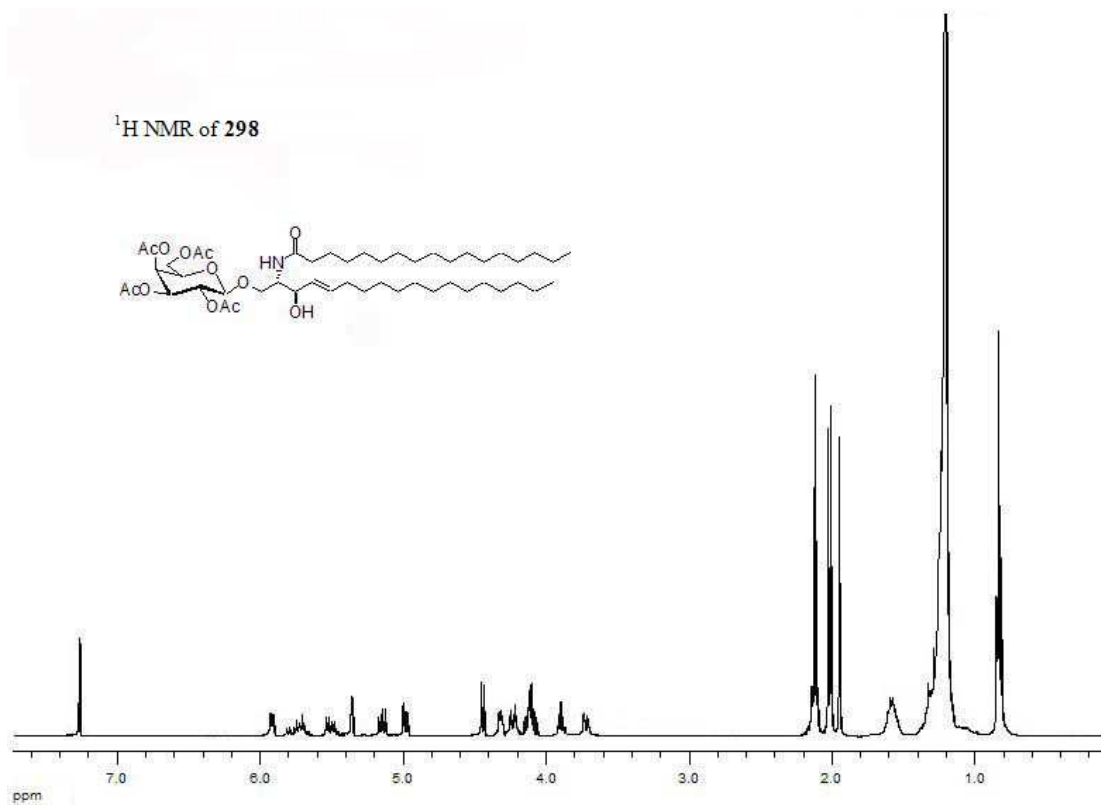
^1H NMR of 296



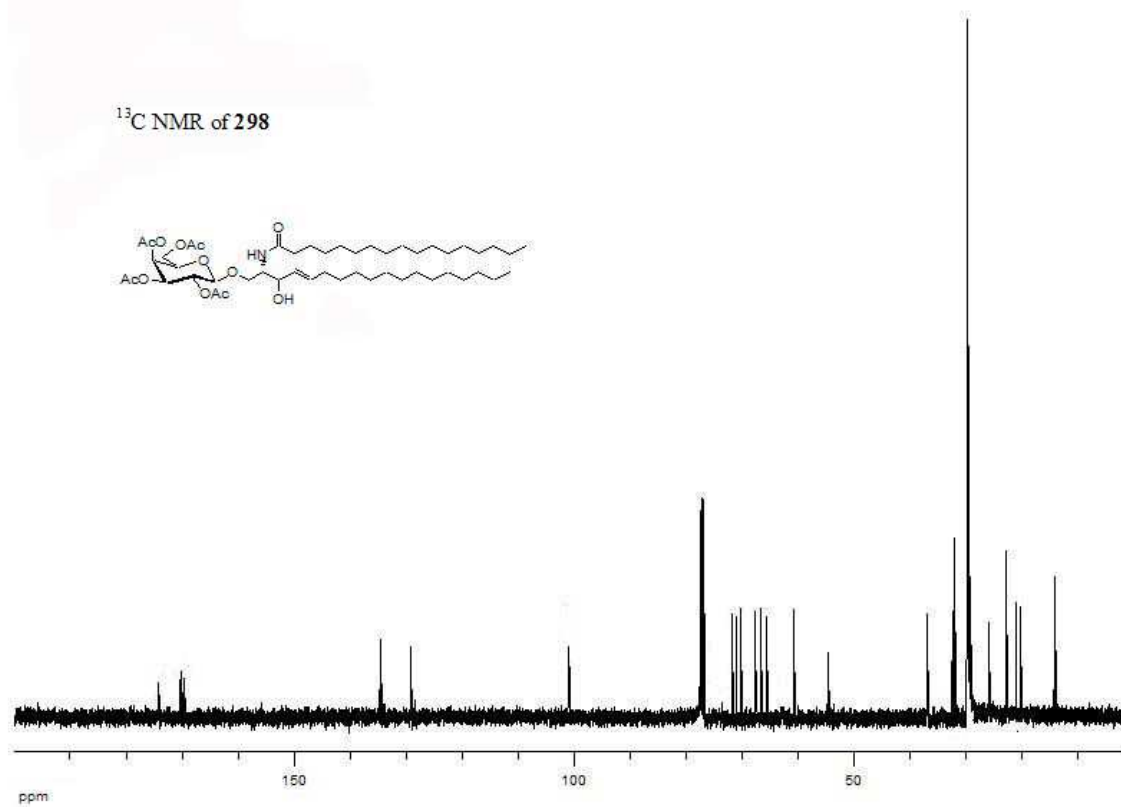
^{13}C NMR of 296



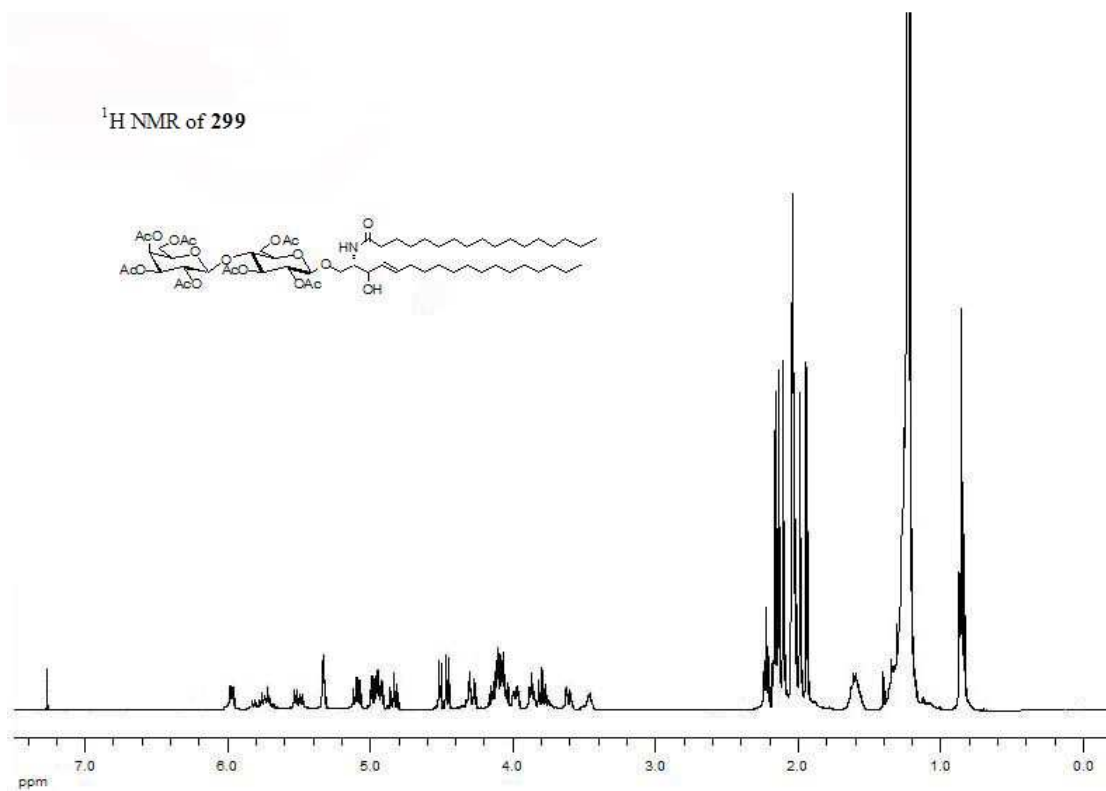
^1H NMR of **298**



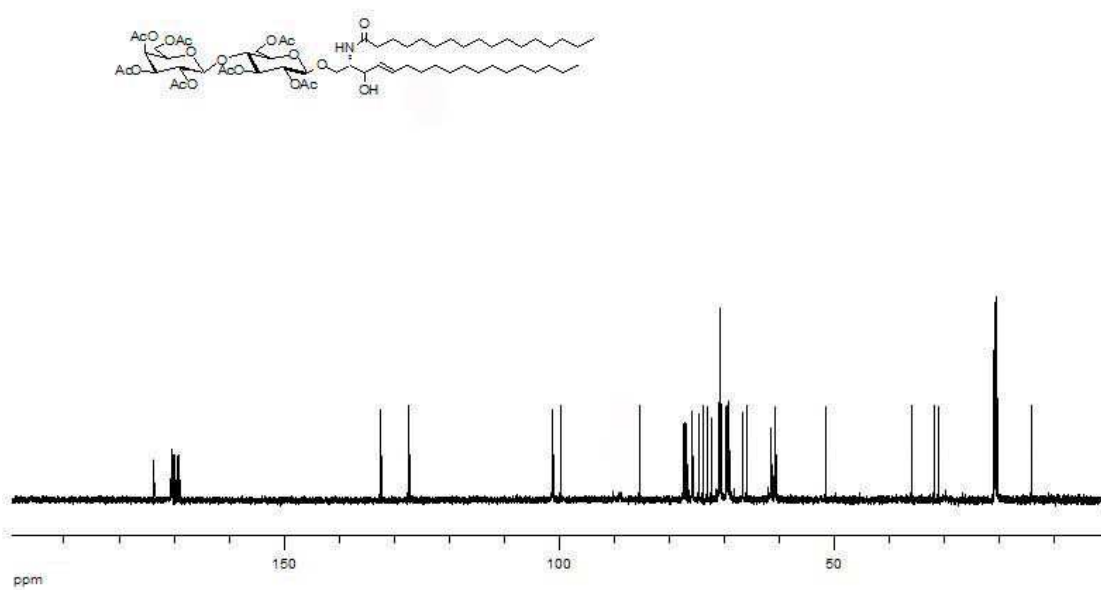
^{13}C NMR of **298**

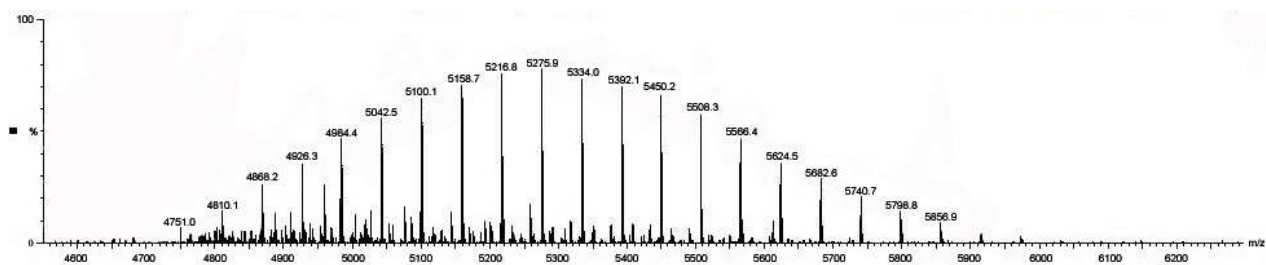


¹H NMR of 299

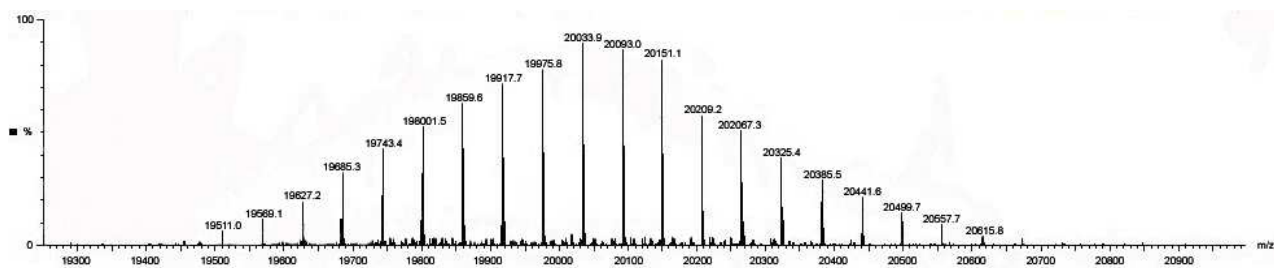


¹³C NMR of 299

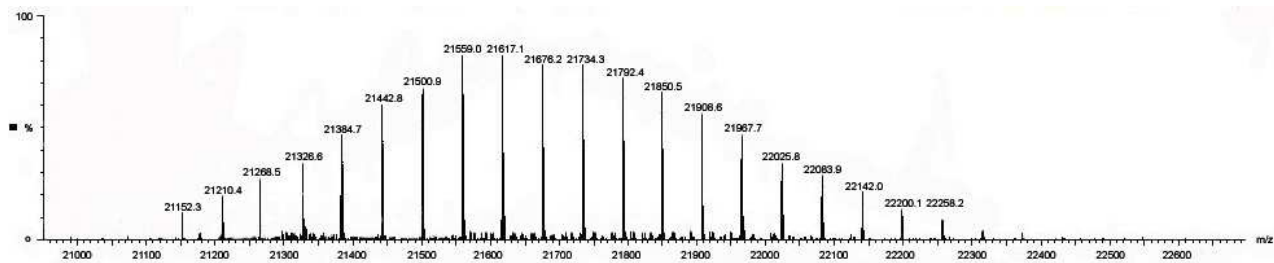




MALDI-TOF MS of 324



MALDI-TOF MS of 325



MALDI-TOF MS of 326